UNIVERSITY OF SOUTHAMPTON

FACULTY OF MEDICINE

Academic Unit of Clinical and Experimental Sciences

Investigating the relationship between *Streptococcus pneumoniae* biofilm and the human host

by

Matthew Wilkins

Thesis for the degree of Doctor of Philosophy

October 2017

UNIVERSITY OF SOUTHAMPTON

ABSTRACT

FACULTY OF MEDICINE

Thesis for the degree of Doctor of Philosophy

INVESTIGATING THE RELATIONSHIP BETWEEN STREPTOCOCCUS PNEUMONIAE BIOFILM AND THE HUMAN HOST

by Matthew Wilkins

Streptococcus pneumoniae (pneumococcus) is a leading cause of worldwide morbidity and mortality. Recent studies have demonstrated that *S. pneumoniae* may colonise the adenoidal mucosal epithelium in the human nasopharynx as aggregated and surface-attached bacteria, known as a biofilm. Biofilms are clinically important due to greater recalcitrance to antibiotics and the immune system than free-living bacteria.

Pneumococcal biofilms have also been found in the middle ear. Adenoidectomy is effective in treating chronic middle ear (otitis media) infections in some children, suggesting an etiological role of nasopharyngeal biofilms in the pathogenesis of otitis media, which remains the most common infection in young children and the primary cause of antibiotic prescriptions in paediatrics. However, studies directly investigating the interaction between pneumococcal biofilms and the host are lacking.

In this study, the interaction between pneumococcus and host cells in adenoid tissue was examined. Specifically, to find evidence of pneumococcal biofilm formation, and whether aggregates of pneumococcus co-localised with macrophages and neutrophils (phagocytic cells). Immunohistochemistry was used to stain for a serotype 14 (S14) pneumococcal strain, which is prevalent in pneumococcal disease, using pure cultures and spiked adenoids. Optimisation was achieved by using different dilutions of a polyclonal rabbit anti-*S. pneumoniae* antibody, alongside various antigen retrieval techniques and different counterstains. Aggregates of pneumococcus were found in each spiked adenoid that was examined. However, evidence of co-localisation with phagocytes was inconclusive with immunohistochemistry and sequential section staining. To obtain results more representative of the *in vivo* host-pathogen environment, pneumococcus was stained in non-spiked patient adenoids with an alternative antibody reactive against over 90 different serotypes. Optimisation was achieved through different antibody dilutions and staining pure cultures of pneumococcus using immunofluorescence. Although individual pneumococcal cells only were found in two of the four patient adenoids examined,

macrophages were in close proximity, and the established methods in this project demonstrated that they are suitable for staining pneumococcus in adenoid tissue and for further examination of assessing co-localisation between pneumococcal biofilms and immune cells in patient adenoids.

Since pneumococcus is predominantly an asymptomatic coloniser, the biofilm phenotype is reasoned to account for persistence in the upper respiratory tract. To date, *in vitro* studies recapitulating pneumococcal biofilms have been developed either on abiotic surfaces, on epithelial cells with a short contact time of up to 4 hours, on non-viable epithelial cells, or are transplanted from prefixed epithelia onto live epithelial cells. In this project, pneumococcal biofilms successfully grew on a confluent and viable bronchial epithelial cell line for up to 12 hours of culture with different pneumococcal loads (multiplicities of infection). Evidenced by scanning electron microscopy, nascent biofilms formed on viable epithelial monolayers using transwell membrane inserts, with morphological structure and topology reflective of mucosal epithelial samples found in *ex vivo*, with *in vitro* models and *in vivo* in mice. Epithelial cell integrity and viability was confirmed through transepithelial resistance, lactate dehydrogenase production and photomicrographic images. This more biologically representative model can be used for advanced modelling of the *in vivo* relationship between pneumococcal biofilms and the host.

Table of Contents

List of Figures

List of Tables

Declaration of Authorship

I, Matthew Wilkins, declare that this thesis and the work presented in it are my own and has been generated by me as the result of my own original research.

Investigating the relationship between *Streptococcus pneumoniae* biofilm and the human host.

I confirm that:

1. This work was done wholly or mainly while in candidature for a research degree at this University;
2. Where any part of this thesis has previously been submitted for a degree or any other qualification at this University or any other institution, this has been clearly stated;
3. Where I have consulted the published work of others, this is always clearly attributed;
4. Where I have quoted from the work of others, the source is always given. With the exception of such quotations, this thesis is entirely my own work;
5. I have acknowledged all main sources of help;
6. Where the thesis is based on work done by myself jointly with others, I have made clear exactly what was done by others and what I have contributed myself;
7. None of this work has been published before submission;

Signed: .....

Date: .....

Acknowledgements

First and foremost, I need to express my deepest gratitude to my supervisors, **Professor Saul Faust**, **Dr Luanne Hall-Stoodley**, **Dr Raymond Allan and Dr Susan Wilson**, who have provided me with guidance and support for these past four years.

I would like to genuinely thank **Jon Ward** and **Jenny Norman** of the ***Histochemistry Research Unit*** for their help throughout this project.

I am also grateful for all the members of staff in the ***Biomedical Imaging Unit***, including **Dr Anton Page**, **Dr Elizabeth Angus** and **Dr Claire Jackson**. In particular, a special mention must go to **James Thompson** and **Dr Dave Johnston** for their invaluable expertise.

I wish to extend my thanks to **Georgia Halladay** and **Sanjita Brito-Mutunayagam** for obtaining consent for the tissue used in this study.

Finally, I must acknowledge ***The Sir Jules Thorn Charitable Trust*** for granting me the opportunity to undertake this PhD by funding the work.

Abbreviations

AOM	Acute otitis media
ATP	Adenosine triphosphate
BHI	Brain heart infusion
BSA	Bovine serum albumin
CBA	Columbia blood agar
CbpA	Choline-binding protein A
CbpD	Choline-binding protein D
CFU	Colony forming units
ChoP	Cell-wall phosphocholine
CLSM	Confocal laser scanning microscopy
COM	Chronic otitis media
CPS	Capsular polysaccharide
CSP	Competence-stimulating peptide
DAPI	4',6-diamidino-2-phenylindole
eDNA	Extracellular deoxyribonucleic acid
ENT	Ear, nose and throat
FCS	Fetal calf serum
GFP	Green fluorescent protein
H&E	Haematoxylin and eosin
HBE	Human bronchial epithelial
HBSS	Hanks balanced salt solution
IAV	Influenza A virus
IPD	Invasive pneumococcal disease
LDH	Lactate dehydrogenase
MOI	Multiplicity of infection
NanA	Neuraminidase
NETs	Neutrophil extracellular traps
NE	Neutrophil elastase
OD	Optical density
OM	Otitis media
OME	Otitis media with effusion

OSA	Obstructive sleep apnea
PavA	Pneumococcal adhesin
PavB	Pneumococcal virulence
PCV	Pneumococcal conjugate vaccine
PPV	Pneumococcal polysaccharide vaccine
PsaA	Pneumococcal surface adhesin A
PspA	Pneumococcal surface protein A
PsrP	Pneumococcal serine-rich repeat protein
QS	Quorum sensing
RaM	Rabbit anti-mouse
RAOM	Recurrent acute otitis media
RT-PCR	Reverse transcription polymerase chain reaction
SaR	Swine anti-rabbit
SEM	Scanning electron microscopy
sMEM	Supplemented minimum essential medium
TBS	Tris-buffered saline
TEER	Transepithelial electrical resistance

1 Chapter 1 - Introduction

1.1 *Streptococcus pneumoniae*

Streptococcus pneumoniae (pneumococcus) is a Gram positive, facultative anaerobic bacterium. Typically, *S. pneumoniae* is observed in pairs known as diplococci, but can also be found as single cells or occurring in short chains. Individual pneumococcal cells are 0.5 to 1.25 µm in diameter, are lancet-shaped and are nonmotile. Similar to other streptococci, pneumococci lack the enzyme catalase and ferment glucose to lactic acid. When cultured on blood agar, pneumococcal cultures produce an area of alpha (green) haemolysis due to the partial breakdown of red blood cells, which helps to differentiate *S. pneumoniae* from group B (beta haemolytic) streptococci that induce a complete lysis of erythrocytes. *S. pneumoniae* can be distinguished from the alpha haemolytic viridans (commensal) streptococci by solubility in bile and susceptibility to optochin.

1.2 Serotyping of *S. pneumoniae*

Tracking the geographical and temporal prevalence of pneumococci is achieved by serotyping the capsular polysaccharide (CPS). The extracellular capsule coats the outer surface of pneumococcus and 97 structurally and serologically distinct serotypes have been discovered to date (Geno et al., 2015). Each serotype is distinguished by the ability of antibody to bind to specific antigens that form the chemical structure of the capsular polysaccharide and are unique to each serotype (Brueggemann et al., 2003).

The virulence factors of pneumococcus can be divided into three categories: the capsule, cytotoxic products (pneumolysin and hydrogen peroxide) and surface proteins. Despite being highly immunogenic, the capsule is the most important virulence factor as it protects pneumococci from phagocytosis (Watson and Musher, 1999). If capsular polysaccharide expression is reduced, antibodies and complement have greater access to the pneumococcal surface, which promotes pneumococcal clearance (Magee and Yother, 2001).

1.3 The nasopharynx

The pharynx connects the oral and nasal cavities to the oesophagus and the larynx, and is divided between the nasopharynx, the oropharynx and the laryngopharynx. The nasopharynx is the most anterior part of the pharynx and is located at the top of the throat behind the internal nares (back of the nose) and the soft palate (roof of the mouth). The nasopharynx is situated at a crossroads that connects the nose, ears (Eustachian tube), mouth and the lower respiratory tract (trachea) (Figure 1.1).

The nasopharynx also contains the tonsils and the adenoids (Figure 1.1), which are aggregates of lymphoid tissue lined with ciliated pseudostratified columnar epithelial cells. The epithelial cells are covered with a mucus layer, which is produced by goblet cells found throughout the epithelial layer, and serve to entrap microorganisms within the nasopharynx. The pneumococcus colonises these mucosal surfaces that line the human nasopharynx (Austrian, 1986), and is associated with mostly asymptomatic carriage (Ghaffar et al., 1999). The nasopharynx is also the ecological niche for other bacteria including, *Staphylococcus aureus*, *Haemophilus influenzae*, *Moraxella catarrhalis* and *Neisseria meningitidis*.

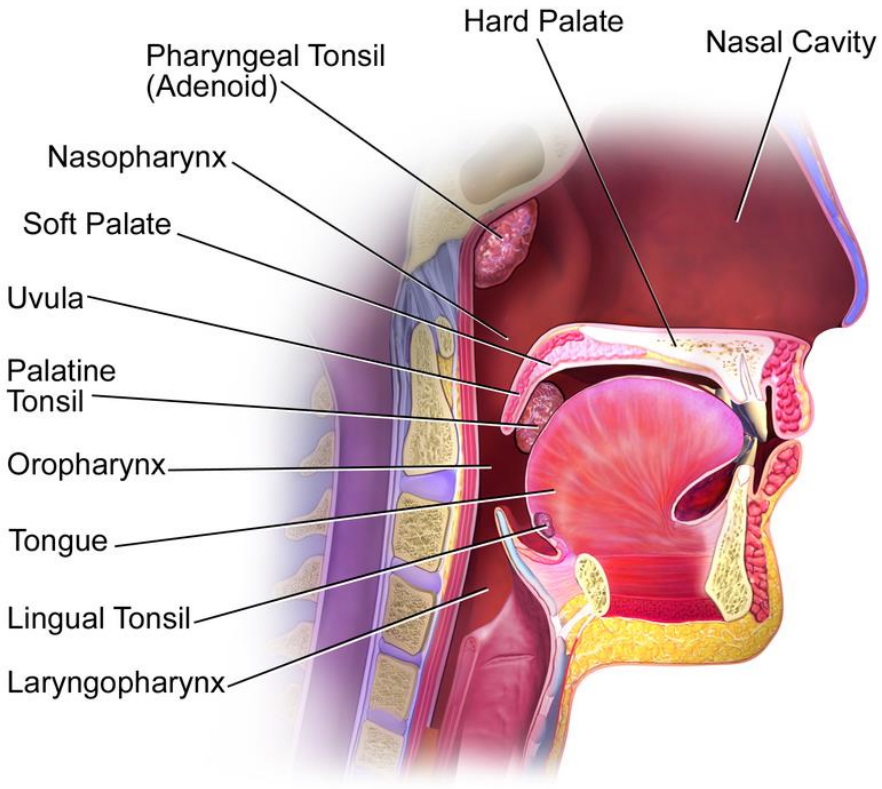

Figure 1.1: The upper respiratory tract in the human host.

The pharynx is divided into the nasopharynx, the oropharynx and the laryngopharynx. The nasopharynx is located at the top of the pharynx and lies close to the paranasal sinuses and the Eustachian tubes. The lymphoid tissues, tonsils and adenoids, help to entrap microorganisms from the external environment. Image taken from http://www.dovemed.com/common-procedures/procedures-surgical/tonsil-and-adenoid-removal-tonsil/.

1.4 Pneumococcal carriage

Colonisation with pneumococcus occurs very early in life, typically within the first few months, and usually peaks at around 2-3 years of age (Bogaert et al., 2004). Colonisation with multiple strains may occur simultaneously (co-colonisation) or sequentially (Wyllie et al., 2014). Up to the age of 9, the carriage rate is 30-40% but then steadily declines thereafter with 10% of the adult population believed to be carriers of pneumococcus (Bogaert et al., 2004, Hussain et al., 2005). This inverse correlation with age has been attributed to the development of the immune system and, in particular, the development of immunological memory induced by repeated exposure to pneumococcal colonisation (Högberg et al., 2007, Weinberger et al., 2008, Malley, 2010).

Pneumococcal carriage rates may be influenced by multiple factors. For instance, large families and overcrowding in places such as nursing homes, hospitals, army barracks and prisons has been shown to expose individuals to a greater number of pneumococcal serotypes (Millar et al., 1994, Hoge et al., 1994, Principi et al., 1999). Typically, pneumococcal carriage is transient, with the duration of colonisation ranging from days to weeks between serotypes (Högberg et al., 2007). In one study, the duration of carriage among common serotypes was estimated to range from ~6 weeks (serotype 15C) to ~20 weeks (serotype 6B) (Sleeman et al., 2006). The prevalence of pneumococcal carriage also varies widely between the pneumococcal serotypes, with some serotypes (4, 5, 7F) infrequently found and others (1) rarely found at all (Sleeman et al., 2006, Ritchie et al., 2012). The serotype distribution also varies geographically (Brueggemann et al., 2004).

The factors that are responsible for this discrepancy in serotype distribution are not completely understood, but the prevalence of pneumococcal carriage appears to correlate with the extent of encapsulation, with a study in mice showing higher carriage rates for serotypes possessing larger capsules (Weinberger et al., 2009). The capsule is able to confer protection against immune-mediated clearance via several mechanisms including limiting complement and antibody deposition (opsonins), avoiding mucus entrapment and being resistant to opsonin-independent phagocytosis (Nelson et al., 2007, Hyams et al., 2010). Additionally, the negative surface charge of the capsule correlates with enhanced resistance to negatively charged phagocytes, with serotypes possessing the greatest negative charge more frequently found in carriage (Li et al., 2013).

1.5 Pneumococcal disease

S. pneumoniae is an opportunistic pathogen and a leading global cause of morbidity and mortality. Pneumococcal disease takes place when resident pneumococcus disseminates from the nasopharynx and migrates to other areas of the host (Bogaert *et al.*, 2004). Pneumococcal disease can range from non-invasive infections such as otitis media, sinusitis and blood culture negative pneumonia, to invasive pneumococcal disease (IPD) including sepsis and meningitis. IPD diagnosis is determined by isolating pneumococcus from a normally sterile site such as the blood or the cerebrospinal fluid.

Although pneumococcal carriage is typically asymptomatic, the high prevalence of colonisation means that the transition to disease occurs frequently enough to ensure that *S. pneumoniae* remains the leading cause of otitis media, community acquired pneumonia, sepsis and meningitis in both developed and developing countries (O'Brien et al., 2009). Despite pneumococcal vaccines and the availability of antibiotics, a report in 2010 estimated that 1.3 million deaths occur each year due to pneumococcal disease (Walker et al., 2013).

The most common pneumococcal diseases are otitis media and pneumonia. Otitis media is the number one reason why a child will visit a doctor, require an antibiotic prescription and undergo surgery (Plasschaert et al., 2006, Monasta et al., 2012). Pneumococcal pneumonia caused 411,000 deaths in young children globally in 2011 (Walker et al., 2013). Pneumonia is the primary pneumococcal disease burden in the elderly, with comorbidities, impaired mucociliary clearance and a waning immune system all increasing the risk (Fung and Monteagudo-Chu, 2010). Concurrent pneumococcal septicaemia has a fatality case rate of approximately 20% (Lim et al., 2001), whilst meningitis is responsible for more than 60,000 deaths or long-term disabilities in children under 5 years of age every year (O'Brien et al., 2009).

1.6 Pathogenesis of pneumococcal disease

Transmission of *S. pneumoniae* occurs through direct person-to-person contact via aerosol droplets, and nasopharyngeal colonisation is a prerequisite for the pathogenesis of all pneumococcal disease (Bogaert et al., 2004, Simell et al., 2012). Transmission exclusively occurs from human carriers as pneumococcus does not colonise animals.

Free-floating (planktonic) pneumococcal cells enter the airways and adhere to the epithelial cells of the nasopharynx through the interactions of bacterial surface adhesins and mammalian cell receptors. Pneumococcus will then most commonly be cleared or will remain as an innocuous coloniser. Infrequently, however, pneumococcal cells may migrate to other areas of the body including nearby organs, such as the ears and the sinuses, or travel via the bronchi down to the lungs. Pneumococci may then penetrate the mucosal barrier to cause septicaemia, or even cross the blood-brain barrier to cause meningitis. Therefore, the virulence factors of pneumococci are likely to represent an adaptation for persisting either in the nasopharynx, transmitting to a new host and leading to the development of disease (Weiser, 2010).

1.7 Invasive disease potential

Invasive pneumococcal disease (IPD) is a major cause of worldwide morbidity and mortality. Individuals with a predisposed risk to IPD are the very young and the very old. Additionally, individuals with immunodeficiencies are more susceptible to IPD including, those with an absent (congenital or splenectomy) or dysfunctional spleen, renal failure or cancer. Immunocompetent individuals with a normal immune system are also at a higher risk of IPD if they have comorbidities, such as cardiovascular or pulmonary disease (van Hoek et al., 2012, Torres et al., 2015) (Table 1).

Table 1: Risk factors for invasive pneumococcal disease

Risk factor	**Individuals affected**	**References**
Age	Persons younger than 2 years of age and persons 65 years and older.	(van Hoek et al., 2012) (Torres et al., 2015)
Chronic illness	Persons with cardiovascular disease, pulmonary disease, chronic liver disease, cirrhosis, diabetes mellitus, cochlear implant and persons with asthma and who smoke cigarettes.	
Immunodeficiency	Persons with splenic dysfunction or absence, chronic renal failure, human immunodeficiency (HIV), Hodgkin's disease, multiple myeloma, lymphoma and persons immunosuppressed due to chemotherapy or organ transplantation.	

Pneumococcal serotypes differ markedly in their capacity for disease. Certain pneumococcal serotypes are prevalent in invasive disease while others are mainly associated with carriage. Despite the existence of over 90 different serotypes of pneumococcus, only a small number are responsible for 70-80% cases of IPD (Hausdorff et al., 2005). Several studies have examined the invasive disease potential of pneumococcal serotypes, which is defined as the ratio of IPD to carriage. For example, serotypes 1, 4, 5, 7F, 8, 12F, 14, 18C and 19A are considered to have a high invasive disease potential, while 6A, 6B, 11A, 15B, 15C and 23F are considered less likely to cause IPD (Brueggemann et al., 2003, Shouval et al., 2006, Kronenberg et al., 2006, Sleeman et al., 2006, Rivera-Olivero et al., 2011, Sá-Leão et al., 2011). It has been found that individuals infected with a pneumococcal serotype of a low invasive potential frequently have an underlying illness prior to the infection (Sjöström et al., 2006, Pilishvili et al., 2010b).

Similar to pneumococcal carriage, it is believed that the differences in invasive disease potential can be attributed to the capsular polysaccharide (Brueggemann et al., 2003, Brueggemann et al., 2004, Sandgren et al., 2004). Specifically, virulence is correlated with the thickness and chemical structure of the pneumococcal capsule, which reflects the serotype-specific capacity for resisting phagocytosis (Hostetter, 1986). The importance of the capsule for pneumococcal disease is emphasised by serotype-specific antibodies conferring high protection against IPD by strains belonging to the same serotype (Pilishvili et al., 2010a). However, several studies have highlighted that the capsule is not

the sole virulence factor accountable for pneumococcal disease. Clinical isolates of the same serotype can vary in their virulence (Kelly et al., 1994), while an enhanced likelihood of invasive disease is not always guaranteed when an isolate changes its capsule to that of another serotype (capsular switching) (Browall et al., 2014). Finally, pneumococcal virulence is affected if surface proteins such as choline-binding protein A (CbpA) and pneumococcal surface protein A (PspA) are deleted (Gosink et al., 2000, Orihuela et al., 2004).

In addition to the discrepancy between serotypes that cause either asymptomatic colonisation or IPD, certain serotypes have been shown to have a propensity for causing non-invasive pneumococcal disease. For instance, serotypes 3, 6A, 6B, 9V, 14, 19A, 19F and 23F are frequently reported to cause acute otitis media in young children worldwide (Rodgers et al., 2009), while serotypes 1, 3, 8, 14 and 19A are the most common causes of pneumococcal pneumonia in adults (Bewick et al., 2012).

1.8 Pneumococcal adherence and colonisation of the nasopharynx

Pneumococcal colonisation requires adherence to the ciliated epithelial lining of the nasopharynx (Figure 1.2). These epithelial cells are covered with a thick mucus layer that acts as a physical barrier to colonisation and also contains antibacterial components; the antimicrobial peptide, lysozyme, may induce cell wall degradation (Nash et al., 2006), while lactoferrin can sequester free iron to inhibit growth and possesses bactericidal properties (Arnold et al., 1980). Additionally, negatively charged mucin glycoproteins are capable of binding to positively charged bacteria and mediating mucociliary clearance (Voynow and Rubin, 2009).

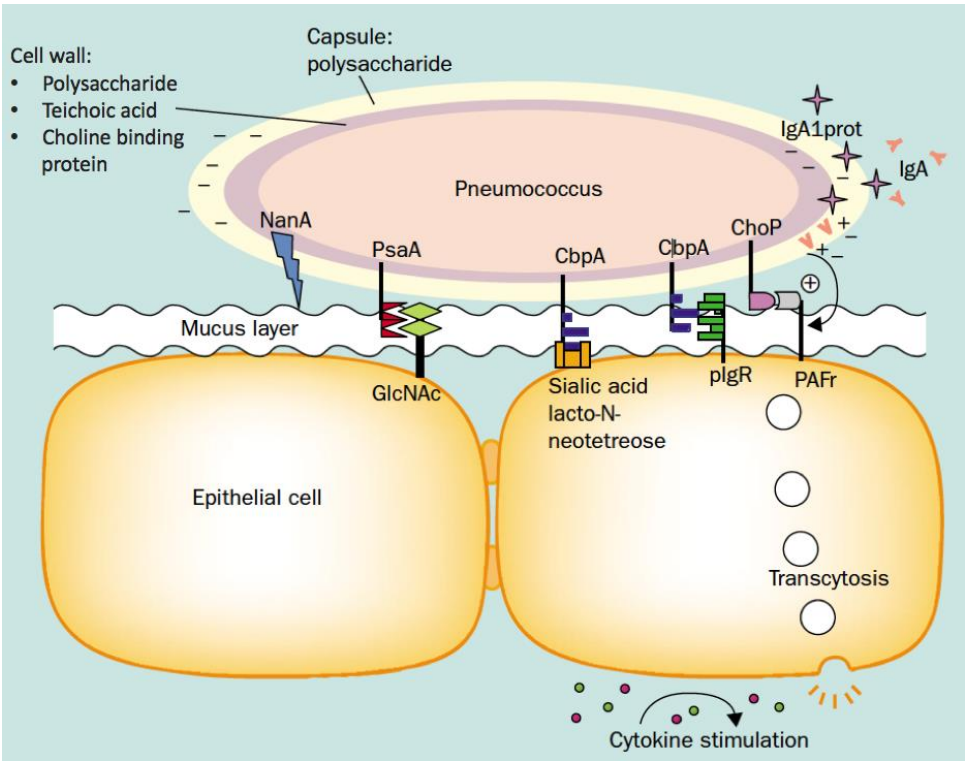

Figure 1.2: *S. pneumoniae* colonisation on epithelial cells.

Pneumococcal neuraminidase (NanA) enables *S. pneumoniae* to bind to epithelial cells by reducing the viscosity of the overlying mucus and exposing *N*-acetyl-glycosamine (GlcNAc) receptors for the pneumococcal surface adhesin A (PsaA) to bind to. Cell-wall phosphocholine (ChoP) binds to platelet-activating-factor receptors (PAFr), whilst another choline-binding protein (CbpA) binds to sialic acid and lacto-N-neotreatose receptors and to the polymeric immunoglobulin receptor (pIgR). Pneumococcal IgA1 protease cleaves host immunoglobulin IgA, which increases the proximity between ChoP and PAF receptors whilst reducing opsonisation. Image taken from Bogaert et al. (Bogaert et al., 2004).

However, pneumococcus can circumvent these physical defences and antibacterial components of the mucosal layer (Table 2). Firstly, pneumococcus can alter the structure of the peptidoglycan layer by incorporating D-alanine into the teichoic acid component of the cell wall thereby masking it from lysozymal degradation (Kovács et al., 2006). Secondly, PspA can bind to lactoferrin to inhibit its bactericidal activity (Hammerschmidt et al., 1999). Finally, the majority of the pneumococcal serotypes are negatively charged, and none are positively charged due to the capsule (Li et al., 2013). Therefore, repulsive forces facilitate the translocation of pneumococcus across the mucus layer and permits access to the underlying epithelial cells (Nelson et al., 2007). Concomitantly, the pneumococcal pore-forming toxin, pneumolysin, impairs the ciliary beating of epithelial cells and reduces mucociliary clearance as a result (Kadioglu et al., 2002). The pneumococcus may also out-compete other bacteria colonising the finite space in the nasopharynx through the production of hydrogen peroxide via the *spxB* gene, which has been shown to kill other bacteria *in vitro* (Pericone et al., 2000).

After translocating through the mucus layer, *S. pneumoniae* adhere to epithelial cells via the action of pneumococcal exoglycosidases including neuraminidase (NanA), β-galactosidase (BgaA) and *N*-acetylglucosaminidase (StrH) (King et al., 2006, Xu et al., 2011). These enzymes sequentially remove terminal sialic acid residues from glycoconjugates on epithelial cells to expose galactose and cell-surface *N*-acetyl-glycosamine (GlcNAc) receptors for pneumococcal surface adhesin A (PsaA) to bind to (King et al., 2006, Blanchette et al., 2016). Additionally, the pneumococcal cell-wall-associated CbpA (also referred to as PspC or SpsA) specifically binds to the polymeric immunoglobulin receptor (pIgR) and immobilised sialic acid and lacto-N-neotreatose receptors (Rosenow et al., 1997), while ChoP binds to platelet-activating-factor receptors (PAFr) (Cundell et al., 1995a). Enolase (Eno) and pneumococcal adhesin and virulence (PavA and PavB) then promote colonisation by binding to the extracellular-matrix components plasminogen and fibronectin, respectively (Bergmann et al., 2001, Holmes et al., 2001, Jensch et al., 2010, Bergmann et al., 2013).

The most abundant natural antibody in mucosal epithelial surfaces is immunoglobulin A (IgA), which can promote phagocytosis through opsonisation (opsonophagocytosis), and also attenuate the pathogenicity of bacteria and its toxins via neutralisation and agglutination i.e. coating the bacteria to inhibit colonisation and subsequent epithelial cell invasion and establishment of an infection (Fasching et al., 2007, Roche et al., 2015). However, pneumococci express a cell surface proteolytic enzyme known as IgA1 protease. This enzyme separates the Fab and Fc domains of IgA by cleaving the immunoglobulin at the hinge region, and has two advantages (Kilian et al.,

1979). It increases the physical proximity of ChoP to the PAF receptors on epithelial cells (Weiser et al., 2003), whilst IgA-bound pneumococci facilitates evasion of complement and phagocytosis due to the absence of Fc domains (Bender and Weiser, 2006, Nakamura et al., 2011).

Table 2: Pneumococcal virulence factors that facilitate colonisation of the nasopharynx

Virulence factor	**Function**	**References**
PspA	Binds to lactoferrin to inhibit lactoferrin killing.	(Hammerschmidt et al., 1999)
Modified peptidoglycan	Prevents lysozymal-induced killing.	(Kovács et al., 2006)
Capsule	Prevents mucus entrapment; reduced expression enables surface proteins to bind to the host.	(Li et al., 2013)
Pneumolysin	Impairs mucociliary clearance.	(Kadioglu et al., 2002)
Hydrogen peroxide	Kills other bacteria competing for space in the nasopharynx.	(Pericone et al., 2000)
NanA, BgaA, StrH	Cleave terminal sialic acid residues from glycoconjugates.	(King et al., 2006)
PsaA	Binds to *N*-acetyl-glycosamine (GlcNAc) receptors.	(Blanchette et al., 2016)
CbpA (also referred to as PspC or SpsA)	Binds to polymeric immunoglobulin receptor.	(Rosenow et al., 1997)
ChoP	Binds to platelet-activating-factor receptors.	(Cundell et al., 1995a)
Enolase	Binds to plasminogen.	(Bergmann et al., 2001)
PavA, PavB	Binds to fibronectin.	(Holmes et al., 2001, Jensch et al., 2010)
IgA1 protease	Cleaves IgA antibody.	(Kilian et al., 1979)

1.9 The role of the capsule during pneumococcal colonisation and pathogenesis

Studies have highlighted that unencapsulated pneumococcal mutants possess greater adhesion properties and are more likely to form robust bacterial structures *in vitro* compared to encapsulated pneumococci (Waite et al., 2001, Moscoso et al., 2006, Allegrucci and Sauer, 2007, Muñoz-Elías et al., 2008, Qin et al., 2013). However, unencapsulated mutants in a mouse model are shown to be poor colonisers (Nelson et al., 2007); displaying reduced density and duration in comparison to encapsulated strains (Cundell et al., 1995b, Nelson et al., 2007). The prevailing theory is that unencapsulated pneumococci remain agglutinated within the mucus lining and are unable to reach the epithelial surface for stable colonisation. Therefore, capsule production is required for effective colonisation *in vivo* (Shainheit et al., 2014), but a thick capsule can act as a physical barrier and inhibit the attachment of cell-surface associated proteins to host cells (Hammerschmidt et al., 2005, Moscoso et al., 2006). Consequently, a minimum amount of capsule is a prerequisite for colonisation *in vivo* by evading mucus entrapment and facilitating efficient adhesion (Magee and Yother, 2001). Importantly, the capsule must then be fully recovered during invasive disease to protect against phagocytosis (López, 2006) and, as such, unencapsulated mutants have been found to be avirulent in animal models (Nelson et al., 2007). Taken together, *S.pneumoniae* must strive to find a balance of CPS production for effective nasopharyngeal colonisation and invasive disease.

To accomplish this, pneumococci undergo spontaneous and reversible phase variation in its CPS production, and transitions between a transparent and an opaque colony morphology (Weiser et al., 1994, Weiser et al., 1996). The transparent morphology is associated with a thinner capsule layer and high levels of cell wall teichoic acid and other adhesins, such as CbpA, while with the opaque morphology the reverse is true (Kim and Weiser, 1998). During colonisation in the nasopharynx, pneumococci shed their capsule (Hammerschmidt et al., 2005) and exhibit a transparent colony morphology to mediate enhanced binding to the mucosal epithelium (Weiser et al., 1994, Cundell et al., 1995b, Moscoso et al., 2006, Muñoz-Elías et al., 2008, Marks et al., 2012a, Marks et al., 2013). Therefore, during colonisation, pneumococcus increases its ability to adhere to epithelial cells at the expense of its invasive potential. In contrast, during IPD in mice and in humans, pneumococcus exhibits an opaque colony morphology with increasing amounts of CPS to confer greater resistance against opsonophagocytosis (Kim et al., 1999, Weiser et al., 2001).

1.10 Transition from asymptomatic colonisation to pneumococcal disease

The transition from pneumococcal carriage to the dissemination of free-living, planktonic bacteria and the onset of pneumococcal disease remains poorly understood. However, passive dispersal of planktonic cells from the nasopharynx may occur via shear forces in the host (i.e. air flow, sneezing, the cough reflex and the movement of mucus), which can then colonise new hosts or disseminate to new sites leading to pneumococcal disease. In addition, the progression from colonisation to infection has been strongly linked with a preceding or concomitant viral infection (McCullers, 2006, Bakaletz, 2010, Pettigrew et al., 2011, Launes et al., 2012, Chertow and Memoli, 2013, Short et al., 2013), with the same pneumococcal strains isolated from the nasopharynx and sites of pneumococcal disease in children and adults with a viral co-infection (Jansen et al., 2008, Peltola et al., 2011, Zhou et al., 2012).

The role of the influenza A virus (IAV) in pneumococcal disease has drawn particular interest. Co-infection with IAV promotes pneumococcal colonisation and increases susceptibility for pneumococcal pneumonia in humans and in animal models (Tong et al., 2000, García-Rodríguez and Fresnadillo Martínez, 2002, Diavatopoulos et al., 2010, Vu et al., 2011, Shrestha et al., 2013, McCullers, 2014, Wolter et al., 2014). IAV infection can predispose the nasopharynx for pneumococcal adherence by attenuating the mucociliary velocity of epithelial cells, whilst viral neuraminidase (NA) removes sialic acid residues from host cells which, along with pneumococcal NanA activity, can expose receptors for pneumococcal adherence (McCullers and Bartmess, 2003, Pittet et al., 2010). Furthermore, IAV neuraminidase activity increases the availability of sialic acid to enhance pneumococcal growth and density in an otherwise nutritionally-poor environment (Siegel et al., 2014).

To facilitate pneumococcal invasion, IAV invades and kills epithelial cells triggering the production of a localised anti-viral inflammatory response (Grebe et al., 2010). This immune response permits pneumococcal escape (Sun and Metzger, 2008), and is characterised with various host responses including, the release of adenosine triphosphate (ATP) and nutrients from injured epithelial cells, and an increase in body temperature (fever) (Weiser, 2010). Co-infection in mice has been shown to increase the density of pneumococcal colonisation through a synergistic increase in the levels of type I interferons in the nasopharynx, which inhibits the recruitment of macrophages and pneumococcal clearance (Nakamura et al., 2011).

1.11 The immune response to a bacterial infection

The human body possesses numerous physical and chemical barriers to protect against the entry of pathogenic microorganisms. However, once bacteria breach the anatomical barriers of the host they can invade the body by adhering to and crossing the mucosal epithelial surface in the respiratory, gastrointestinal or urogenital tract. The cell surface expression of different pattern recognition receptors (PRRs) on host cells enables the recognition of invariant bacterial antigens. These bacterial motifs are known as pathogen-associated molecular patterns (PAMPs), and allows epithelial cells and innate immune cells to recognise and discern between innocuous host cells (self-antigens) and foreign invaders (non-self antigens) (Janeway and Medzhitov, 2002). The most extensively studied PRRs are the Toll-like receptors (TLRs), which activate NFκB transcription factors that regulate the expression of pro-inflammatory cytokines and chemokines (Medzhitov et al., 1997). As a result of the pattern-recognition system, phagocytic cells known as macrophages and neutrophils can bind to, engulf and destroy bacteria, and subsequently release pro-inflammatory cytokines (TNF-α, IL-1, IL-6) and chemokines (CXCL8 and CCL2). These inflammatory mediators increase the permeability of blood vessels, recruit monocytes and neutrophils from the blood (chemotaxis) and cause extravasation of these leukocytes to the site of infection. This process is known as an inflammatory response. During phagocytosis a variety of toxins are produced to assist in killing engulfed bacteria including, antimicrobial peptides (defensins and cathelicidins), reactive nitrogen species (nitric oxide) and reactive oxygen species (hydrogen peroxide and superoxide anion), which is known as the respiratory burst. The same toxins may also be released into the extracellular environment causing toxicity to host cells and extensive tissue damage (Janeway and Medzhitov, 2002).

The inflammatory response can also be triggered by the complement system, which is comprised of a series of serum proteins that bind to bacteria (alternative pathway) and mark them for destruction after the deposition of the effector molecule, C3b. The coating of bacteria with complement (opsonisation) can induce bacterial cell lysis through the membrane attack complex, and also strongly enhance (complement) the binding of macrophages and neutrophils (opsonophagocytosis). Additionally, the release of TNF-α, IL-1 and IL-6 triggers the production of acute phase proteins from the liver, such as mannose binding lectin (MBL) and C-reactive protein (CRP). Acute phase proteins and natural antibody may also bind to bacteria and activate complement via the classical pathway (McGrath et al., 2006).

If the innate immune response cannot contain and resolve a bacterial infection, the adaptive arm of the immune response is triggered. Immature phagocytic dendritic cells are recruited to the site of infection, phagocytose bacteria and migrate as mature cells to lymphoid tissue where they act as an antigen presenting cell (APC) for naive T-cells. An activated T-cell triggers proliferation and induction of effector functions including, the enhanced production, extravasation and bactericidal activity of phagocytes, and the production of antigen-specific acquired antibodies through B-cell activation, which promotes opsonophagocytosis and activates complement (classical pathway).

1.12 The immune response to pneumococcal colonisation

As previously mentioned, an individual is typically only transiently colonised with pneumococcus. It has been shown in both human and mouse studies that colonisation with pneumococcus is an immunising event, activating both cell- and humoral-mediated immune responses, which protects against re-colonisation and invasive disease (McCool et al., 2002, Goldblatt et al., 2005, Malley et al., 2005, Zhang et al., 2006, Zhang et al., 2009, Richards et al., 2010, Cohen et al., 2011, Cohen et al., 2012, Ferreira et al., 2013, Wilson et al., 2015). The pattern recognition receptors (PRR) on epithelial cells, such as TLR2 and TLR4, recognise lipoteichoic acids and pneumolysin (Malley et al., 2003, van Rossum et al., 2005), while the cytosolic receptor known as nucleotide-binding oligomerisation domain (Nod) recognises lysozymal-induced digestion of pneumococcal cell wall peptidoglycan (Davis et al., 2011). Sensing of these pneumococcal components triggers the production of type I interferons and an inflammatory response (Davis et al., 2011, Parker et al., 2011).

Inoculation of mice with pneumococcus results in binding of the TLR2 receptor on epithelial cells, followed by intracellular signalling events and an infiltration of neutrophils. However, the infiltrate of neutrophils is insufficient for pneumococcal clearance. Instead, colonisation is only resolved after a gradual and prolonged increase in the recruitment of macrophages, which is reliant on $CD4^+$ T cells and IL-17 signalling (Zhang et al., 2009). Initially, it was believed that naïve $CD4^+$ T cells could be primed to differentiate into Th1 or Th2 lymphocytes characterised by the production of IFN-γ and IL-4. However, in 2005 it was discovered that $CD4^+$ T cells can also differentiate into a Th17 cell lineage characterised by the production of IL-17 (Curtis and Way, 2009). IL-17 secreting Th17 cells are essential for orchestrating an enhanced infiltration of monocytes/macrophages and neutrophils into the nasopharynx (Zhang et al., 2009).

Although acquired antibody is produced, it has been shown that clearance of pneumococcal colonisation is antibody-independent during primary exposure in mice, with antibody playing a limited role (McCool and Weiser, 2004, Malley et al., 2005, Trzciński et al., 2008, Zhang et al., 2009). In contrast, $CD4^+$ T cells and IL-17 are both indispensable for pneumococcal clearance from the nasopharynx (Malley et al., 2005, Lu et al., 2008, Zhang et al., 2009). However, duration of carriage upon re-colonisation in humans and in mice is reduced by both cell-mediated and humoral-mediated immune responses. The already primed $CD4^+$ T cells and IL-17 induces a quicker and more robust infiltration of phagocytes, while acquired antibody (mucosal and systemic) from prior colonisation is available to facilitate opsonophagocytosis (Zhang et al., 2009, Richards et al., 2010). Studies in humans and in mice have also revealed that the induced production of $CD4^+$ T cells, IL-17 and antibody from previous colonisation and clearance of pneumococcus protects against lung infection (Richards et al., 2010, Wright et al., 2013, Wilson et al., 2015). This protection is lost in the absence of either $CD4^+$ T cells or IL-17 (Wilson et al., 2015). In contrast, resolution of invasive disease after previous colonisation is unaffected by loss of $CD4^+$ T cells, but is dependent on antibody (Cohen et al., 2011). Thus, the site of secondary infection appears to dictate the nature of the immune response.

As a result of the development of serotype-specific anti-capsular antibodies in vaccinated individuals, it was presumed that natural immunity against IPD is reliant on anti-capsular antibody. However, it has been shown in both humans (McCool et al., 2002, Goldblatt et al., 2005, Zhang et al., 2006) and in mouse models (Richards et al., 2010, Cohen et al., 2011, Ferreira et al., 2013) that pneumococcal colonisation induces antibody production against various pneumococcal surface proteins as well. Moreover, a study in mice showed that human serum after experimental pneumococcal challenge confers protection against IPD in mice after invasive challenge with an alternative capsular serotype (Ferreira et al., 2013). In a similar study, depletion of only anti-capsular antibody had no detrimental effect on human immunoglobulin binding to pneumococcus, or inducing opsonophagocytosis or conferring protection against IPD in mouse models (Wilson et al., 2017). In comparison, binding of pneumococci was reduced after surface proteins were genetically removed. Additionally, there is epidemiological evidence that low anti-protein antibody levels correlates with an increased risk of middle ear infections in children (Kaur et al., 2011, Sharma et al., 2012). Collectively, the most current opinion is that anti-protein antibody appears to have the dominant role in naturally acquired immunity, protecting against both non-invasive and IPD in a serotype-independent manner.

1.13 Pneumococcal mechanisms of resistance against the immune system

A pneumococcal infection can trigger the recruitment and influx of neutrophils to the site of infection and rapid phagocytosis. Neutrophil-mediated phagocytosis is heavily opsonin-dependent (Yuste et al., 2008), with unopsonised pneumococcus relatively resistant to phagocytosis (Hyams et al., 2010). The importance of opsonin-dependent phagocytosis is underscored in persons with deficiencies in complement components, who suffer from susceptibility to pneumococcal pneumonia, septicaemia and meningitis (Jönsson et al., 2005, Yuste et al., 2008), with similar findings reported in mouse studies (Brown et al., 2002, Yuste et al., 2005, Rupprecht et al., 2007, Li et al., 2011). The classical complement pathway is triggered after natural or acquired antibody or acute phase proteins (e.g. CRP) bind to ChoP (Mold et al., 2002). These complexes result in the binding of C1q - the first component of the classical pathway - and eventual C3b deposition on the pneumococcal cell surface. The alternative pathway can be spontaneously activated after C3b binds directly to pneumococcus (Winkelstein and Tomasz, 1977).

1.13.1 The pneumococcal capsule

It has been shown that the pneumococcal capsule can confer resistance against complement by preventing the binding of complement (alternative pathway) and CRP (classical pathway) (Hyams et al., 2010). Furthermore, the capsule can directly inhibit the interaction between pneumococcus and anti-protein antibody (classical pathway), and with nonopsonic receptors on phagocytes such as mannose and scavenger receptors (Hyams et al., 2010). There is a close correlation between the extent of complement resistance and the propensity for invasive disease (Hyams et al., 2013). This association may account for the discrepancy seen between serotypes and invasive disease potential due to differences in capsular polysaccharides and capsule thickness (Kim and Weiser, 1998, Brueggemann et al., 2004, Weinberger et al., 2009). Indeed, Hostetter et al. identified serotype differences in the amount of complement deposition and the extent of bound C3b degradation (Hostetter, 1986). Finally, the pneumococcal capsule confers steric hindrance, which appears to prevent the Fc region of bound antibody and bound C3b complement component from interacting with specific receptors on phagocytes (Winkelstein, 1981, Musher, 1992).

1.13.2 Pneumococcal cell proteins

It has been discovered that pneumococcal cell wall proteins can also confer resistance to opsonophagocytosis. For instance, the surface level expression of PspA competes with CRP for binding to ChoP residues (Tu et al., 1999, Mukerji et al., 2012, Ren et al., 2012a). Additionally, a recent study suggests that the major autolysin, LytA, can also reduce the classical complement pathway by preventing the interaction of CRP with ChoP residues (Ramos-Sevillano et al., 2015). Similarly, CbpA facilitates increased binding to the negative regulator of the alternative complement pathway, factor H, preventing opsonisation (Dave et al., 2001, Walport, 2001, Jarva et al., 2002, Quin et al., 2005, Yuste et al., 2010). The extent of binding to factor H is serotype dependent and correlates with invasive disease potential (Yuste et al., 2010, Hyams et al., 2013). CbpA and enolase can also bind to the complement-inhibitory protein known as C4b-binding protein (C4BP), which inhibits the classical complement pathway by increasing the dissociation of complement components prior to C3b deposition (Dieudonné-Vatran et al., 2009, Agarwal et al., 2012). More recently, it has been revealed that LytA can increase the recruitment of factor H and C4BP to the pneumococcal cell wall and degrade complement components (Ramos-Sevillano et al., 2015). Moreover, pneumococcal exoglycosidases such as NanA can inhibit opsonophagocytosis by deglycosylating complement components (Dalia et al., 2010). Finally, in comparison to the aforementioned virulence factors, pneumolysin can promote the classical complement pathway but, crucially, this toxin is released extracellularly and facilitates complement evasion by activating the classical pathway from a distant site (Paton et al., 1984, Mitchell et al., 1991).

1.13.3 Neutrophil-mediated killing

The aforementioned mechanisms to inhibit opsonisation also serve to protect pneumococcus from phagocytosis by neutrophils. Neutrophils may kill bacteria by producing neutrophil extracellular traps (NETs), consisting of bactericidal fibres that contain deoxyribonucleic acid (DNA) (Brinkmann et al., 2004). However, pneumococcus can resist NET killing by repulsive forces that prevent entrapment (Wartha et al., 2007), and via the production of an endonuclease enzyme, EndA, which degrades the DNA of the NETs (Zhu et al., 2013). Pneumolysin can also impair the function of neutrophils by reducing chemotaxis, and inhibiting the respiratory burst and bactericidal activity of neutrophils (Paton and Ferrante, 1983).

1.14 Treatment of pneumococcal disease: vaccines and antibiotic therapy

Historically, pneumococcal infections have been treated with the antibiotic, penicillin. However, resistance to penicillin was first reported in the 1960s. The widespread overprescription and overuse of penicillin in the decades since has caused the development of penicillin-resistant pneumococcal strains (Butler et al., 1998, Nasrin et al., 2002), with pneumococcus also showing an increasing resistance to alternative β-lactam antibiotics and even non-β-lactam antibiotics (Musher, 1992, Tomasz, 1995, Chen et al., 1999, Davidson et al., 2002, Nasrin et al., 2002).

Currently, the first-line antibiotic treatment for pneumococcal infections is amoxicillin, especially in the case of otitis media. However, with infections that are refractory to this antibiotic, amoxicillin is frequently prescribed alongside clavulonic acid (also known as co-amoxiclav) or with azithromycin, as a course of second-line therapy (Harmes et al., 2013). The increasing prevalence of antibiotic-resistant *S. pneumoniae* is highlighted by the global emergence of non-susceptible pneumococcus in both carriage and disease isolates (Cho et al., 2014, Kumar et al., 2014, Lee et al., 2014). The high morbidity and mortality caused by pneumococcal disease, and the increasing prevalence of antibiotic resistant pneumococcal cases, necessitated the urgent need to prevent pneumococcal infections via immunisation.

1.15 Pneumococcal vaccines

There are currently two different types of pneumococcal vaccine (Table 3). The pneumococcal polysaccharide vaccine (PPV) consists of purified capsular polysaccharide antigen from 23 different serotypes of pneumococci (PPSV23). In contrast, pneumococcal conjugate vaccines (PCV) consist of purified capsular polysaccharide antigen from multiple different serotypes conjugated to a nontoxic form of a diphtheria toxin.

Table 3: Serotypes included in licensed pneumococcal vaccines

Vaccine	**Serotypes covered**	**Manufacturer**	**Year of licensure**	**References**
23-valent polysaccharide (PPSV23)	1, 2, 3, 4, 5, 6A, 7F, 8, 9N, 9V, 10A, 11A, 12F, 14, 15B, 17F, 18C, 19A, 19F, 20, 22F, 23F, and 33F.	Merck and Co	1983	(Daniels et al., 2016)
7-valent pneumococcal conjugate vaccine (PCV7)	4, 6B, 9V, 14, 18C, 19F, 23F.	Wyeth (now Pfizer)	2000	
10-valent pneumococcal conjugate vaccine (PCV10)	1, 4, 5, 6B, 7F, 9V, 14, 18C, 19F and 23F.	GlaxoSmithKline	2009	
13-valent pneumococcal conjugate vaccine (PCV13)	1, 3, 4, 5, 6A, 6B, 7F, 9V, 14, 18C, 19A, 19F, 23F.	Pfizer	2010	

1.15.1 The pneumococcal polysaccharide vaccine (PPSV23)

In 1983, a serotype-specific 23-valent pneumococcal polysaccharide vaccine (PPSV23) was licensed in the United States. Although the PPSV23 vaccine did not confer protection from pneumococcal disease caused by non-vaccine serotypes, the 23 vaccine-type serotypes accounted for 85% of IPD cases at the time (Robbins et al., 1983). The PPSV23 vaccine was recommended for anyone above the age of two years with an increased risk of IPD (section 1.7) and healthy persons above the age of 64.

The PPSV23 vaccine was successful in reducing prevalence of IPD. For example, the PPSV23 vaccine was 50-70% effective in preventing pneumococcal bacteraemia in persons older than 2 years of age (Fedson, 1999, Melegaro and Edmunds, 2004). However, epidemiological studies comparing the patterns of pneumococcal carriage before and after the introduction of the PPSV23 vaccine did not show a clinically significant decrease in carriage rates among those that were vaccinated (Herva et al., 1980). This observation was due to the PPSV23 vaccine not inducing mucosal immunity. Consequently, the vaccine did not affect asymptomatic colonisation, protect individuals from non-invasive infections, such as otitis media, or protect unvaccinated individuals from pneumococcal transmission (Rubin, 2000).

1.15.2 Pneumococcal conjugate vaccines

The PPSV23 vaccine was proven to be ineffective in children less than 2 years of age due to an inability to develop effective antibody responses (Fedson, 1999). Therefore, in 2000, a pneumococcal conjugate vaccine (PCV) was licensed in the United States to cover the 7 serotypes most commonly found in cases of IPD (Table 3). The PCV7 vaccine was effective in triggering a more robust immune response in a T-cell dependent manner. Specifically, B-cells bind and internalise the polysaccharide-diphtheria toxin complex and activate the recruitment of type 2 helper T-cells, which induces humoral immunity through the production of antibodies and the generation of memory B-cells. The PCV7 vaccine also induced mucosal immunity, enabling clearance of vaccine-type serotypes from asymptomatic carriers to eradicate colonising pneumococci (Table 4). Thus, non-vaccinees are protected as pneumococcus is unable to circulate in the population. This phenomenon is known as herd immunity.

Studies in the United States and in the United Kingdom revealed that PCV7-vaccine-type IPD and non-invasive pneumococcal disease decreased in all age groups (Miller et al., 2011, Richter et al., 2013). These dramatic results, alongside a significant increase in the prevalence of non-vaccine serotypes causing IPD, resulted in the licensure of a 10-valent

vaccine (PCV10) in 2009, followed by a 13-valent pneumococcal conjugate vaccine (PCV13) being approved in 2010. In addition to the 7 serotypes of the PCV7 vaccine, the PCV13 vaccine included a further 6 different pneumococcal serotypes/groups, which were collectively accountable for over 70% of global IPD (Webster et al., 2011) (Table 3).

Table 4: Advantages and disadvantages of the PPSV and PCV vaccines

Vaccine	**Advantages**	**Disadvantages**	**References**
PPSV	A large number of vaccine-type serotypes covered.	No mucosal immunity.	(Robbins et al., 1983)
		Carrier rates not affected.	(Herva et al., 1980)
		No protection from non-invasive pneumococcal infections.	(Rubin, 2000)
		Herd immunity is not induced.	
Vaccine	**Advantages**	**Disadvantages**	
PCV	Mucosal immunity is induced.	A smaller number of vaccine-type serotypes covered.	(O'Brien et al., 2007)
	Reduction in carriage rates.		(Simell et al., 2012)
	Confers some protection from non-invasive pneumococcal infections.		
	Herd immunity occurs.		

PPSV, pneumococcal polysaccharide vaccine; PCV, pneumococcal conjugate vaccine.

1.16 The direct and indirect effects of pneumococcal conjugate vaccines

PCVs have caused a reduction in pneumococcal carriage of vaccine-type serotypes (Käyhty et al., 2006, O'Brien et al., 2007, Tocheva et al., 2010, Tocheva et al., 2011, Fleming-Dutra et al., 2014). As pneumococcal carriage always precedes pneumococcal disease (Bogaert et al., 2004, Simell et al., 2012), the advantages of a decrease in carriage are two-fold. Firstly, vaccinees are provided with direct protection against pneumococcal disease (direct effect). Secondly, widespread vaccination reduces transmission, carriage and subsequent pneumococcal disease in unvaccinated persons (indirect effects) (O'Brien et al., 2007, Simell et al., 2012). The PCVs have also had a significant impact in decreasing IPD caused by serotypes covered in the vaccines (Whitney et al., 2003, Whitney et al., 2006, Pilishvili et al., 2010a, Conklin et al., 2014, Harboe et al., 2014). By reducing IPD and pneumococcal carriage, the PCVs have caused a reduction in the requirement for prescribing and using antibiotics, limiting the development of antibiotic resistance.

Importantly, pneumococcal carriage of vaccine-type serotypes can only be reduced through immunisation with the PCVs and not completely eradicated. Consequently, carriage and transmission of vaccine-type serotypes continues in the population, especially in regions where widespread immunisation cannot be achieved. Furthermore, despite the success of the PCVs in significantly reducing IPD and carriage by vaccine-type serotypes, there has been an increase in carriage and in pneumococcal disease by non-vaccine serotypes in the population (Hicks et al., 2007, Muñoz-Elías et al., 2008, Millar et al., 2010, Tocheva et al., 2010, Flasche et al., 2011, Tocheva et al., 2011, Weinberger et al., 2011, Levy et al., 2014). This phenomenon is known as serotype replacement, and can result from vaccine-type pneumococci acquiring the capsule of a non-vaccine serotype or, more commonly, the expansion of existing non-vaccine serotypes in the population (Coffey et al., 1998, Pai et al., 2005, Wyres et al., 2013, Balsells et al., 2017).

Serotype replacement has undermined the effectiveness of the conjugate vaccines as the overall prevalence of all pneumococcal serotype carriage has remained unaffected (Hammitt et al., 2006, Millar et al., 2006, O'Brien et al., 2007, Sá-Leão et al., 2009, Cohen et al., 2010, Flasche et al., 2011). Additionally, the selective pressure of the PCV vaccines and continuation of antibiotic misuse can result in the emergence of more virulent serotypes (Porat et al., 2004, Temime et al., 2005). However, the invasive disease potential of the majority of non-vaccine serotypes is inferior to vaccine-type serotypes (Flasche et al., 2011), and this potential appears to be unaffected by time or the introduction of the vaccine (Scott et al., 2012). Therefore, the potential of colonising non-vaccine serotypes to cause

IPD in the population is less likely than the potential of colonising vaccine-type serotypes to cause IPD in unvaccinated persons.

1.17 Biofilms – a structured, complex community of bacterial cells

In addition to existing as free-living, planktonic cells, bacteria can also aggregate and grow on an abiotic (inert) or biotic (living) surface. Sessile and aggregated bacteria are known as biofilms (Costerton et al., 1999, Donlan and Costerton, 2002). Unlike single, planktonic bacteria, a biofilm is a community of bacterial cells that are enclosed in a self-produced extracellular polymeric substance (EPS), comprised of polysaccharides, proteins, lipids and extracellular DNA (eDNA) (Flemming and Wingender, 2010). It is now widely acknowledged that the biofilm lifestyle is the predominant mode of growth for bacteria (Hall-Stoodley et al., 2004).

Biofilm formation is environmentally driven and significantly increases bacterial survival during unfavourable conditions. As a result, biofilms are inherently more tolerant to antibiotic treatment (Costerton et al., 1999, Lewis, 2001, Stewart and Costerton, 2001, Parsek and Singh, 2003, Lewis, 2008, Høiby et al., 2010a), and to the host innate and adaptive immune responses (Donlan and Costerton, 2002).

1.18 The clinical impact of biofilms

Surface-attached bacteria were first observed in 1684 by Antonie van Leeuwenhoek, who described the presence of animals (“animiculae”) in the plaque on his teeth. However, it was not until the late 1970s when publications in the medical field began to acknowledge the existence of clumps of bacteria, and it was not until the 1980s that the pathogenic role biofilms play during persistent infections was described, with Costerton et al. using the term biofilm for the first time in 1981 (McCoy et al., 1981, Costerton et al., 1999). The American Society of Microbiology recognised the microbiological relevance of biofilm growth in 1993 (Costerton et al., 1994). In the intervening years, the importance of biofilms has become increasingly apparent, with the amount of literature on the subject matter increasing exponentially (Figure 1.3).

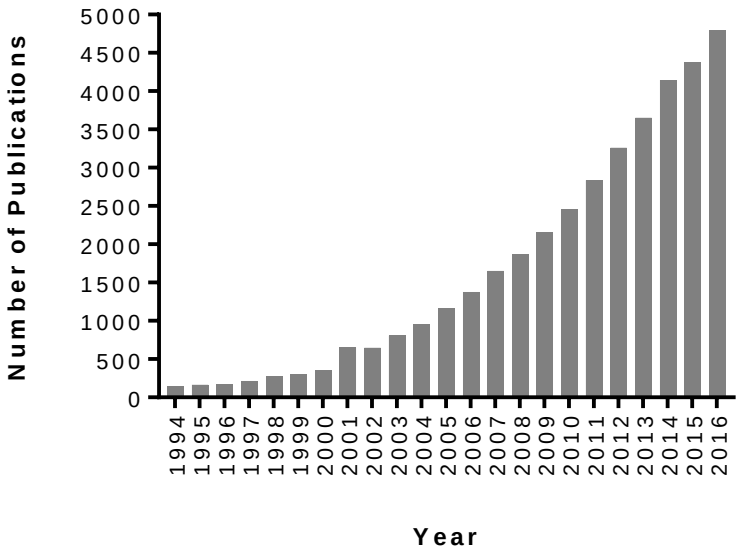

Figure 1.3: Biofilm publications from 1994 to 2016.

CSV data from PubMed was used to generate the graph. The search term 'biofilm' was used.

Biofilms are of enormous importance in medicine as they contribute to persistent infections (Hall-Stoodley and Stoodley, 2009, Høiby et al., 2011). Biofilms are responsible for a range of infections, such as cystic fibrosis-related lung infection (Høiby et al., 2010b), wound infections (Percival et al., 2012), otitis media (Hall-Stoodley et al., 2006), sinusitis (Jain and Douglas, 2014, Sanderson et al., 2006) and endocarditis (Høiby et al., 1986) (Figure 1.4). It is estimated that in excess of 60% of all human bacterial infections, and up to 80% of chronic infections, are attributed to bacterial growth in the form of a biofilm (Costerton et al., 1999, Potera, 1999, Wolcott and Ehrlich, 2008).

Biofilms also have a high propensity for contaminating numerous medical devices including, catheters (Tran et al., 2012), prosthetic heart valves (Donlan, 2001), joint prostheses (Song et al., 2013), cardiac pacemakers (Santos et al., 2011), intrauterine devices (Auler et al., 2010), dentures (Murakami et al., 2015) and contact lenses (Abidi et al., 2013) (Figure 1.4). The US Centres of Disease Control and Prevention (CDC) estimates that biofilms are responsible for more than 65% of hospital, healthcare-associated (nosocomial) infections (Percival et al., 2012).

Taken together, substantial economic costs are annually accrued by medical biofilms due to their high frequency, the prevalence of treatment failure and the necessity to often

remove an infected foreign body (Francolini and Donelli, 2010, Høiby et al., 2011, Römling and Balsalobre, 2012).

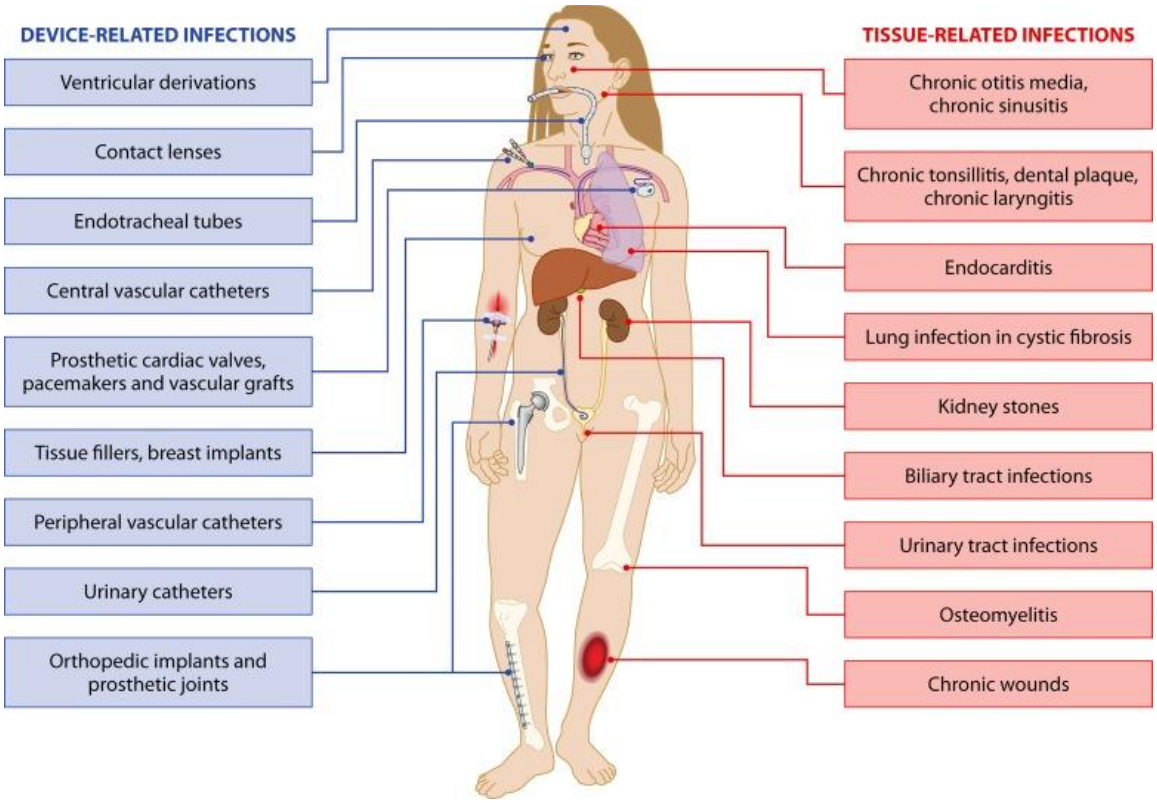

Figure 1.4: Biofilm-associated tissue-related and device-related infections.

A partial list of biofilm-associated infections, which affect many different regions of the human host. Image taken from Lebeaux et al. (Lebeaux et al., 2014).

1.19 The life cycle of a bacterial biofilm

The biofilm life cycle (Figure 1.5) is regarded as a dynamic process consisting of sequential but separate stages (Costerton et al., 1999, O'Toole et al., 2000, Hall-Stoodley et al., 2004): (i) individual planktonic bacteria attach to the surface of a foreign body or tissue. At this stage, bacteria remain susceptible to antibiotics and can be sloughed off due to shear forces; (ii) irreversible binding to the surface leads to an aggregation of cells to form microcolonies, with typically mushroom- or tower-like structures *in vitro.* Cell division enables further recruitment and binding of other planktonic cells; (iii) a mature biofilm begins to emerge: the self-produced EPS forms (Flemming and Wingender, 2010), water channels intersperse bacterial clusters to facilitate circulation of nutrients and oxygen and the removal of waste products (Stoodley et al., 1994), and cell-to-cell communication (quorum sensing) begins to regulate numerous physiological processes (Davies et al., 1998). At this stage, recalcitrance of a biofilm to antibiotics and the immune system is at its greatest; (iv) individual bacterial cells are shed from the biofilm. Dispersal from a biofilm enables propagation to new sites and subsequent colonisation and formation of a new biofilm (O'Toole et al., 2000, Hall-Stoodley and Stoodley, 2005).

The life cycle and recalcitrance of a biofilm ensures that a biofilm-associated infection is typically chronic or recurrent, characterised by persistent inflammation and tissue damage. Although conventional antibiotics and/or host defences can control the acute infection caused by the intermittent dispersal of planktonic cells, the biofilm itself is not eradicated (Costerton et al., 1999). To determine if an infection is biofilm-associated, diagnostic criteria have been proposed: (i) the presence of aggregated cell clusters; (ii) association with a surface (i.e. a medical device or the mucosal epithelium); (iii) the presence of an EPS; (iv) recalcitrance to antibiotics and host clearance; (v) culture-negative samples, despite the detection of live bacteria and the presence of innate immune cells, such as macrophages and neutrophils (Hall-Stoodley and Stoodley, 2009).

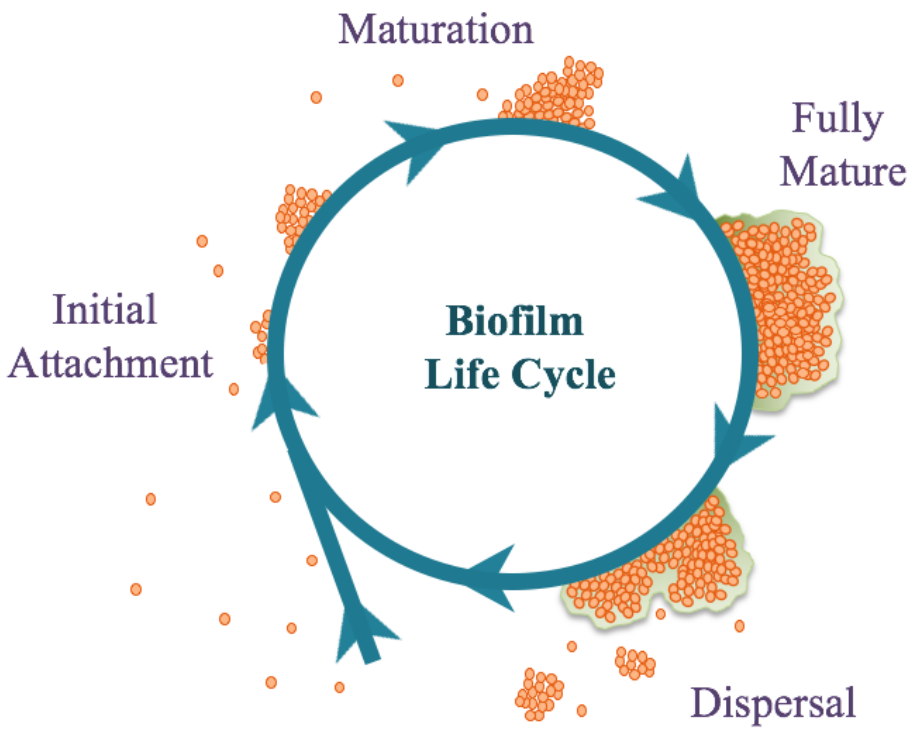

Figure 1.5: The life cycle of a biofilm in the human host.

For initial attachment, bacteria adhere to the epithelial cell surface and irreversibly bind through the interaction of bacterial surface proteins and mammalian cell receptors. Further bacterial attachment ensures the development of microcolonies, the start of intercellular communication and the emergence of an extracellular polymeric substance, as a mature biofilm begins to form. Individual cells of the biofilm are shed, enabling dispersed cells to attach to the host at new sites to form a new biofilm.

1.20 Pneumococcal biofilm formation in the human host

Recent studies have identified the presence of *S. pneumoniae* biofilms *in vivo* on the human middle ear epithelial mucosa of children undergoing treatment for recurrent or chronic otitis media (COM) (Hall-Stoodley et al., 2006), as well as on the mucosa of adenoids (Hoa et al., 2009, Nistico et al., 2011), and on the sinus mucosa of patients with chronic rhinosinusitis (Sanderson et al., 2006). Pneumococcal biofilms have also been observed in a chinchilla animal model of otitis media (Reid et al., 2009). These studies demonstrate two hallmarks of biofilms: evasion of the host immune response (Donlan and Costerton, 2002) and increased recalcitrance to antibiotics (Costerton et al., 1999, Lewis, 2001, Stewart and Costerton, 2001, Parsek and Singh, 2003, Lewis, 2008, Høiby et al., 2010a).

In vitro studies have shown that, unlike planktonic bacteria, the cells in a biofilm are significantly more tolerant to antibiotic treatment (Hall-Stoodley et al., 2008, del Prado et al., 2010, Sanchez et al., 2011b, Marks et al., 2012a, Vandevelde et al., 2014), and that while *in vivo* treatment eradicates planktonic bacteria at the site of infection, bacteria in the nasopharynx are commonly more persistent (Cohen et al., 1997, Dabernat et al., 1998, Dagan et al., 1998, Cohen et al., 1999, Varon et al., 2000). As previously mentioned, although colonisation of the nasopharynx always precedes pneumococcal disease (Bogaert et al., 2004, Simell et al., 2012), carriage is typically asymptomatic. Taken together, although there is a paucity of knowledge concerning how *S. pneumoniae* colonises and persists in the human nasopharynx, the recent literature strongly suggests that pneumococcal biofilm formation plays a key role.

Biofilms of pneumococcus and other middle ear pathogens were found on adenoids in children prone to COM (Hoa et al., 2009), which supports the argument that biofilm communities can act as a reservoir for the dispersal of planktonic cells to cause pneumococcal disease (Nistico et al., 2011). It has also been shown that pneumococcus forms highly structured biofilms during nasopharyngeal colonisation in mice (Marks et al., 2012a, Blanchette-Cain et al., 2013). Colonisation in the form of a biofilm provides an insight into how pneumococcus can persist in the nasopharynx for greater longevity, but also be able to transmit to a new host or disseminate to cause overt infection (Hall-Stoodley and Stoodley, 2005).

1.21 Ultrastructure of a pneumococcal biofilm

Unencapsulated *S. pneumoniae* grown on abiotic surfaces, such as glass and polystyrene, revealed that pneumococcus forms complex three-dimensional biofilms. Confocal laser scanning microscopy (CLSM) was used to visualise the depth and spatial distribution of adherent pneumococci after forming a biofilm. CLSM identified structures that were between 25-30μm thick, in addition to the presence of small voids interspersing pneumococcal aggregates, and a heterogenic population of live and dead cells (Moscoso et al., 2006). Additionally, scanning electron microscopy (SEM) revealed pneumococcal microcolonies were in the form of a honeycomb-like structure, and the existence of fibre-like material linking pneumococcal cells to each other and to the self-produced EPS (Moscoso et al., 2006).

The EPS of a biofilm acts as a scaffold for the embedded bacterial cells and has many roles: providing structure and cohesion to the community; contributing to the resistance against antibiotics and host defenses; permitting circulation of nutrients and oxygen and the removal of waste-products; and facilitating cell-to-cell communication (quorum sensing) and horizontal gene transfer between cells (Domenech et al., 2012).

Extracellular DNA (eDNA) is a significant constituent of the matrix, playing a key role in the formation and maintenance of biofilms (Whitchurch et al., 2002, Moscoso et al., 2006, Rice et al., 2007, Qin et al., 2007, Jurcisek and Bakaletz, 2007). eDNA is released upon pneumococcal cell death (autolysis) and confers structural integrity for the biofilm by enabling individual pneumococcal cells to adhere to one another and by enhancing adhesion to epithelial cells. The use of DNA degrading enzymes, such as DNase I, have been found to significantly inhibit or disintegrate pneumococcal biofilms *in vitro*, which underscores the importance of eDNA for biofilm growth (Moscoso et al., 2006, Hall-Stoodley et al., 2008).

1.22 Intercellular communication in pneumococcal biofilms

Transformation is the ability of bacteria to uptake foreign DNA and incorporate genetic material into chromosomal DNA. This genetic exchange (horizontal gene transfer) is known as competency and is regulated by quorum sensing (QS). QS is a population density-dependent system that relies on the production of small, diffusible signalling molecules (autoinducers). These autoinducers bind to specific receptors on other bacterial cells in the local environment (von Bodman et al., 2008). In pneumococcus, the

autoinducer is a pheromone called competence-stimulating peptide (CSP), which is regulated by the *ComC* gene (Håvarstein et al., 1995).

The increase in cell number within a biofilm community correlates with an increase in the extracellular concentration of CSP. Once a threshold concentration is reached, a profound and co-ordinated change in gene expression is triggered at the population level. Specifically, CSP binds to the membrane bound ComD, a histidine kinase that phosphorylates the response regulator, ComE. Phosphorylated ComE binds to a promoter to induce the expression of approximately 20 early competence genes. The product of one of these genes, ComX, activates the expression of more than 80 late competence genes. Together, these genes facilitate DNA uptake and homologous recombination (Kowalko and Sebert, 2008, Moscoso et al., 2009, Vidal et al., 2013).

One of the physiological processes governed by QS is the production of the EPS. Cell death (autolysis) of pneumococcal cells results in the release of eDNA, which facilitates bacterial aggregation and confers structural integrity for the biofilm (Moscoso et al., 2006, Hall-Stoodley et al., 2008). Investigations have demonstrated that the pneumococcal cell wall murein hydrolases LytA, LytC and CbpD are responsible for autolytic eDNA release (Moscoso and Claverys, 2004). In addition to autolytic eDNA, pneumococci can lyse non-competent pneumococcal cells via LytA and CbpD in a process known as “microbial fratricide”, to provide an essential source of eDNA that can be taken up by competent pneumococcal cells (Steinmoen et al., 2002, Moscoso and Claverys, 2004, Guiral et al., 2005, Håvarstein et al., 2006, Claverys and Håvarstein, 2007, Claverys et al., 2007, Eldholm et al., 2009, Montanaro et al., 2011, Wei and Håvarstein, 2012). This competence-induced lysis of a subset of pneumococcal cells ensures that biofilm growth is associated with a close network of pneumococcal cells and an EPS containing copious amounts of eDNA, which acts as an excellent source for genetic exchange (Steinmoen et al., 2002, Wei and Håvarstein, 2012).

It has been discovered that the majority of cells in a pneumococcal biofilm are transparent phase variants, and a significant proportion of the community is non-viable (Sanchez et al., 2011b). Taken together, it is proposed that fratricide of opaque phase variants provides eDNA for enhancing the persistence of the biofilm, whilst the larger numbers of transparent phase variants can facilitate efficient adherence to epithelial cells *in vitro* and effective colonisation in the nasopharynx *in vivo* (Sanchez et al., 2011b).

In addition to CSP-mediated transfer of genetic material, *S. pneumoniae* possesses another signalling molecule known as autoinducer-2 (AI-2). AI-2 is biosynthesised by the *luxS* gene, which is conserved in most Gram-positive and Gram-negative bacteria (Schauder et al., 2001). *LuxS*-mediated QS is closely associated with competence, EPS

production and enhancing the efficiency of genetic exchange by promoting microbial fratricide (Trappetti et al., 2011, Wei and Håvarstein, 2012), while mouse studies have shown that *luxS* is required for persistent pneumococcal nasopharyngeal colonisation and for pneumococcus to spread effectively to the lungs and the bloodstream (Stroeher et al., 2003, Joyce et al., 2004). Therefore, both CSP and AI-2 signalling networks regulate the expression of genes required upon the transition to the biofilm mode of growth, with Vidal et al. showing that *luxS* and *ComC* are indispensable for early pneumococcal biofilm formation on epithelial cells as determined by biomass (Vidal et al., 2011, Vidal et al., 2013).

1.23 Biofilm growth enhances pneumococcal fitness

It has been demonstrated that several factors contribute towards providing the optimal conditions for transformation: the presence of oxygen, a low concentration of ions and nutrients and a temperature between 30-34°C (Chen and Morrison, 1987, Trombe, 1993, Echenique et al., 2000). The same optimal conditions for efficient transformation are found in the nasopharynx. Epidemiological studies suggest that nasopharyngeal colonisation, rather than invasive disease, is the driving force for horizontal gene transfer due to high carriage rates and environmental stress including, these suboptimal conditions for growth, and exposure to vaccines, antibiotics and the immune system (Dowson et al., 1989, Coffey et al., 1991, Coffey et al., 1998, Ding et al., 2009, Domenech et al., 2009, Croucher et al., 2011).

As pneumococcus may colonise as a biofilm, recent studies have examined the extent of DNA transformation in biofilms. Compared with broth-grown bacteria, biofilms have been shown to upregulate competence genes and have a much higher rate of transformation (Oggioni et al., 2006, Trappetti et al., 2011, Marks et al., 2012b, Wei and Håvarstein, 2012). The importance of competence for biofilm formation was demonstrated *in vitro* whereby competence mutants failed to form a biofilm on abiotic surfaces (Trappetti et al., 2011). In comparison to planktonic bacteria, pneumococcal cells in a biofilm downregulate capsule production when grown on abiotic and biotic surfaces, with this phenotypic change more pronounced during growth on epithelial cells (Hammerschmidt et al., 2005, Hall-Stoodley et al., 2008, Marks et al., 2012b). In fact, it has been shown that capsule deficient mutants form the most robust biofilms *in vitro* (Moscoso et al., 2006, Qin et al., 2013). As capsule production is inversely proportional to transformation efficiency (Ravin, 1959), biofilm formation during nasopharyngeal colonisation may provide the optimal environment for genetic exchange due to the transition to the transparent phase variant.

The rate of transformation *in vitro* has been found to be higher during biofilm growth on fixed epithelia than on an abiotic surface (Marks et al., 2012b).

Horizontal gene transfer is vital for adapting to environmental stress and increasing the fitness of pneumococci. In the nasopharynx, pneumococcus is exposed to a higher concentration of oxygen that can lead to DNA damage. Oxidative stress may also occur via leukocytes and antibiotics that can induce oxidative damage due to reactive oxygen species (ROS) (Kohanski et al., 2010). As unrepaired DNA damage can be lethal to a cell, damages must be quickly and efficiently repaired. One of the genes expressed during pneumococcal competence is *recA*, which is essential for homologous recombination and DNA repair (Mortier-Barrière et al., 1998). Interestingly, the major autolysin gene, *lytA*, is also induced by the same operon (Lewis, 2000), suggesting that fratricide is an adaptation for overcoming oxidative stress in the nasopharynx.

The nasopharynx can be colonised with multiple pneumococcal strains either at the same time or sequentially. A few studies have shown that 9-49% of individuals colonised with pneumococcus had two or more strains, with some individuals colonised with up to six different strains (Brugger et al., 2009, Donkor et al., 2011, Leung et al., 2011). Future intraspecies co-colonisation studies may reveal even higher carriage rates due to advancements in culture-independent detection techniques (Turner et al., 2011). In addition to co-colonisation increasing the density of pneumococcal carriage and the likelihood of pneumonia (Brugger et al., 2010, Albrich et al., 2012), co-colonisation is clinically relevant as the extensive pool of eDNA (due to fratricide of non-competent cells) can be reciprocally shared between different pneumococcal strains (Wei and Håvarstein, 2012). Significant genetic transfer has been found among multiple pneumococcal strains in a study of chronic otitis media (Hiller et al., 2011), and the rate of transformation between pneumococcal strains was revealed to be much higher during biofilm growth compared to planktonic pneumococci in a mouse model and *in vitro* (Marks et al., 2012b). Interspecies co-colonisation, such as between *M. catarrhalis* or *H. influenzae* and *S. pneumoniae* has shown to confer pneumococcal resistance against antibiotics both *in vitro* and in animal models (Weimer et al., 2011, Perez et al., 2014). This resistance may help to explain otitis media (OM) cases that are refractory to antibiotic treatment, since OM is frequently a polymicrobial biofilm-associated infection (Hall-Stoodley et al., 2006).

Finally, the capsule locus of the pneumococcus is flanked by genes which code for proteins that are targets for β-lactam antibiotics (Trzciński et al., 2004). As a result of selection pressure from host defences and antibiotics, pneumococcus can change its serotype (serotype switching) via changes in capsule genes and also alter its antibiotic resistance profile through homologous recombination at the same time. Serotype switching

has been found in paediatric carriage strains in Gambia (Donkor et al., 2011), and transfer of genetic material to facilitate antibiotic resistance has been observed in mice and *in vitro* (Marks et al., 2012b).

1.24 Pneumococcal biofilms subvert the immune response

Pneumolysin has been shown to play an important role in biofilm formation (Shak et al., 2013a). However, normal pneumolysin expression can cause tissue damage and initiate full-scale inflammation, which would presumably promote pneumococcal clearance (Orihuela et al., 2004, Mitchell and Dalziel, 2014). The profound difference between the inflammatory response during colonisation and during an acute infection, suggests that pneumococcus modifies its interaction with the host. Consequently, it is believed that in a similar way to the pneumococcal capsule, pneumococcus finely controls the expression of pneumolysin, to mediate initial attachment and persistence in an immunoquiescent host.

1.24.1 Evading opsonophagocytosis

Recent studies have revealed numerous mechanisms that a pneumococcal biofilm may deploy to facilitate persistent colonisation *in vivo*. For example, Domenech et al. demonstrated that the binding of the acute-phase protein, CRP, was significantly reduced on pneumococcal biofilms in comparison to planktonic cultures (Domenech et al., 2013). This limitation of the classical complement pathway has been attributed to the biofilm-associated enhanced surface level expression of PspA, which competes with CRP in the binding of ChoP (Mukerji et al., 2012).

Domenech et al. also measured the *in vitro* surface deposition of the key complement component C3b on pneumococcal biofilms compared to planktonic cultures. Although pneumococcal cells in an *in vitro* or *in vivo* biofilm are predominantly of the transparent phase variant (Sanchez et al., 2011b), C3b coated only very small areas of a pneumococcal biofilm. In contrast, C3b coated the entire bacterial surface of the planktonic cultures. Limited recognition of pneumococcal biofilms by C3b was attributed to the increased surface expression of CbpA and an enhanced recruitment of factor H, the negative regulator of the alternative complement pathway (Domenech et al., 2013).

Finally, it has been demonstrated that, in the absence of opsonising complement, the extent of phagocytosis by human neutrophils of a pneumococcal biofilm is significantly reduced and, compared to planktonic bacteria, the level of phagocytosis is impaired even in the presence of complement (Domenech et al., 2013). Consequently, similar to other

bacteria, such as *S. aureus*, pneumococcal biofilms are more resistant to opsonophagocytosis than planktonic cells (Cerca et al., 2006, Thurlow et al., 2011).

Taken together, despite an increase in bacterial aggregate size recently found to correlate with an enhanced agglutinating effect of antibody and an increase in complement deposition and subsequent opsonophagocytosis (Dalia and Weiser, 2011), a pneumococcal biofilm is able to limit the surface deposition of acute phase proteins, complement and natural and acquired antibody. These biofilm-associated mechanisms of impaired activation and enhanced downregulation of the classical and alternative complement pathways have a direct inhibitory effect on the activation of an inflammatory response, the efficacy of phagocytosis and the onset of an adaptive immune response.

1.24.2 The role of the extracellular matrix

In addition to providing structural integrity and cohesion, the EPS of a pneumococcal biofilm may also contribute to the enhanced protection against complement, antibody and phagocytes. Studies with other bacteria have shown that species-specific acquired antibody fail to penetrate the EPS and activate complement (Fux et al., 2005). Therefore, it is conceivable that the matrix may prevent nasopharyngeal clearance of *S. pneumoniae*. Additionally, due to the constituents and complexity of the EPS the matrix may mask immunogenic pneumococcal proteins. The inclusion of host molecules in the EPS, such as factor H, C4BP and degraded complement components, may result in a pneumococcal biofilm being perceived as containing innocuous self-antigens (Blanchette and Orihuela, 2012).

1.24.3 Promoting the expansion and activation of regulatory T-cells

In the absence of infection, regulatory T cells (Tregs) suppress the activation of immune responses via the production of the anti-inflammatory cytokines TGF-β and IL-10, which also prevents the development of autoimmunity. Studies have shown that Treg numbers are greatly increased at mucosal sites in patients with human immunodeficiency virus (HIV), but Treg numbers in the blood are similar with those found in healthy controls, suggesting that the persistent presence of antigen in local tissues can promote the expansion of Treg cells (Andersson et al., 2005, Epple et al., 2006). A recent study by Zhang et al. revealed that pneumococcal carriage in children is associated with an increase in the number of Treg cells in adenoid tissue and the amount of IL-10, which may be contributing to the delayed clearance or persistence of pneumococcus in children (Zhang et al., 2011). Future research may focus on whether Treg cells preferentially recognise

biofilm pneumococci over planktonic cells, to help to explain why a robust immune response is suppressed during biofilm colonisation with any species of bacteria.

1.25 Pneumococcal biofilms are hyper-adhesive but less invasive

Since biofilm-associated infections are recalcitrant to antibiotics and the immune response, it was believed that biofilms were highly invasive. However, isolates of pneumococcus from the bloodstream appear as lancet-shaped diplococci (Tomasz et al., 1964), which is the same morphology as broth-grown planktonic pneumococcus, and have been shown to rapidly invade and kill epithelial cells *in vitro* (Blanchette-Cain et al., 2013). In contrast, pneumococcal biofilms are detected on adenoids and in the middle ear (Hall-Stoodley et al., 2006, Hoa et al., 2009, Nistico et al., 2011). As previously mentioned, although pneumococcal mutants lacking capsular polysaccharide demonstrate enhanced biofilm formation (Moscoso et al., 2006, Marks et al., 2012a, Qin et al., 2013), they are avirulent *in vivo* as they are unable to prevent opsonophagocytosis in the bloodstream (Hyams et al., 2010, Melin et al., 2010). In contrast, invasive strains are encapsulated. Due to this discordance between *in vitro* biofilm formation and IPD *in vivo*, it was suggested that the biofilm mode of growth is avirulent in comparison to planktonic bacteria.

To directly test this hypothesis, Sanchez et al. challenged mice with equal colony forming units (CFU) of either planktonic or biofilm pneumococci (Sanchez et al., 2011b). The development of septicaemia occurred in mice that were intratracheally challenged with planktonic pneumococci. However, the majority of mice challenged with biofilm pneumococci did not contain any bacteria in their blood (Sanchez et al., 2011b). In comparison to planktonic cells, pneumococcal biofilms have also been found to be hyperadhesive on epithelial cells *in vitro* but, again, considerably less invasive (Sanchez et al., 2011b, Blanchette-Cain et al., 2013, Marks et al., 2013, Qin et al., 2013).

1.26 Gene expression of avirulent pneumococcal biofilms

Microarray analysis, mass spectroscopy and reverse transcription polymerase chain reaction (RT-PCR) studies have shown that biofilm pneumococci downregulate the expression of several virulence factors compared to planktonic cells *in vitro* including, enolase, pneumolysin and pilus (an invasin) (Allegrucci et al., 2006, Sanchez et al., 2011a, Sanchez et al., 2011b, Marks et al., 2013). Conversely, the expression of *SpxB*, *NanA*, *CbpA*, and pneumococcal serine-rich repeat protein (*PsrP*) are upregulated during biofilm growth (Parker et al., 2009, Sanchez et al., 2011b, Blanchette-Cain et al., 2013, Shenoy

and Orihuela, 2016). These adhesin proteins facilitate aggregation of pneumococcus by enabling either direct or indirect connections via bridging molecules to form (Sanchez et al., 2010, Blanchette and Orihuela, 2012). The quorum sensing system LuxS is also upregulated, which has been shown to facilitate biofilm formation, competence and fratricide, and is required for persistent carriage (Joyce et al., 2004, Trappetti et al., 2011, Vidal et al., 2011). Cell wall hydrolases (LytA and LytC) and PspA are also associated with biofilm formation (Moscoso et al., 2006). The importance of biofilm-associated proteins has been illustrated with mutants (e.g. CbpA, LytA, LytC and PspA) showing a decreased capacity to form a biofilm *in vitro* and impaired nasopharyngeal colonisation in mice (Moscoso et al., 2006, Muñoz-Elías et al., 2008, Marks et al., 2012a).

Additionally, biofilm growth is associated with changes in metabolism, protein synthesis, energy production and capsule production (Oggioni et al., 2006, Hall-Stoodley et al., 2008, Sanchez et al., 2011a, Sanchez et al., 2011b, Marks et al., 2012b, Yadav et al., 2012, Allan et al., 2014). Oggioni et al. showed that the gene expression of pneumococcal strains isolated from the nasopharynx of mice was almost identical to that of pneumococcal biofilms *in vitro* (Oggioni et al., 2006). Taken together, the finely controlled regulation of the capsule, cytotoxic products and surface proteins facilitates effective colonisation of the mucosal epithelia in the nasopharynx without triggering an intense, localised inflammatory response.

1.27 Virulence and gene expression of biofilm-dispersed pneumococci

Oggioni et al. demonstrated that the pattern of gene expression of pneumococci isolated from the bloodstream in mice was similar to that of planktonic, broth grown pneumococci. In contrast, the expression pattern of pneumococci from tissue was almost identical to that of pneumococcal biofilms *in vitro* (Oggioni et al., 2006). As colonisation always precedes pneumococcal disease, studies have been performed to assess whether the virulence of pneumococci actively-dispersed from a biofilm is restored.

In an *in vivo* mouse model, infection with the influenza A virus caused the active dispersal of pneumococcal cells, which subsequently translocated to the middle ear and the lungs in greater numbers than biofilm pneumococci (Marks et al., 2013). Furthermore, while intraperitoneal challenge with biofilm pneumococci resulted in rapid clearance from the bloodstream, the majority of mice that were challenged with biofilm-dispersed cells had to be sacrificed before they became moribund. Unexpectedly, it was discovered that actively-dispersed pneumococci induced an infection that was even more aggressive than

planktonic, broth-grown bacteria; actively-dispersed pneumococci triggered more inflammation and mice were terminally ill with significantly lower numbers of pneumococcal cells in the bloodstream (Marks et al., 2013). Collectively, actively-dispersed pneumococci were responsible for causing an infection that most closely resembles IPD in humans.

As a result of the observed differences in the virulence of planktonic, biofilm and actively-dispersed pneumococci, the gene expression of each cell population was examined. For actively-dispersed pneumococci, the expression of pneumolysin and numerous other genes (e.g. *CPS* and *pavA*) were significantly higher than both biofilm and planktonic, broth-grown pneumococci (Marks et al., 2013). The expression of the gene responsible for the opaque phenotype, *licD2*, was also significantly upregulated (Table 5). This phenotypic transition is integral to the virulence of actively-dispersed pneumococci to avoid opsonophagocytosis. Although actively-dispersed opaque pneumococci are associated with poor adherence to epithelial cells, they are more effective at invading and causing cell death both *in vitro* and *in vivo* compared to biofilm pneumococci, and they also induce the production of more pro-inflammatory cytokines (Marks et al., 2013).

Table 5: The transcriptional profile of biofilm and biofilm-dispersed pneumococci

Pneumococcal biofilm	**Virulence factor**	**Dispersed pneumococci**	**References**
↓ (Downregulated)	Capsular polysaccharide (*cps*)	↑ (Upregulated)	(Moscoso et al., 2006)
↓	Opaque phenotype (*licD2*)	↑	(Hall-Stoodley et al., 2008)
↓	Pneumolysin (*ply*)	↑	
↓	Pneumococcal adhesin and virulence (*pavA*)	↑	(Parker et al., 2009, Trappetti et al., 2011)
↓	Pneumococcal surface protein A (*PspA*)	↑	
↓	Autolysins (*CbpD*, *lytA*)	↑	(Sanchez et al., 2011b)
↑	Competence-stimulating peptide (*ComC*)	↓	(Marks et al., 2012b)
↑	Autoinducer-2 (*luxS*)	↓	
↑	Pneumococcal serine-rich repeat protein (*PsrP*)	↓	(Blanchette-Cain et al., 2013)
↑	Pyruvate oxidase (*SpxB*)	↓	(Marks et al., 2013)
↑	Neuraminidase (*NanA*)	↓	
↑	Phosphocholine (*ChoP*)	↓	(Vidal et al., 2013)
↑	Choline binding protein A (*CbpA*)	↓	

In addition to changes in the gene expression of virulence genes, studies have identified that dispersed pneumococcal cells downregulate genes associated with competence, purine and pyrimidine metabolism and translation, whilst upregulating carbohydrate metabolism (Pettigrew et al., 2014). Consequently, planktonic, biofilm and actively-dispersed pneumococcus display markedly different transcriptional profiles, which is indicative of three phenotypically distinct populations. These studies correlate very nicely with a study by Sanchez et al; convalescent sera obtained from individuals that had invasive disease preferentially reacted with planktonic cell lysates instead of biofilm lysates (Sanchez et al., 2011a). However, the opposite effect was discovered when sera from mice immunised with an ethanol-killed pneumococcal biofilm were obtained. Taken together, a developed immune response to either planktonic or biofilm pneumococci is not

equally effective against both phenotypes due to differences in protein expression. These results are also consistent with the findings that invasive disease is caused by planktonic diplococci (Tomasz et al., 1964), whilst pneumococcus asymptomatically colonises in the form of a biofilm (Muñoz-Elías et al., 2008, Sanchez et al., 2011b, Marks et al., 2012a, Blanchette-Cain et al., 2013).

In summary, biofilm formation during nasopharyngeal colonisation is thought to confer long-term, indolent persistence of pneumococcus against unfavourable environmental conditions. Sloughing, or changes in the microenvironment (e.g. a viral co-infection), lead to the dispersal of planktonic cells. This transforms the pneumococcal biofilm to become a source of infection and undergo the transition from a passive coloniser to a virulent pathogen, fully primed for successful invasion. As the capability for biofilm formation *in vivo* varies amongst pneumococcal strains, dispersed planktonic cells can lead to two different forms of pneumococcal infection. Dispersed pneumococcal cells that possess a high propensity for biofilm formation may transmit to the sinuses or the middle ear (Hall-Stoodley et al., 2006, Sanderson et al., 2006, Hoa et al., 2009, Al-Mutairi and Kilty, 2011), and dispersed pneumococcal cells that possess a lower propensity for biofilm formation but, have a more invasive phenotype, can penetrate the lower respiratory tract and enter the bloodstream to cause IPD (Orihuela et al., 2004).

1.28 Biofilm tolerance to antibiotics

Traditionally, antibiotics were developed for the eradication of planktonic cells and so their efficacy was assessed *in vitro* against planktonic bacteria, whilst research on antibiotic resistance was focused on resistance at the cellular level. However, bacteria that have had no known genetic basis for antibiotic resistance have shown increased tolerance when they form a biofilm (Anderl et al., 2000), and dispersed bacteria from a biofilm often become quickly susceptible to antibiotics (Anwar et al., 1989, Williams et al., 1997, Anderl et al., 2003). This observation highlights an important distinction between antimicrobial resistance and tolerance; while resistant bacteria can continue to divide and multiply in the presence of an antibiotic, tolerance refers to the absence of growth but the ability of bacteria to withstand an antibiotic.

This means that in addition to any conventional resistance at the planktonic level, bacteria in a biofilm also exhibit tolerance to antibiotics, which is not driven by mutations or mobile genetic elements. Reduced susceptibility means that bacteria in a biofilm can withstand antimicrobial agents at a concentration up to a thousand times greater than that which is efficacious in eradicating corresponding planktonic cells (Ceri et al., 1999, Parsek

and Singh, 2003, Römling and Balsalobre, 2012). This increased tolerance is dependent on the multicellular nature of biofilms, and can be understood through three main categories of antimicrobial recalcitrance: attenuated antibiotic penetration, heterogeneous microenvironments and bacterial persistence. These mechanisms may act in a synergistic manner to confer even greater recalcitrance against antibiotics (O'Toole et al., 2000, Mah and O'Toole, 2001, Lebeaux et al., 2014).

Although there is no generic barrier to the diffusion of antibiotics into the self-produced matrix to permeate a biofilm (Anderl et al., 2000, Stone et al., 2002, Zheng and Stewart, 2002), certain antibiotics can be deactivated or adsorbed into the biofilm matrix resulting in slow transport or incomplete penetration. For example, studies have shown that a concerted concentration of β-lactamases in the matrix of *Pseudomonas aeruginosa* biofilms can degrade routinely used β-lactam based antibiotics (Dibdin et al., 1996, Ciofu et al., 2000), and negatively charged polymers, such as eDNA and alginate, can bind to positively charged aminoglycoside antibiotics (Mulcahy et al., 2008, Tseng et al., 2013). However, limited antibiotic penetration cannot account for cases where different antibiotics fully penetrate different species of biofilm bacteria but are unable to eradicate a biofilm (Anderl et al., 2000, Walters et al., 2003).

A hallmark of biofilms is the presence of nutrient and oxygen gradients. In growth medium, nutrient-limited bacteria can become highly tolerant to antibiotics (Nguyen et al., 2011). In a biofilm, nutrient and oxygen availability decreases in the depths of a biofilm resulting in the existence of a slow-growing or a starvation state of bacteria, with low metabolic activity in a hypoxic environment (de Beer et al., 1994, Costerton et al., 1995). Consequently, a biofilm is a heterogenic population of cells (Rani et al., 2007, Stewart and Franklin, 2008). As many antibiotics are only effective against metabolically active and growing bacteria, cells in the outer layers of the biofilm may be damaged by conventional antibiotics but, cells in the more central and deeper regions that are slowly metabolising, may tolerate these antibiotics (Walters et al., 2003, Borriello et al., 2004).

The mechanisms of biofilm tolerance cannot fully account for the ineffectiveness of antibiotics that are capable of penetrating a biofilm and killing non-dividing cells (Spoering and Lewis, 2001). Instead, it is widely believed that ‘persister cells’ play a key role in biofilm recalcitrance to antibiotics. Persister cells are a subpopulation of deeply buried cells that are insensitive to killing by antibiotics, persevere throughout antibiotic treatment and repopulate the biofilm once treatment ceases (Lewis, 2001, Lewis, 2008, Lewis, 2010). Persisters represent a physiological state with low levels of translation in association with switching off of genes that encode for metabolic proteins (Shah et al., 2006). Antibiotics have a severely attenuated effect against this metabolic quiescent cell

population as many antibiotics target dividing cells. The persister phenotype is not due to mutations since, under conditions that stimulate growth, the persister state is reversible and the susceptibility to antibiotics is similar with the non-persister cells from the original biofilm (Singh et al., 2009). Instead, the formation of these dormant phenotypic variants is dependent on a slow growth state and metabolic inactivity, and may be a survival mechanism to forego replication in favour of ensuring that, while other cells may be killed, they can survive, regrow and cause relapsing infections (Mulcahy et al., 2010).

1.29 Therapeutic strategies for eradicating established biofilms

Once a biofilm is established, bacteria characteristically withstand antibiotic treatment. Both *in vitro* and *in vivo* experiments have shown that the minimum inhibitory concentration (MIC) and the minimum bactericidal concentration (MBC) for bacteria in a biofilm are frequently significantly higher than their planktonic counterparts (Ceri et al., 1999, Høiby et al., 2011, Hengzhuang et al., 2012), to the extent that an effective MBC for biofilms *in vivo* cannot be reached due to toxic side effects in the host. Ideally, a biofilm would be treated with early and aggressive antibiotic regimens, but the majority of clinical biofilm infections are associated with already mature biofilms. Moreover, sub-inhibitory concentrations of antibiotics have been known to stimulate *P. aeruginosa* and *Escherichia coli* biofilm growth (Dunne, 1990, Hoffman et al., 2005), and ineffective antibiotic treatment can select for the development of antibiotic resistance.

In light of the high recalcitrance against conventional antibiotics, recent research has shifted towards focussing on alternative, non-antibiotic compounds that may be used either alone (to replace these antibiotics) or alongside antibiotic treatment (to improve their efficacy), in order to increase the likelihood of eradicating an established biofilm. To improve the efficacy of treating biofilms *in vivo*, it is widely accepted that anti-biofilm treatments should be used in conjunction with conventional antibiotics. Any treatment that leads to dispersal but does not kill the dispersed cells may cause rapid re-establishment of biofilms at new sites via these planktonic cells. Conversely, if antibiotics that only target dispersed planktonic cells are used, then the biofilm is not removed and acute symptoms caused by released bacteria may reoccur.

One anti-biofilm approach is to investigate potential mechanisms of degrading the EPS in biofilms to lead to reduced stability and structural integrity. Enzymes, such as dispersin B and DNases, have been used to target exopolysaccharides and eDNA, respectively. Dispersin B has proven effective against *Staphylococcus epidermidis*

(Chaignon et al., 2007), and DNase I has shown efficacy against a range of bacterial species including, pneumococcus, *P. aeruginosa* and *S. aureus* (Hall-Stoodley et al., 2008, Okshevsky et al., 2015). An alternative anti-biofilm approach has focussed on inducing biofilm dispersal. Non-toxic levels of exogenous nitric oxide have been shown to trigger dispersal of *P. aeruginosa* biofilms and other bacterial species (Barraud et al., 2006, Barraud et al., 2009, Barraud et al., 2015). This has recently been shown to be relevant in human disease in a small pilot study (Howlin et al., 2017). Similarly, nitric oxide has been found to enhance the susceptibility of pneumococcal biofilms towards traditional antibiotics by modulating pneumococcal metabolism (Allan et al., 2016). Quorum sensing (QS) has also offered another avenue for anti-biofilm treatment. The synergistic effect of a QS inhibitor and an antibiotic (tobramycin) in a mouse model has been shown to reduce the biomass of a *P. aeruginosa* biofilm and enhance clearance due to phagocytosis (Hentzer et al., 2003, Christensen et al., 2012). A novel QS inhibitor has also shown promise in the prevention of pneumococcal biofilm formation in an animal model of otitis media (Cevizci et al., 2015). Specifically, biofilm formation was not detected on small Cochlear implants implanted into guinea pigs.

Despite numerous *in vitro* and animal studies showing promising anti-biofilm treatments, very few *in vivo* preclinical or clinical studies have demonstrated an improvement in the treatment of biofilm-associated infections. Only one anti-biofilm therapy that targets already established biofilms is currently in established clinical use. Recombinant human DNase I (dornase alfa) has been found to degrade both bacteria-derived eDNA and neutrophil-derived DNA (NETs), helping to reduce the viscosity of sputum in cystic fibrosis patients (Konstan and Ratjen, 2012, Manzenreiter et al., 2012). NETs and eDNA in bacterial biofilms in the middle ear are currently being investigated as a potential target for dornase alfa in patients suffering from recurrent ear infections, to reduce the viscosity of the effusion (Thornton et al., 2013).

1.30 Otitis Media

Acute otitis media (AOM) is the most common infection in young children and is the leading cause for doctor appointments, antibiotic prescriptions and surgery in this age demographic (Plasschaert et al., 2006, Monasta et al., 2012). AOM is characterised with an inflamed tympanic membrane, middle ear effusion, earache and fever (Gates et al., 2002). Many children can suffer from 3 or more episodes in a 6 month period known as recurrent AOM (RAOM), with effusion resolving between episodes. In comparison, otitis media with effusion (OME) is characterised with middle ear effusion but without any clinical symptoms of acute infection, and is diagnosed as COM if effusion persists beyond 3 months (Daly et al., 1999). A clinical side effect of RAOM or COM is conductive hearing loss (Bennett et al., 2001), which can have significant socioeconomic consequences due to the effects on a child's behaviour, education and development of language (Winskel, 2006).

The three primary causative agents of AOM are *S. pneumoniae, H. influenzae* and *M. catarrhalis* (Giebink, 1989, Casey and Pichichero, 2004, Güvenç et al., 2010). The majority of AOM infections are self-limiting, with symptoms typically resolving in less than a week (Toll and Nunez, 2012). Although analgesia is integral to treatment, with non-steroidal anti-inflammatory drugs (NSAIDs) shown to significantly reduce symptoms (Bertin et al., 1996), treatment with antibiotics is frequently of primary consideration for clinicians (Toll and Nunez, 2012). The overprescription and overuse of antibiotics for the medical management of AOM has selected for the development of antibiotic resistant bacteria including the predominant otopathogens of OM (Green and Wald, 1996, McLinn and Williams, 1996, Cohen et al., 1997, Pichichero, 2000, Bakaletz, 2007). Surgical treatment for RAOM or COM that is refractory to antibiotic treatment requires the insertion of a tympanostomy tube (grommet) into the eardrum to drain the middle ear effusion and ameliorate the painful symptoms (Hall-Stoodley et al., 2006, Daniel et al., 2012). However, tympanostomy tube placement does not prevent OM and may act as a substratum for biofilm growth (Bothwell et al., 2003). Furthermore, despite the PCVs culminating in a reduction in IPD, the vaccines have not appreciably reduced the incidence of OM (Taylor et al., 2012, Ochoa-Gondar et al., 2015).

OM occurs when bacteria that reside in the nasopharynx migrate through the Eustachian tube, colonise the middle ear mucosal epithelium and establish an infection. The Eustachian tube, which connects the back of the nose to the middle ear, equalises air pressure in the middle ear and facilitates drainage of built-up fluid. Deficiencies in the innate and adaptive immune responses have been reported to increase susceptibility to OM (Shimada et al., 2008, Li et al., 2012, Xu et al., 2015). There is also a clear association

between a preceding viral infection and the onset of OM (Bakaletz, 2010). A viral infection such as IAV causes nasopharyngitis, thicker mucus production, increased bacterial carriage and a dysfunctional Eustachian tube. A dysfunctional Eustachian tube reduces middle ear pressure and the nasopharyngeal mucus is sucked into the middle ear along with any microorganisms present (Nokso-Koivisto et al., 2015).

To directly investigate the effect of a virus and the resulting host responses on the dispersal of an established pneumococcal biofilm, Marks et al. developed a biofilm model on epithelial cells *in vitro* and *in vivo* and treated the biofilm with IAV and various components of an IAV-associated host response (Marks et al., 2013). *In vitro* treatment of a pneumococcal biofilm on live epithelial cells with IAV (after initially being allowed to form a biofilm on fixed cells) resulted in a 10-fold increase in the number of pneumococcal cells in the supernatant, which supports the role of IAV inducing the release of bacteria from biofilms, contributing to the pathogenesis of OM. Exogenous addition of ATP, glucose and an increase in temperature also induced the release of pneumococcal cells from a pneumococcal biofilm on fixed epithelial cells. *In vivo* treatment with IAV resulted in an increase in nasopharyngeal colonisation in mice, and IAV and IAV-associated host responses also increased dispersal and dissemination to the middle ear and the lungs (Marks et al., 2013).

Initially, COM was believed to be an inflammatory but "sterile" process due to repeatedly negative cultures from middle ear effusions (Giebink et al., 1982, Diamond et al., 1989, Hendolin et al., 1999); a trait which is also common for bacteria in a biofilm (Potera, 1999). However, with the advent of culture-independent approaches such as PCR, effusions were frequently found to contain pathogenic bacteria, with viable bacteria even detected after antibiotic treatment (Post et al., 1995, Post et al., 1996b, Post et al., 1996a, Aul et al., 1998, Rayner et al., 1998, Hall-Stoodley et al., 2006). Effusions have contained the same spectrum of bacteria as those found in acute infections (Rayner et al., 1998). To account for the culture negative results and persistent and recurrent infections despite antibiotic treatment, it was postulated that COM is a biofilm-associated infection (Ehrlich et al., 2002, Bakaletz, 2007).

Hall-Stoodley et al. demonstrated that COM is a biofilm-associated infection by demonstrating that aggregated and pathogenic bacteria were present on the mucosal epithelium in the middle ear of children undergoing tympanostomy tube placement (Hall-Stoodley et al., 2006). Every effusion was found to contain at least one of the principle OM pathogens by PCR (Hall-Stoodley et al., 2006). These pathogens have been shown to form biofilms *in vitro* (Allegrucci et al., 2006, Pearson et al., 2006, Starner et al., 2006, Hall-Stoodley et al., 2008, Marks et al., 2012a). Animal studies have also shown biofilm

formation on the middle ear mucosa of experimentally infected animals (Ehrlich et al., 2002, Dohar et al., 2005, Reid et al., 2009, Weimer et al., 2010). Biofilms were detected in middle ear mucosal biopsies from children with either RAOM or COM, yet not in patients without a history of COM but undergoing surgery for a cochlear implant (Hall-Stoodley et al., 2006, Post et al., 2007). These observations indicated that biofilm bacteria are not usually found in the middle ear in the absence of infection.

Conversely, pneumococcal biofilms and all other major otopathogens have been detected on the mucosal epithelium on adenoid tissue in children undergoing adenoidectomy for the treatment of either COM or obstructive sleep apnea (OSA), suggesting that the adenoid harbours pathogenic bacteria regardless of whether pneumococcal disease is present or not (Hoa et al., 2009, Nistico et al., 2011). Currently, the hypothesis is that adenoids can act as a reservoir for otopathogenic biofilm bacteria leading to the pathogenesis of OM. Specifically, during favourable changes in the host such as a viral infection and, due to anatomical proximity to the Eustachian tube (Gates, 1999), shed planktonic cells may access and reside within the middle ear. As COM is a biofilm-associated infection, infrequent shedding of planktonic cells may occur resulting in acute infection (i.e. RAOM) and inflammation (Hall-Stoodley et al., 2006, Tonnaer et al., 2006, Bakaletz, 2007, Post et al., 2007). Although the immune system and/or antibiotics may control the acute infection, the established biofilm itself remains unperturbed, which promotes recurrent infections and antibiotic resistance.

Several studies have reported identical paired isolates from adenoid tissue and from middle ear effusions in patients with OM (Hotomi et al., 2004, Tonnaer et al., 2005, Emaneini et al., 2013). In support of the role of nasopharyngeal biofilms giving rise to OM, the most common otopathogens have frequently been found in the adenoids of otitis-prone children (McClay, 2000, Karlidağ et al., 2002, Kania et al., 2008, Hoa et al., 2009). In a study by Saafan et al. the adenoids of children with COM were analysed for the presence of *S. pneumoniae*, *H. influenzae*, *M. catarrhalis* and *S. aureus* biofilms (Saafan et al., 2013). 96% of the adenoid samples contained at least one of these otopathogens, while 80% of middle ear effusions also contained at least one of these predominant otopathogens, demonstrating an association between adenoidal biofilm formation and COM (Saafan et al., 2013). Additional studies have also reported denser and more extensive biofilms in the adenoids of children with OM compared to those without OM (Zuliani et al., 2009, Hoa et al., 2010, Saylam et al., 2010, Tawfik et al., 2016).

1.31 Adenoidectomy for the treatment of otitis media

Adenoidectomy, either alone or as an adjunctive therapy alongside tympanostomy tube placement, has been shown in some children to effectively treat COM and reduce further incidence (Gates et al., 1987, Gates et al., 1988, Paradise et al., 1990, Gates, 1999, Coyte et al., 2001, Kadhim et al., 2007, van den Aardweg et al., 2010, Boonacker et al., 2014). Adenoidectomy is also performed for the treatment of OSA due to an enlarged adenoid (hypertrophy) that can obstruct the Eustachian tube, thereby preventing mucus drainage and maintenance of normal air pressure (Bluestone, 1996). Therefore, the true reason behind the efficacy of adenoidectomy for the treatment of COM has been debated. However, adenoidectomy has been effective in reducing recurrence of COM irrespective of adenoid size in children older than 3 years of age (Gates, 1999, McClay, 2000, Pagella et al., 2010). Furthermore, recent studies comparing adenoidal biofilm formation in patients with adenoid hypertrophy and OME (group 1), to patients with adenoid hypertrophy alone (group 2), have shown no correlation between adenoid size and biofilm formation, and that the extent of nasopharyngeal bacterial colonisation (much greater in group 1) is the main determinant factor in the pathogenesis of OME (Saylam et al., 2010, Saafan et al., 2013, Tawfik et al., 2016). Taken together, these findings support the argument that adenoidectomy can be clinically effective in some children by removing a reservoir of pathogenic bacteria.

In the majority of studies that have examined the presence of pneumococcal biofilms on adenoid tissue, aggregates of pneumococcus have been observed on the mucosal epithelial surface and within the crypts of the adenoid (Kania et al., 2008, Nistico et al., 2011). However, it has been reported that otopathogens, including pneumococcus, can be found intracellularly within epithelial cells from OM biopsies (Coates et al., 2008, Thornton et al., 2011), and that intracellular aggregates of pneumococcus have been detected in the epithelial cells of adenoid tissue and surrounded with an extracellular matrix, which is indicative of a biofilm (Nistico et al., 2011). These findings may further explain the ineffectiveness of current antibiotic treatments, which are empirically chosen due to their effectiveness against planktonically grown bacteria.

Despite the clinical relevance of biofilms in the pathogenesis of OM, there is little research on why host immune mechanisms are unable to clear a biofilm in the nasopharynx and in the middle ear in the same way as planktonic bacteria. Based on the literature, which has predominantly focused on the *in vitro* interaction between host innate immunity and either *P. aeruginosa* (Jesaitis et al., 2003, Leid et al., 2005, Jensen et al., 2007, Alhede et al., 2009) or *S. aureus* biofilms (Leid et al., 2002, Günther et al., 2009, Thurlow et al.,

2011, Scherr et al., 2014), our hypothesis was that macrophages and/or neutrophils may play a role in the host innate response to a pneumococcal biofilm in patient adenoids.

1.32 Studying the interactions between pneumococcal biofilms and the host

The vast majority of *in vitro* biofilm studies have been performed on an abiotic (polystyrene or glass) surface. Although a wealth of information on pneumococcal biofilm formation has been provided, the relevance and implications for *in vivo* pneumococcal biofilm formation and nasopharyngeal colonisation is limited. For instance, although all pneumococcal isolates, whether invasive or nasopharyngeal strains, are able to produce biofilms *in vitro* (Allegrucci et al., 2006, Muñoz-Almagro et al., 2008, Tapiainen et al., 2010), there is no correlation between the ability to form a robust biofilm *in vitro* and the virulence potential of a pneumococcal isolate obtained from different anatomical sites in humans and in mice (Lizcano et al., 2010, Tapiainen et al., 2010, Sanchez et al., 2011b).

In addition, these models do not facilitate interrogation of host-pneumococcal biofilm interactions, which is an important and unexplored area of biofilm research. Incorporation of a host component will more accurately recapitulate the dynamics between host-pneumococcal biofilms *in vivo*, and facilitate a deeper and more pertinent understanding of these complex communities. Accordingly, recent studies have involved more appropriate model systems. For instance, Parker et al. and Sanchez et al. demonstrated a clear relationship between epithelial cells and pneumococcal adherence and biofilm formation. In comparison to planktonic pneumococci, biofilm bacteria displayed better adherence to epithelial cells after both populations were grown on abiotic surfaces (Sanchez et al., 2011b), whilst bacteria recovered from epithelial cells formed more structured biofilms on abiotic surfaces than bacteria without previous epithelial cell exposure (Parker et al., 2009). Marks et al. and Blanchette-Cain et al. have since shown that pneumococcus forms a biofilm on epithelial cells *in vivo* in the nasopharynx in mice (Marks et al., 2012a, Blanchette-Cain et al., 2013), and that pneumococcal biofilms grown on epithelial cells *in vitro* and *in vivo* form more quickly, are more structured, have a higher biomass and exhibit a more reflective *in vivo* antibiotic resistance profile than pneumococcal biofilms grown on an abiotic surface (Sanchez et al., 2011b, Marks et al., 2012a, Vidal et al., 2013).

These studies represent surrogate models for pneumococcal biofilm formation on epithelial cells in the human host. However, current co-culture models that examine the *in*

vitro interaction between pneumococcus and the human host have relied on the following: (i) using fixed epithelial cells; pneumococcal biofilms from various serotypes have been grown on lung (A549), pharyngeal (Detroit 562) and bronchial (NCI-H292) epithelial cell lines prefixed with paraformaldehyde (Marks et al., 2012a, Shak et al., 2013, Vidal et al., 2013); (ii) having only a short contact time between pneumococcus and live epithelial cells; several research groups have used unfixed, viable epithelia to study pneumococcal biofilms but for a limited time only (maximum of 4 hours) (Pracht et al., 2005, Bootsma et al., 2007, Sanchez et al., 2011b, Brittan et al., 2012, Blanchette-Cain et al., 2013, Blanchette et al., 2016); (iii) growing a pneumococcal biofilm on either an abiotic or a fixed biotic surface that is then transplanted on to live epithelial cells; in a model developed by Marks et al. pneumococcal biofilms were developed on prefixed human respiratory epithelial cells (HRECs) for 48 hours and then transplanted onto live HREC cultures, with media changes every 4 hours to ensure that the biofilms were maintained (Marks et al., 2013). The drawbacks to these approaches include the following: (i) interrogation of the host innate response to pneumococcal biofilm formation is not permitted; (ii) initial bacterial attachment only can be investigated; (iii) in the absence of viable host cells biofilm formation is arbitrarily created. As the aim of *in vitro* experiments is to extrapolate the results to explain and/or predict observations *in vivo*, it is important to recapitulate the *in vivo* environment as much as possible during *in vitro* experiments. In this project, therefore, the aim was to develop a co-culture model enabling live epithelial cells to be inoculated with planktonic pneumococcal cells, and for biofilm formation to occur without compromising epithelial cell integrity.

1.33 Aims and objectives

Aim 1: To assess pneumococcal co-localisation with phagocytes in adenoid tissue (Chapters 3 and 4).

- Objective 1: Stain a clinically relevant pneumococcal strain by using a well-established immunohistochemistry technique.
- Objective 2: Perform immunolabelling of pneumococcus and macrophages and neutrophils in spiked adenoid tissue.
- Objective 3: Determine the presence of *S. pneumoniae* biofilms.
- Objective 4: Investigate pneumococcal-host immune cell co-localisation in patient adenoids.

Aim 2: To establish a co-culture model with pneumococcal biofilms and an epithelial cell line (Chapters 5 and 6).

- Objective 1: Develop confluent and healthy respiratory epithelial cell monolayers on transwell membranes.
- Objective 2: Assess epithelial cell monolayer integrity and viability with different *S. pneumoniae* loads (multiplicities of infection).
- Objective 3: Measure pneumococcal adherence and early biofilm formation with viable counts and scanning electron microscopy analyses.
- Objective 4: Explore the host response to a nascent pneumococcal biofilm with an optimised co-culture model.

This work will allow for a better understanding of the relationship between a pneumococcal biofilm and human innate immune cells, and will provide a co-culture model that can be used as an advantageous tool for the translational investigation of the interaction between early-phase pneumococcal biofilms and live epithelial cells.

2 Chapter 2 - Materials and Methods

2.1 Bacterial strains

Single strains representing *S. pneumoniae* serotypes 14 and 2 (D39) were used in this project.

Serotype 14 (S14) is a blood sample isolate provided by the UK Public Health England (Health Protection Agency) Microbiology Services laboratory, Southampton. S14 was chosen for this study as it is prevalent in pneumococcal disease including otitis media, and previous work in our laboratory has shown this particular strain to have good biofilm-forming capacity (Hall-Stoodley et al., 2008, Hiller et al., 2007). Pure cultures of S14 and S14 spiked paediatric adenoid tissue were used for immunohistochemistry and immunofluorescence experiments.

The D39 strain (kindly gifted by Dr. Stuart Clare's laboratory, University of Southampton) was used for all *in vitro* co-culture experiments with a bronchial epithelial cell line. A plasmid (pMV158) that constitutively expresses a green fluorescent protein (GFP) had been incorporated into the D39 genome (Nieto and Espinosa, 2003). To induce the regulon and subsequent fluorescence, the strain was grown in medium containing 2% maltose (Sigma-Aldrich, U.K.). The metabolism of maltose by viable pneumococcal cells activates the expression of the fluorescent protein. In this way, the amount of fluorescence could be used to assess the number of viable cells and the extent of biofilm formation by using fluorescence microscopy. The use of a GFP-expressing pneumococcal strain meant that the surface area of pneumococcal biofilms on the epithelial cell surface could be determined using confocal microscopy.

2.2 Glycerol stocks of bacterial strains

10 µl of S14 and D39 was streaked onto Columbia blood agar (CBA) plates with 5% horse blood (Oxoid, U.K.) and incubated overnight at 37°C/5% CO_2. Bacterial growth was resuspended in 2 ml Brain Heart Infusion (BHI) broth (Oxoid, U.K.) and centrifuged at 3200 x *g* for 5 minutes to remove any cell debris and lytic enzymes. The supernatant was used to make a 1:10 dilution in BHI in a 15 ml conical centrifuge tube (Fisher Scientific, U.K.) and incubated at 37°C/5% CO_2 until the bacteria had reached mid-exponential phase ($1x10^8$ bacterial cells per ml). The bacteria were then stored in a 22% glycerol solution (Sigma-Aldrich, U.K.) at -20°C. To check for the growth of only pneumococcus, 10 µl of a

glycerol stock for each strain was streaked onto a CBA plate for overnight incubation at 37°C/5% CO_2 and assessed for the presence of pure cultures.

2.3 Growth kinetics of the D39 laboratory strain

Regression analysis is a widely used microbiology technique to estimate the relationship between the number of live bacterial cells within a culture in relation to absorbance over a set period of time. Regression analysis was performed for D39 to determine what optical density (OD) equated to $1x10^8$ bacterial cells per ml (mid-exponential phase). Regression analysis for S14 had already been performed and optimised in our laboratory. This assay enabled standardisation of inoculation with *S. pneumoniae* for all immunohistochemistry (S14), immunofluorescence (S14) and co-culture (D39) experiments.

10 µl of a frozen D39 aliquot (section 2.2) was streaked onto a CBA plate and incubated overnight at 37°C/5% CO_2. A broth culture was set up as previously described (section 2.2) and incubated at 37°C/5% CO_2. 1 ml of fresh BHI was pipetted into a 1 ml cuvette (Fisher Scientific, U.K.) and placed in a Jenway 6300 spectrophotometer (Keison Products, U.K.) at a wavelength of 600 nm for calibration. After every hour of incubation, 1 ml of the broth culture was removed and the absorbance at 600 nm was measured, whilst a 96-well plate (Fisher Scientific, U.K.) was used to perform 10-fold serial dilutions with 200 µl of the broth and 180 µl of fresh BHI media per well. A spot plating method was then performed by pipetting 20 µl of each dilution onto a CBA plate five times, and the CBA plates were then incubated for ~18 hours at 37°C/5% CO_2. The number of colony forming units (CFUs) were counted to measure the number of viable pneumococcal cells, and a calibration curve was drawn by plotting CFUs versus OD at 600 nm from which the OD correlating to $1x10^8$ cells per ml was measured. This assay was performed in three separate experiments, with the average OD taken and used for all future experiments.

2.4 Assessment of GFP expression in *S. pneumoniae* D39 biofilms

To determine if the D39 strain successfully fluoresced in the biofilm phenotype, a broth culture of D39 was set up as before (section 2.2). For biofilm formation, a mid-exponential planktonic culture (2 ml $x10^8$ cells) was used to inoculate two cell culture glass bottom dishes (CELLview) (Greiner Bio One, U.K.) and supplemented with 2 ml BHI diluted 1:5 in non-pyrogenic sterile dH_2O. These nutrient-starved conditions would help the transition to the biofilm mode of growth.

The culture dishes were incubated at 37°C/5% CO_2 under static conditions. After 24 hours of incubation, 0.4 g of maltose was dissolved in 10 ml of 1:5 BHI, mixed well and filter sterilised with a polyethersulfone membrane (0.4 µm pore size) (Fisher Scientific, U.K.) to produce a 4% solution. 2 ml of the spent medium was removed from the culture dishes and replaced with either 2 ml of the maltose solution (for a final maltose solution of 2%) or 2 ml of fresh 1:5 BHI. After a further 24 hours of incubation, the spent medium was removed from both dishes and replaced with 2 ml of Hank's Balanced Salt Solution (HBSS) (Fisher Scientific, U.K.). The culture dishes were rocked gently to remove unattached planktonic cells and any residual medium, and 2 ml of 70% glycerol was added. The extent of GFP expression and biofilm formation was then analysed by confocal laser scanning microscopy (CLSM), with a Leica SP8 microscope using a 488 laser line (excitation at 488 nm and emission at 498 nm), and an inverted stand using a x63 oil immersion lens.

2.5 Clinical adenoid samples

Anonymised paediatric adenoid tissue (<12 years of age) was obtained at Southampton General Hospital from patients undergoing adenoidectomy for the treatment of suspected inflammatory (obstructive sleep apnea, OSA) or infective ear, nose and throat (ENT) disease, with written informed parental consent. Adenoids were collected under NHS Research Ethics approval 09/H0501/74 (Appendix 9.4).

2.6 Processing of adenoid tissue

Adenoids were collected from surgery on ice in individual 50 ml conical centrifuge tubes (Fisher Scientific, U.K.) consisting of 4750 µl HBSS and 250 µl fetal calf serum (FCS) (Sigma-Aldrich, U.K.) to provide the cells with essential inorganic ions, water and growth supplements. As a positive control for staining pneumococcus in adenoid tissue, adenoids (n = 4) were spiked with S14. A broth culture of S14 was set up as before (section 2.2) and the bacteria grown to mid-exponential phase. Adenoid tissue was typically collected from surgery early-afternoon, however, where appropriate, sub-culturing of the broth culture (1:10 dilution in fresh BHI) was performed. Adenoid tissue was washed twice with 1 ml HBSS to remove unattached bacteria and incubated in the S14 broth at 37°C/5% CO_2 for 2 hours. In order to prevent autolysis and necrosis of the adenoid tissue, the adenoid tissue was then immediately fixed in 15 ml of 10% neutral buffered formalin (NBF) (Leica Biosystems, U.K.). NBF served to preserve the structure of the tissue and to enhance the resistance of the cells in the tissue against downstream processing

by improving the mechanical strength of the tissue through cross-link bridges. Non-spiked patient adenoids (n = 4) were obtained and washed in the same way before fixing in NBF.

2.6.1 Paraffin-embedding

After formalin-fixation (section 2.6), each adenoid was processed for paraffin-embedding; crucial to preserve tissue morphology and provide physical support for sectioning. Embedding in paraffin wax is the most widely used method for solidifying tissue samples whilst minimising damage to the natural shape and architecture of the tissue. Paraffin-embedding was performed using a Tissue-Tek VIP5 junior automated processor by a laboratory technician (Sakura, Newbury, U.K.), with the steps outlined below (Table 6). Steps 1-10 were carried out at 37°C and steps 11-14 were carried out at 60°C under vacuum. Alcohol denatured with industrial methylated spirit (74 O.P.) (Fisher Scientific, U.K.) was used for the appropriate steps.

Table 6: The steps and reagents used to paraffin-embed adenoid tissue

Step	**Reagent**	**Time (hours)**
1	70% alcohol	1
2	80% alcohol	1
3	90% alcohol	1
4	100% alcohol	1
5	100% alcohol	1
6	100% alcohol	2
7	100% alcohol	2
8	Clearene	1.5
9	Clearene	1.5
10	Clearene	1.5
11	Wax	1.5
12	Wax	1
13	Wax	1
14	Wax	1

2.6.2 Microtome sectioning

To obtain sections of adenoid tissue for subsequent experiments, formalin-fixed, paraffin-embedded adenoid tissue was sectioned using a microtome (Leica Biosystems, U.K.). 4 µm sections were floated out on a water bath at 40°C, mounted onto APES coated microscope slides (CellPath, U.K.), and dried at 37°C for at least 48 hours to ensure thorough drying and adherence of the tissue sections prior to immunohistochemistry and immunofluorescence experiments.

2.7 Fixation of pure cultures of S14 using a Shandon Cytoblock kit

A broth culture of S14 was set up to obtain pure bacteria cultures (section 2.2). Pure cultures of pneumococcus were initially used to optimise staining of pneumococcus with anti-pneumococcal antibodies, and then to act as a positive control for each assay that stained for pneumococcus in spiked and non-spiked adenoid tissue. At the point of mid-exponential phase, S14 in a 15 ml conical centrifuge tube was centrifuged at 3200 x *g* for 5 minutes, the supernatant was discarded and 5 ml of NBF was added. After overnight incubation at 4°C, the sample was centrifuged at 10,956 x *g* for 5 minutes, the supernatant removed and 5 ml of 70% ethanol (Fisher Scientific, U.K.) was added. The sample was centrifuged at 10,956 x *g* for another 5 minutes and the ethanol was removed. 1 drop of Reagent 1 and Reagent 2 from the Shandon Cytoblock Kit (Thermo Shandon Inc., U.S.) were added to the centrifuge tube and vortexed vigorously to obtain a well-formed pellet. Each pellet was placed in a Cytoblock Cassette and submerged in 70% ethanol. After paraffin-embedding (section 2.6.1), S14 was sectioned 4 µm thick using a microtome, as previously described (section 2.6.2). This technique enabled pure cultures of pneumococcus to be in a format suitable for immunohistochemistry staining.

2.8 Haematoxylin and Eosin stain

A haematoxylin and eosin (H&E) stain was performed for pure cultures of sectioned S14 to determine the morphology of pneumococcus to help identify pneumococcus in S14 spiked adenoids during subsequent experiments. The sections were dewaxed in clearene (2x10 minutes), hydrated through 100% alcohol (2x5 minutes), 70% alcohol (5 minutes) and placed in tap water (5 minutes). After staining the slides in Mayer's haematoxylin (5 minutes) (Appendix 9.1), which stains nuclear chromatin blue/purple, the sections were placed under running tap water (5 minutes) and stained in eosin (5 minutes) (Appendix 9.1)

to stain cytoplasmic proteins pink. The sections were rinsed very briefly in tap water and dehydrated through graded alcohols in 70% alcohol (1 minute) and 100% alcohol (1 minute), cleared in clearene (3x2 minutes), and mounted in pertex mounting medium (Leica Biosystems, U.K.).

2.9 Immunohistochemistry

Immunohistochemistry is a well-established experimental technique that uses antibodies to show the distribution and localisation of a protein of interest at the cellular level in tissue sections (Hsu et al., 1981). This method was chosen as it allowed targets to be observed in intact tissue *in situ*, and offered a more cost effective alternative to immunofluorescent staining.

To stain for a protein of interest using immunohistochemistry, a primary antibody is used that recognises and binds to the target protein with high specificity. In comparison to direct immunohistochemistry, in which just one (labelled) antibody is used to detect and stain for the target antigen, the avidin-biotin indirect method involves two antibodies. The use of a secondary antibody allowed for signal amplification of the target protein as more than one secondary antibody would bind to the tissue-bound primary antibody. However, the working dilution (i.e. optimal concentration) of both the primary and secondary antibody had to be optimised in order to prevent either a too high or a too low concentration of antibody that would otherwise result in non-specific staining or insufficient staining, respectively. Furthermore, it was important that the secondary antibody was directed against the species in which the primary antibody was raised in. For instance, if the primary antibody was raised in rabbit then an anti-rabbit secondary antibody that was raised in any species other than rabbit could be applied.

The secondary antibody was conjugated to biotin and acted as a link between the antigen-bound primary antibody and avidin biotin-reporter enzyme (horseradish peroxidase) complexes (Hsu et al., 1981). As avidin possesses four binding sites for biotin, unoccupied biotin-binding sites in these avidin-biotin complexes enabled avidin to bind to the biotinylated secondary antibody. A substrate was then applied to form a coloured precipitate (brown) at the site of the detected antigen (Figure 2.1).

To act as a positive control, a section of tissue that is known to possess a particular antigen was stained for the detection of that antigen. A positive result from this positive control indicated that the immunohistochemistry protocol was optimised and working, and suggested that any negative result from a tested sample was valid (as detailed in section 2.12). In order to verify that a positive result from a tested sample was valid, a negative

control was also performed whereby the primary antibody was omitted and replaced with the diluent, tris-buffered saline (i.e. TBS), and the appropriate secondary antibody was used as normal. This negative control helped to confirm that any positive staining from a tested sample was the direct result of the secondary antibody binding to the primary antibody, and not to other antigens in the tissue (as detailed in section 2.12).

Immunohistochemistry was used to stain for: (i) pure cultures of S14 and (ii) pneumococcus (S14), macrophages and neutrophils in spiked adenoid tissue.

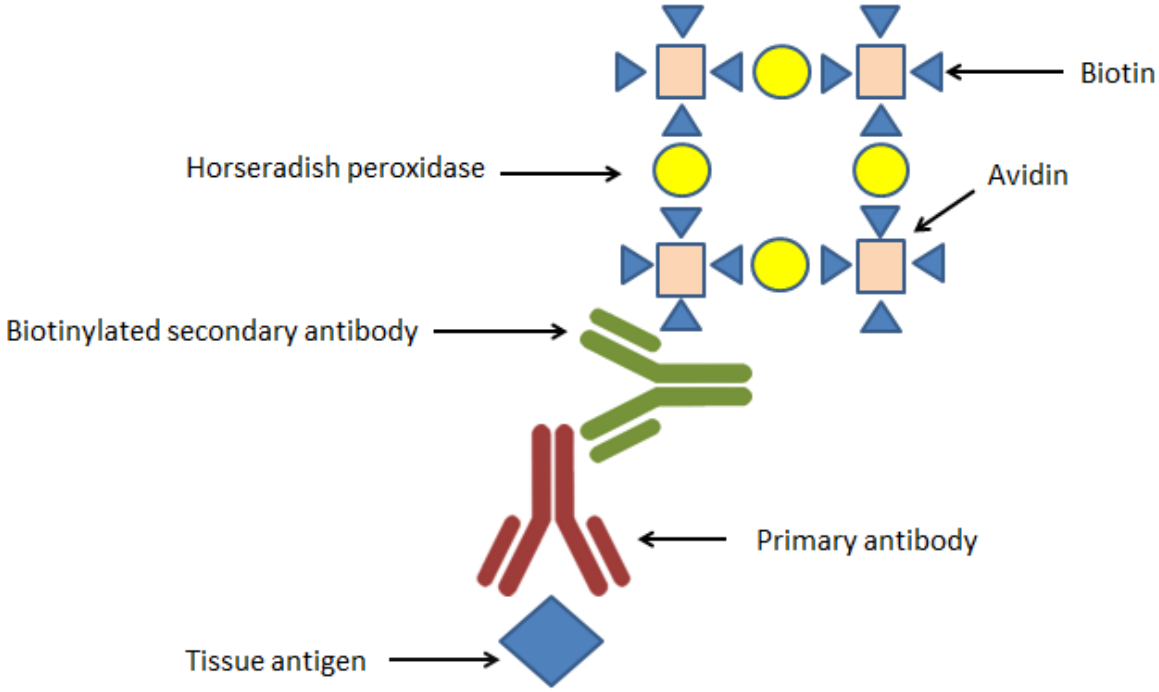

Figure 2.1: The avidin-biotin complex immunohistochemistry method.

2.10 Immunohistochemistry antigen retrieval techniques

As the process of fixation (section 2.6) can mask epitopes on the target antigen it was important to establish the need or not of using a technique to unmask these epitopes. Exposing target antigens may require proteolytic-induced epitope retrieval (PIER), heat-induced epitope retrieval (HIER) or no pre-treatment at all. The enzyme pronase was used for PIER, and a microwave and a pressure cooker were used to act as a source of heat for HIER. Therefore, in addition to optimising the working dilution of the primary and

secondary antibodies for optimal immunohistochemistry staining, the appropriate antigen retrieval technique had to be determined in order for the primary antibody to bind to its target antigen.

2.10.1 Pronase antigen retrieval

A 100 µl vial of pronase stock (Dako, U.K.) was added to 1.9 ml of TBS (Appendix 9.1) and mixed well. The drained slides were covered with the working pronase solution (0.01%) for 10 minutes and then washed with TBS (2x5 minutes).

2.10.2 Microwave antigen retrieval

Citrate buffer pH 6.0 or ethylenediaminetetraacetic acid (EDTA) buffer pH 8.0 was made by adding 2.1 g citric acid crystals or 0.37 g EDTA (both Fisher Scientific, U.K.) with 1 litre of distilled water. The pH was adjusted to 6.0 with ~25 ml 1 M sodium hydroxide (citrate buffer), or pH 8.0 with ~8 ml 0.1 M sodium hydroxide (EDTA buffer) (Fisher Scientific, U.K.). The slides were placed into a plastic staining rack inserted in a polystyrene box. To maintain a constant load, three boxes were used with blank slides to make up a total of 72 slides per box. Each box was filled with 330 ml of prepared citrate or EDTA buffer and then microwaved (25 minutes) at 50% power. The boxes were removed and placed under running cold water (3 minutes). The slides were then placed back into the staining trays, and washed in TBS (2x5 minutes).

2.10.3 Pressure cooker antigen retrieval

Citrate buffer pH 6.0 was made by adding 2.1 g citric acid crystals with 1 litre of distilled water and adjusted with ~25 ml 1 M sodium hydroxide. Once the citrate buffer had boiled in a pressure cooker, stainless steel staining racks containing the slides were placed into the pressure cooker. The regulator valve was turned to position 2 (13 lb pressure) to allow the pressure to build. After 2 minutes, the pressure cooker was removed and submerged in cold water until atmospheric pressure had been reached. The vessel was filled with cold water and the slides removed. The slides were placed back into the staining trays and washed in TBS (2x5 minutes).

2.11 Immunohistochemistry protocol

Formalin-fixed (section 2.6), paraffin-embedded (section 2.6.1) sections were deparaffinised in clearene (2x5 minutes) and rehydrated through 100% alcohol (2x5 minutes) and 70% alcohol (5 minutes). Experimental tissue can contain endogenous peroxidase activity that will result in non-specific false-positive background. To account for this, endogenous peroxidase activity was suppressed with 0.5% hydrogen peroxide in methanol (both Sigma-Aldrich, U.K.) (10 minutes), and the sections were washed with TBS (3x2 minutes). The appropriate antigen retrieval pre-treatment for the target antigen was then performed to expose the antigenic epitopes in the tissue. Next, avidin solution (Vector Laboratories, U.K.) was applied to block any endogenous biotin in the tissue and the sections were rinsed with TBS (3x2 minutes). Biotin solution (Vector Laboratories, U.K.) was then applied to block the remaining biotin binding sites on avidin and the sections were rinsed with TBS (3x2 minutes). Blocking medium (Appendix 9.1) was added (20 minutes), and a primary antibody at the appropriate dilution was applied to form antigen-antibody complexes against the target of interest (*S. pneumoniae*, macrophages or neutrophils) after overnight incubation at 4°C (Hsu et al., 1981).

To detect these complexes, the sections were washed with TBS (3x5 minutes) and a biotinylated second stage antibody was applied at the appropriate dilution (30 minutes) to bind to the primary antibody. The biotinylated enzyme, horseradish peroxidase, was bound to free avidin solution (Vector Laboratories, U.K.) and left at room temperature for at least 30 minutes prior to use to allow avidin-biotin-peroxidase complexes to form. The sections were washed with TBS (3x5 minutes) and the avidin biotin-peroxidase complexes were applied to the sections for 30 minutes. The sections were washed with TBS (3x5 minutes) and the chromogen, diaminobenzidine (DAB) (BioGenex, U.S.) (Appendix 9.1), was applied (5 minutes). This enzyme substrate was catalysed by horseradish peroxidase to induce a colorimetric reaction, which produced an insoluble-brown precipitate in the vicinity of the target antigen. The sections were washed under tap water (5 minutes), counterstained with Mayer's haematoxylin (1 minute) and washed with tap water again (5 minutes). Counterstaining enabled optimal contrast between the stained cells of interest (brown) and the unstained cells (blue) in the tissue by binding to cell nuclei. Finally, the sections were dehydrated through 70% alcohol (1 minute), 100% alcohol (2x1 minute) and clearene (3x2 minutes) in order to enhance image quality during microscopy, and then mounted in pertex mounting medium and covered with a coverslip (Sigma-Aldrich,U.K.) (Hsu et al., 1981).

2.12 Antibodies used for immunohistochemistry

A polyclonal rabbit antibody (Abcam, U.K.) was used to stain for *S. pneumoniae*, with known reactivity against *S. pneumoniae* serotypes 3, 4, 6, 7, 9, 14, 18, 19 and 23, but was un-titrated and untested for immunohistochemistry application. To determine the optimum working dilution, a range of antibody dilutions were tested with pneumococcal S14 pure cultures. The optimal dilution was assessed by the antibody dilution that resulted in the highest proportion of stained (brown) versus counterstained (blue) pneumococcal cells, in addition to the uniformity of staining. For each tested dilution, enzymatic, heat-induced and no treatment antigen retrieval techniques (section 2.10) were performed in order to determine the optimum pre-treatment for unmasking the target antigen (i.e. S14) for the primary antibody to successfully bind to. For each antigen retrieval technique, a negative control was used, as previously described (section 2.9). A swine anti-rabbit (SaR) antibody (Dako, U.K.) was used as the secondary antibody at a dilution of 1:400. This antibody was optimised prior to this project.

Pure cultures of S14 were also used as a positive control for pneumococcal staining in S14 spiked adenoid tissue, while a negative control was used as previously described (section 2.9). To optimise visualisation of pneumococcus against the counterstained cells in S14 spiked adenoid tissue, two different counterstains - Mayer's haematoxylin and Methyl green (BDH Chemicals, U.K.) (Appendix 9.1) - were used.

Monoclonal mouse anti-human CD68 (Dako, U.K.) and mouse monoclonal anti-human neutrophil elastase (NE) (Dako, U.K.) primary antibodies were selected for staining for macrophages and neutrophils, respectively, as they are frequently used to detect these immune cells in tissue. The optimum working dilutions and pre-treatments for visualising CD68 and NE had previously been optimised in the laboratory in tonsil tissue prior to this project. A rabbit anti-mouse (RaM) antibody (Dako, U.K.) at an also previously optimised dilution was used as the secondary antibody to stain for both macrophages and neutrophils, and a negative control was used to stain for CD68 and NE in adenoid tissue, as previously described (section 2.9). The positive controls for CD68 and NE were performed by staining with monoclonal mouse anti-human Ki67 (Dako, U.K.) and monoclonal mouse anti-human Pan CK (Sigma-Aldrich, U.K.) primary antibodies, respectively, in tonsil tissue. Staining for Ki67 and Pan CK had also previously been optimised in the laboratory prior to this project; requiring the same secondary RaM antibody for staining CD68 and NE, and requiring the same antigen pre-treatments as CD68 (microwave citrate) and NE (pronase). A full list of the antibodies used for immunohistochemistry experiments is shown in Table 7.

Table 7: Antibodies used for immunohistochemistry experiments

Primary antibody	**Target antigen**	**Antigen retrieval technique**	**Dilution**	**Supplier**
Polyclonal rabbit anti-*S. pneumoniae*	*S. pneumoniae* serotypes 3, 4, 6, 7, 9, 14, 18, 19 and 23	No pre-treatment	1:1200 (Chapter 3, sections 3.4 and 3.5)	Abcam
Monoclonal mouse anti-human CD68 IgG3	Macrophages	Microwave citrate	1:200	Dako
Monoclonal mouse anti-human NE IgG1	Neutrophils	Pronase	1:200	Dako
Monoclonal mouse anti-human Ki67	All growing cells, not G0 resting cells	Microwave citrate	1:100	Dako
Monoclonal mouse anti-human pan cytokeratin (Pan CK)	Cytokeratins 1, 4, 5, 6, 8, 10, 13, 18 and 19	Pronase	1:4000	Sigma-Aldrich
Secondary antibody				
Swine anti-rabbit (SaR)	*S. pneumoniae* primary antibody	Not applicable	1:400	Dako
Rabbit anti-mouse (RaM)	CD68, NE, Ki67 and Pan CK primary antibodies	Not applicable	1:400	Dako

2.13 Immunofluorescence to stain for S14 and macrophages in spiked adenoid tissue

To perform dual fluorescent staining of pneumococcus and macrophages in the same adenoid section, a technique known as immunofluorescence was used. In a similar way to immunohistochemistry, immunofluorescence involves incubation of the chosen tissue with a primary antibody. However, a secondary antibody that is conjugated to a fluorophore is then applied to the tissue. Fluorophores are excited via the use of wavelength-appropriate lasers to emit different colours of light, which can be used to identify the presence and localisation of different cell markers in the same section of tissue.

The same primary antibodies and optimised dilutions for staining pneumococcus and macrophages using immunohistochemistry (Table 7) were used for immunofluorescence experiments. In a similar way to optimising the polyclonal rabbit anti-*S. pneumoniae* primary antibody, secondary conjugated goat antibodies were optimised in order to discover their optimum working concentrations. Pure cultures of S14 were used to optimise the secondary conjugated antibody for pneumococcal staining, and S14 spiked sections were used to optimise the secondary conjugated antibody for macrophage staining. To act as a negative control, the primary antibody was omitted and replaced with TBS. Additionally, the secondary antibodies were used to stain for both targets of interest to ensure that there was no cross-reactivity between the secondary and primary antibodies.

2.14 Immunofluorescence protocol

Formalin-fixed (section 2.6), paraffin-embedded (section 2.6.1) sections were deparaffinised in clearene (2x5 minutes) and rehydrated through 100% alcohol (2x5 minutes) and 70% alcohol (5 minutes). The sections were then pre-treated with the pronase antigen retrieval technique as previously described (section 2.10.1), and permeabilised where appropriate (macrophage staining) with 0.5% saponin (Sigma-Aldrich, U.K.) in TBS for 10 minutes, followed by further washes in TBS (2x5 minutes). The sections were stained with 10% serum (Dako, U.K.) from the species from which the secondary antibody was raised in (i.e. goat) for 30 minutes. This step prevented Fc receptor binding of both the primary and the secondary antibody, and also helped to minimise the secondary antibody cross-reacting with endogenous immunoglobulins in the tissue. After two further washes in TBS (2x5 minutes), the primary antibody at the optimised dilution was applied in 1% bovine serum albumin (BSA) (Sigma-Aldrich, U.K.) for overnight incubation at 4°C.

The sections were washed in TBS (3x5 minutes) and the secondary conjugated antibody was applied in 1% BSA for 1 hour to bind to the primary antibody. After washing the sections in TBS (3x5 minutes), the sections were counterstained with a fluoroshield mounting medium with 4',6-diamidino-2-phenylindole (DAPI) (Abcam, U.K.) and covered with a coverslip. This aqueous mounting medium contains a fluorescent dye that binds to DNA and stains the nuclei, which can be visualised when illuminated with UV light. Finally, to prevent evaporation of the aqueous medium and movement of the coverslip, the edges of the coverslip were sealed with nail polish. The sections were then viewed with a Leica SP8 confocal microscope, as previously mentioned (section 2.4).

2.15 Antibodies used for immunofluorescence

The primary antibodies that were used to stain pneumococcus and macrophages using the immunohistochemistry protocol (Table 7) were used to stain for the same cell markers in spiked adenoid tissue using indirect immunofluorescence. To detect and visualise pneumococcus in patient adenoid tissue a rabbit pneumococcal Omni primary antibody (Oxford Biosystems, U.K.) was used, which is reactive against 91 pneumococcal serotypes. A goat anti-rabbit IgG secondary antibody conjugated with Alexa Fluor 488 (Fisher Scientific, U.K.) was used to bind to the polyclonal rabbit anti-*S. pneumoniae* primary antibody (in spiked adenoids) and to the primary pneumococcal Omni antibody (in patient adenoids) for pneumococcal staining. A goat anti-mouse IgG secondary antibody conjugated with Alexa Fluor 568 (Fisher Scientific, U.K.) was used to bind to the monoclonal mouse anti-human CD68 IgG3 primary antibody (in spiked and patient adenoids) for macrophage staining. A full list of antibodies used for immunofluorescence experiments is shown in Table 8.

Table 8: Antibodies used for immunofluorescence experiments

Primary antibody	**Target antigen**	**Antigen retrieval technique**	**Dilution**	**Supplier**
Polyclonal rabbit anti-*S. pneumoniae*	*S. pneumoniae* types 3, 4, 6, 7, 9, 14, 18, 19 and 23	Pronase	1:1200	Abcam
Monoclonal mouse anti-human CD68 IgG3	Macrophages	Pronase	1:200	Dako
Polyclonal rabbit pneumococcal Omni	91 serotypes of pneumococcus	Pronase	1:100 (Chapter 4, section 4.7)	Oxford Biosystems
Secondary antibody				
Goat anti-rabbit IgG, Alexa Fluor 488 conjugate	Polyclonal rabbit anti-*S. pneumoniae* and Omni antibody	Not required	1:2000 (Chapter 4, section 4.4)	Fisher Scientific
Goat anti-mouse IgG, Alexa Fluor 568 conjugate	Monoclonal mouse anti-human CD68 IgG3	Not required	1:400 (Chapter 4, section 4.4)	Fisher Scientific

2.16 Cell culture and co-culture methods

16HBE14o- cells are an adenovirus transformed epithelial cell line (16HBE cells) derived from human bronchial epithelium (kindly gifted by Dr. Dieter Gruenert, University of California), and were used for all co-culture experiments in this project. This cell line is referred to from now on as 16HBE cells. As this project involved developing an established co-culture model, an epithelial cell line was more preferable in order to generate reproducible results and limit inter-assay variation that can occur when primary cells are used.

Minimum essential medium (MEM) (Gibco, Life Technologies, U.K.) was used for all co-culture experiments in order to represent the nutritionally poor nasopharynx *in vivo*, and since Marks et al. and Moscoso et al. showed inferior biofilm formation (as measured by CFUs and transformation efficiency) when a nutrient-rich medium was used (Marks et al., 2012a, Marks et al., 2012b, Moscoso et al., 2006). Each 500 ml bottle of MEM was supplemented (sMEM) with 50 ml fetal calf serum (FCS), 5 ml L-glutamine (200 mM), 5 ml penicillin-streptomycin (50 μg/ml) (all Gibco, Life Technologies, U.K.) and 1 ml nystatin (100 μg/ml) (Sigma-Aldrich, U.K.). The purpose of these additives is listed in Table 9.

Table 9: Constituents of minimum essential medium (MEM) used for co-culture experiments

Constituent	**Purpose**
Fetal calf serum	Fetal blood to provide the cells with nutrients and growth factors
L-glutamine	An essential amino acid required for cell growth and function
Penicillin-streptomycin	Antibiotics used for reducing the risk of a bacterial contamination
Nystatin	Antifungal used to reduce the risk of a fungal contamination

2.17 Culture of human bronchial epithelial cells

16HBE cells from a frozen stock were used to seed a T75 flask (Corning Life Sciences, Fisher Scientific, U.K.) with 2-3 million cells and supplemented with 13 ml of sMEM at 37°C/5% CO_2 until at least 90% confluent. Confluence was assessed with an inverted microscope at x10 magnification. Once confluent, the sMEM was replaced with 10 ml of HBSS to remove any residual medium and incubated for 5 minutes at 37°C/5% CO_2. The HBSS was replaced with 5 ml of 0.25% trypsin/EDTA (Gibco, Life Technologies, U.K.) and incubated at 37°C/5% CO_2 for 5 minutes to detach the 16HBE cells from the surface of the T75 flask. As trypsin is a proteolytic enzyme, it causes the breakdown of proteins that cells use to attach to the flask. The flask was then gently knocked to encourage further dissociation and the cells were checked for dissociation using the inverted microscope. If the cells had not sufficiently dissociated then dissociation was monitored after every minute of additional incubation.

After the 16HBE cells were floating freely, 13 ml of sMEM was added in order for the FCS to competitively inhibit the enzymatic activity of trypsin. The suspension was placed into a 30 ml universal tube (Greiner Bio-One, U.K.) and centrifuged for 5 minutes at 1000 x *g*. The supernatant was removed and the pellet was resuspended in 1 ml of sMEM. 150 µl of this cell suspension was pipetted into a new T75 flask with 13 ml of sMEM ready for the next passage; the 16HBE cells were given fresh sMEM after two days and passaged once a week. In addition, 20 µl of the cell suspension was used to perform a cell count (below).

2.18 16HBE cell count: enumeration for multiplicities of infection

In order to obtain single 16HBE cells, the 30 ml universal tube containing the resuspended pellet was flicked several times to encourage separation of any clumps of cells in the tube. 20 µl of the resuspended pellet was then immediately placed into a 1.5 ml microcentrifuge tube (Fisher Scientific, U.K.) and supplemented with 20 µl 0.4% trypan blue viability dye (Fisher Scientific, U.K.). The microcentrifuge tube was flicked several times and 10 µl of this suspension was then used to perform a cell count using a haemocytometer chamber (Weber Scientific International, U.S.A.).

The 16HBE cells were counted under the haemocytometer in four 4x4 square grids with each grid representing 1 mm^2, and the average cell count from each 4x4 square grid was obtained. To account for the dilution with trypan blue, the average cell count was

multiplied by two, adjusted to read as X $x10^6$ cells/ml and multiplied by the volume of cell suspension to obtain the total number of cells.

2.19 Seeding a 12-well plate with transwell inserts

12-well co-culture plates with transwell membrane inserts (12 mm, 0.4 µm pore size, Corning, Fisher Scientific, U.K.) were used for all co-culture experiments. For seeding a transwell membrane in a 12-well plate, the total number of confluent 16HBE cells was obtained, as previously described (sections 2.17 and 2.18). Each transwell membrane was then seeded with 2.5 x 10^5 cells and supplemented with sMEM for a final volume of 0.5 ml. This suspension was pipetted on top of each membrane (apical surface), and 1 ml of sMEM was pipetted under each transwell (baso-lateral surface). The apical and baso-lateral medium was replaced with fresh sMEM daily.

2.20 Transepithelial resistance

Transepithelial resistance (TEER) is a surrogate measure of tight junction formation and cellular integrity by measuring resistance across the 16HBE cell monolayer. The TEER (Ohms.cm^2) was measured in each transwell by using a EVOM 2 epithelial voltohmmeter (World Precession Instruments, U.S.A.).

The voltohmmeter has two measuring prongs. The longer prong was placed to rest in the baso-lateral medium and the shorter prong was placed in the apical medium of each transwell and the readings were recorded. For standardisation, the TEER measurements were taken daily at the same time (one hour after changing the apical and baso-lateral medium with fresh sMEM) until confluent 16HBE cell monolayers had formed (typically, ~9000 Ohms.cm^2). For each reading, TEER was measured in each transwell three times with the means taken, and corrected by subtracting the mean TEER value of a transwell membrane containing sMEM without 16HBE cells (a baseline value typically at ~2000 Ohms.cm^2). TEER readings were measured in the same way at various time-points after infecting confluent 16HBE cell monolayers with pneumococcus.

2.21 Trypsinising 16HBE cell monolayers

To determine the number of 16HBE cells on the transwell membranes once confluent, a cell monolayer was trypsinised to obtain a cell count. Firstly, the apical and baso-lateral medium was replaced with 0.2 ml HBSS and the co-culture plate was incubated for 5 minutes at 37°C/5% CO_2. The HBSS was removed and 0.2 ml of 0.25% trypsin/EDTA was placed into the transwell insert. The co-culture plate was then incubated at 37°C/5% CO_2 for 5 minutes. The trypsin was removed and inactivated in 2.5 ml of antibiotic-free sMEM (10% FCS, 1% L-glutamine and 0.2% nystatin) in a 15 ml conical centrifuge tube. 0.5 ml of fresh trypsin was pipetted onto the apical surface of the cell monolayer and the co-culture plate was incubated at 37°C/5% CO_2 for 10 minutes. The plate was then gently knocked to encourage dissociation. If sufficient dissociation had not occurred, dissociation was monitored after every minute of additional incubation.

When the 16HBE cells were floating freely, the 0.5 ml of trypsin was pipetted into the 15 ml centrifuge tube and centrifuged at 1000 x *g* for 5 minutes. The supernatant was removed and the pellet was resuspended in 0.4 ml antibiotic-free sMEM. 20 µl of the cell suspension was added to 20 µl of 0.4% trypan blue solution to perform a cell count, as previously described (section 2.18).

2.22 Multiplicity of infection

By using the 16HBE cell count from a confluent monolayer of 16HBE cells (section 2.21), the epithelial cells were inoculated with a range of D39 pneumococcal loads for different multiplicities of infections (MOIs). MOI refers to the ratio of pneumococcal cells to epithelial cells. An uninoculated epithelial cell monolayer was used as a negative control in each experiment.

24 hours prior to, and immediately before inoculation with D39, the apical and baso-lateral medium from each transwell was replaced with antibiotic-free sMEM to ensure that any residual antibiotics (i.e. penicillin and streptomycin) were removed. For inoculation, 5 ml of mid-exponential-phase D39 (5 x 10^8 cells) (section 2.2) was centrifuged at 10,956 x *g* for 5 minutes, and the pellet resuspended in 5 ml antibiotic-free sMEM. To determine the dilution factor, 5 x 10^8 was divided by the 16HBE cell count total and divided by 5000 (equating to 5 ml). This answer was multiplied by two to provide the total resuspended volume required in 1 ml of fresh antibiotic-free sMEM. 10-fold serial dilutions were performed in antibiotic-free sMEM for a range of MOIs. Finally, the apical medium from each transwell was removed and replaced with 0.5 ml of each dilution.

2.23 Enumeration of pneumococcal cells on infected 16HBE cell monolayers

To ascertain how many individual D39 pneumococcal cells adhered to the infected 16HBE cell monolayers, CFUs were determined at numerous time-points after infection. At each time-point, the apical suspension was withdrawn and each transwell membrane was removed with sterile forceps and a scalpel and placed into a 12-well plate (Corning Incorporated, Costar, U.S.A.), which was supplemented with 0.5 ml of fresh antibiotic-free sMEM per well. The 12-well plate was gently rocked to remove unattached planktonic cells and the medium was replaced with 0.5 ml of fresh antibiotic-free sMEM. This washing step was repeated once more. Using a sterile cell scraper (Fisher Scientific, U.K.), the transwell membranes were vigorously scraped and each 0.5 ml cell suspension was briefly vortexed in 1.5 ml microcentrifuge tubes for 5 seconds to break up any remaining bacteria aggregates. 10-fold serial dilutions were performed in antibiotic-free sMEM and the spot plating method was performed, as previously described (section 2.3). The CFUs were counted after 18 hours.

2.24 Scanning electron microscopy co-culture analysis of a D39 pneumococcal biofilm and a 16HBE cell layer

To visualise adherent pneumococci on confluent 16HBE cell monolayers at various time-points post-infection, the epithelial cells were processed for SEM analysis. SEM analysis was performed twice for each MOI at every time-point that was measured; a minimum of three images were obtained for each MOI from the two samples. For each time-point, the transwell membranes were removed with a scalpel and placed in a 12-well plate supplemented with 0.5 ml of antibiotic-free sMEM per well. The 12-well plate was gently rocked to remove any unattached planktonic cells and the medium was replaced with 0.5 ml of fresh antibiotic-free sMEM. This washing step was repeated once more. The epithelial cells were fixed by placing them into individual wells of another 12-well plate containing 1 ml of 3% glutaraldehyde with 0.15% alcian blue in 0.1 M cacodylate buffer (all Agar Scientific, U.K.) for 24 hours at 4°C. The addition of alcian blue was performed to enhance the resolution of the samples by improving the deposition of the fixative, osmium tetroxide (below). The samples were rinsed in a 0.1 M cacodylate buffer for two 10 minute washes and post-fixed in 1% osmium tetroxide (Sigma-Aldrich, U.K.) in 0.1 M cacodylate buffer for 1 hour, followed by two 10 minute washes in 0.1 M cacodylate buffer. The samples were gradually dehydrated by placing them through an ethanol series of 30%, 50%, 70%, and 95% for 5 minutes in each solution, and stored in 100% ethanol for 24

hours at room temperature. The samples were critical point dried using a Balzers CPD 030 critical point dryer (BAL-TEC, Liechtenstein) by exchanging the 100% ethanol with liquid carbon dioxide, which was then heated to 31°C under pressure to ensure thorough drying of the samples. Finally, the samples were sputter coated using an E5100 sputter coater (Polaron, U.K.) to enhance the signal to noise ratio under the microscope, and all of the samples were examined using a FEI Quanta 250 scanning electron microscope.

2.25 Lactate dehydrogenase cytotoxicity assay

The cytotoxicity of D39 pneumococcus was determined by measuring the level of lactate dehydrogenase (LDH) released from the 16HBE cells. 16HBE cell monolayers were inoculated with a range of MOIs as previously described (section 2.22). At the end-point of the co-culture assay, the LDH Cytotoxicity Assay (Fisher Scientific, U.K., catalogue number 88953 88954), with all of the controls (Table 10), was performed according to the manufacturer's instructions (n = 3). Uninfected and non-lysed 16HBE cells were used to measure baseline, spontaneous levels of LDH release from epithelial cells, and served as a negative control (0% cytotoxicity). Uninfected but lysed 16HBE cells - lysed with lysis buffer solution - were used to determine the maximum release of LDH from epithelial cells, and served as a positive control (100% cytotoxicity). 50 µl of a LDH Positive Control (Appendix 9.2) - a reagent provided in the kit - was used in triplicate wells to demonstrate that the assay had worked. Absorbance was measured at 490 nm using an iMark Microplate Absorbance Reader (Bio-Rad, U.K.). To calculate cytotoxicity levels, the average LDH value of experimental wells (infected epithelial cells) was divided by the average value of maximum LDH (uninfected and lysed epithelial cells) using the following equation:

% Cytotoxicity = (Average Experimental value / Average Maximum LDH Release value) X 100

Table 10: Controls used for the LDH Cytotoxicity assay

Control	**Purpose**
Uninfected and non-lysed 16HBE cells	To determine the baseline value of LDH (0% cytotoxicity) from the epithelial cells
Uninfected but lysed 16HBE cells	To determine the maximum value of LDH (100% cytotoxicity) from uninfected and lysed epithelial cells
LDH positive control (reagent provided in the kit)	To demonstrate that the LDH cytotoxicity assay was functioning normally and experimental readouts could be trusted

2.26 Human Cytokine Magnetic Buffer Reagent Luminex assay

The apical medium of infected and uninfected 16HBE cell monolayers was harvested at various time-points post-infection, centrifuged at 1000 x *g* for 15 minutes at 4°C and the samples stored at -80°C until use. The concentration of extracellular cytokines released by the 16HBE cells was measured using a Human Cytokine Magnetic Buffer Reagent Kit (Fisher Scientific, U.K.) according to the manufacturer's instructions. Firstly, magnetic beads conjugated to antigen specific (cytokine) antibodies were used to bind to experimental samples containing unknown cytokines at unknown concentrations. Biotinylated detector antibodies were used to bind to the bead-immobilised cytokines. Next, streptavidin, which is conjugated to a fluorescent protein known as R-Phycoerythrin (RPE), was added. The amount of bead-associated fluorescence was analysed to measure the concentration of a panel of cytokines (Figure 2.2).

Standards were reconstituted in a solution of 50% Assay Diluent and 50% antibiotic-free sMEM for a total volume of 1 ml, and mixed well. A standard curve of the reconstituted standards was performed and used in duplicate along with blanks (Appendix 9.3). 25 µl of diluted Antibody Beads (Appendix 9.3) was pipetted into each well of a provided 96-well plate and protected from light for the remainder of the assay. The wells were washed twice with 200 µl of Wash Solution (Appendix 9.3).

50 µl of Incubation Buffer was added to all of the wells. 100 µl of the reconstituted and diluted standards was pipetted into the standard wells, 100 µl of the blanks was

pipetted into the background wells, and 50 µl of Assay Diluent and 50 µl of the harvested samples were pipetted into the sample wells. The plate was protected from light and incubated on an orbital plate shaker at 700 rpm for 2 hours at room temperature. The liquid was decanted and the wells were washed twice in the usual way. 100 µl of diluted Biotinylated Detector Antibody (Appendix 9.3) was added to each well. The plate was protected from light and incubated on an orbital plate shaker at 700 rpm for 1 hour. The liquid was decanted and the wells were washed twice. 100 µl of diluted Streptavidin-RPE solution (Appendix 9.3) was added to each well, the plate was protected from light and incubated on an orbital plate shaker at 700 rpm for 30 minutes. The liquid was decanted and the wells were washed 3 times. 150 µl of Wash Solution was added to each well and the plate was incubated on an orbital plate shaker at 700 rpm for 3 minutes. Finally, the plate was read with Bio-Plex 200 System software (Bio-Rad, U.K.) and the concentration of the harvested samples was determined from the standard curve.

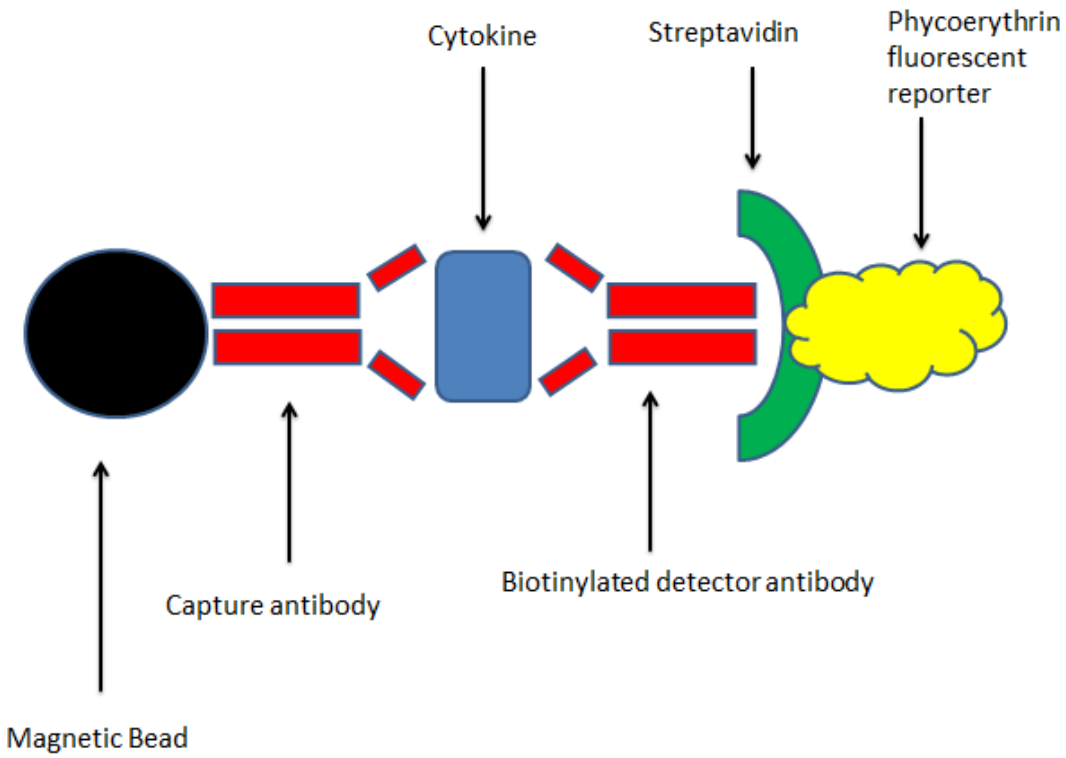

Figure 2.2: A Luminex magnetic bead-based immunoassay for the detection of cytokines.

2.27 Microscopic images of 16HBE cells

Photomicrographic images of 16HBE cells on transwell membranes were taken with the following camera and set-up:

Olympus, model number C-5060, and 4x high quality wide zoom lens with 5.1 mega pixels.

2.28 Statistical analysis

Statistical analysis was performed using GraphPad Prism version 7 software.

Gaussian distribution was determined via normality tests and histogram plots. For normal distribution of data, parametric tests were performed. Non-parametric tests were used for non-normal distribution of data.

One-way ANOVA with either Tukey's multiple comparisons test or Dunn's multiple comparisons test was used to compare each group with every other group from more than two groups.

One-way ANOVA and two-way ANOVA with Dunnett's multiple comparisons test were used to specifically test experimental groups (infected 16HBE cells) against a control group (uninfected 16HBE cells) at one time-point or over several time-points.

A Wilcoxon matched pairs test was used for two-group comparisons of cytokine concentrations from treated (infected) and controlled (uninfected) epithelial cells.

A statistical significance level of 0.05 was used throughout.

3 Chapter 3 - Development of an *ex vivo* model for studying the interaction between *S. pneumoniae* and host immune cells in adenoid tissue

3.1 Introduction

Pneumococcal biofilms have been shown to form on both the epithelial surface of adenoid tissue and on the middle ear mucosal epithelium (Hall-Stoodley et al., 2006, Hoa et al., 2009, Nistico et al., 2011). These studies suggest that nasopharyngeal biofilms on adenoids may act as a reservoir for otopathogenic bacteria and contribute to the pathogenesis of otitis media. Recent studies also suggest that despite being hyperadhesive on epithelial cells either *in vitro* or in mice, pneumococcal biofilms are less virulent and less invasive than their planktonic counterparts (Sanchez et al., 2011b, Marks et al., 2012a, Marks et al., 2013, Blanchette-Cain et al., 2013). These studies support the current theory that *S. pneumoniae* may colonise the nasopharynx as a biofilm and persist in the upper respiratory tract where they can resist antibiotic treatment and host defences. Such persistence may favour the transmission of pneumococcus to a new host or to different anatomical sites during favourable conditions. However, the detailed role of the cellular host innate immune response to a pneumococcal biofilm in adenoid tissue has not been directly investigated. In particular, it is unknown whether phagocytic cells have the capacity to engulf pneumococci residing in the biofilm phenotype.

3.2 Aims

The individual aims for the experiments described in this chapter were as follows:

- Assess the morphology of the S14 laboratory strain by using a haematoxylin and eosin (H&E) stain.
- Optimise protocols for using a polyclonal rabbit anti-*S. pneumoniae* primary antibody in order to stain pure cultures of the S14 strain using immunohistochemistry.
- Examine the S14 strain *in situ* in spiked adenoid tissue using the optimised anti-*S. pneumoniae* antibody.
- Evaluate pneumococcal biofilm aggregates in adenoid tissue.

- Identify macrophages and neutrophils in spiked adenoid tissue.
- Perform sequential section staining for pneumococcus, macrophages and neutrophils in spiked adenoid tissue to investigate co-localisation between pneumococcus and these innate immune cells.

3.3 Visualisation of a S14 pneumococcal strain in adenoid tissue using haematoxylin and eosin staining

A *S. pneumoniae* S14 pure culture (Chapter 2, section 2.7) and two adenoids spiked with S14 (Chapter 2, section 2.6) were sectioned with a microtome to obtain two sections per sample (Chapter 2, section 2.6.2) and then underwent H&E staining (Chapter 2, section 2.8).

This method stained pneumococcus alone (Figure 3.1, A) and also identified pneumococci in adenoid tissue (Figure 3.1, B-D). Pneumococcal cellular morphology was similar in both the pure culture and adenoid tissue, with pneumococci appearing as lancet-shaped cells, approximately 1 µm in diameter. Pneumococci were stained violet due to the negatively charged DNA of the bacteria binding to positive charges in the basic haematoxylin dye. Cells in the adenoid tissue also stained violet, whilst positively charged proteins in the tissue were reddish/pink due to the negative charge of the acidic eosin dye. Pneumococci in the spiked adenoids were in distinct clusters, with individual cells observed (Figure 3.1, B-D). However, due to the dark pigmentation of the other cells in the adenoid, it was difficult to determine whether pneumococci were present unless they were in the periphery of the tissue or where there were clear areas in the tissue (Figure 3.1, B-D). H&E staining was performed for subsequent adenoids to assess the structural morphology of the tissue prior to performing immunolabelling experiments.

A Pure culture of pneumococcus (positive control)

B Pneumococcus in spiked adenoid tissue

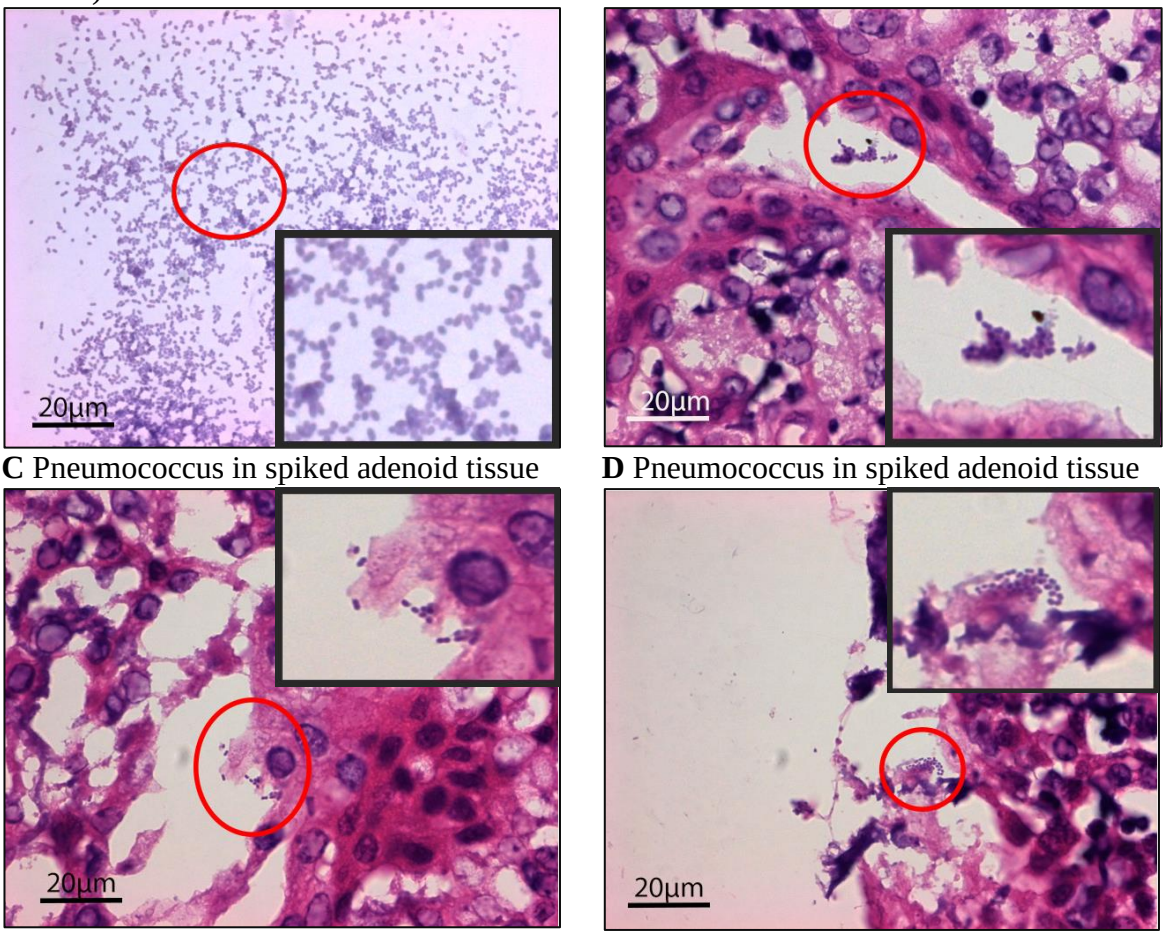

C Pneumococcus in spiked adenoid tissue

D Pneumococcus in spiked adenoid tissue

Figure 3.1: Identification of *S. pneumoniae* S14 in adenoid tissue by haematoxylin and eosin staining

Representative images from two sections of a pure culture sample and from two sections per spiked adenoid. Pneumococcus alone stained with haematoxylin following H&E staining (A), and was also detected in both spiked adenoids (as indicated with red circles) (B-D). In both cases, pneumococci were lancet-shaped and approximately 1 µm in diameter. In spiked adenoid tissue, pneumococci were found in distinct clusters, evidenced more clearly in the inlaid images. Images were taken using a Zeiss light microscope with a x100 oil immersion lens.

3.4 Optimisation of a polyclonal rabbit anti-*S. pneumoniae* antibody using immunolabelling

Pure cultures of *S. pneumoniae* S14 strain were used to determine the optimum antigen retrieval technique and the appropriate dilution of the polyclonal rabbit anti-*S. pneumoniae* primary antibody to identify pneumococci without nonspecific or background staining. Serial dilutions of the primary antibody in TBS ranging from 1:250 to 1:8000 were performed. A separate pure culture section was used for each dilution and for each pre-treatment. For each dilution, no pre-treatment, pronase, microwave citrate, microwave EDTA and pressure cooker citrate pre-treatments were used (Chapter 2, 2.10), and a negative control was also included for each pre-treatment (Table 11), as previously described (Chapter 2, section 2.9).

Table 11: Antigen retrieval techniques and dilutions used to optimise protocols using a primary rabbit anti-*S. pneumoniae* antibody for *in situ* labelling of bacteria in tissue

Antigen retrieval technique	**Tested dilutions of polyclonal rabbit anti-*S. pneumoniae* primary antibody**	**Negative control**
No treatment	1:250, 1:500, 1:1000, 1:2000, 1:4000, 1:8000	Omission of the primary antibody
Pronase	1:250, 1:500, 1:1000, 1:2000, 1:4000, 1:8000	
Microwave citrate	1:250, 1:500, 1:1000, 1:2000, 1:4000, 1:8000	
Microwave EDTA	1:250, 1:500, 1:1000, 1:2000, 1:4000, 1:8000	
Pressure cooker citrate	1:250, 1:500, 1:1000, 1:2000, 1:4000, 1:8000	

Individual S14 pneumococcal cells stained brown for each pre-treatment (data not shown), and when no pre-treatment was used (Figure 3.2). Regardless of the treatment, there was little difference in the degree of staining (intensity of the brown stain) when the primary antibody was diluted 1:250, 1:500 and 1:1000 (Figure 3.2, A-C). At higher dilutions, 1:2000, 1:4000 and 1:8000, staining became progressively weaker, with a proportion of the pneumococcal cells stained blue with the counterstain, Mayer's haematoxylin (Figure 3.2, D-F). Although the counterstain procedure was consistent between the different pre-treatments and different dilutions, counterstain staining was not observed with high concentrations of the primary antibody; binding to all of the pneumococcal cells. As expected, all of the individual pneumococcal cells were stained

blue with the counterstain when the primary antibody was omitted and buffer (TBS) was used (negative control) (Figure 3.2, G).

A 1:250 anti-*S.pneumoniae* primary antibody

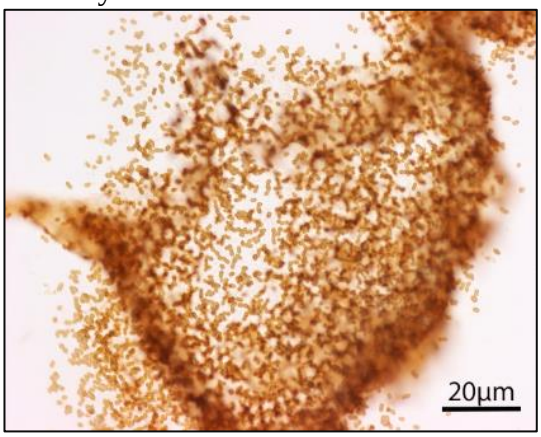

B 1:500 anti-*S.pneumoniae* primary antibody

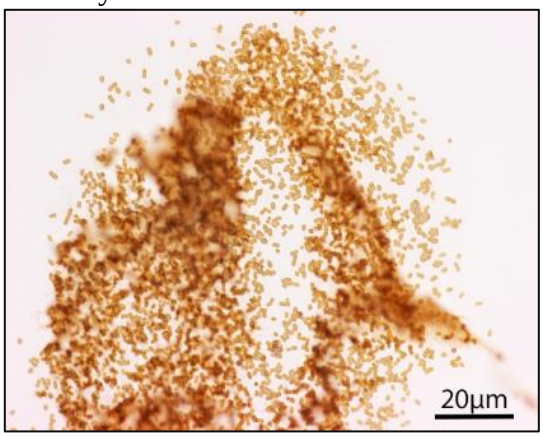

C 1:1000 anti-*S.pneumoniae* primary antibody

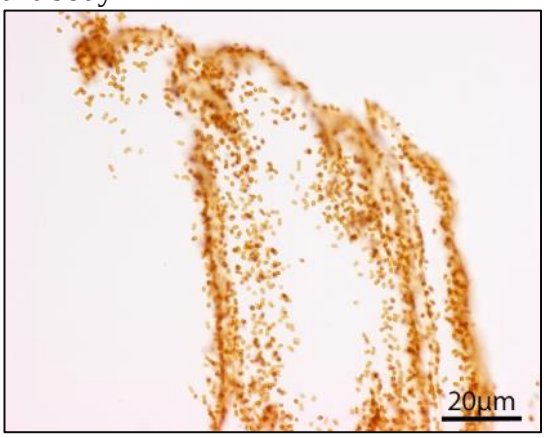

D 1:2000 anti-*S.pneumoniae* primary antibody

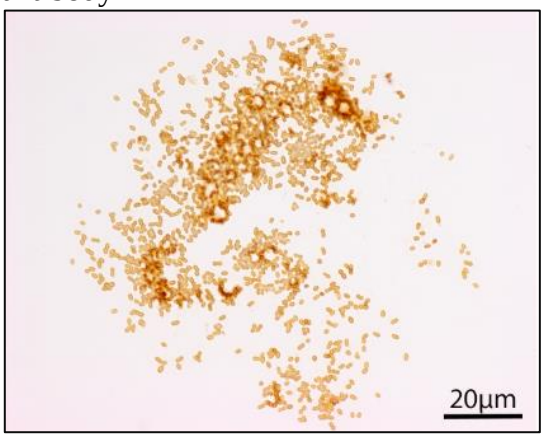

E 1:4000 anti-*S.pneumoniae* primary antibody

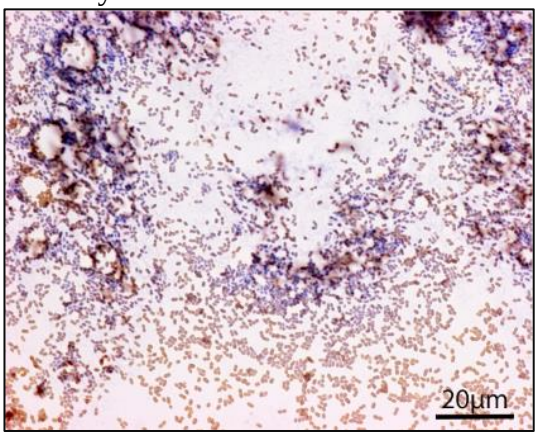

F 1:8000 anti-*S.pneumoniae* primary antibody

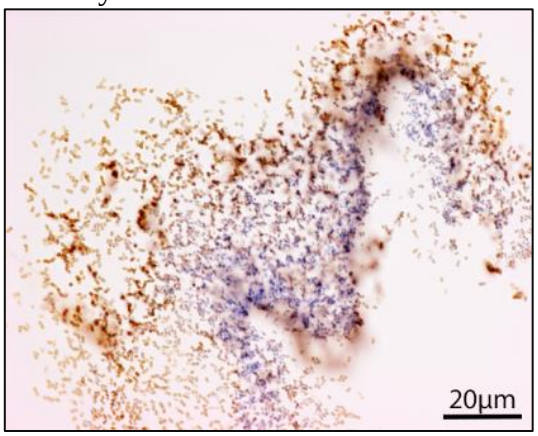

G Omitted primary antibody (negative control)

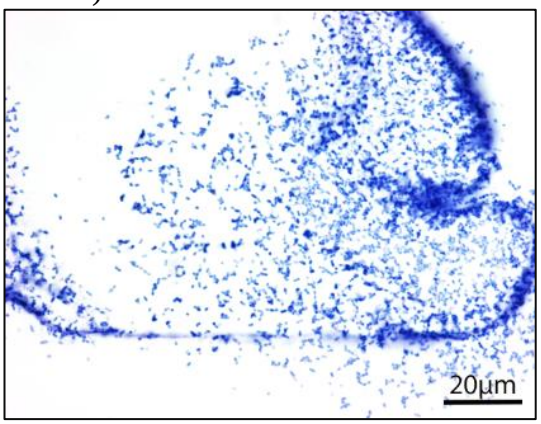

Figure 3.2: Titration of a polyclonal rabbit anti-*S. pneumoniae* primary antibody without an antigen retrieval protocol.

S. pneumoniae S14 stained evenly (brown) with the following dilutions: 1:250 (A), 1:500 (B) and 1:1000 (C). Ineffective staining was observed with dilutions 1:2000 (D), 1:4000 (E) and 1:8000 (F). Pneumococci were stained (blue) with the counterstain Mayer's haematoxylin in the absence of the anti-*S. pneumoniae* primary antibody (G). Images were taken using a Zeiss light microscope with a x100 oil immersion lens.

3.5 Fine-tune titration of polyclonal rabbit anti-*S. pneumoniae* antibody

Pure cultures of pneumococcus were stained with a dilution of 1:1000 (Figure 3.2, C), but the staining became progressively weaker above 1:2000 (Figure 3.2, D-F). Therefore, further titrations were tested to further resolve the dilution of the anti-*S. pneumoniae* antibody for the best sensitivity. Dilutions 1:1200, 1:1400, 1:1600 and 1:1800 were tested. Since all antigen retrieval pre-treatments were successful in staining pneumococcus, these same antigen retrieval techniques were used at each dilution except for the pressure cooker pre-treatment. Pressure cooker pre-treatment is the most abrasive antigen retrieval technique, since heating methods that unmask a target antigen can cause unbalanced epitope retrieval due to the formation of hot and cold spots in the tissue. A separate pure culture sample was again used for each dilution and for each pre-treatment. Negative controls were included for each treatment, as previously described (Chapter 2, section 2.9).

Pneumococcal cells were stained with all of the tested dilutions, even without any pre-treatment (Figure 3.3). Optimal staining intensity and uniformity without any pre-treatment was seen with the 1:1200 dilution (Figure 3.3, A). No staining was observed without the primary antibody (Figure 3.3, E). Therefore, the anti-*S. pneumoniae* primary antibody was used at a dilution of 1:1200 for all subsequent assays to identify pneumococcus in adenoid tissue.

A 1:1200 anti-*S.pneumoniae* primary antibody

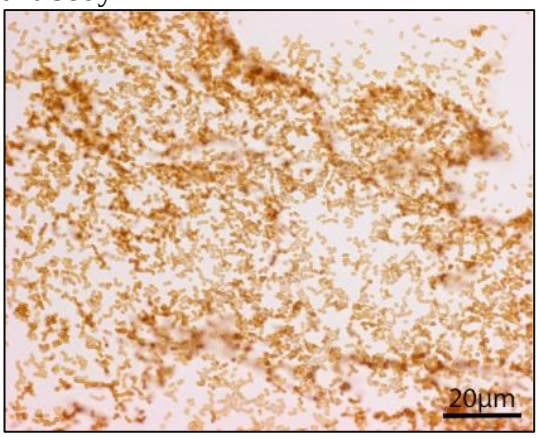

B 1:1400 anti-*S.pneumoniae* primary antibody

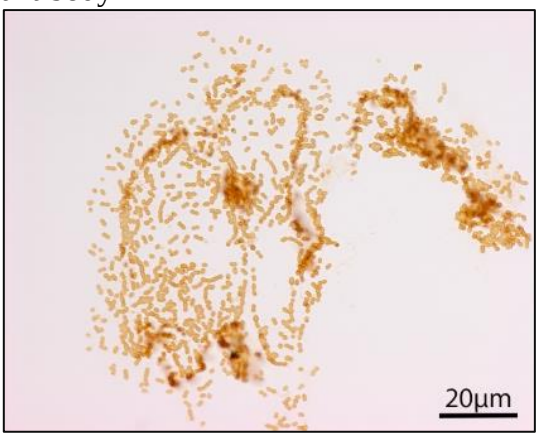

C 1:1600 anti-*S.pneumoniae* primary antibody

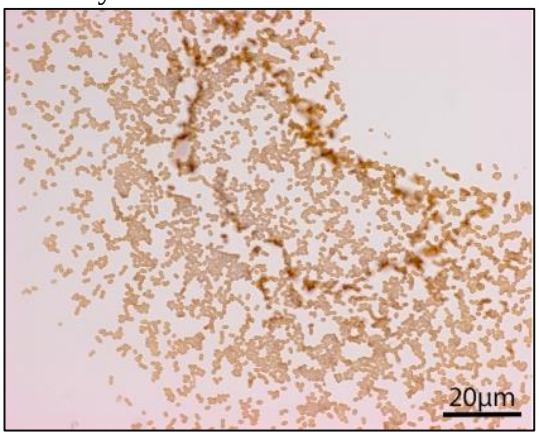

D 1:1800 anti-*S.pneumoniae* primary antibody

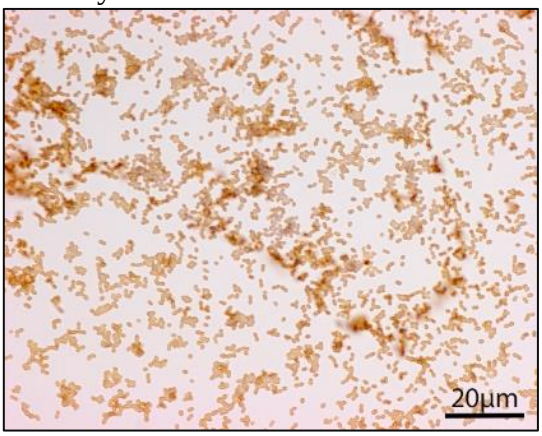

E Omitted primary antibody (negative control)

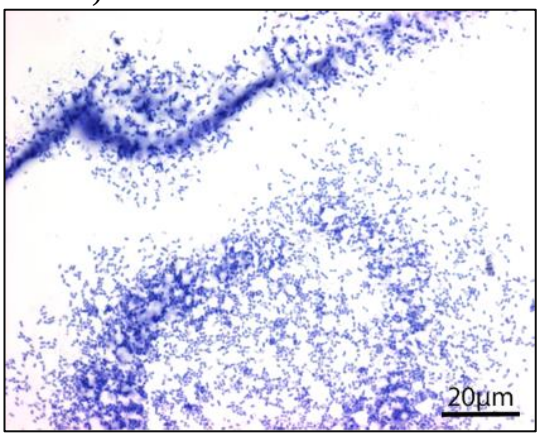

Figure 3.3: Fine-tune titration of a polyclonal rabbit anti-*S. pneumoniae* primary antibody without an antigen retrieval technique.

S. pneumoniae S14 was stained (brown) with the following dilutions 1:1200 (A), 1:1400 (B), 1:1600 (C) and 1:1800 (D). Optimal staining intensity and uniformity was achieved with 1:1200 dilution (A). Pneumococci were stained (blue) with the counterstain Mayer's haematoxylin in the absence of the anti-*S. pneumoniae* primary antibody (E). Images were taken using a Zeiss light microscope with a x100 oil immersion lens.

3.6 Staining for S14 in spiked adenoid tissue

No pre-treatment, together with a primary antibody dilution of 1:1200, were used in order to stain pneumococcus in two adenoids spiked with the S14 strain, as previously described (Chapter 2, section 2.6). Two sections were stained on the same day from one adenoid, followed by two sections on another day from the other spiked adenoid. The immunohistochemistry protocol and inclusion of a negative control per adenoid were used as previously described (Chapter 2, sections 2.9 and 2.11). As a positive control, a S14 pure culture of pneumococcus was stained per adenoid with the optimised antibody dilution (1:1200), with no pre-treatment. The counterstain, Mayer's haematoxylin, was used to highlight the nuclei and the morphological structure of host cells in the tissue.

As expected, appropriate staining was observed for both the positive and negative controls (data not shown). Pneumococci were successfully stained in both sections from both of the two spiked adenoids, and clusters of pneumococci were detected (Figure 3.4, A). However, locating the pneumococcus in the tissue using light microscopy was extremely time-consuming, and visualisation of the pneumococcus was frequently impaired by the dark pigmentation of the counterstain.

To enhance visualisation of pneumococcus in adenoid tissue, the experiment was repeated with the same spiked adenoids and the same controls, but the incubation period with Mayer's haematoxylin was shortened. Although this experimental change made it easier to visualise pneumococcal cells in the adenoid tissue, the shorter incubation time with the counterstain did not provide sufficient contrast between the stained pneumococcal cells and the faintly counterstained cells (Figure 3.4, B). It was also difficult for the stained and counterstained cells to be resolved simultaneously in the same focal plane. Consequently, the experiment was repeated using sections from the same adenoids but with an alternative counterstain (Methyl green) to improve resolution. Similar to Mayer's haematoxylin, Methyl green is a widely used counterstain for immunohistochemistry with a lighter pigmentation, and resulted in clearer visualisation of the pneumococcal cells, and provided sufficient contrast to the counterstained cells (Figure 3.4, C). These experiments demonstrated that, irrespective of the type of counterstain used or the incubation time, distinct clusters of pneumococcal cells were identified in spiked adenoid tissue, with an optimal primary antibody dilution of 1:1200 and no pre-treatment of the tissue.

A Pneumococcus with Mayer's haematoxylin counterstain (prolonged incubation)

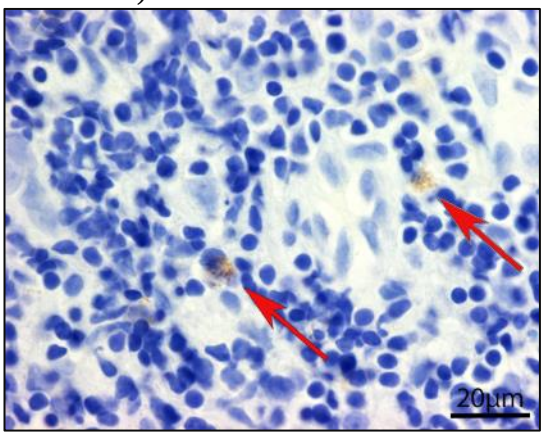

B Pneumococcus with Mayer's haematoxylin counterstain (shortened incubation)

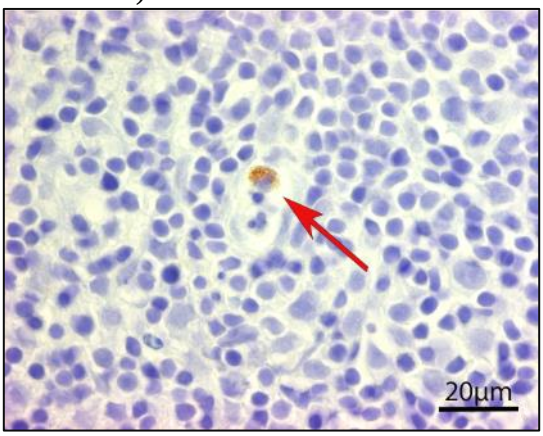

C Pneumococcus with Methyl green counterstain

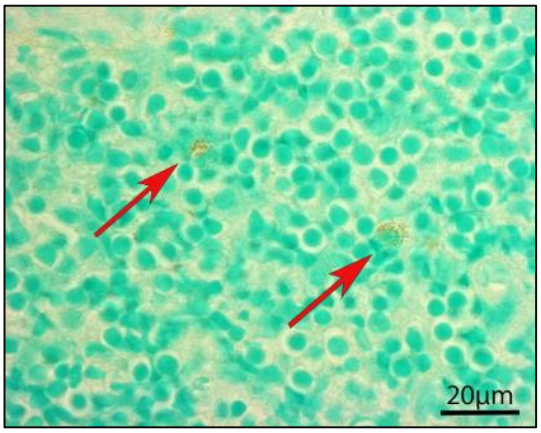

Figure 3.4: Nuclear counterstaining for *S. pneumoniae* in S14 spiked adenoid tissue.

S. pneumoniae was successfully stained (brown; depicted with red arrows) in spiked adenoid tissue using Mayer's haematoxylin (A-B) and Methyl green (C) counterstains. Representative images from the same two adenoids for each condition are shown. Although a shorter incubation time with Mayer's haematoxylin permitted clearer visualisation of the pneumococcus (B), incubation with Methyl green provided sufficient contrast between pneumococci and counterstained host cells (C). Images were taken using a Zeiss light microscope with a x100 oil immersion lens.

3.7 Staining for macrophages in spiked adenoid tissue

Having optimised the staining protocol for pneumococcus in spiked adenoid tissue (Figure 3.4) the immunohistochemistry protocol was used to identify macrophages in one of the spiked adenoids used to stain for pneumococcus (section 3.6).

Two adenoid sections were treated with a microwave citrate antigen retrieval protocol, and a monoclonal mouse anti-human CD68 IgG3 primary antibody was used (1:200 dilution), followed by a rabbit anti-mouse secondary antibody (1:400 dilution). Omission of the primary antibody served as a negative control. A monoclonal mouse anti-human Ki67 primary antibody was used (1:100 dilution) in a section of tonsil tissue to act as a positive control, as previously described (Chapter 2, section 2.12). These antibodies had already been optimised prior to this project.

Macrophages were stained in both sections of the adenoid tissue using the monoclonal mouse anti-human CD68 primary antibody and Methyl green as the counterstain (Figure 3.5, A). Macrophages were not labelled without the primary antibody (Figure 3.5, B). In comparison, Ki67 was successfully stained in tonsil tissue (Figure 3.5, C). The results from the negative and positive control confirmed that the immunohistochemistry protocol identified macrophages in the tissue.

A 1:200 anti-CD68 primary antibody

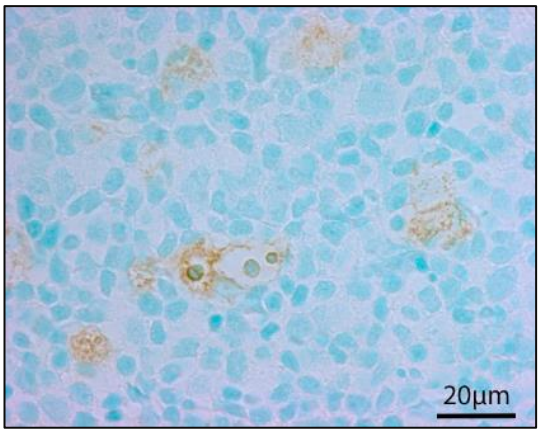

B Omitted primary antibody (negative control)

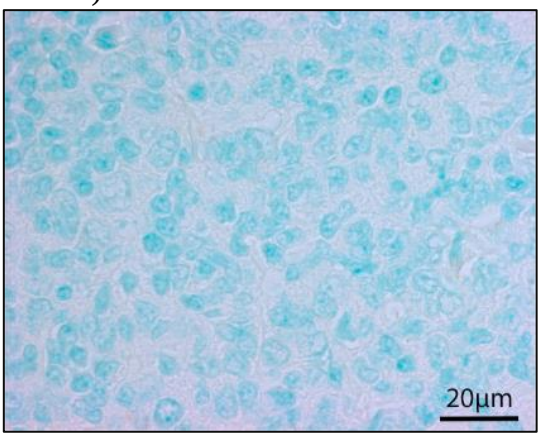

C 1:100 anti-Ki67 primary antibody (positive control)

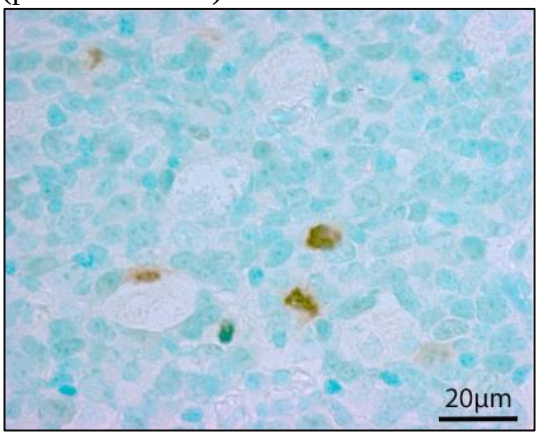

Figure 3.5: Staining for the macrophage cell marker CD68 in S14 spiked adenoid tissue.

Representative images of two sections from a spiked adenoid show macrophages were stained (brown) with a monoclonal mouse anti-human CD68 primary antibody (1:200 dilution), followed by a rabbit anti-mouse secondary antibody (1:400 dilution), with microwave citrate pre-treatment of the tissue (A). Macrophages were not stained without the primary antibody (B). As a positive control, Ki67 was stained in a section of tonsil tissue, with the same antigen retrieval technique and secondary antibody (C). Images were taken using a Zeiss light microscope with a x100 oil immersion lens.

3.8 Staining for neutrophils in spiked adenoid tissue

To stain for neutrophils, the same adenoid that was used to stain pneumococcus (section 3.6) and macrophages (section 3.7) was pre-treated with pronase and incubated with a monoclonal mouse anti-human NE IgG1 primary antibody (1:200 dilution), followed by a rabbit anti-mouse secondary antibody (1:400 dilution). Omission of the primary antibody served as a negative control. Cytokeratin was stained in a section of tonsil tissue with a monoclonal mouse anti-human Pan CK primary antibody (1:4000 dilution), to serve as a positive control, as previously described (Chapter 2, section 2.12). These antibodies had been optimised prior to this project.

Similar to macrophage staining in spiked adenoid tissue (Figure 3.5, A), neutrophils were successfully stained in both of the adenoid sections (Figure 3.6, A). Neutrophils were not stained without the primary anti-human NE antibody (Figure 3.6, B). Cytokeratin was stained with the anti-human Pan CK antibody, with copious staining detected on the edges of the tonsil tissue (Figure 3.6, C). These results were indicative that the immunohistochemistry protocol identified neutrophils in adenoid tissue.

A 1:200 anti-NE primary antibody

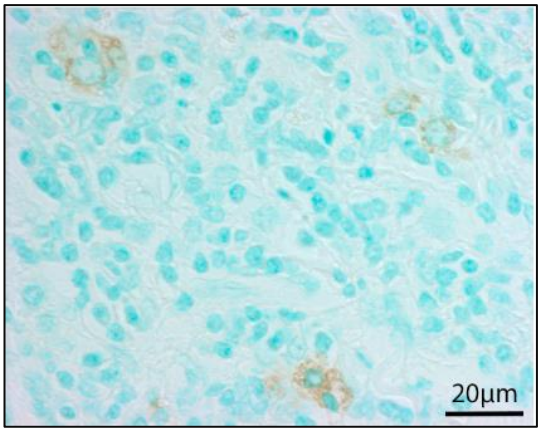

B Omitted primary antibody (negative control)

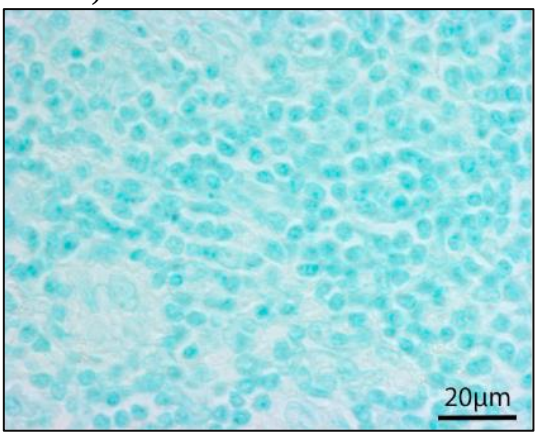

C 1:4000 anti-Pan CK primary antibody (positive control)

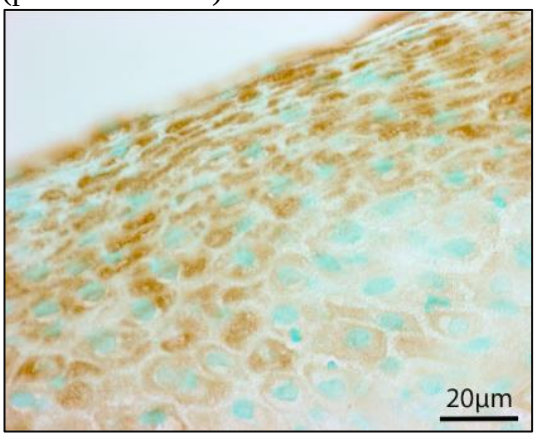

Figure 3.6: Staining for the neutrophil cell marker NE in S14 spiked adenoid tissue.

Representative images of two sections from a spiked adenoid show neutrophils were stained (brown) with a monoclonal mouse anti-human NE primary antibody (1:200 dilution), followed by a rabbit anti-mouse secondary antibody (1:400 dilution), with pronase pre-treatment of the tissue (A). Neutrophils were not stained without the primary antibody (B). As a positive control, cytokeratin was stained in a section of tonsil tissue, with the same antigen retrieval technique and the same secondary antibody (C). Images were taken using a Zeiss light microscope with a x100 oil immersion lens.

3.9 Sequential section staining to detect pneumococcal-host co-localisation in spiked adenoid tissue

To demonstrate pneumococcal co-localisation with macrophages and/or neutrophils in S14 spiked adenoid tissue an immunohistochemistry technique known as sequential section staining was tested. Three consecutive (sequential) sections per spiked adenoid were prepared using a microtome (4 µm sections), and individually stained for macrophages, pneumococci or neutrophils, as previously described (Chapter 2, section 2.11).

Four spiked adenoids were used to examine co-localisation, with one adenoid section per cell marker (i.e. pneumococcus, macrophages or neutrophils) used for each adenoid. The optimised antibody dilutions, antigen retrieval techniques and counterstains were used for each cell marker, and omission of the primary antibodies served as a negative control (Table 12). A pure culture section of pneumococcus and staining of the cell markers, Ki67 and Pan CK, in a section of tonsil tissue were used for each spiked adenoid and served as the positive controls (data not shown).

Table 12: List of antibody dilutions and antigen retrieval techniques used to stain pneumococcus and immune cells in spiked adenoid tissue using immunohistochemistry

Cell type	**Macrophages**	***S. pneumoniae***	**Neutrophils**
Target antigen	CD68	3, 4, 6, 7, 9, 14, 18, 19 and 23	NE
Primary antibody	Monoclonal mouse anti-human CD68 (IgG3)	Polyclonal rabbit anti-*S. pneumoniae*	Monoclonal mouse anti-human NE (IgG1)
Dilution of primary antibody	1:200	1:1200	1:200
Antigen retrieval technique	Microwave citrate	No pre-treatment	Pronase
Secondary antibody	Rabbit anti-mouse (RaM)	Swine anti-rabbit (SaR)	Rabbit anti-mouse (RaM)
Dilution of secondary antibody	1:400	1:400	1:400
Counterstain	Methyl green		
Negative control	Omitted primary antibody		
Positive control	Monoclonal mouse anti-human Ki67 (1:100) in tonsil tissue	Pure culture (S14) of pneumococcus	Monoclonal mouse anti-human Pan CK (1:4000) in tonsil tissue

To evaluate co-localisation, images of pneumococcus were captured at a high resolution (x100 objective lens) with a Zeiss microscope. High resolution images of pneumococcus were viewed on a computer screen, and the stained pneumococcal cells and the counterstained host cells were drawn on an acetate sheet with different colours to act as a reference point for comparison. The same area of the adenoid section was captured using a lower power lens and used as a guide to find the same area in adenoid sections stained for macrophages or neutrophils. Once located, a high resolution image was captured and stained macrophages or neutrophils and the counterstained host cells were drawn on the acetate sheet. By drawing all of the stained cell markers and landmarks of counterstained cells in the tissue, bacterial-host co-localisation was assessed.

Pneumococci were closely associated with macrophages in one sample (Figure 3.7) and with macrophages and neutrophils in another sample (Figure 3.8). There were, however, major limitations in using this immunohistochemistry approach to demonstrate

co-localisation in spiked adenoids: 1) images had to be combined from sequential sections that were stained for different cell markers; 2) it was extremely time-consuming to locate pneumococcus in tissue sections; 3) it was difficult to identify the same counterstained structural cells/landmarks at a high power magnification when aligning the same area of the tissue from the three adenoid sections. In summary, co-localisation of pneumococcus and innate immune cells *in situ* using an immunohistochemistry approach was not convincing.

A *S. pneumoniae* section

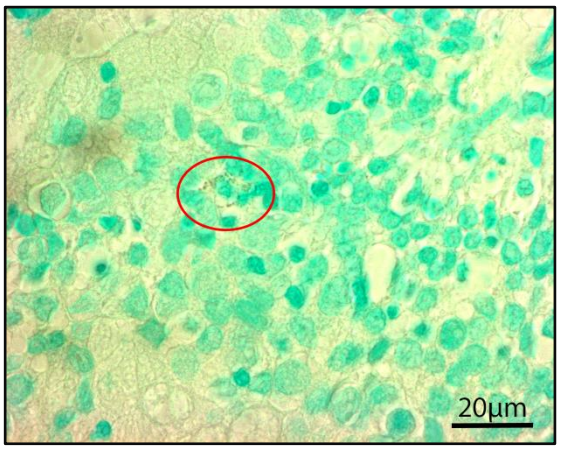

B Macrophage section

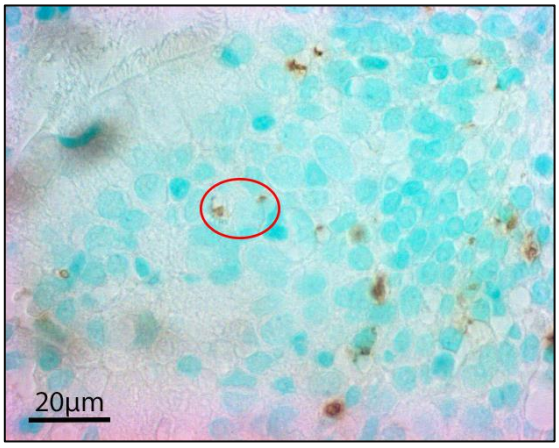

C Neutrophil section

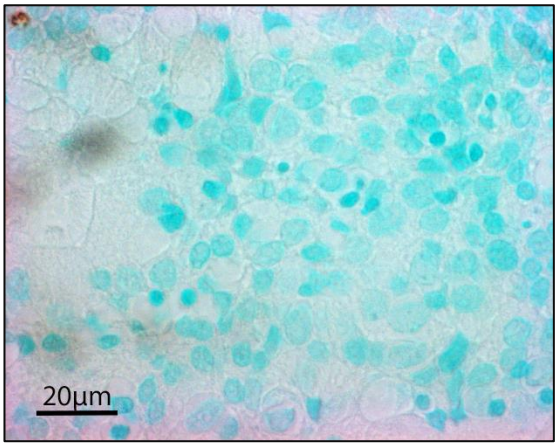

D Acetate sheet

E H&E stain

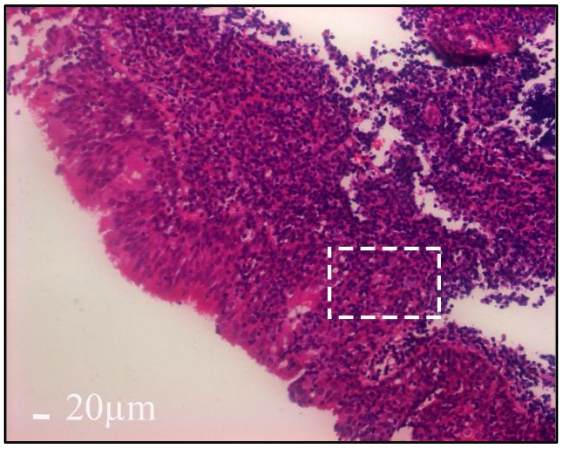

Figure 3.7: A co-localisation composite image showing association between *S. pneumoniae* and macrophages in spiked adenoid tissue.

Sequential sections were used to stain *S. pneumoniae* (A), macrophages (B) or neutrophils in a spiked adenoid (C). Pneumococci (red), macrophages (blue) and counterstained host cell structures (green and yellow) were drawn on an acetate sheet (D). Pneumococci (red) were closely associated with macrophages (blue) (depicted with red circles in A, B and D) (D). A H&E stain demarcates where co-localisation was identified in the tissue (E). Images were taken using a Zeiss light microscope with a x100 oil immersion lens. Scale bar, 20 µm (images A-C).

A *S. pneumoniae* section

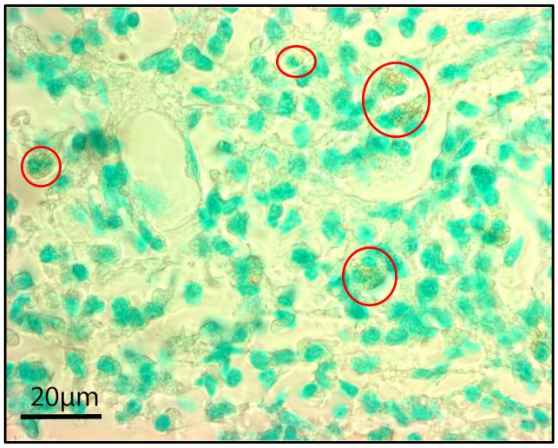

B Macrophage section

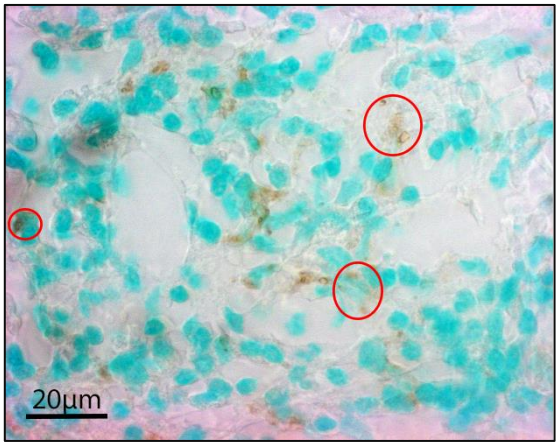

C Neutrophil section

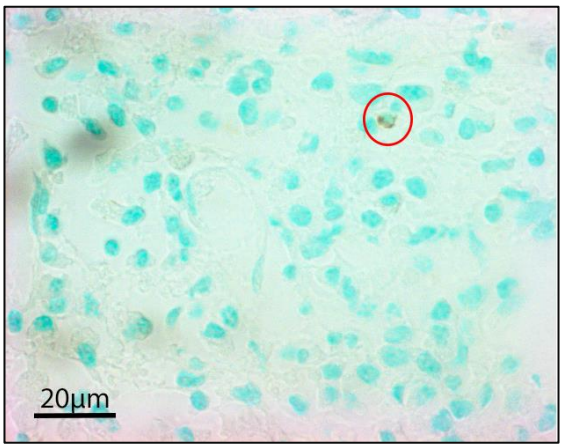

D Acetate sheet

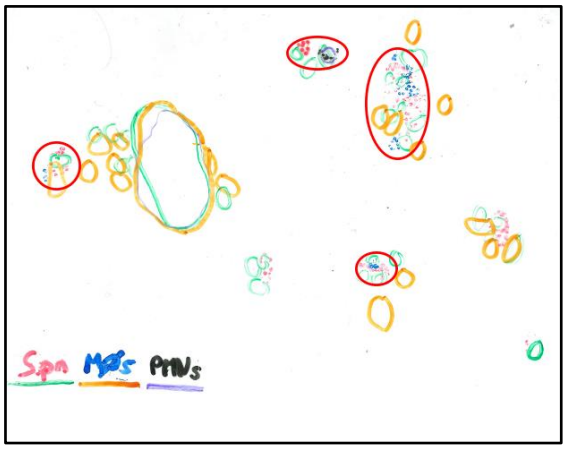

E H&E stain

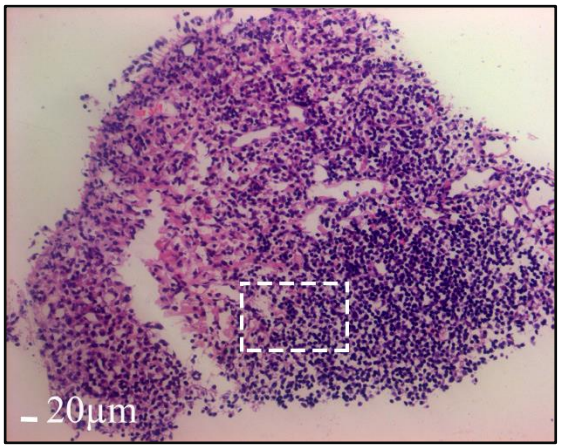

Figure 3.8: A co-localisation composite image showing association between *S. pneumoniae* and macrophages and neutrophils in spiked adenoid tissue.

Sequential sections were used to stain *S. pneumoniae* (A), macrophages (B) and neutrophils (C) in a spiked adenoid. Pneumococci (red), macrophages (blue), neutrophils (black) and counterstained host cell structures (green, yellow and purple) were drawn on an acetate sheet (D). Pneumococci (red) were closely associated with macrophages (blue) and neutrophils (black) (depicted with red circles in A-D) (D). A H&E stain demarcates where co-localisation was identified in the tissue (E). Images were taken using a Zeiss light microscope with a x100 oil immersion lens. Scale bar, 20 µm (images A-C).

3.10 Discussion

In this methods development chapter, it was demonstrated S14 pneumococci alone and in spiked adenoid tissue were successfully stained using immunohistochemistry with a polyclonal rabbit anti-*S. pneumoniae* primary antibody. Pneumococcal staining with this antibody was optimised using a broad titration (Figure 3.2), followed by a fine-tune titration (Figure 3.3), to test a range of antibody dilutions in conjunction with different antigen retrieval techniques. These experiments determined that a dilution of 1:1200 and no pre-treatment of the tissue was optimal for staining pneumococcus alone (Figure 3.3, A).

Different counterstains and incubation times were tested in order to visualise pneumococci in spiked adenoid tissue, and both the stained and counterstained cells in the same focal plane. Incubation without the primary antibody and pure cultures of pneumococcus served as the negative and positive controls, respectively. Although there was a certain trade-off between clearly visualising clusters of pneumococcal cells and ensuring sufficient contrast with the counterstained cells, counterstaining with Methyl green provided the clearest visualisation (Figure 3.4, C). Macrophages and neutrophils were also stained in spiked adenoid tissue using the cell markers CD68 (Figure 3.5, A) and NE (Figure 3.6, A), respectively.

The co-localisation of pneumococcus, CD68 and NE in consecutive (sequential) spiked adenoid sections in four separate adenoids was investigated (Figure 3.7 and Figure 3.8). Pneumococci were successfully identified and found throughout the tissue in small clusters in each of the four adenoids. Macrophages and neutrophils were also successfully stained in each adenoid sample. Although the co-localisation experiments provided proof of principle, with pneumococci closely associated with macrophages in one adenoid (Figure 3.7) and with macrophages and neutrophils in another (Figure 3.8), due to the limitations of this approach, the results were not conclusive to definitively demonstrate co-localisation. In addition, co-localisation in spiked adenoid tissue is not representative of conditions *in vivo*.

As a result of the development of fluorescent laboratory techniques, scientific papers in the literature detail the use of immunofluorescence for identifying two or more cell markers in a section of tissue. However, immunofluorescence requires expensive conjugated secondary antibodies and a confocal microscope that is expensive to purchase and run. Since the aim in this project was to develop and trial a more cost-effective approach, which would also benefit from the use of light microscopes that are more readily available in research laboratories, immunohistochemistry and sequential section staining was the preferred initial method of choice. An alternative approach could have been to

perform double immunolabelling in the same section of adenoid tissue using immunohistochemistry (Falini et al., 1986). However, there were concerns about being able to visualise pneumococci if it was located at the same site in the tissue as that of macrophages and/or neutrophils, as well as any potential cross-reactivity between antibodies and also subjecting the thin sections of tissue to multiple incubation steps.

The experiments in this chapter clearly demonstrated that immunohistochemistry was a cost-effective tool to visualise pneumococcus in human adenoid tissue, yet it was not sufficient to investigate pneumococcal co-localisation with innate immune phagocytic cells *in situ* in adenoid samples *ex vivo.* In light of this, and due to the limitations of trying to locate stained pneumococci in adenoid tissue, the aim for the next chapter was to determine whether pneumococcus and macrophages and neutrophils could all be stained in spiked adenoid tissue with the same antigen retrieval technique and, if so, to investigate co-localisation in patient (non-spiked) adenoids by performing multiple immunofluorescent staining in the same section of tissue.

4 Chapter 4 - Staining for *S. pneumoniae* and macrophages in patient adenoids using immunofluorescence

4.1 Introduction

The overarching aim in this project was to determine which phagocytic cells pneumococci co-localised with in adenoid tissue. In this chapter, patient (non-spiked) adenoids were used to determine pneumococcal-host innate immune cell co-localisation. Co-localisation in patient adenoid samples will more accurately depict conditions *in vivo* in the nasopharynx.

The polyclonal rabbit anti-*S. pneumoniae* antibody used to stain pneumococci in spiked adenoid tissue only recognises and binds to a limited number of serotypes (Chapter 2, section 2.12), all of which are covered in the available pneumococcal vaccines (PPSV23 and PCV13) (Chapter 1, Table 3). In order to stain for any pneumococcus, regardless of the pneumococcal vaccination status of the adenoid donor, an Omni antibody with known reactivity against over 90 different pneumococcal serotypes was used. In addition, due to the limitations of using immunohistochemistry for co-localisation experiments, immunofluorescence was used for immunolabelling of pneumococci and macrophages and neutrophils. Immunofluorescence uses fluorophore-conjugated secondary antibodies, allowing for a more rapid detection of (rare) pneumococci in the tissue with greater sensitivity. Furthermore, the fluorescent-conjugates permit individual identification of co-localised cell targets (i.e. pneumococci and phagocytic cells).

4.2 Aims

The individual aims for the experiments described in this chapter were as follows:

- Stain pneumococci, macrophages and neutrophils using immunohistochemistry and a pronase antigen retrieval technique.
- Optimise protocols for staining pneumococcus alone, and pneumococcus and host innate immune cells in spiked adenoid tissue using immunofluorescence.

- Investigate co-localisation in patient (non-spiked) adenoids using these optimised immunolabelling protocols.

4.3 Staining for pneumococci and macrophages in spiked adenoid tissue with pronase pre-treatment

To identify individual co-localised cell targets in the same patient adenoid sample using immunofluorescence, it was important to initially show that pneumococci and macrophages and neutrophils could all be stained in spiked adenoid tissue using the same antigen retrieval technique. Previous optimisation experiments (Chapter 3, section 3.5) showed that a pure culture of pneumococcus was successfully stained brown with an anti-*S. pneumoniae* antibody dilution of 1:1200 and pronase pre-treatment (Figure 4.1).

A 1:1200 anti-*S.pneumoniae* primary antibody

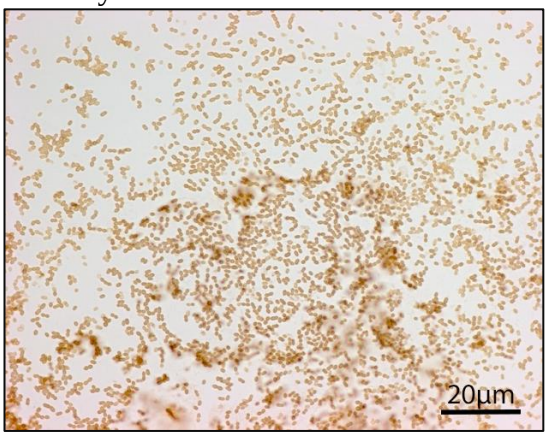

B Omitted primary antibody (negative control)

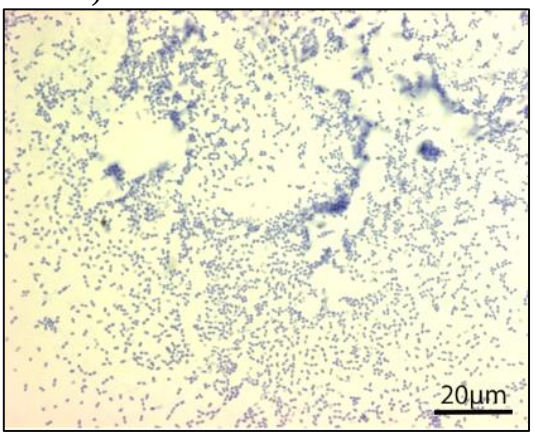

Figure 4.1: *S. pneumoniae* staining with pronase pre-treatment.

Pneumococci were stained (brown) with a polyclonal rabbit anti-*S. pneumoniae* primary antibody (1:1200 dilution), using pronase as an antigen retrieval technique (A). Pneumococci were stained (blue) with the counterstain Mayer's haematoxylin in the absence of the primary antibody (B). Images were taken using a Zeiss light microscope with a x100 oil immersion lens.

However, experiments staining for neutrophils were no longer performed in this project for the following reasons: 1) macrophages were more abundant in the adenoid samples; 2) macrophages are tissue-resident cells, whereas neutrophils are chemotactic cells requiring stimulation from pro-inflammatory cytokines; 3) inclusion criteria for obtaining patient adenoids included OM and OSA patients; 4) time-constraints in optimising immunolabelling protocols. Therefore, the aim was to stain for pneumococcus and macrophages using pronase as the antigen retrieval technique.

Spiked adenoid tissue used to optimise pneumococcal and macrophage staining (Chapter 3, sections 3.6 and 3.7) were used, with Methyl green as the counterstain and the appropriate antibodies at the optimised dilutions, as listed in Table 12 (Chapter 3, section 3.9). Two adenoids were used, with two sections per adenoid used to stain for pneumococcus or macrophages. Omission of the primary antibodies served as a negative control. As a positive control, a pure culture of pneumococcus was stained with pronase pre-treatment, whilst macrophages were stained in a section of spiked adenoid tissue with microwave citrate as the antigen retrieval technique (data not shown).

Pneumococci and macrophages were stained in each section of the two spiked adenoids with pronase pre-treatment (Figure 4.2). These results indicated that pneumococcus and macrophages could be stained simultaneously in the same adenoid section using pronase pre-treatment of the tissue. Therefore, immunofluorescence was used to identify pneumococcus and macrophages in spiked adenoid tissue and, thereafter, to investigate co-localisation in patient adenoid samples.

A Pneumococci with pronase pre-treatment

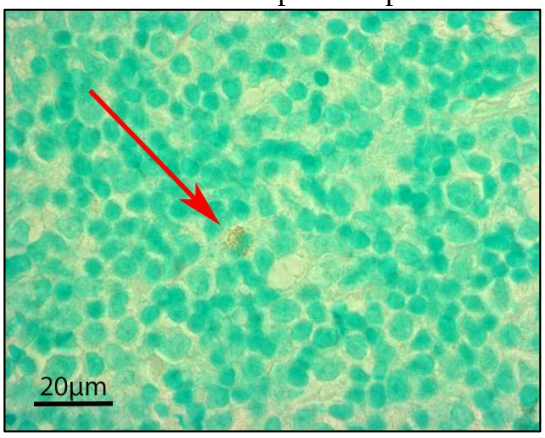

B Macrophages with pronase pre-treatment

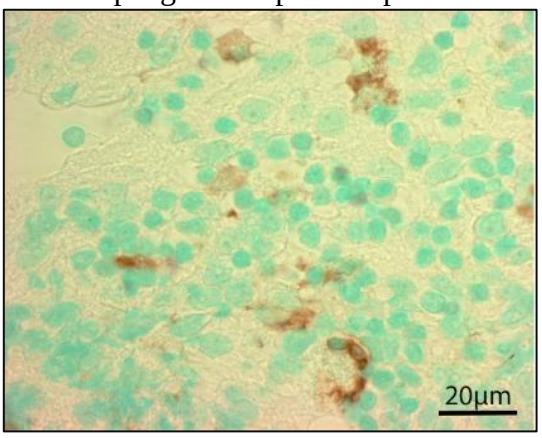

C Omitted anti-*S.pneumoniae* primary antibody (negative control)

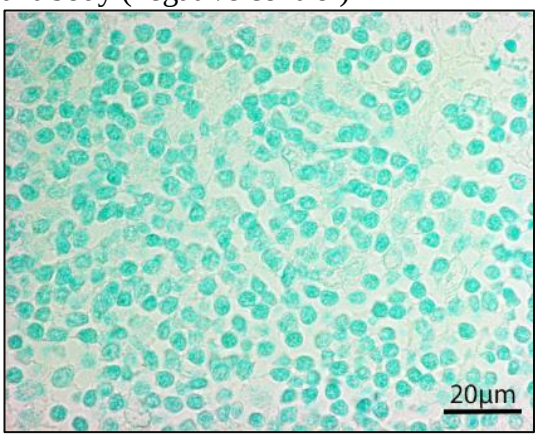

D Omitted anti-CD68 primary antibody (negative control)

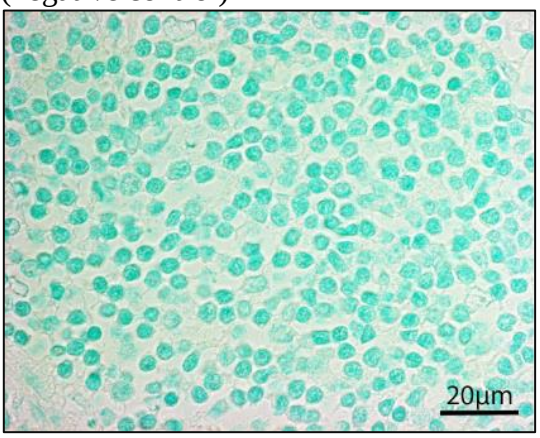

Figure 4.2: *S. pneumoniae* and macrophage staining in spiked adenoid tissue with pronase pre-treatment.

Representative images of two sections from two spiked adenoids show that pneumococci (A) (indicated with red arrows) and macrophages (B) were stained (brown) with pronase pre-treatment of the tissue. Pneumococci (C) and macrophages (D) were not stained without the primary antibodies. Images were taken using a Zeiss light microscope with a x100 oil immersion lens.

4.4 Optimisation of conjugated secondary antibodies

To label different cell markers using immunofluorescence, fluorophore-conjugated secondary antibodies specific for a primary antibody were used. Each fluorophore is excited at a different wavelength to emit a different colour, thereby identifying separate cell markers in the same section of tissue. Conjugated secondary antibodies were used to stain pneumococcus and macrophages. To determine the optimal dilutions for subsequent assays, these two conjugated antibodies were titrated.

4.4.1 Optimisation of a goat anti-rabbit IgG conjugated antibody using *S. pneumoniae* pure cultures

Pure cultures of pneumococcus were used to titrate a goat anti-rabbit IgG conjugated secondary antibody, with a separate section used to stain pneumococcus with one of the following antibody dilutions: 1:100, 1:200, 1:400, 1:800, 1:1200, 1:1600 and 1:2000 (Table 13). The polyclonal rabbit anti-*S. pneumoniae* primary antibody was used at the optimised dilution of 1:1200 (Chapter 3, section 3.5). To demonstrate that the secondary antibody was specific to the primary antibody, the primary antibody was omitted.

Table 13: The conditions used to optimise pneumococcal staining with a goat anti-rabbit IgG conjugated secondary antibody

Primary antibody	Polyclonal rabbit anti-*S. pneumoniae*
Antigen retrieval technique	Pronase
Dilution of titrated primary antibody	1:1200
Secondary antibody	Goat anti-rabbit IgG, Alexa Fluor 488 Conjugate (excitation max. 496 nm, emission max. 519 nm)
Tested dilutions	1:100, 1:200, 1:400, 1:800, 1:1200, 1:1600 and 1:2000
Negative control	Omitted primary antibody

Pneumococci stained equally well for all of the tested dilutions (data not shown), including 1:100 (Figure 4.3, A) and 1:2000 (Figure 4.3, B) dilutions. In some cases, the entirety of a pneumococcal cell fluoresced, whilst for some pneumococcal cells only the outside of the cell fluoresced, giving these cells a halo-like appearance. Pneumococci were not stained without the primary antibody (negative control). Instead, pneumococci were stained with the DAPI counterstain (Figure 4.3, C). Since pneumococci were successfully

stained with a dilution of 1:2000, this dilution was used to stain pneumococci in spiked adenoid tissue.

A 1:100 Alexa Fluor 488 conjugated antibody

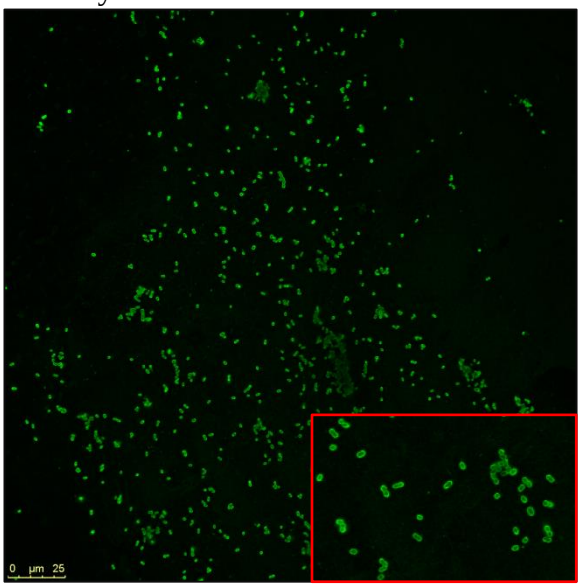

B 1:2000 Alexa Fluor 488 conjugated antibody

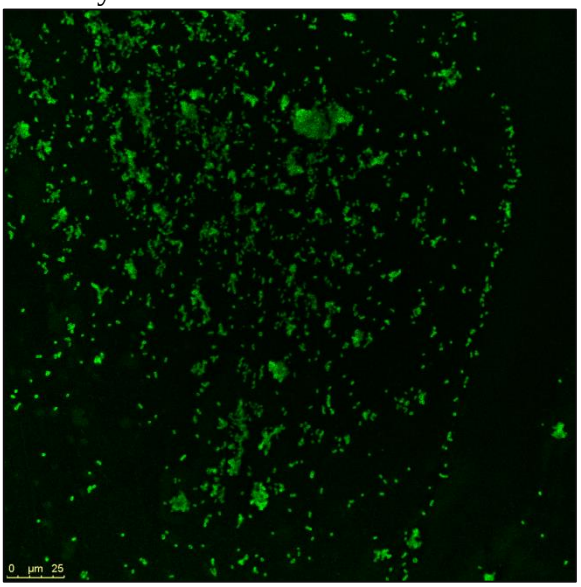

C Omitted anti-*S.pneumoniae* primary antibody (negative control)

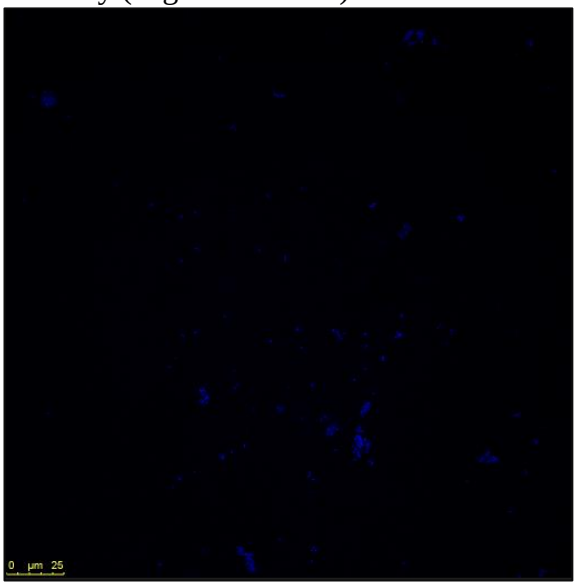

Figure 4.3: Titration of a goat anti-rabbit IgG conjugated secondary antibody.
S. pneumoniae pure cultures were stained with 1:100 (A) and 1:2000 (B) dilutions with a goat anti-rabbit conjugated Alexa Fluor 488 secondary antibody (excitation max. 496 nm, emission max. 519 nm). Pneumococcal staining is depicted with green fluorescence, evidenced more clearly in the inlaid image. Pneumococci were not stained without the rabbit anti-*S. pneumoniae* primary antibody, but were labelled with the DAPI counterstain instead (evidenced with blue fluorescence) (C). Images were taken with a Leica SP8 confocal microscope and an inverted stand using a x63 oil immersion lens.

4.4.2 *S. pneumoniae* staining in spiked adenoid tissue with a goat anti-rabbit IgG conjugated antibody

To stain for pneumococcus in two spiked adenoids, the polyclonal primary anti-*S. pneumoniae* antibody was used at a dilution of 1:1200, followed by the goat anti-rabbit IgG conjugated secondary antibody at the optimised dilution of 1:2000 (section 4.4.1). Two sections were used per adenoid. To demonstrate that the secondary antibody was specific to the primary antibody, the primary antibody was omitted; without a primary antibody, staining was not expected. A pneumococcal pure culture was used as a positive control.

Pneumococci were successfully stained in both sections from both of the two spiked adenoids, with a conjugated secondary antibody dilution of 1:2000 and pronase pre-treatment of the tissue (Figure 4.4, A-C). Pneumococci were in small, distinct clusters, ranging approximately from four to twelve individual cells. Pneumococci were not stained in either adenoid without the primary antibody (negative control) (Figure 4.4, D). Pure cultures of pneumococcus were successfully stained with the primary and secondary antibodies (Figure 4.4, E).

A Pneumococcus with 1:1200 and 1:2000 dilutions

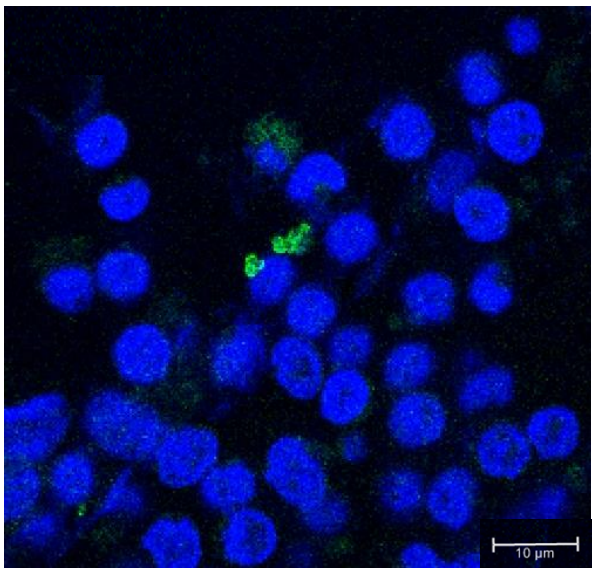

B Pneumococcus with 1:1200 and 1:2000 dilutions

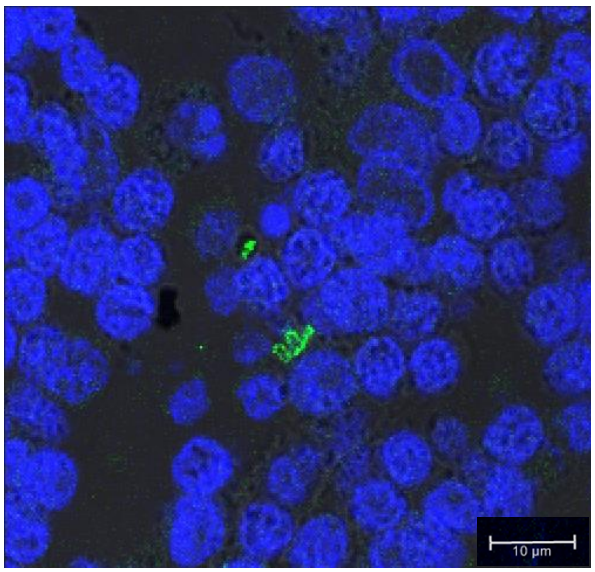

C Pneumococcus with 1:1200 and 1:2000 dilutions

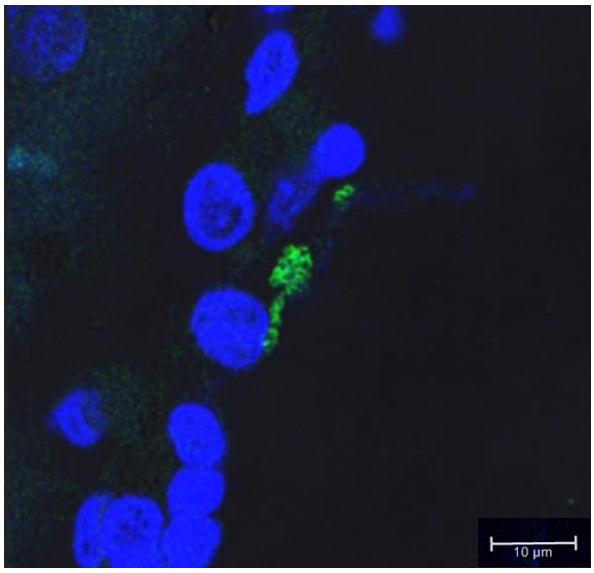

D Omitted anti-*S.pneumoniae* primary antibody (negative control)

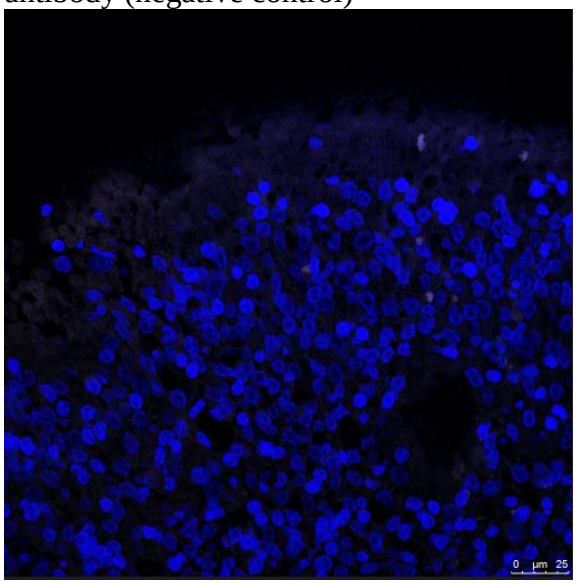

E Pure culture of pneumococcus (positive control)

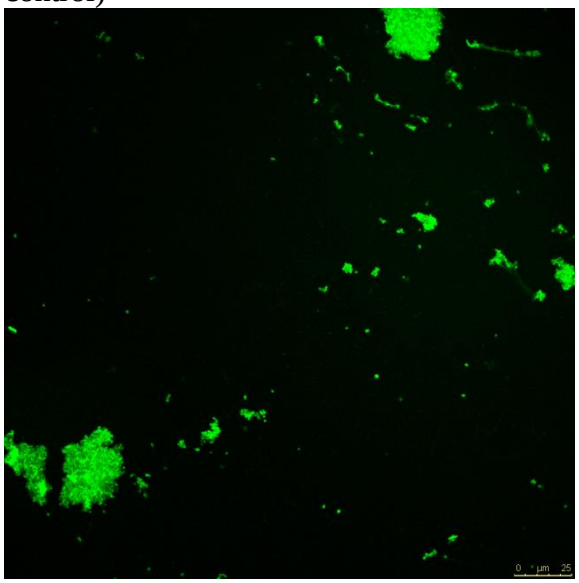

Figure 4.4: Immunofluorescent staining of pneumococci in spiked adenoid tissue.

Representative images of *S. pneumoniae* stained in two spiked adenoids (depicted as green fluorescence), using pronase pre-treatment and primary and secondary antibody dilutions of 1:1200 and 1:2000, respectively (A-C). An Alexa Fluor 488 conjugated secondary antibody was used (excitation max. 496 nm, emission max. 519 nm). Multiple pneumococcal cells were found in small clusters. Pneumococci were not stained without the primary antibody (D). A pure culture of *S. pneumoniae* was successfully stained (E). Images were taken with a Leica SP8 confocal microscope and an inverted stand using a x63 oil immersion lens. Scale bar, 10 µm (images A-C).

4.4.3 Optimisation of a goat anti-mouse IgG Alexa Fluor conjugated antibody in a spiked adenoid

To stain for macrophages (cell marker, CD68) using immunofluorescence, a spiked adenoid used to stain for pneumococcus (section 4.4.2) was used to optimise a goat anti-mouse IgG conjugated secondary antibody, with a separate section of the same adenoid used to stain with one of the following dilutions: 1:100, 1:200, 1:400, 1:800, 1:1200, 1:1600 and 1:2000 (Table 14). The monoclonal mouse anti-human CD68 primary antibody was used at the optimised dilution of 1:200. A negative control was performed, as previously described (sections 4.4.1 and 4.4.2), and the experiment was performed twice in the same adenoid.

Table 14: The conditions used to optimise macrophage staining with a goat anti-mouse IgG conjugated secondary antibody

Primary antibody	Monoclonal mouse anti-human CD68
Antigen retrieval technique	Pronase
Dilution of titrated primary antibody	1:200
Secondary antibody	Goat anti-rabbit IgG, Alexa Fluor 568 Conjugate (excitation max. 578 nm, emission max. 603 nm).
Tested dilutions	1:100, 1:200, 1:400, 1:800, 1:1200, 1:1600 and 1:2000
Negative control	Omitted primary antibody

Macrophages were successfully stained in the spiked adenoid using immunofluorescence and pronase pre-treatment (Figure 4.5, A-C). Macrophages were not stained without the primary antibody (Figure 4.5, D), and were not labelled with dilutions higher than 1:800 (data not shown). Optimal staining was achieved with a 1:400 dilution (Figure 4.5, B), with non-specific background staining found with a 1:100 dilution (Figure 4.5, A) and staining too weak with a 1:800 dilution (Figure 4.5, C). As a result, a conjugated secondary antibody dilution of 1:400 was used for subsequent assays that stained for macrophages in adenoid samples.

A 1:100 Alexa Fluor 568 conjugated antibody

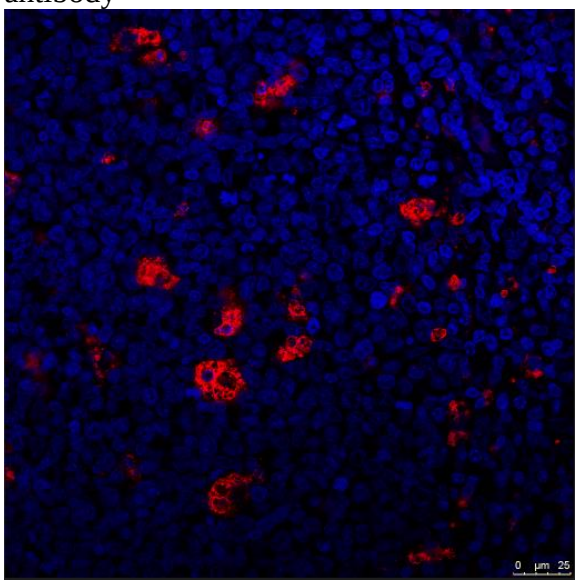

B 1:400 Alexa Fluor 568 conjugated antibody

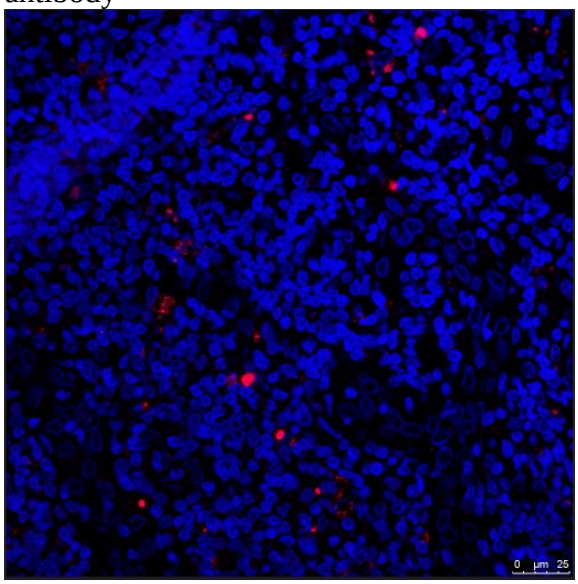

C 1:800 Alexa Fluor 568 conjugated antibody

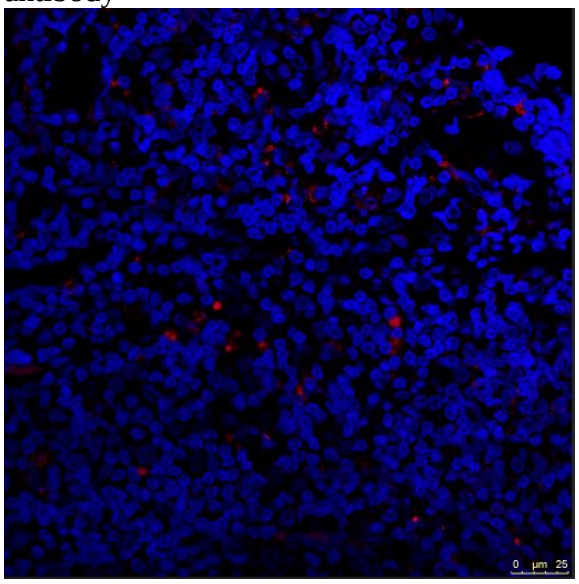

D Omitted anti-CD68 primary antibody (negative control)

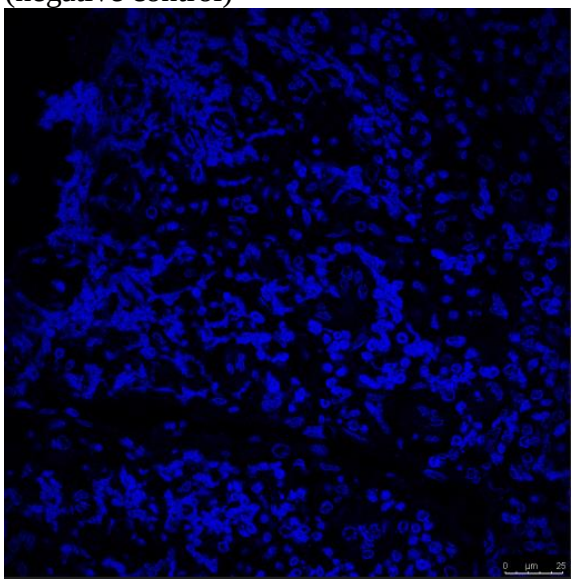

Figure 4.5: Immunofluorescent staining of macrophages in spiked adenoid tissue.

Macrophages were stained in spiked adenoid tissue with dilutions 1:100 (A), 1:400 (B) and 1:800 (C) as shown with red fluorescence, by using a goat anti-mouse IgG conjugated Alexa Fluor 568 secondary antibody (excitation max. 578 nm, emission max. 603 nm). Macrophages were not labelled without the primary antibody (D). Images were taken with a Leica SP8 confocal microscope and an inverted stand using a x63 oil immersion lens.

4.5 Determining specificity to rule out cross-reactivity between conjugated secondary antibodies and primary antibodies in a spiked adenoid

The aim of the next experiment was to show no cross-reactivity between the conjugated secondary antibodies and the species-specific primary antibodies. Specifically, that the goat anti-mouse secondary antibody would only bind with the mouse anti-human CD68 primary antibody, and the goat anti-rabbit secondary antibody would only bind with the anti-*S. pneumoniae* rabbit primary antibody.

A pneumococcal pure culture was incubated with the anti-*S. pneumoniae* primary antibody, followed by the goat anti-mouse secondary antibody. Similarly, the same spiked adenoid from the previous experiment (section 4.4.3) was incubated with the CD68 primary antibody, followed by the goat anti-rabbit secondary antibody. To serve as a negative control, spiked adenoid tissue was incubated without the primary antibodies. The optimised conditions for immunolabelling pneumococci pure cultures (section 4.4.1) and macrophages in spiked tissue (section 4.4.3) were used for the positive controls.

No cross-reactivity was found between the conjugated secondary antibodies and the primary antibodies (Figure 4.6). Specifically, the goat anti-mouse antibody did not bind to the rabbit anti-*S. pneumoniae* primary antibody (Figure 4.6, A), and the goat anti-rabbit antibody did not bind to the mouse anti-human CD68 primary antibody (Figure 4.6, B). Pneumococci and macrophage staining was not found in adenoid tissue incubated without the primary antibodies (Figure 4.6, C). Pneumococci and macrophages were stained with the positive controls (Figure 4.6, D-E).

These experiments confirmed that dual immunofluorescence in adenoid tissue could be performed, with both pneumococci and macrophages stained in the same section of adenoid tissue.

A 1:1200 anti-*S.pneumoniae* primary antibody and Alexa Fluor 568 conjugate

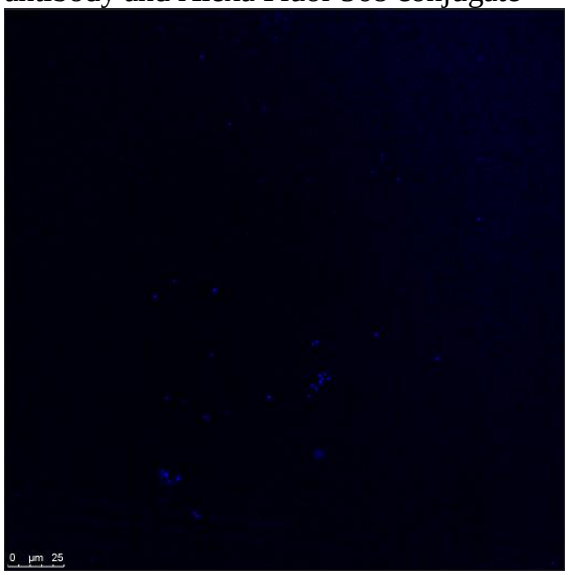

B 1:200 anti-CD68 primary antibody and Alexa Fluor 488 conjugate

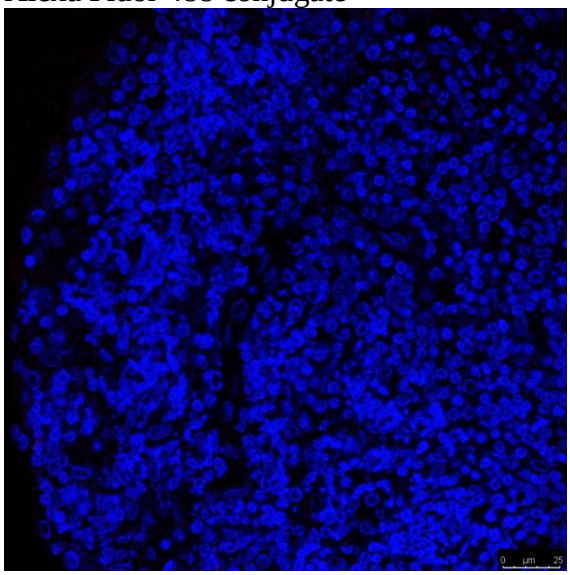

C Omitted anti-*S.pneumoniae* and anti-CD68 primary antibodies (negative control)

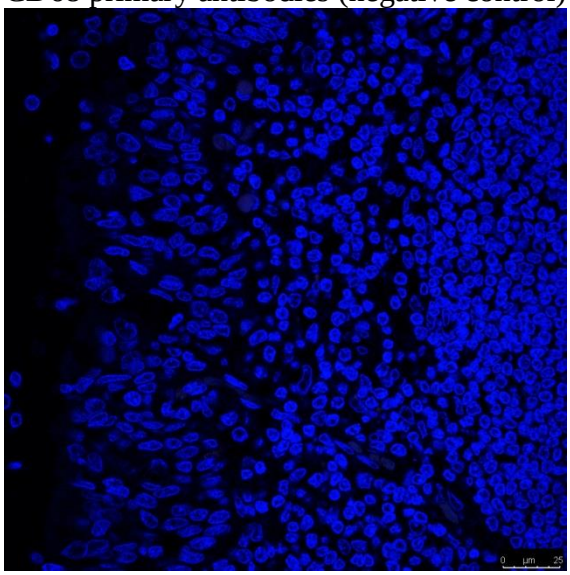

D Pure culture of pneumococcus (positive control)

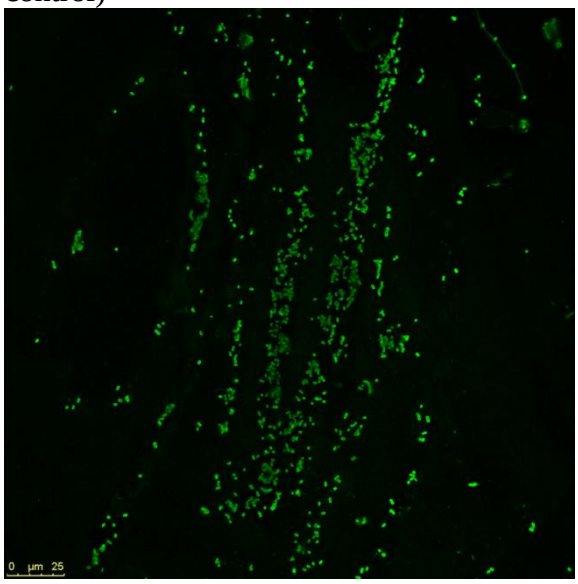

E Macrophage staining (positive control)

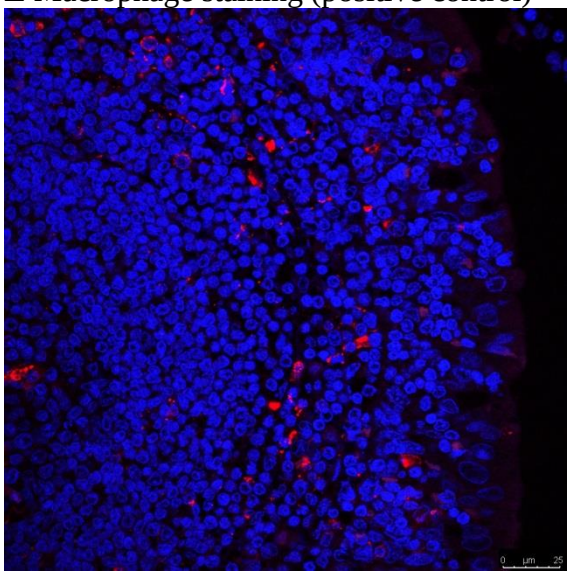

Figure 4.6: Examining cross-reactivity between conjugated secondary antibodies and primary antibodies in spiked adenoid tissue.

No cross-reactivity was found between conjugated secondary antibodies and the primary antibodies, evidenced by an absence of green and red fluorescence (A-B). Instead, pneumococci and host cells (including macrophages) were stained with the DAPI counterstain (depicted with blue fluorescence) (A-B). Pneumococci and macrophages were not found in adenoid tissue incubated without the primary antibodies (C). A pneumococcal pure culture (D) and macrophages in spiked adenoid tissue (E) were stained (depicted with green and red fluorescence, respectively) with the appropriate secondary antibodies: Alexa Fluor 488 (excitation max. 496 nm, emission max. 519 nm) for pneumococcus, and an Alexa Fluor 568 (excitation max. 578 nm, emission max. 603 nm) for macrophages. Images were taken with a Leica SP8 confocal microscope and an inverted stand using a x63 oil immersion lens.

4.6 Summary of staining for pneumococci and macrophages in spiked adenoid tissue using immunofluorescence

In this chapter, the following was demonstrated: 1) pneumococci pure cultures were stained using an immunofluorescent protocol and optimising a conjugated secondary antibody (Figure 4.3); 2) pneumococci were stained in spiked adenoid tissue with this antibody, with distinct clusters of pneumococcal cells found in different regions of the adenoid (Figure 4.4); 3) macrophages were also labelled using immunofluorescence and a conjugated secondary antibody, in a spiked adenoid sample that was positive for pneumococci (Figure 4.5), and 4) the conjugated secondary antibodies did not cross-react with the primary antibodies (Figure 4.6).

Optimising these protocols for *in situ* immunolabelling of pneumococci and macrophages enabled a dual immunofluorescence staining protocol to be performed to stain pneumococci and macrophages in the same tissue section of patient adenoids (Table 15).

Table 15: The antibody dilutions and antigen retrieval techniques used for staining pneumococci and macrophages in spiked adenoid tissue using immunofluorescence

Cell type	***S. pneumoniae***	**Macrophages**
Target antigen	*S. pneumoniae* serotypes 3, 4, 6, 7, 9, 14, 18, 19 and 23	CD68
Primary antibody	Polyclonal rabbit anti-*S. pneumoniae*	Monoclonal mouse anti-human CD68 (IgG3)
Dilution of primary antibody	1:1200	1:200
Antigen retrieval technique	Pronase	Pronase
Secondary antibody	Goat anti-rabbit IgG (Alexa Fluor 488) conjugate (excitation max. 496 nm, emission max. 519 nm)	Goat anti-mouse IgG (Alexa Fluor 568) conjugate (excitation max. 578 nm, emission max. 603 nm)
Dilution of secondary antibody	1:2000	1:400
Counterstain	DAPI	DAPI

4.7 Optimisation of a pneumococcal primary Omni antibody using a S14 pure culture

To stain for any of the possible pneumococcal serotypes in patient adenoids an Omni antibody was used. The Omni polyclonal rabbit antibody contained a pool of antisera, which binds to each pneumococcal serotype. Since the Omni antibody had not been optimised for use with immunohistochemistry or immunofluorescence, it was titrated and optimised by using pure cultures of pneumococcus. A separate section of a pure culture sample was used to stain with one of the following antibody dilutions: 1:100, 1:200, 1:400, 1:800, 1:1200, 1:1600 and 1:2000. The conjugated goat anti-rabbit secondary antibody was used at the optimised dilution of 1:2000, whilst pneumococci were incubated without the primary Omni antibody to serve as a negative control. Finally, a pneumococcal pure culture section was incubated with the Omni antibody at the highest tested dilution (i.e. 1:100), followed by the conjugated goat anti-mouse secondary antibody at the optimised dilution (i.e. 1:400) to show that the secondary antibody did not cross-react with the primary Omni antibody.

Pneumococci were stained with each dilution (Figure 4.7, A-C), with optimal staining achieved at a 1:100 dilution (Figure 4.7, A). This dilution was therefore used to stain for pneumococcus in subsequent patient adenoids. Pneumococci were not stained without the Omni antibody (Figure 4.7, D), or when incubation with the Omni antibody was followed by the conjugated goat anti-mouse secondary antibody (Figure 4.7, E). Thus, there was no cross-reactivity and dual fluorescent staining in patient adenoids could be performed.

A 1:100 Omni antibody

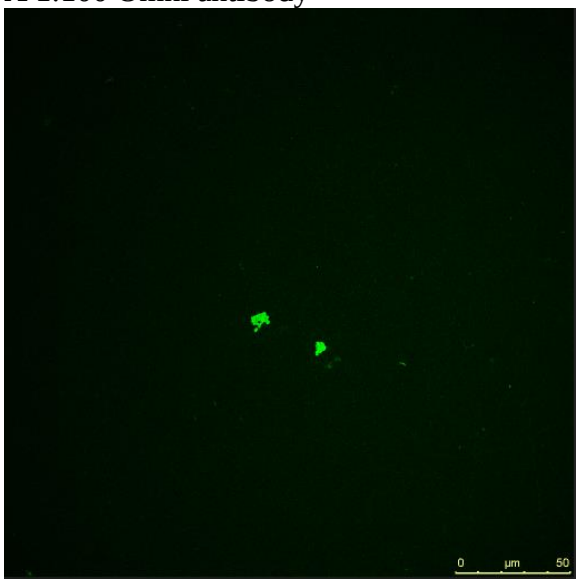

B 1:800 Omni antibody

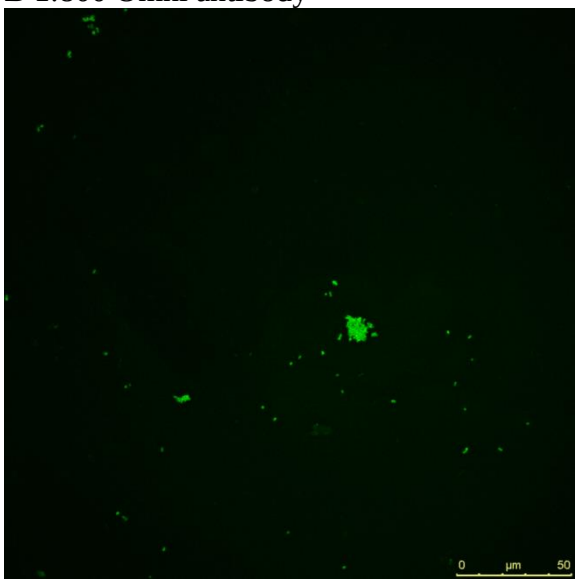

C 1:2000 Omni antibody

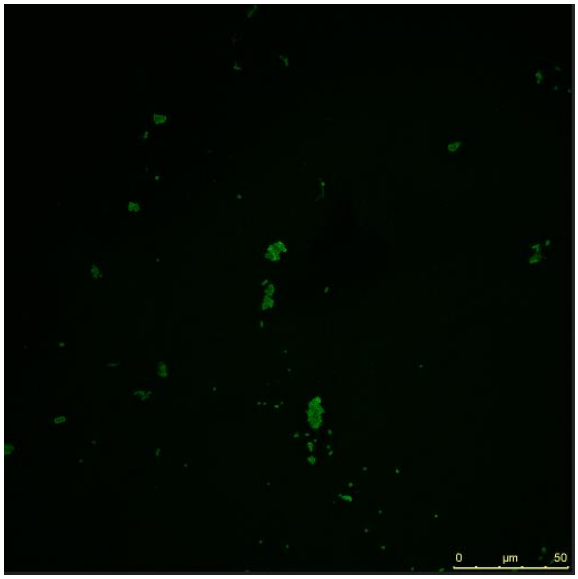

D Omitted primary antibody (negative control)

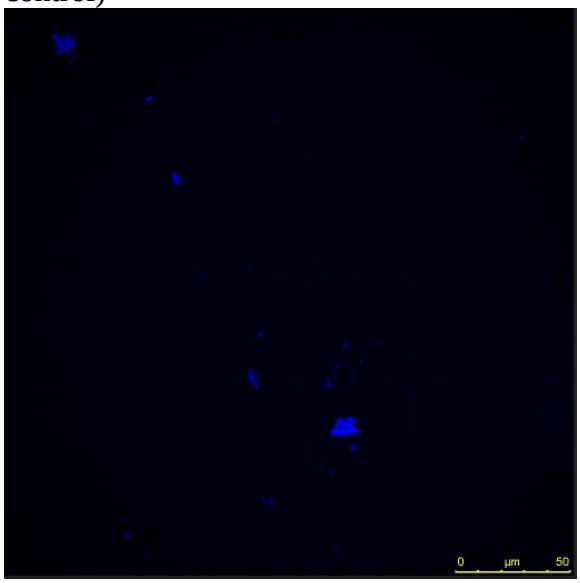

E 1:100 Omni antibody and Alexa Fluor 568 conjugate (1:400)

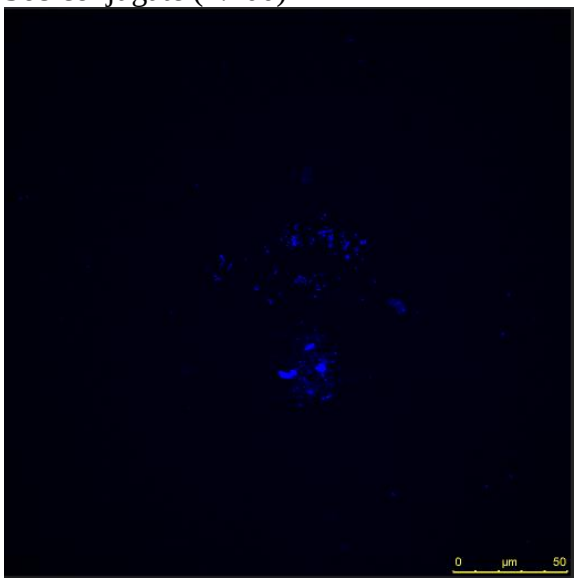

Figure 4.7: Titration of an Omni pneumococcal primary antibody.
S. pneumoniae pure cultures (depicted with green fluorescence) were stained with dilutions 1:100 (A), 1:800 (B) and 1:2000 (C), with an Omni antibody and an Alexa Fluor 488 secondary antibody (excitation max. 496 nm, emission max. 519 nm). Pneumococci were stained with the DAPI counterstain (depicted with blue fluorescence) in the absence of the Omni antibody (D). Pneumococci were not stained with the goat anti-mouse conjugated secondary antibody (Alexa Fluor 588; excitation max. 578 nm, emission max. 603 nm) (E). Images were taken with a Leica SP8 confocal microscope and an inverted stand using a x63 oil immersion lens.

4.8 Dual fluorescent labelling of pneumococci and macrophages in adenoid tissue samples

To perform dual immunofluorescence staining of pneumococcus and macrophages in patient adenoids, four adenoids were sectioned with a microtome, as previously described (Chapter 2, section 2.6.2). The immunofluorescence protocol was used (Chapter 2, section 2.14), with the following amendments: the first conjugated secondary antibody in 1% BSA was applied for 1 hour to bind to the first primary antibody. The adenoid sections were then washed in TBS (3x5 minutes) before the second primary antibody (in 1% BSA) was applied and the tissue sections incubated overnight at 4°C. The sections were then washed in TBS (3x5 minutes), and the second conjugated secondary antibody (in 1% BSA) was applied for 1 hour at room temperature. The sections were washed in TBS (3x5 minutes), counterstained with DAPI and covered with a coverslip. Finally, the sections were viewed with a Leica SP8 confocal microscope.

To serve as the positive controls, a pure culture of pneumococcus was stained with the Omni primary antibody followed by the goat anti-rabbit conjugated secondary antibody, and the same spiked adenoid from previous experiments (section 4.4.3) was used to stain macrophages with the mouse anti-human CD68 primary antibody and the goat anti-mouse conjugated secondary antibody (data not shown). Dual immunofluorescence staining was performed in patient adenoid tissue without the primary antibodies to serve as a negative control (data not shown). A list of the antibodies and dilutions used for dual immunolabelling in patient adenoid tissue is shown in Table 16.

Table 16: The conditions used to stain for pneumococcus and macrophages in patient adenoid tissue using dual immunofluorescence

Primary antibodies	Polyclonal rabbit pneumococcal Omni and monoclonal mouse anti-human CD68
Antigen retrieval technique	Pronase
Dilution of primary antibodies	1:100 (pneumococcus) and 1:200 (macrophages)
Secondary antibodies	Goat anti-rabbit IgG Alexa Fluor 488 conjugate (excitation max. 496 nm, emission max. 519 nm) for pneumococcus, and a goat anti-mouse IgG Alexa Fluor 568 conjugate (excitation max. 578 nm, emission max. 603 nm) for macrophages
Dilution of secondary antibodies	1:2000 (pneumococcus) and 1:400 (macrophages)
Positive controls	Pure culture of S14 (pneumococcus) and a spiked adenoid (macrophages)
Negative control	Primary antibodies replaced with TBS

Pneumococci were found in two of the four patient adenoids that were examined (Figure 4.8 and Figure 4.9). The green fluorescence (depicting the pneumococcal cells) was not similar to the halo-like structure that was observed in previous experiments, which stained pure cultures of S14 (Figure 4.3 and Figure 4.7) and S14 in spiked adenoid tissue (Figure 4.4). However, the size of the cells (~1 µm diameter) was similar. Thus, it may be that differences in the appearance of the fluorescence resulted from growing S14 in optimum conditions in the laboratory. Additionally, aggregates of pneumococci were not found; rather an individual cell was seen, which was associated with macrophages (Figure 4.8 and Figure 4.9).

Pneumococci and macrophages were not labelled in spiked adenoid tissue incubated without the primary antibodies, whilst pure cultures of pneumococcus and macrophages in spiked adenoid tissue were stained with the positive controls (data not shown).

A Pneumococcus, macrophages and DAPI counterstain

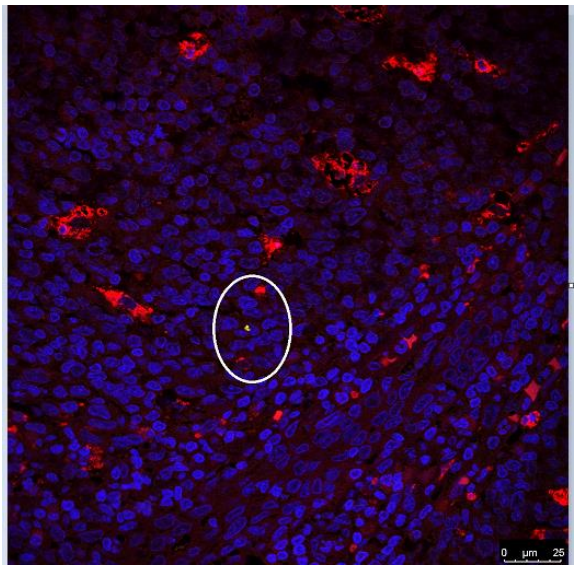

B Macrophages and DAPI counterstain

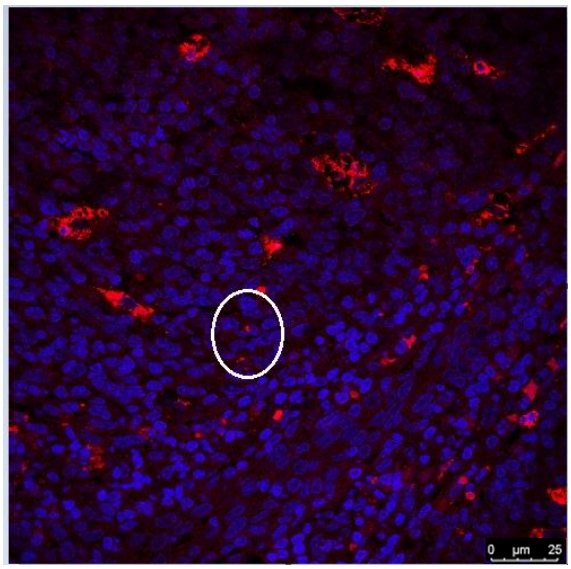

C Pneumococcus and DAPI counterstain

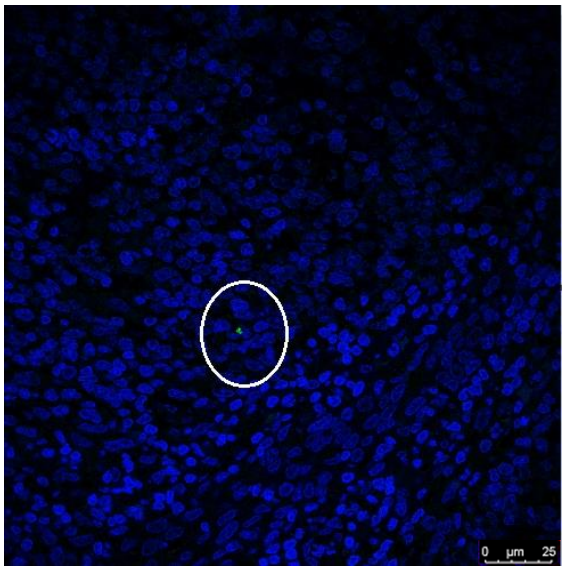

D Pneumococcus and DAPI counterstain (enlarged image of [C])

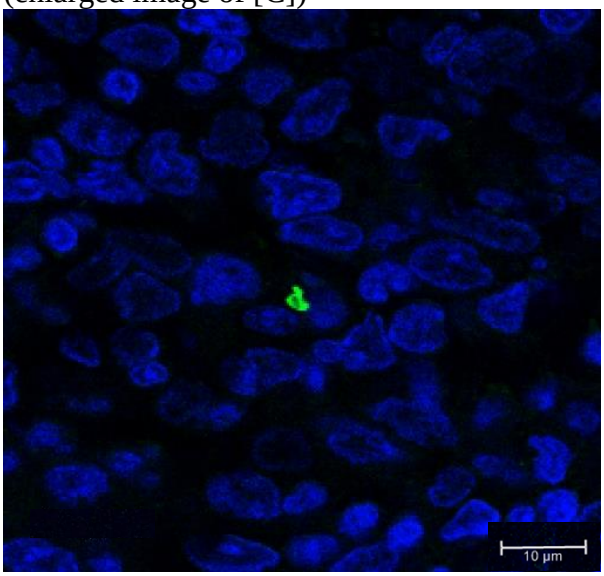

Figure 4.8: Dual immunofluorescence labelling of pneumococci and macrophages in a patient adenoid.

Pneumococci and macrophages were stained in a patient adenoid (A) using dual immunofluorescence. Image A shows stained pneumococci (depicted with green fluorescence), macrophages (red fluorescence) and counterstained host cells (blue fluorescence). Immunolabelling without the green fluorescence channel (B) and without the red fluorescence channel (C) show macrophage and pneumococcal staining, respectively, with an enlarged image of pneumococcal staining shown in D. White circles demarcate where pneumococcus and macrophages were closely associated in the tissue. Images were taken with a Leica SP8 confocal microscope and an inverted stand using a x63 oil immersion lens.

A Pneumococcus, macrophages and DAPI counterstain

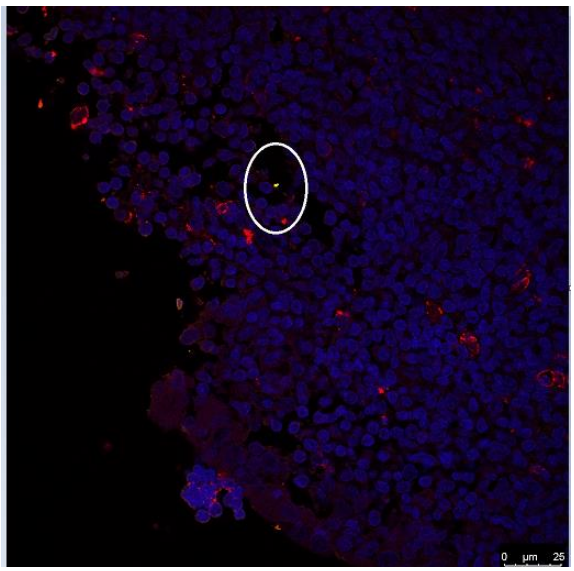

B Macrophages and DAPI counterstain

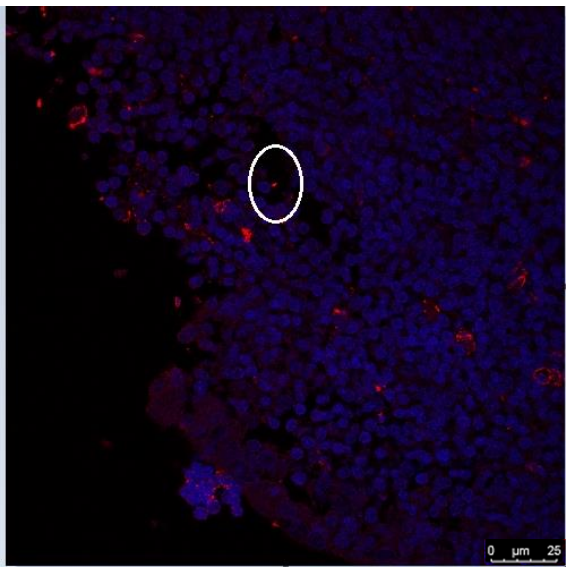

C Pneumococcus and DAPI counterstain

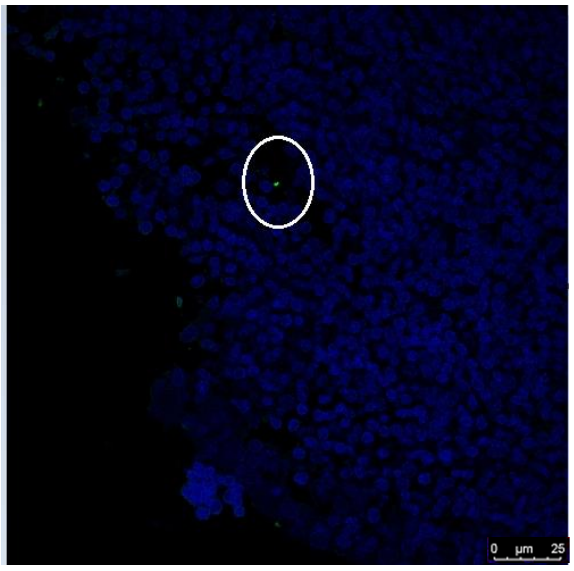

D Pneumococcus and DAPI counterstain (enlarged image of [C])

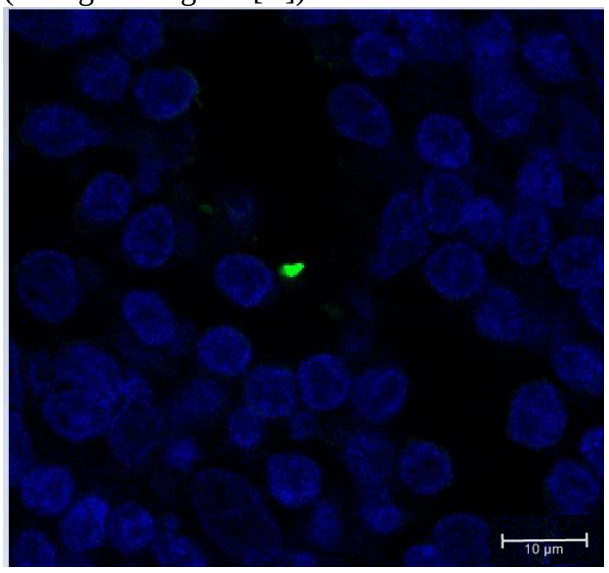

Figure 4.9: Dual immunofluorescence labelling of pneumococci and macrophages in a second patient adenoid.

Pneumococci (depicted with green fluorescence) and macrophages (red fluorescence) were successfully stained in a second patient adenoid (A). Immunolabelling without the green fluorescence channel (B) and the red fluorescence channel (C) show macrophage and pneumococcal staining, respectively, with an enlarged image of pneumococcal staining shown in D. White circles demarcate where pneumococcus and macrophages were closely associated in the tissue. Images were taken with a Leica SP8 confocal microscope and an inverted stand using a x63 oil immersion lens.

4.9 Discussion

The overarching aim in this chapter was to determine whether pneumococcus co-localised with macrophages in patient adenoid tissue using immunofluorescence. To perform dual staining of pneumococcus and the macrophage cell marker, CD68, in the same section of tissue, it was initially determined if pneumococcus and macrophages could be stained in spiked adenoid tissue using the same antigen retrieval technique. Based on the optimisation experiments for the polyclonal rabbit anti-*S. pneumoniae* primary antibody in Chapter 3, the enzyme pronase was selected as the antigen retrieval technique. Although both pneumococcus and macrophages were successfully stained in spiked adenoid tissue with pronase (Figure 4.2), the aim was to investigate co-localisation in patient adenoids using dual immunofluorescence. Immunofluorescence would permit rapid detection of pneumococci and any co-localisation and, therefore, would be more efficient than the immunohistochemistry methods used so far. Immunofluorescence would also provide higher quality images of stained and counterstained cells in adenoid tissue.

Therefore, conjugated secondary antibodies were optimised for dual immunofluorescence labelling of pneumococcus and macrophages using pneumococcus alone (Figure 4.3) and spiked adenoid tissue (Figure 4.5), respectively. Pneumococci were also successfully stained in spiked adenoid tissue, with distinct clusters of pneumococcal cells clearly evident in the tissue (Figure 4.4). Finally, it was shown that the two conjugated antibodies did not cross-react with primary antibodies specific for pneumococci and macrophage staining (Figure 4.6).

An Omni primary antibody was used to stain pneumococcus in patient adenoid samples, but was initially titrated with pure cultures (S14) of pneumococcus (Figure 4.7). Dual immunofluorescence experiments showed pneumococci were stained in two of the four patient adenoids and macrophages were labelled in all four (Figure 4.8 and Figure 4.9). The pneumococcal cells were amorphous in appearance rather than the halo-like structure found when S14 was stained using pure cultures (Figure 4.3 and Figure 4.7) and spiked adenoids (Figure 4.4). This discrepancy may be due to the fact that S14 was grown in the laboratory under optimum conditions, whereas pre-existing pneumococci in patient adenoids were present in *in vivo* conditions. Taken together, growing *in vivo* may have accounted for the differences in structure between spiked and patient adenoids, especially as the size of the fluorescently stained pneumococcal cells was similar from both type of adenoids (Figure 4.4, Figure 4.8 and Figure 4.9). Pneumococcal aggregates were not found in patient adenoid samples. Instead, only an individual pneumococcal cell was found, which appeared to be associated with macrophages (Figure 4.8 and Figure 4.9).

Several studies have examined the presence of biofilms on the surface of adenoids from children suffering from chronic adenoiditis, COM or adenoid hypertrophy which causes OSA (Al-Mazrou and Al-Khattaf, 2008, Kania et al., 2008, Hoa et al., 2009, Zuliani et al., 2009, Hoa et al., 2010, Saylam et al., 2010, Nistico et al., 2011, Saafan et al., 2013, Tawfik et al., 2016). Three findings are relevant. Firstly, that the presence of biofilms on adenoid tissue is proportionately higher from patients with a chronically inflamed adenoid or middle ear. Secondly, that the grade of the biofilm and the mucosal surface area coverage of the biofilm are significantly greater on the adenoids of children suffering from either adenoiditis or COM compared to children suffering from OSA. Thirdly, that adenoid biofilm formation appears to be associated with the pathogenesis of COM.

To visualise the presence of biofilms on adenoid tissue, SEM, fluorescence *in* situ hybridisation (FISH) and confocal microscopy, or histological staining, are often used. Attached aggregates are typically found along the surface of adenoid tissue and in the vicinity of small crypts, interspersed with areas of normal-appearing mucosa. These findings may explain why aggregates were not found in the patient adenoids examined in this project. Furthermore, the absence of surface-attached pneumococci may have been due to the fact that it was not readily evident whether the epithelial cell surface was present in the sections, because of the difficulty in orientating the tissue for paraffin-embedding. Finally, the epithelial surface may have been damaged during surgical removal of the tissue.

Winther et al. and Ivarrson et al. used May Grünwald Giemsa in their studies to stain for phagocytosis of unidentified bacteria in adenoid tissue (Ivarsson and Lundberg, 2001, Winther et al., 2009). In both studies, neutrophils were found to have ingested planktonic bacteria in the surface secretions of the adenoid and, as a result, the bacteria were not stained with a eubacterial FISH probe, suggesting that they were no longer metabolically active. Ivarrson et al. also showed through immunohistochemistry staining that immunoglobulins (IgG, IgA, IgM) and plasma cells were found in the surface secretions of adenoids, whilst neutrophils and macrophages were seen in the epithelium and penetrating the epithelial surface. The authors of this study concluded that phagocytes were leaving the adenoid, entering into the surface secretions and phagocytosing the bacteria (Ivarsson and Lundberg, 2001). The authors postulated that any bacteria penetrating the adenoid epithelium are ingested and killed by macrophages and/or neutrophils, whereas bacteria on the epithelial surface that form biofilms are refractory to the action of phagocytes. These findings may also explain why bacteria, individual cells or clusters of cells, were not seen in subepithelial parenchyma tissue in either study.

In support of these studies, despite being hyperadhesive on epithelial cells, pneumococcal biofilms have been found to be considerably less invasive *in vitro* and in mice models compared to planktonic cells (Sanchez et al., 2011b, Blanchette-Cain et al., 2013, Marks et al., 2013, Qin et al., 2013).

In the patient adenoids samples, aggregates of pneumococcus were not found, but rather, an individual cell was found in two of the four adenoids. Since the number of patient adenoids that were examined in this project were small (n = 4), more samples are required to further investigate evidence of pneumococcal aggregates and co-localisation in adenoid tissue before conclusive conclusions can be made.

Convincing evidence of pneumococcal co-localisation with innate immune cells was not found in his project, but in the literature it has been shown that pneumococci co-localises with epithelial cells on patient adenoids *ex vivo* during pneumococcal colonisation and biofilm development (Hoa et al., 2009, Nistico et al., 2011). Biofilms were found in COM and OSA patient groups, suggesting that the adenoidal epithelial surface serves as a reservoir for pathogenic pneumococci (and other otopathogens), even in the absence of overt (middle ear) infection. However, current *in vitro* models attempting to recapitulate pneumococcal biofilms on viable epithelial cells have only been developed with a short contact time (maximum of 4 hours) (Pracht et al., 2005, Bootsma et al., 2007, Sanchez et al., 2011b, Brittan et al., 2012, Blanchette-Cain et al., 2013, Blanchette et al., 2016).

Therefore, the aim for the next chapter was to develop a prolonged *in vitro* co-culture model to enable nascent pneumococcal biofilm formation on live epithelial cells, which would facilitate interrogation of bacterial and host components in a more biologically representative model.

5 Chapter 5 – Development of a *S. pneumoniae* and respiratory epithelial cell co-culture model

5.1 Introduction

Previous research has shown pneumococci form biofilms on the surface of adenoid tissue and on the respiratory mucosa of patients suffering from chronic rhinosinusitis (Sanderson et al., 2006, Hoa et al., 2009, Nistico et al., 2011), as well as on the nasal septa of experimentally infected mice (Marks et al., 2012a, Blanchette-Cain et al., 2013, Shak et al., 2013b). Additionally, pneumococcal biofilms are present on the middle ear mucosa of both experimentally infected chinchillas and in children with chronic otitis media (Hall-Stoodley et al., 2006, Hoa et al., 2009, Reid et al., 2009). Taken together, it is now believed that the biofilm mode of growth plays a key role during colonisation in the nasopharynx in the human host. Given the fact that carriage is a prerequisite for pneumococcal disease, a deeper understanding of pneumococcal biofilm-host interactions is of great importance in delineating how pneumococcus are able to persist in the upper respiratory tract. However, the vast majority of studies on pneumococcal biofilms have been performed on abiotic surfaces and, as such, these models are not representative of the host environment. Therefore, more biologically-relevant models are required to investigate this relationship.

The importance of pneumococcal-host interactions for the development of a nascent biofilm was initially shown by Parker et al. who demonstrated that recovered bacteria from epithelial cells formed a more pronounced biofilm on abiotic surfaces than bacteria without any previous exposure to epithelial cells (Parker et al., 2009). Marks et al. and Vidal et al. have since shown that pneumococcal biofilms grown on fixed epithelial cells have a significantly greater biomass from as little as 6 hours post-challenge than pneumococcal biofilms grown on an abiotic surface (Marks et al., 2012a, Vidal et al., 2013). Although pneumococcal biofilms grown on abiotic surfaces have revealed the importance of virulence factors, extracellular DNA and the extracellular matrix for biofilm formation *in vitro* (Muñoz-Elías et al., 2008, Sanchez et al., 2011b), no correlation has been found between the ability of a clinical isolate to form a biofilm on an abiotic surface and its virulence potential *in vivo* (Lizcano et al., 2010, Tapiainen et al., 2010).

Pneumococcal biofilms on abiotic surfaces lack the structural morphology (i.e. a robust EPS, filamentous material and interconnected bacterial aggregates) that is observed

in vivo in mice and on respiratory epithelial cells *in vitro* (Marks et al., 2012a). Marks et al. have also shown a direct correlation between the ability of pneumococcal strains with mutations in virulence factors to form a biofilm either on epithelial cells *in vitro* or in the nasopharynx in mice; a correlation which is lost when abiotic surfaces are used for biofilm growth (Marks et al., 2012a).

In two independent studies that focussed on direct infection of epithelial cells, a cytotoxic effect was induced within 4 hours of pneumococcal challenge, with epithelial cellular damage confirmed through LDH release, TEER measurements and cell lysis (Brittan et al., 2012, Smith et al., 2013). In another infection study, gentamicin was added to pneumococcal challenged epithelial cells at 2 hours post-infection to prevent overgrowth of bacteria and loss of epithelial cell viability (Marriott et al., 2012). To circumvent the cytotoxic effect that pneumococcus can have on epithelial cells, existing pneumococcal biofilm and epithelial co-culture models have relied on growing biofilms on either non-viable primary cells or an epithelial cell line prefixed with paraformaldehyde, or growing biofilms on either an abiotic surface or a fixed biotic surface before transplanting the biofilm onto live epithelial cells (Marks et al., 2012a, Marks et al., 2012b, Marks et al., 2013, Vidal et al., 2013). The caveat to these co-culture models is that biofilms are either arbitrarily created without the presence of viable host cells, or the host innate response cannot be measured.

Vidal and colleagues have been successful in developing a flow system co-culture model with living cultures of human respiratory epithelial cells (Vidal et al., 2013). A bioreactor with a continuous flow of nutrients and a complete exchange of the culture medium every 25 minutes allowed a pneumococcal biofilm to develop without having a cytotoxic effect. However, expensive and specialised laboratory experiment is required for this type of model.

As pneumococcal biofilms have been found on human mucosal epithelial samples *ex vivo* (Hall-Stoodley et al., 2006, Sanderson et al., 2006, Hoa et al., 2009, Nistico et al., 2011), the aim for this project was to develop a prolonged *in vitro* co-culture model that would facilitate pneumococcal biofilm formation on living cultured epithelial cells. This model would be an advantageous tool in examining pneumococcal biofilm-host interactions in a system that is more reflective of conditions *in vivo*.

5.2 Aims

The individual aims for the experiments described in this chapter were as follows:

- Assess the growth kinetics and biofilm formation of the D39 pneumococcal strain to be used in the co-culture model.
- Establish confluent and healthy respiratory epithelial cell monolayers to be inoculated with pneumococcus.
- Assess epithelial cell layer integrity and viability towards different pneumococcal loads (multiplicities of infection).
- Determine the extent of bacterial association on the epithelial cells through CFU enumeration and analyse the formation of an early pneumococcal biofilm by using SEM microscopy.
- Establish the optimal number of pneumococcus to seed the co-culture with, and determine the maximum infection time that does not compromise 16HBE cell integrity.

5.3 Growth kinetics of the D39 pneumococcal laboratory strain

16HBE cells were to be challenged with the D39 pneumococcal strain for all co-culture experiments. To ensure that the 16HBE cells were challenged with the same MOIs of pneumococcus for each co-culture experiment, regression analysis was performed for the D39 strain (n = 3) (Chapter 2, section 2.3). Regression analysis shows the relationship between the number of live pneumococcal cells (CFUs) in relation to absorbance over time. The aim of the experiment was to determine the OD absorbance value that equated to $1x10^8$ pneumococcal cells per ml of suspension. This OD would then be used to create different pneumococcal inoculums for co-culture experiments.

The equation on the representative graph was used to determine the OD value for $1x10^8$ pneumococcal cells, which measured 0.054 (Figure 5.1). The average OD value for the three separate experiments was 0.050 and was used to create different pneumococcal inoculums for all of the co-culture experiments.

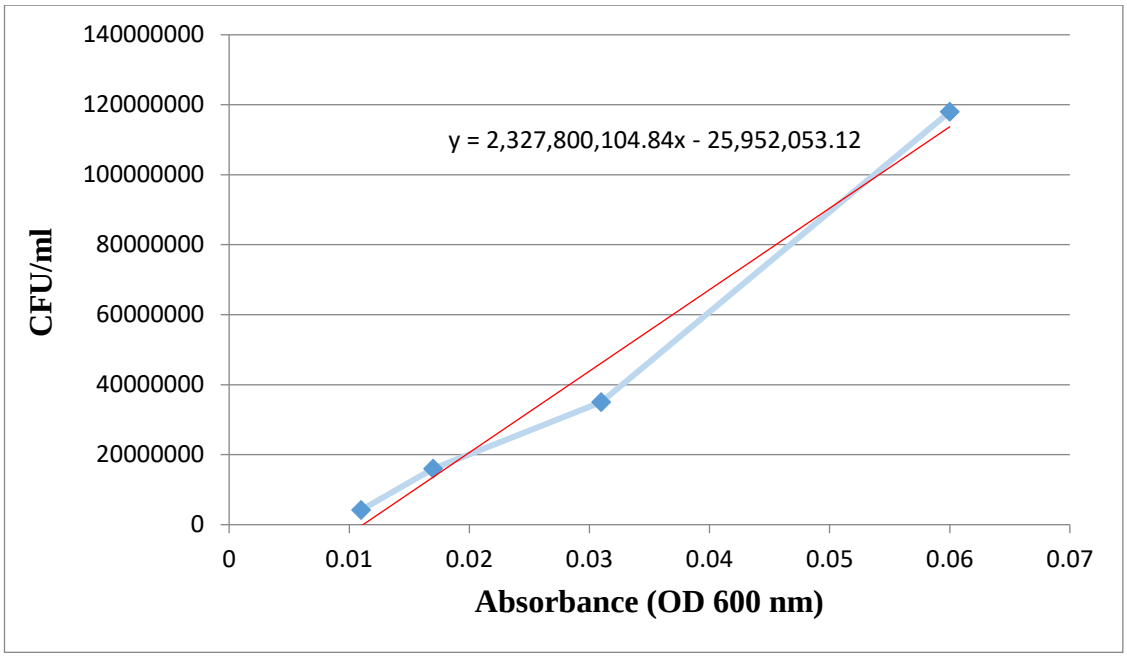

Figure 5.1: Regression analysis for the D39 pneumococcal laboratory strain.
Regression analysis for the D39 pneumococcal strain to determine the absorbance value at an OD of 600 nm that equated to $1x10^8$ pneumococcal cells. A representative graph from three independent experiments is shown.

5.4 Confocal microscopy analysis of a GFP-expressing D39 biofilm

One of the aims for the pneumococcal (D39) and 16HBE co-culture model was to assess the surface area coverage of pneumococcal biofilms on the epithelial cell surface using confocal microscopy. Consequently, confocal microscopy was initially used to determine whether or not the D39 pneumococcal strain fluoresced in the biofilm phenotype (n = 1). D39 was grown in a broth culture (Chapter 2, section 2.2) and biofilm formation was assessed, as previously described (Chapter 2, section 2.4). Briefly, 2 ml of the broth (2 ml x10^8 cells) was pipetted onto CELLView plates and supplemented with 2 ml BHI diluted 1:5 with non-pyrogenic sterile dH_2O. After 24 hours incubation at 37°C/5% CO_2, the spent media from both plates was removed and replaced with either 2 ml of 0.4 g of maltose in 10 ml of 1:5 BHI (4% solution) or 2 ml of 1:5 BHI. After 24 hours incubation at 37°C/5% CO_2, the plates were then processed for confocal microscopy analysis (Chapter 2, section 2.4). The extent of biofilm formation was determined by measuring the amount of fluorescence as an indicator of GFP expression.

D39 pneumococcal cells that were incubated with maltose fluoresced, with green fluorescence detected (Figure 5.2, A). This result indicated that the pneumococcal cells had metabolised the maltose present in the culture medium to activate the expression of the fluorescent protein. In comparison, pneumococcal cells that were cultured without maltose did not fluoresce (Figure 5.2, B).

As the D39 strain successfully fluoresced in the biofilm phenotype, this well-characterised laboratory strain was suitable for subsequent co-culture experiments with 16HBE cells.

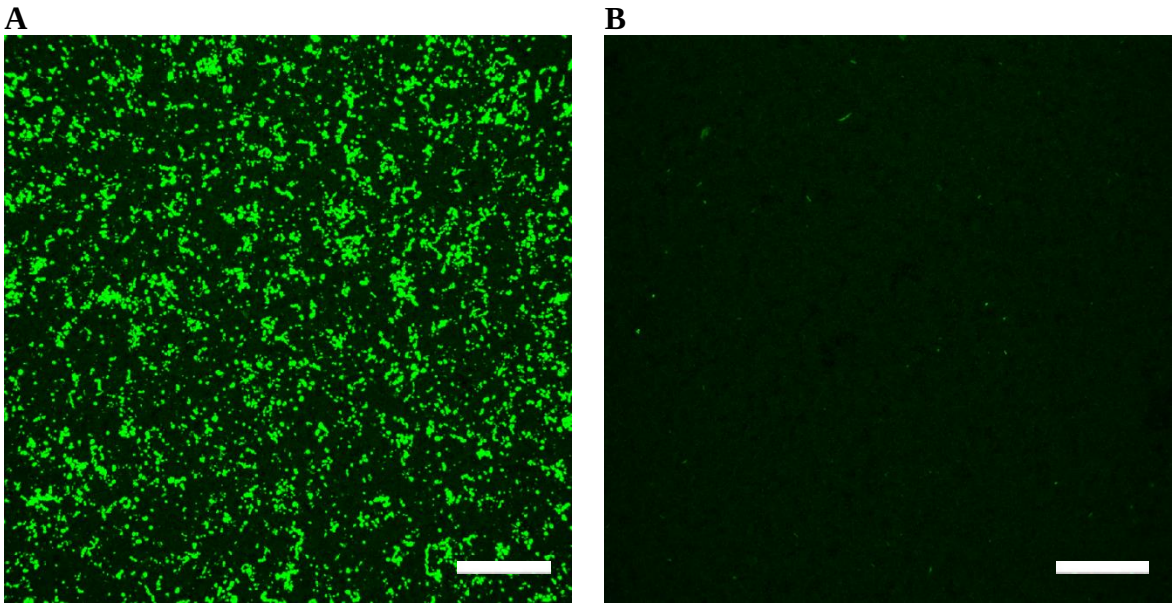

Figure 5.2: Biofilm formation of a D39 pneumococcal strain expressing a GFP plasmid

Confocal microscopy was used to assess the level of green fluorescence as a measure of the number of viable pneumococcal cells and the extent of biofilm formation. In the presence of maltose, GFP-expressing pneumococci successfully fluoresced in the biofilm phenotype (A). In the absence of maltose, GFP-expressing pneumococci did not fluoresce in the biofilm phenotype, with minimal background fluorescence detected (B). Scale bar, 40 μm.

5.5 Establishing a confluent monolayer of 16HBE cells on transwell membranes

The aim for the first co-culture experiment was to determine whether 16HBE cells formed a confluent monolayer on transwell membrane inserts in a 12-well plate, and how long it would take for confluence to be reached. Six transwell membranes were each seeded with $2.5x10^5$ 16HBE cells (Chapter 2, section 2.19), and the TEER was measured daily in each transwell as previously described (Chapter 2, section 2.20). The experiment was then performed two more times (n = 3).

The average TEER value of all 18 transwells on day 1 was less than 1000 Ohms.cm^2 (Figure 5.3). From day 1 to day 3, the TEER increased, with a statistically significant increase from day 1 to day 2 (p<0.0001) and from day 2 to day 3 (p<0.0001). However, there was no significant difference in the TEER values from day 3 to day 4 or from day 4 to day 5 as the TEER began to plateau, with readings of approximately 7000 Ohms.cm^2 recorded.

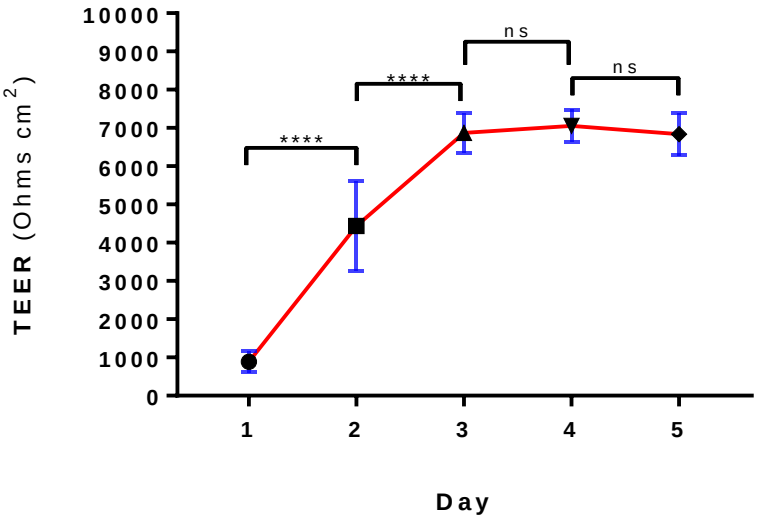

Figure 5.3: TEER measurement of a 16HBE cell line grown on transwell membrane inserts.

Six transwell membrane inserts were each seeded with $2.5x10^5$ 16HBE cells supplemented with 500 µl of sMEM (day 0), in each of three independent experiments. For the next 5 days, the TEER across each membrane was recorded. The graph shows the TEER readings from all three experiments combined; the mean TEER from all 18 transwells on each day. The TEER increased from days 1 to 3, with a significant increase from day 1 to day 2, and from day 2 to day 3. From day 3 to day 5 the TEER began to plateau. Data points represent the mean and the error bars represent the standard errors of the mean, from three independent pooled experiments. Significance indicated as follows: ****, $P < 0.0001$; ns, not significant.

Alongside the TEER experiments, light microscopy images of the 16HBE cells after seeding the transwell inserts were taken daily to visually monitor the development of a confluent monolayer over time (days 1 to 5). For each experiment (n = 3), a photomicrographic image was taken of one transwell for five consecutive days at the same time each day, as previously described (Chapter 2, section 2.27). Images were taken of the same area of the transwell each time.

On day 1, there were large gaps between clusters of 16HBE cells, which varied in size (Figure 5.4, A). This observation explained the low TEER value readings (<2000 Ohms.cm^2) on day 1 (Figure 5.3). Similarly, the clusters of epithelial cells on days 2 and 3 increased in size (Figure 5.4, B and C) and reflected the sharp increase in electrical resistance across the epithelial cells due to the growing confluence of the cell monolayer (Figure 5.3). Finally, on days 4 and 5 there was complete surface coverage of the 16HBE monolayers on the membrane insert (Figure 5.4, D and E), suggesting that the high TEER values on days 4 and 5 (Figure 5.3) were due to the formation of intercellular tight junction complexes. The TEER results, combined with the 16HBE microscopic images, indicated that the 16HBE cells could form a confluent monolayer of healthy cells on transwell membranes. Consequently, the cells could be inoculated with *S. pneumoniae*.

A Day 1

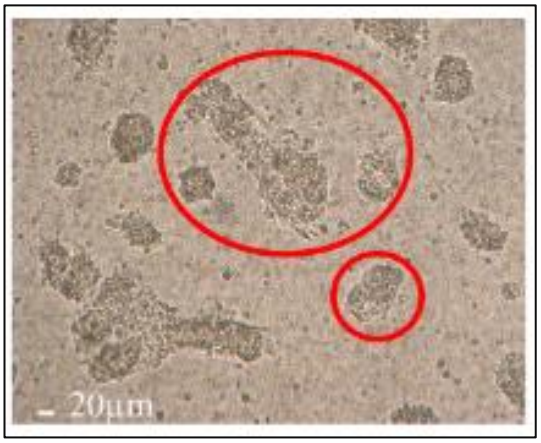

B Day 2

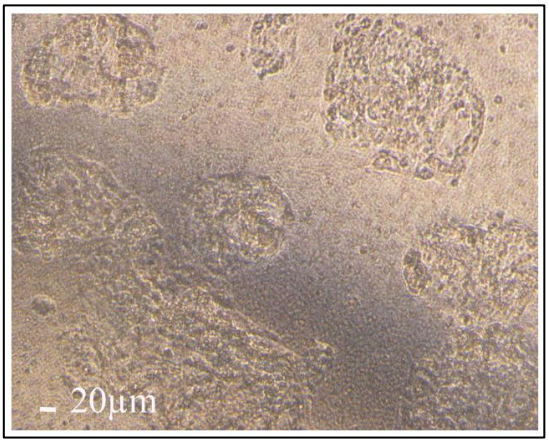

C Day 3

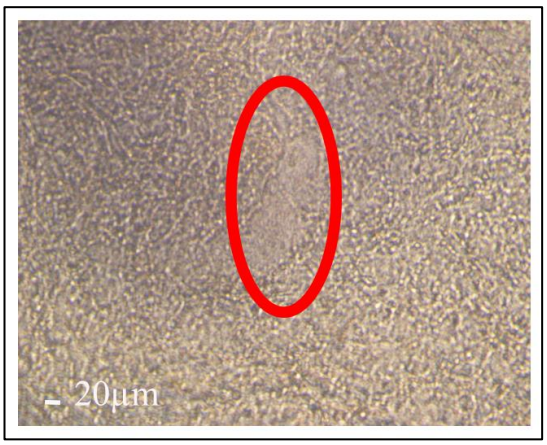

D Day 4

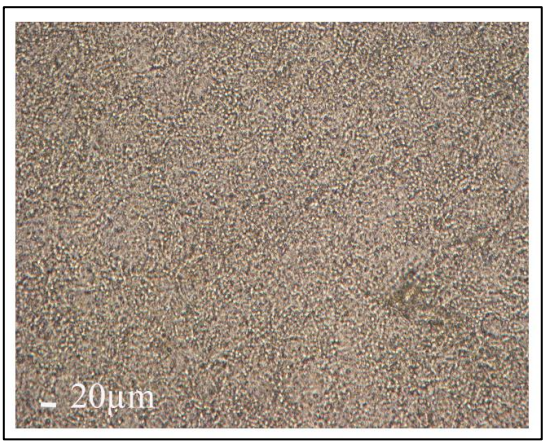

E Day 5

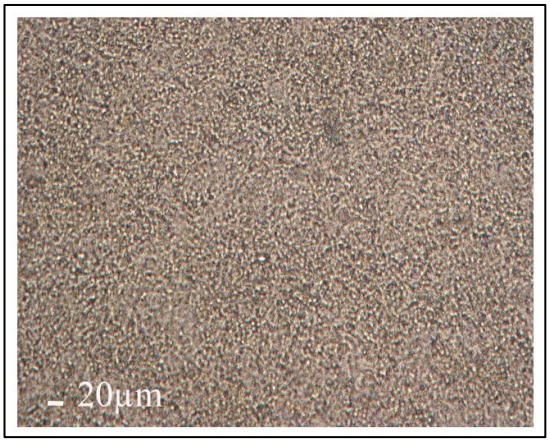

Figure 5.4: 16HBE cells growing on a transwell membrane insert across five days.

On day 1 the 16HBE cells adhered to the transwell membranes, forming variable sized clusters of cells (depicted by the red circles) (A). On day 2, the clusters of cells became larger as the epithelial cells continued to divide and grow, with smaller gaps detected (B). By day 3, only small areas of the underlying membrane (red circle) were not covered with epithelial cells (C). By days 4 and 5, the 16HBE cells completely covered the surface of the transwell membrane to form a confluent monolayer (D and E). Images were taken with an Olympus digital camera, as previously described (Chapter 2, section 2.27).

5.6 Growing 16HBE cells in the absence of antibiotics

The aim for the next experiment was to determine if the absence of antibiotics (i.e. penicillin and streptomycin) in the sMEM impacted the health of the monolayers as reflected in the TEER, since no antibiotics could be present in the co-culture model once pneumococcus was added. Six transwell membranes were seeded with $2.5x10^5$ 16HBE cells as before (section 5.5), and the TEER was measured daily in each transwell. After taking the TEER measurements on day 3, the apical and baso-lateral medium was replaced with antibiotic-free sMEM. TEER was measured on day 4 to determine whether there was a decrease in the TEER. If there was no decrease in the TEER then the 16HBE cell monolayers would be infected on day 4, and the replacement of co-culture medium with antibiotic-free sMEM would be performed 24 hours prior to infection (i.e. day 3). This approach would ensure that pneumococci would not be killed by any residual antibiotics in the co-culture model. The experiment was performed four times.

TEER increased from days 1 to 3 (Figure 5.5). On day 3, the average TEER across the 16HBE monolayers was 7000 $Ohms.cm^2$. On day 4, the average TEER was 7500 $Ohms.cm^2$, indicative that the change to antibiotic-free sMEM did not cause a decrease in the TEER (Figure 5.5). As a result, day 4 was chosen to infect the 16HBE cells with pneumococci, supported by images of epithelial cells demonstrating confluent monolayers on day 4 with no gaps observed (Figure 5.4, D). Collectively, therefore, the cell monolayers would be healthy and stable prior to infection.

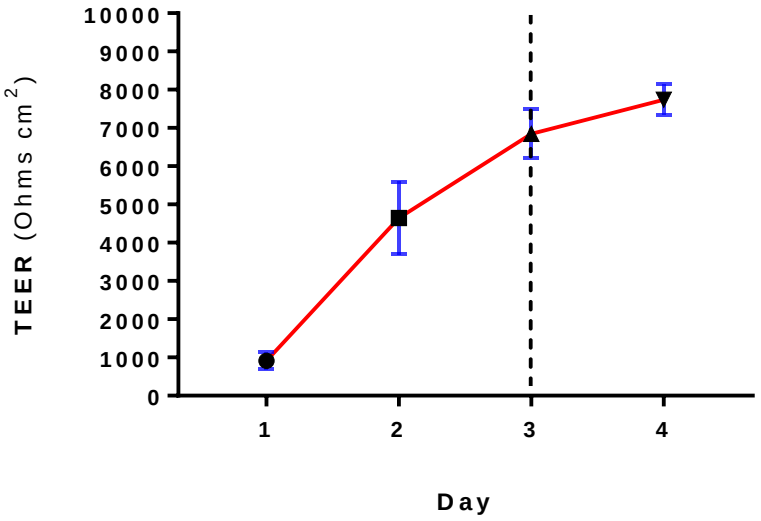

Figure 5.5: TEER measurement of 16HBE cell monolayers in the presence and absence of antibiotics.

Six transwell membrane inserts were each seeded with $2.5x10^5$ 16HBE cells supplemented with 500 µl of sMEM (day 0), in each of four independent experiments, and the TEER was measured for the next 4 days. In each experiment, the apical and baso-lateral medium in each transwell was replaced with antibiotic-free sMEM after the TEER readings were taken on day 3 (depicted with a dashed vertical line). TEER values were taken 24 hours later on day 4. The graph shows the TEER readings from all four experiments combined. The TEER continued to increase from days 1 to 4. Data points represent the mean and the error bars represent the standard errors of the mean, from four independent pooled experiments.

5.7 Inoculation of 16HBE cell monolayers with different ratios of pneumococcal cells (multiplicities of infection)

16HBE cell monolayers were infected with the *S. pneumoniae* laboratory strain D39 on day 4, as previously described (Chapter 2, section 2.22). Brittan et al. and Smith et al. reported cytotoxic effects on primary respiratory epithelial cells within 4 hours of pneumococcal challenge (Pracht et al., 2005, Brittan et al., 2012, Smith et al., 2013); however the MOI was not reported. As a result, a range of MOIs were tested to determine an optimum MOI that would maintain epithelial cell monolayer integrity during co-culture. MOIs of 1:1, 0.1:1, 0.01:1 and 0.001:1 were each tested in one transwell, and an uninfected monolayer and a transwell containing just antibiotic-free sMEM were also used to act as a negative control and represent a baseline value for TEER without a cell monolayer (~2000 Ohms.cm^2), respectively. The sMEM was changed to antibiotic-free sMEM following TEER measurements on day 3. The TEER was then measured before infecting the cells on day 4 (0 h), and at 2, 4, 6 and 18 hours post-infection, as previously described (Chapter 2, section 2.20). The apical and baso-lateral medium from all the monolayers was replaced with fresh antibiotic-free sMEM 1 hour prior to TEER measurements at 18 hours. Medium replacement was not carried out before the other time-points post-infection to ensure bacterial adhesion to the cell monolayer. The experiment was then repeated three times (n = 4).

The aim of the experiment was to assess monolayer health in response to different MOIs and determine the co-culture period. The experiment would indicate at what time 16HBE monolayer integrity was affected in the presence of pneumococci.

There was a drop in the TEER of the uninfected 16HBE cell monolayers after 18 hours of co-culture (Figure 5.6). This decrease in TEER might be attributable to the lack of antibiotics in the sMEM in the co-culture model from day 3 after seeding.

For the infected monolayers, there was not a statistically significant drop in the TEER compared to the uninfected monolayers up to 6 hours post-infection. At 18 hours post-infection, the TEER from all of the infected monolayers had significantly dropped in comparison to the uninfected epithelial cells (p<0.0001), with the mean TEER readings all at the baseline value (i.e. a membrane insert without any epithelial cells) of ~1000 Ohms.cm^2. There was no significant difference in the TEER between the MOIs at 18 hours post-infection (data not shown). As the TEER had drastically decreased for all the MOIs after 18 hours of co-culture compared to the uninfected epithelial cells, this result suggested that this particular TEER change in the pneumococcal-infected transwells was pneumococcal- and time-dependent. Specifically, pneumococci were affecting 16HBE cell

monolayer confluency by disturbing tight junction formation and/or causing epithelial cell death.

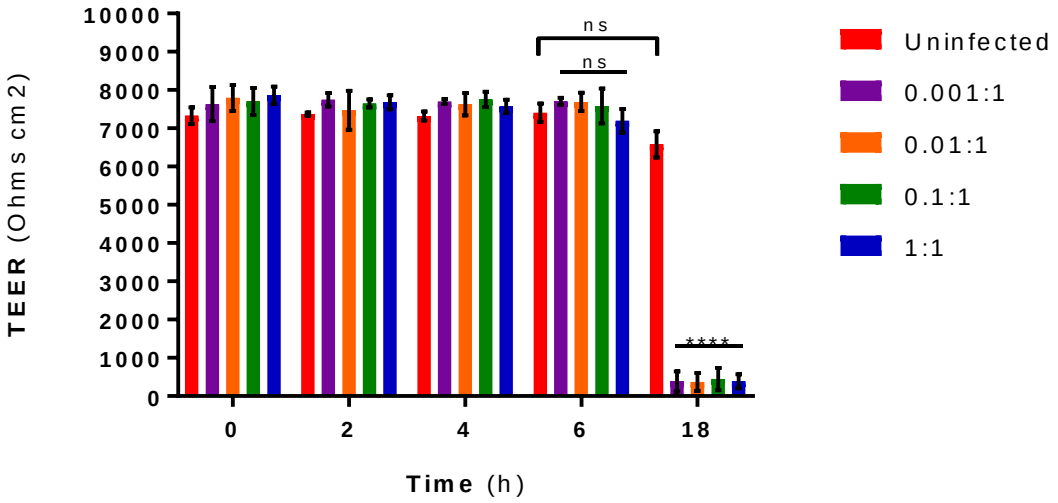

Figure 5.6: Infecting 16HBE cells with different MOIs of a D39 pneumococcal strain.

16HBE cell monolayers were infected with different MOIs of the *S. pneumoniae* strain D39. TEER of uninfected and infected monolayers was measured prior to challenge with pneumococci (0 hours) and at several time-points post-infection. The confluence of the infected monolayers was compromised at 18 hours post-infection, reflected by a significant drop in TEER compared to uninfected epithelial cells. Data points represent the mean and the error bars represent the standard errors of the mean, from four independent pooled experiments. Significance is indicated as follows: ****, $P < 0.0001$; ns, not significant.

5.8 Measuring pneumococcal attachment to 16HBE cells at 2, 4 and 6 hours post-infection

For the next experiment, 16HBE cell monolayers were again infected with a range of MOIs from 1:1 to 0.001:1 and bacterial adherence was measured. The main aim was to determine if pneumococci were adhering to the surface of the 16HBE cell monolayers. Therefore, viable counts (CFUs) of pneumococci were made at 2, 4 and 6 hours post-infection, as previously described (Chapter 2, section 2.23). These time-points had previously been used to measure TEER of infected monolayers and, therefore, were chosen for CFU enumeration. The second aim was to determine if there was an increase in the number of pneumococcal cells adhered to the 16HBE monolayers during co-culture, and if any observed increase was dose-dependent.

Cultures were seeded as previously described (Chapter 2, section 2.19), followed by a change to antibiotic-free sMEM on day 3. At day 4, TEER was measured and epithelial cell monolayers were infected with MOIs of either 1:1, 0.1:1, 0.01:1 and 0.001:1 per transwell, or left uninfected. At 2, 4 and 6 hours post-infection the transwell inserts were processed for calculating total viable counts. For each assay, CFUs were measured for all of the MOIs at a particular time-point (i.e. 2, 4 or 6 hours post-infection). CFUs were measured a total of four times for each time-point.

Pneumococci adhered to the surface of the 16HBE cell monolayers at 2 hours post-infection, with the number of viable *S. pneumoniae* ranging from 10^1 for the lowest MOI of 0.001:1 to 10^4 for the highest MOI of 1:1 (Figure 5.7). At 4 hours post-infection, viable pneumococci ranged from 10^2 to 10^5 for the MOIs of 0.001:1 and 1:1. At 6 hours post-infection, viable pneumococci ranged from 10^4 to 10^6 for the same MOIs. Therefore, co-culture duration correlated with an increase in the number of CFUs for all of the MOIs tested, with the highest number of viable cells observed at 6 hours post-infection.

There was not a statistically significant difference in viable pneumococci between adjacent MOIs at any of the time-points measured, but there was a significant difference between the lowest MOI of 0.001:1 and the highest MOI of 1:1 at 2, 4 and 6 hours post-infection (Figure 5.7, A-C).

The overarching aim for the development of this co-culture model was to determine the optimum infection time and the optimum MOI that would allow viable *S. pneumoniae* to adhere to the 16HBE cells without compromising monolayer integrity. Based on TEER (Figure 5.6) and CFU data (Figure 5.7), the integrity of the 16HBE monolayers was still maintained at 6 hours post-infection despite the presence of more viable pneumococci than at 2 hours or 4 hours. It was hypothesised that more viable cells would translate to an increase in the size and/or number of pneumococcal aggregates, with greater surface area

coverage on the epithelial cells. The higher the number of well-established aggregates would provide for a more robust and reliable co-culture model to not only examine pneumococcal biofilm-host interactions, but also genomics-based analyses or evaluation of treatments against early biofilm formation. Consequently, a 6 hour co-culture model with an MOI of 1:1 could have been used for subsequent assays, but TEER data (Figure 5.6) indicated that the integrity of the 16HBE cells might be maintained beyond 6 hours before the loss of integrity at 18 hours post-infection. Since co-culture models used by other research groups to date have used infection assays up to only 4 hours on live epithelial cells without a flow system model (Pracht et al., 2005, Bootsma et al., 2007, Sanchez et al., 2011b, Brittan et al., 2012, Blanchette-Cain et al., 2013, Blanchette et al., 2016), the aim was to see if the 6-hour co-culture model could be extended further using the same MOIs, and thereby provide a more representative model of biofilm formation.

Prior to this, it was important at first to demonstrate that pneumococci were forming a biofilm at the 6-hour time-point. Originally, confocal microscopy was to be used to assess the surface area coverage of D39 pneumococcal biofilms on confluent 16HBE cell monolayers. However, due to access to inverted microscopes only, this technique would not enable high quality images to be obtained due to the poor refractive index of the transwell membranes. It was decided that SEM would be used instead to detect the presence of pneumococcal biofilms on the epithelial monolayers. SEM is an invaluable tool for visualising the architecture of a biofilm including, the structure, density, spatial organisation, surface coverage, cellular morphology, and even depth to an extent. Whereas, although confocal microscopy does not provide the same level of magnification and resolution that is required to for detailed observation of individual pneumococcal cells, it is often the preferred method of choice for quantifying bacteria due to the fluorescence signal and a greater field of view, as well as for distinguishing between viable and non-viable bacterial cells (Hannig et al., 2010).

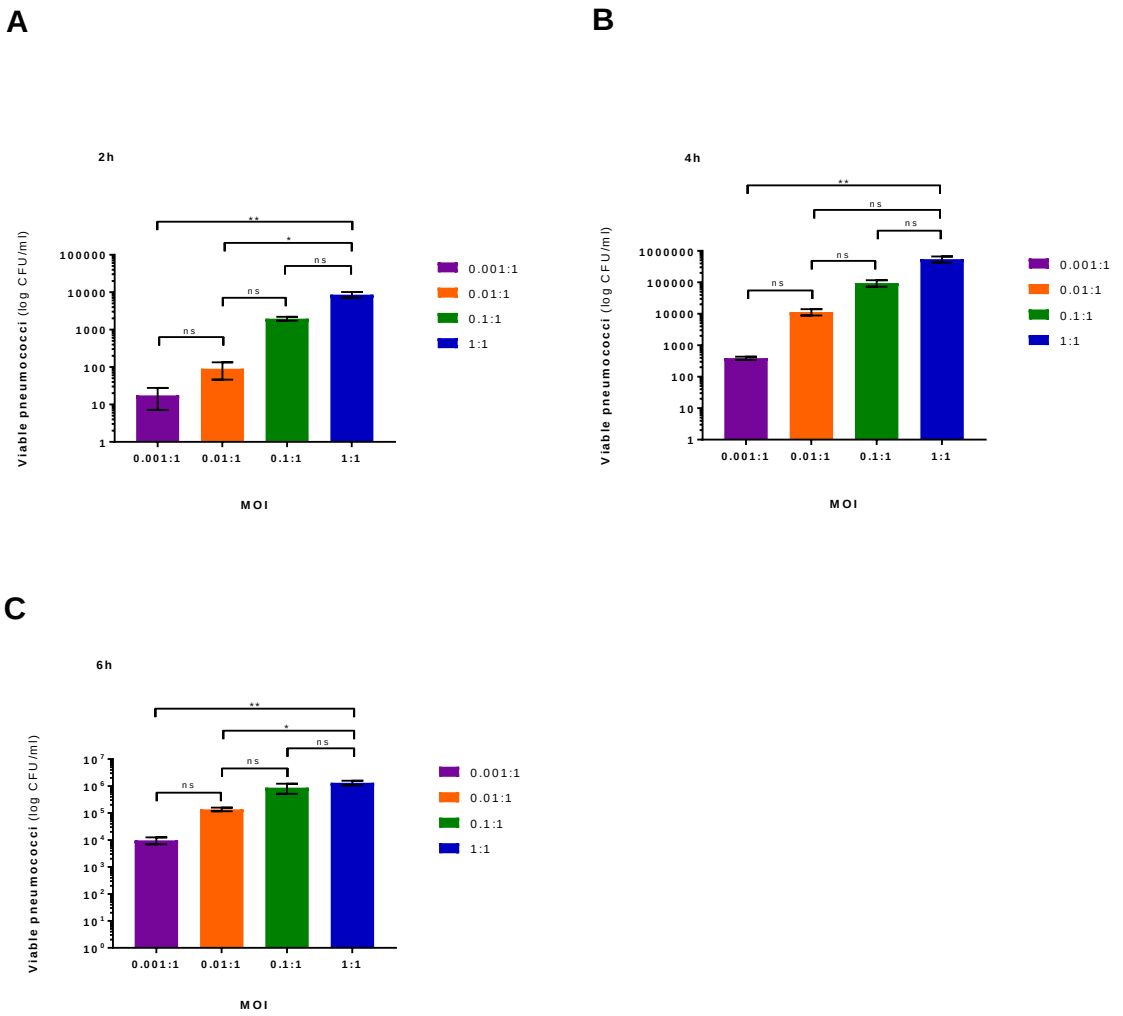

Figure 5.7: Viable pneumococcal cells on 16HBE cell monolayers up to 6 hours post-infection.

16HBE cell monolayers were infected with different MOIs of D39. Viable pneumococcal cells were determined from infected co-cultures at 2 (A), 4 (B) and 6 hours (C) post-infection. An increase in the number of CFUs between each of the MOIs was observed at each time-point (A-C). Pneumococcal colonies were not detected from the uninfected control. Data points represent the mean and the error bars represent the standard errors of the mean, from four independent pooled experiments for each time-point. Significance is indicated as follows: *, $P<0.05$; **, $P < 0.01$; ns, not significant.

5.9 Early pneumococcal biofilm formation on 16HBE cell monolayers at 6 hours post-infection shown by scanning electron microscopy (SEM)

It had previously been shown that the integrity of 16HBE monolayers was preserved up to 6 hours post-infection with different pneumococcal MOIs (Figure 5.6). SEM was used to determine whether the pneumococcal cells formed biofilms. 16HBE cultures were infected with the same MOIs, and each transwell was processed for SEM analysis at 6 hours post-infection, as previously described (Chapter 2, section 2.24) with uninfected 16HBE cells used as a negative control. The experiment was then repeated once more (n = 2).

Surface-attached and aggregated pneumococci of different sizes were seen on the epithelial cell monolayers for all of the MOIs (Figure 5.8). Furthermore, the presence of an extracellular matrix was found encasing some of the aggregates, indicative of the formation of a biofilm (Figure 5.8, D). Pneumococci were not detected on the uninfected epithelial monolayers (Figure 5.8, E). Aside from variability in the overall surface area of each biofilm, the most notable finding was the pleomorphic nature of the individual pneumococcal cells. Pneumococci were not evenly distributed over the surface of the epithelial cell monolayers, and were detected at a magnification of x1000 or greater. For this reason, it was difficult to determine the overall surface area coverage for any of the SEM samples. Pneumococcal biofilms have also been shown to be neither confluent nor contiguous when grown in the nasopharynx of mice, which is in stark contrast to when they are grown on a plastic microtiter plate surface (Blanchette-Cain et al., 2013). Preparing the SEM samples for electron microscopy involved a harsh dehydration process, which might account for why extracellular matrix material (which is a highly hydrated structure in nature) was not detected in all of the images. Nevertheless, the SEM samples demonstrated that pneumococcal biofilms were evident on live epithelial cells at 6 hours post-challenge for all of the MOIs.

A MOI 1:1

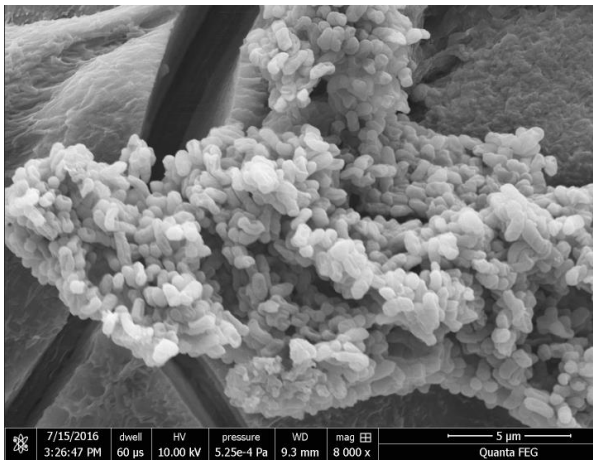

B MOI 0.1:1

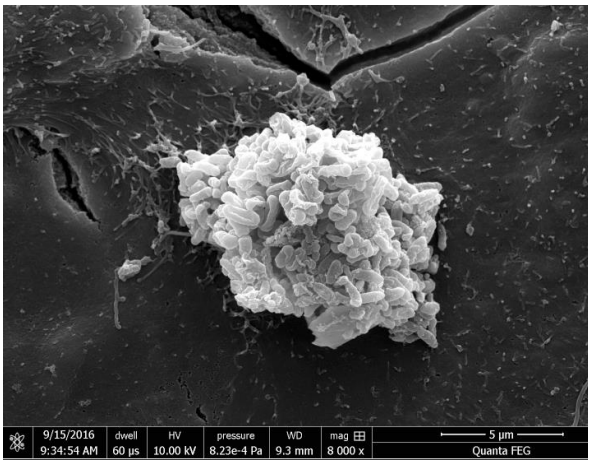

C MOI 0.01:1

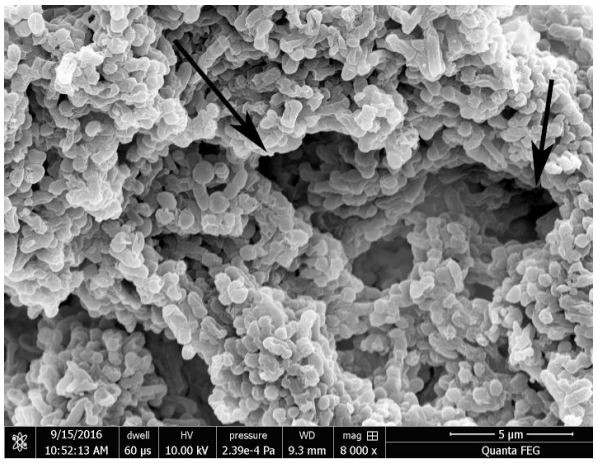

D MOI 0.001:1

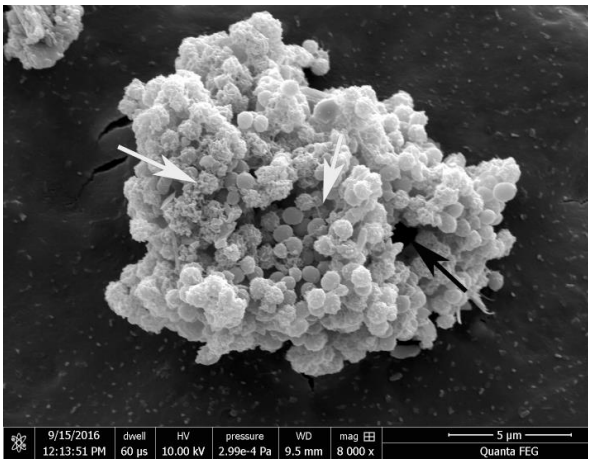

E Uninfected cells

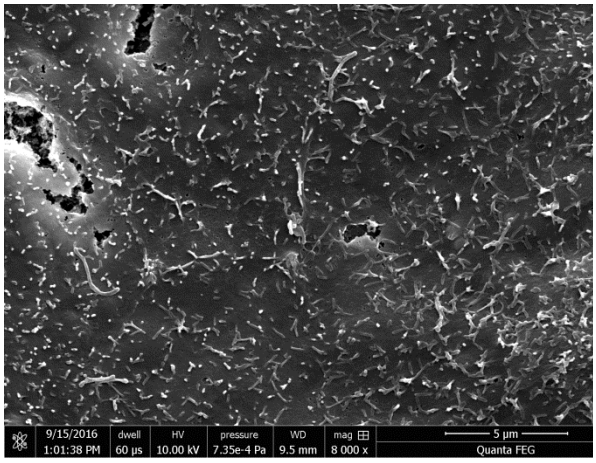

Figure 5.8: Early D39 pneumococcal biofilm formation on bronchial epithelial cells using scanning electron microscopy.

16HBE cell monolayers were infected with different MOIs of the pneumococcal strain D39. At 6 hours post-infection, uninfected and infected monolayers were processed for SEM analysis to assess pneumococcal biofilm formation. Representative images for the MOIs of 1:1 (A), 0.1:1 (B), 0.01:1 (C) and 0.001:1 (D) are shown, as well as an uninfected culture (E) at a magnification of x8000. Surface-attached, pneumococcal aggregates were present for each of the MOIs (A-D). The formation of an extracellular matrix and fibrous material were also detected (white arrows, D), as well as water channels depicting aggregate heterogeneity (black arrows, C and D). Adherent pneumococci were not detected on the uninfected monolayers (E).

5.10 16HBE cell health measured by TEER beyond 6 hours of co-culture with *S. pneumoniae* D39

In this project so far it was shown that 16HBE cells formed confluent monolayers on transwell membranes on day 4 after seeding (section 5.5), and that the confluence/monolayer integrity remained unperturbed in the presence of different bacterial loads (MOIs) of the *S. pneumoniae* laboratory strain D39, for up to 6 hours after inoculation (Figure 5.6). However, at 18 hours post-infection there was a statistically significant decrease in the TEER of the infected monolayers (Figure 5.6). By measuring viable counts at different time-points post-infection (Figure 5.7), and by processing the co-cultured epithelial cells at 6 hours post-infection for SEM analysis (Figure 5.8), it was demonstrated that pneumococci adhered to the surface of the epithelial cells and formed structured, heterogeneous aggregates as an indication of early (nascent) biofilm formation.

Current *in vitro* pneumococcal biofilm studies typically involve at least 24 hours growth on an abiotic (glass or plastic) surface to ensure sufficient biomass (CFUs) and that an extracellular matrix has formed. Furthermore, it would be reasonable to presume that colonising pneumococcal biofilms in the nasopharynx are present for longer than 6 hours. Taken together, the aim for the next part of this chapter was to extend the co-culture duration beyond 6 hours, whilst maintaining a TEER reflective of healthy monolayer integrity. Thus, 16HBE cells were infected as before (one transwell for each MOI) and the TEER was measured at 8, 10 and 12 hours post-infection. The aim was to determine at which time-point the TEER of the infected epithelial monolayers decreased to a level similar to that seen at 18 hours (Figure 5.6), or whether the TEER incrementally decreased. In the event of the latter, the last time-point that preceded this decrease would be used as the new end-point of the co-culture model for subsequent assays. The experiment was repeated three times (n = 4).

After 6 hours of co-culture, there was a significant drop in the TEER of the 16HBE cell monolayers challenged with the two highest MOIs of 1:1 and 0.1:1 in comparison to uninfected 16HBE cells (Figure 5.9, A). This result was not seen in previous experiments (Figure 5.6), whereby there was not a significant drop in the TEER for any of the MOIs at 6 hours post-infection. There was a slight drop (~800 Ohms.cm^2) in the TEER of the uninfected 16HBE cell monolayers after 6 hours of co-culture (data not shown). These observed differences between the two sets of experiments may be attributable to the fact that a higher passage number of the 16HBE cells were used having performed CFU (section 5.8) and SEM analyses (section 5.9). Repeated passaging can cause immortalised cell lines to gradually lose normal physiology or genetic stability.

At 8 hours post-infection, there was a significant decrease in the TEER for the MOI of 0.01:1 (Figure 5.9, B), and TEER significantly decreased for all of the MOIs from 10 hours post-infection (Figure 5.9, C-D). Consequently, an MOI of 0.01:1 and an end-point of 6 hours, or an MOI of 0.001:1 and an end-point of 8 hours, could have been used for subsequent assays.

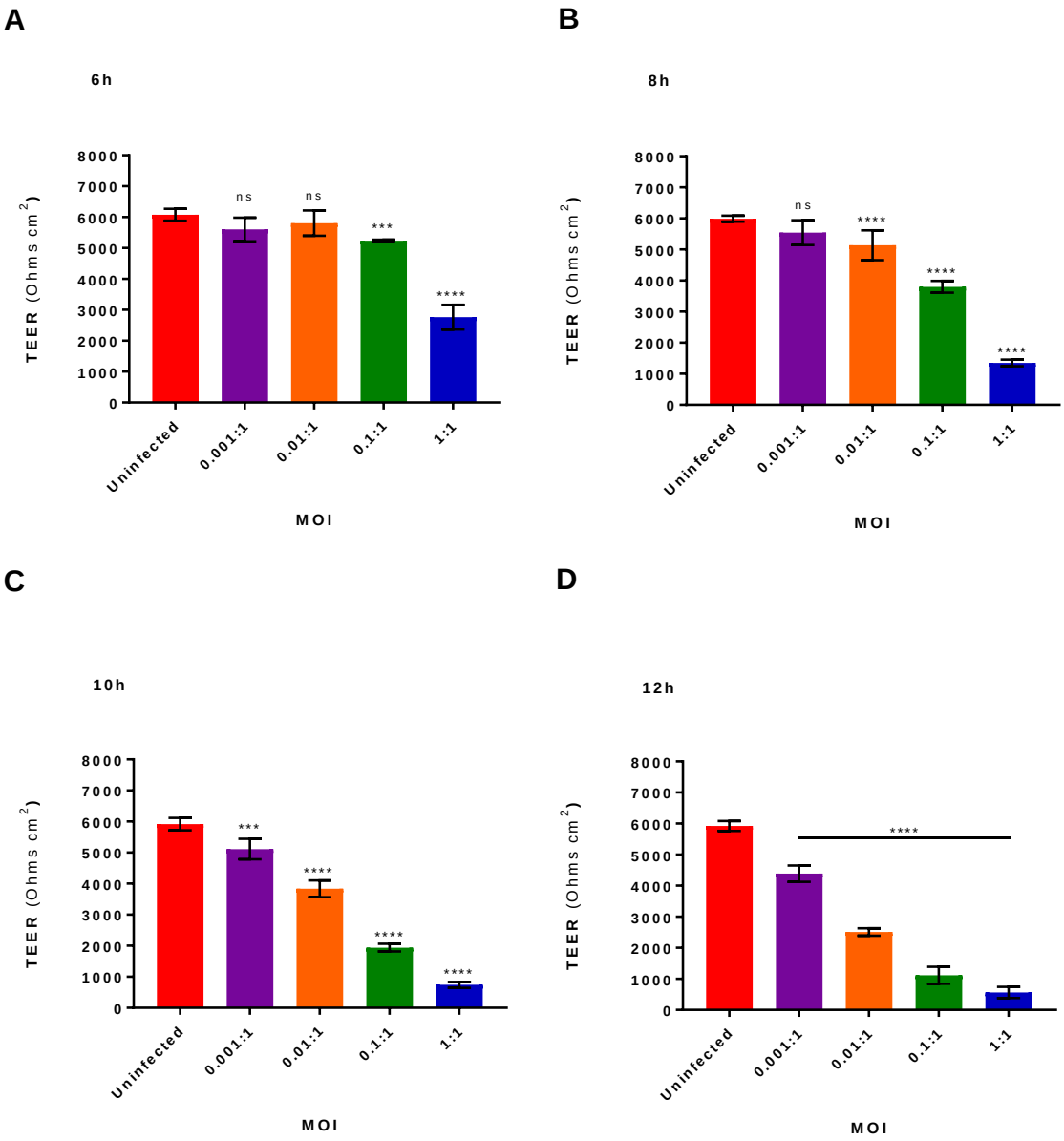

Figure 5.9: TEER of 16HBE cells co-cultured with *S. pneumoniae* from 6 hours to 12 hours post-infection.

16HBE cells were infected with different MOIs of the pneumococcal strain D39. TEER of uninfected and infected monolayers was measured prior to challenge (0 hours) and at 6 (A), 8 (B), 10 (C) and 12 hours (D) post-infection. TEER remained unchanged from 6 hours to 12 hours for the uninfected cultures. TEER for the MOIs of 1:1 and 0.1:1 significantly decreased at all the time-points measured (A-D). TEER significantly decreased at 8 hours (B) and at 10 hours (C) post-infection for the MOIs of 0.01:1 and 0.001:1, respectively. Data points represent the mean and the error bars represent the standard errors of the mean, from four independent pooled experiments. Significance is indicated as follows: ***, $P < 0.001$; ****, $P < 0.0001$; ns, not significant.

The observed decrease in TEER from the infected 16HBE monolayers was postulated to be the direct result of pneumococcal-induced disruption to epithelial transmembrane intercellular tight junctions and/or epithelial cell death. The cytotoxic effects caused by the pneumococcal cells may be due to a number of factors: 1) pneumococci produce and secrete hydrogen peroxide and pneumolysin; two virulence factors that are toxic to epithelial cells and directly induce cellular damage (Feldman et al., 1990, Feldman et al., 1994); 2) pneumococci are able to undergo lysis, which is coupled with the release of pneumolysin (Rubins and Janoff, 1998). Thus, pneumococci in the co-culture model may have lysed from 6 hours post-infection causing the release of toxins, resulting in cytotoxicity and disruption of monolayer integrity; 3) individual pneumococcal cells may have shed from the nascent biofilms and these dispersed planktonic cells could exhibit enhanced virulence with regard to the epithelial cells; a phenomenon which has been observed using *in vivo* mouse models (Marks et al., 2012b, Marks et al., 2013).

In order to try and inhibit the effect of these putative factors to further extend the duration of the co-culture model, different approaches were considered for subsequent assays. A pneumolysin mutant strain could have been used to remove any pneumolysin from the co-culture model. Alternatively, a mutant strain for the gene *spxB* - which codes for the enzyme, pyruvate oxidase, involved in the production of hydrogen peroxide - could have been used. However, pneumolysin and SpxB have been shown to be important for the biofilm mode of growth (Bättig and Mühlemann, 2008, Marks et al., 2012a, Blanchette-Cain et al., 2013, Shak et al., 2013a, Blanchette et al., 2016). Furthermore, the aim of the co-culture model was to recapitulate as much as possible the *in vivo* pneumococcal-host environment in the nasopharynx. Therefore, the preferred approach was to attempt to counteract the activity of hydrogen peroxide rather than using single- or double-mutant strains. Catalase neutralises hydrogen peroxide to water, and has been shown to completely attenuate decreased ciliary motility and epithelial cell damage *in vitro* (at 1000 units/ml) (Feldman et al., 2002).

As a result, 16HBE cell monolayers were infected with pneumococci in antibiotic-free sMEM supplemented with catalase (Sigma-Aldrich, U.K.) for the next set of experiments. Additionally, two other alterations to the co-culture model were implemented. Firstly, 16HBE monolayers were infected on day 5 rather than on day 4 after cultures were initiated. Although there was no statistically significant difference in the TEER between day 4 and day 5 (Figure 5.3), it was thought that infecting on day 5 might permit a more stable cell monolayer at the time of inoculation. Secondly, the apical and baso-lateral catalase-supplemented antibiotic-free sMEM was replaced with fresh co-culture medium at 0.5 hours post-infection and at other time-points. Replacing the medium at 0.5 hours post-

infection was thought to be sufficient time for some pneumococcal cells to adhere to the surface of the cell monolayers, whilst reducing the amount of toxins, such as pneumolysin, that might be present. It was also thought that media replacement at later time-points post-infection might remove any planktonic cells that may have dispersed from the nascent biofilm.

5.11 TEER of 16HBE monolayers beyond 6 hours post-infection with *S. pneumoniae* D39 in catalase-supplemented media

For the next set of experiments, 16HBE monolayers were seeded on transwell inserts, as previously described (Chapter 2, section 2.19). However, after taking TEER measurements on day 4, the apical and baso-lateral medium was replaced with antibiotic-free sMEM. On day 5, TEER measurements were taken and the monolayers were infected with MOIs of 1:1, 0.1:1, 0.01:1 and 0.001:1 per transwell in catalase-supplemented antibiotic-free sMEM (1000 units/ml). An uninfected monolayer was used to determine if catalase had a detrimental effect on epithelial cell integrity, evidenced by a decrease in TEER. Apical and baso-lateral medium was replaced at 0.5 hours post-infection and at 6, 8, 10, 12 and 19 hours post-infection. TEER was measured at 6, 8, 10, 12 and 20 hours post-infection, as previously described (Chapter 2, section 2.20). The experiment was repeated three times (n = 4). The aim was to determine whether the aforementioned changes to the co-culture model (section 5.10) would maintain TEER beyond 6 (0.01:1) to 8 (0.001:1) hours post-infection (Figure 5.9).

TEER readings for the MOI of 1:1 had significantly decreased from 8 hours post-infection in comparison to uninfected 16HBE cultures (Figure 5.10, A-D). In contrast, TEER measurements for the remaining MOIs indicated that there was not a statistically significant decrease after 12 hours of co-culture (Figure 5.10, A-C). However, at 20 hours post-infection there was a significant drop in TEER for all the remaining MOIs (Figure 5.10, D). There was a drop in the TEER (~2000 Ohms.cm^2) of the uninfected monolayers after 6 hours of co-culture (data not shown). This drop was greater than in previous experiments (section 5.10).

In summary, it appeared that the aforementioned changes in the co-culture protocol were successful in extending the model to 12 hours for specific MOIs of pneumococci. Specifically, replacement of the apical and baso-lateral medium with fresh catalase-supplemented antibiotic-free sMEM was pivotal in preserving TEER of infected 16HBE cell monolayers.

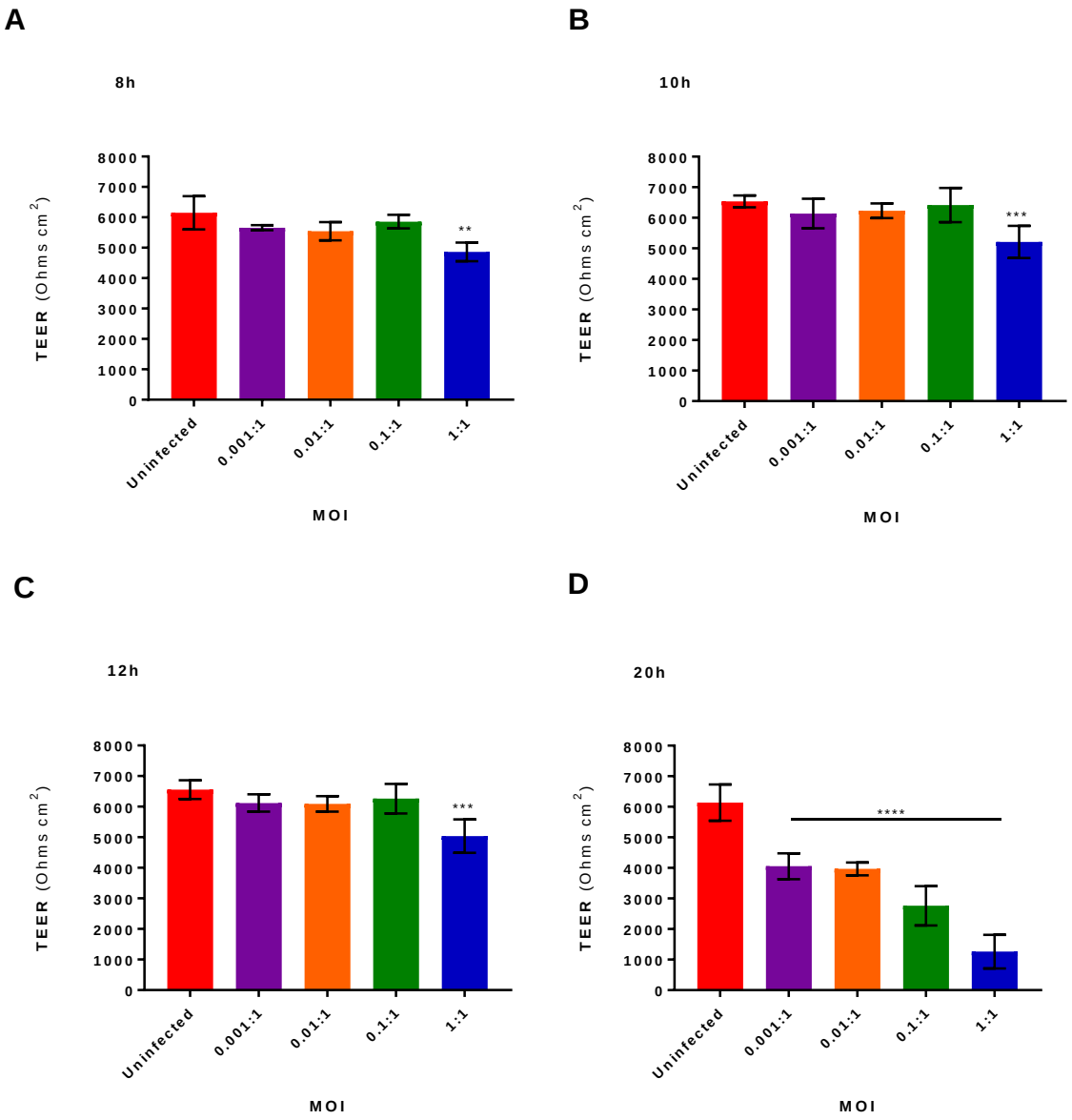

Figure 5.10: TEER of 16HBE monolayers co-cultured with *S. pneumoniae* D39 between 6 hours and 20 hours in the presence of catalase-supplemented media.

16HBE cells were infected with different MOIs of the pneumococcal strain D39 in catalase-supplemented antibiotic-free sMEM (1000 units/ml). TEER for the cultures infected with an MOI of 1:1 significantly decreased from 8 hours in comparison to uninfected 16HBE cells (A-D). TEER for the remaining MOIs only significantly decreased at 20 hours post-infection (D). Data points represent the mean and the error bars represent the standard errors of the mean, from four independent pooled experiments. Significance is indicated as follows: **, $P < 0.01$; ***, $P < 0.001$; ****, $P < 0.0001$; ns, not significant.

Although a 12-hour infection model was established for the MOIs of 0.1:1, 0.01:1 and 0.001:1 (Figure 5.10), the timing of the end-point of the infection assay was logistically problematic for processing the co-cultured cells for either CFU or SEM analyses, or for performing further assays on the same day. Moreover, it had recently been reported in the literature that the presence of catalase can affect the transcription of inflammatory cytokines (Loose et al., 2015). Since the aim was to establish a co-culture model that would permit interrogation of the epithelial response, such as the ability to measure the production of inflammatory cytokines, the use of catalase was not advisable. Therefore, for the next set of experiments the 16HBE cells were infected in the evening and the co-culture medium was replaced with fresh antibiotic-free sMEM without catalase after 0.5 hours and at 6 and 13 hours post-infection only. The aim of the experiment was to determine if the TEER was maintained at 14 hours post-infection on the following morning without catalase, and with fewer changes of the medium, to facilitate processing at 14 hours in order to prolong the co-culture model.

5.12 TEER of 16HBE co-cultures with *S. pneumoniae* D39 beyond 6 hours in the absence of catalase-supplemented media

16HBE cells were seeded on transwell inserts for 5 days, as previously described (section 5.11). TEER measurements were taken and the monolayers were infected with MOIs of 0.1:1, 0.01:1 and 0.001:1 per transwell in antibiotic-free sMEM without catalase. The MOI of 1:1 was no longer used for co-culture experiments since the changes to the co-culture model (section 5.10) did not prevent this MOI from significantly reducing epithelial cell monolayer integrity (Figure 5.10). At 0.5 hours and at 6 and 13 hours post-infection, apical and baso-lateral medium from the monolayers was replaced with fresh antibiotic-free sMEM without catalase. TEER was measured before infecting the epithelial cells (0 hours) and at 14 hours post-infection. The aim of the experiment was to determine if the integrity of the infected cultures was maintained at 14 hours post-infection, despite the absence of catalase and fewer changes of the co-culture medium. The experiment was then repeated three times (n = 4).

The TEER of only the lowest MOI (0.001:1) had not significantly decreased at 14 hours post-infection in comparison to uninfected cultures (Figure 5.11). Whereas, in the 12 hour co-culture model, the TEER of 16HBE cells infected with higher pneumococcal loads (i.e. MOIs of 0.1:1 and 0.01:1) had not significantly decreased compared to uninfected epithelial cells at 12 hours post-infection (Figure 5.10). Additionally, this particular assay would not be useful for measuring the host response over several time-points against a developing pneumococcal biofilm. Taken together, this overnight co-culture assay was not thought to facilitate interrogation of 16HBE cell responses to a high pneumococcal load over time. As a result, the aim for the next experiment was to repeat the 12-hour co-culture model (Figure 5.10), but in the absence of catalase.

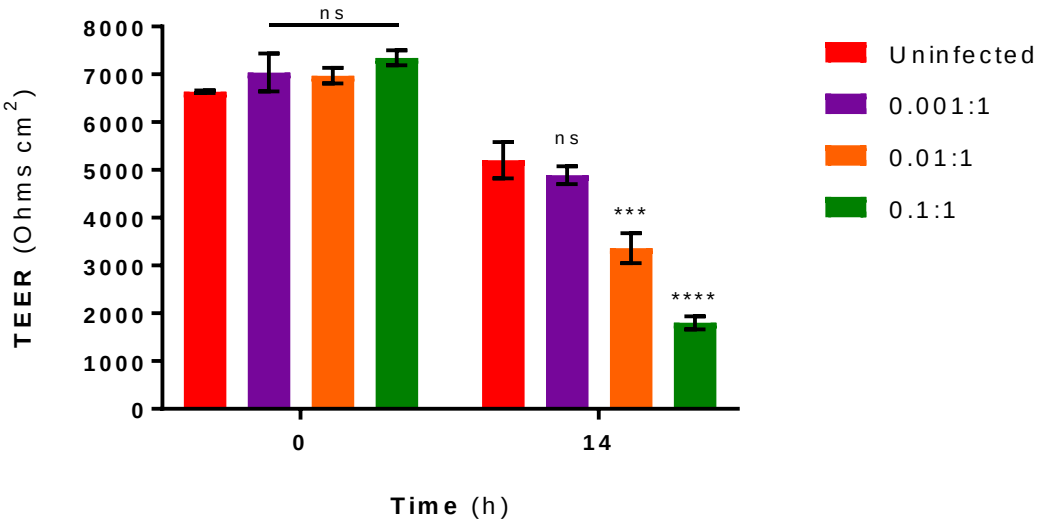

Figure 5.11: TEER of 16HBE monolayers co-cultured with *S. pneumoniae* D39 overnight in the absence of catalase-supplemented media.

16HBE cell monolayers were infected with different MOIs of the pneumococcal strain D39. TEER of uninfected and infected monolayers was measured prior to challenge (0 hours) and at 14 hours post-infection. TEER of only the lowest MOI (0.001:1) had not significantly dropped in comparison to uninfected 16HBE cells. Data points represent the mean and the error bars represent the standard errors of the mean, from four independent pooled experiments. Significance is indicated as follows: ***, $P < 0.01$; ****, $P < 0.0001$; ns, not significant.

5.13 TEER of 16HBE co-cultures infected with *S. pneumoniae* D39 for 12 hours

16HBE cells were seeded on transwell inserts for 5 days, TEER measurements were taken and epithelial cells were infected with MOIs of 0.1:1, 0.01:1 and 0.001:1 per transwell in antibiotic-free sMEM without catalase. An uninfected culture served as a negative control. Apical and baso-lateral medium from all cultures was replaced at 0.5 hours post-infection and at 6, 8 and 10 hours, whilst TEER was measured at 6, 8, 10 and 12 hours post-infection. The experiment was then repeated three times (n = 4). The aim was to determine whether the 12-hour co-culture model with catalase (Figure 5.10) could be reproduced in the absence of catalase.

TEER of all the MOIs was not statistically different from the uninfected cultures at 6, 8, 10 or 12 hours post-infection (Figure 5.12). This set of results suggested that the replacement of apical and baso-lateral medium with fresh antibiotic-free sMEM (without catalase) could preserve 16HBE cell integrity during 12 hours of co-culture.

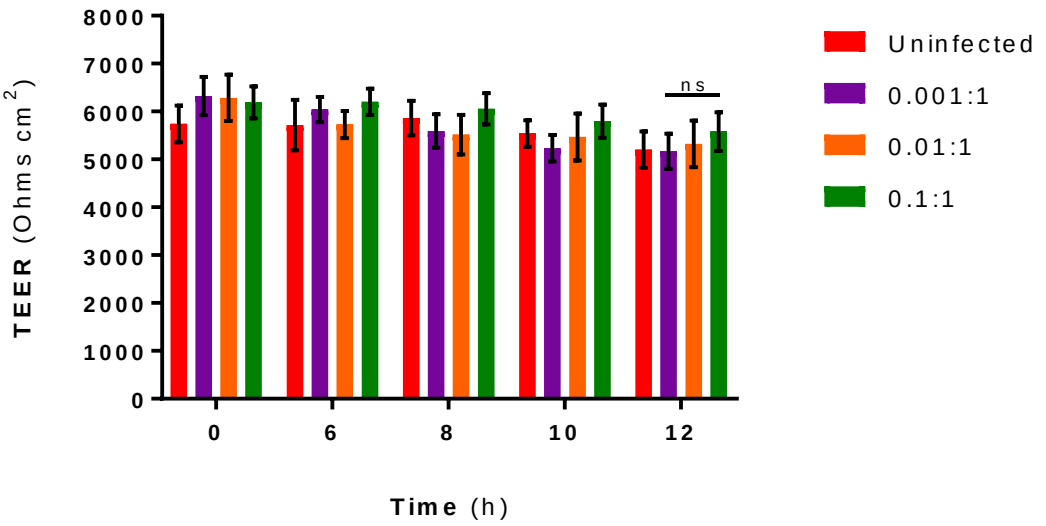

Figure 5.12: TEER of 16HBE monolayers co-cultured with *S. pneumoniae* D39 from 6 hours to 12 hours post-infection in the absence of catalase.

16HBE cell monolayers were infected with different MOIs of the pneumococcal strain D39. TEER of uninfected and infected monolayers was measured prior to challenge (0 hours) and at 6, 8, 10 and 12 hours post-infection. The TEER for all the MOIs had not significantly decreased in comparison to the uninfected 16HBE cells at any of the time-points measured. Data points represent the mean and the error bars represent the standard errors of the mean, from four independent pooled experiments. Significance is indicated as follows: ns, not significant.

5.14 Discussion

In this chapter, a 12-hour co-culture model using a live bronchial epithelial cell line and a *S. pneumoniae* serotype 2 strain (D39) was developed. In order to challenge the 16HBE cell monolayers for as long as possible before epithelial cell integrity was compromised (reflected by TEER) a range of MOIs were tested. Initially, on day 4 after seeding transwell membranes, the confluent epithelial monolayers were challenged with different MOIs in a static model, with no exchange of co-culture medium post-challenge (Figure 5.6). Viable *S. pneumoniae* adherent to epithelial cells was confirmed by CFU enumeration at 2, 4 and 6 hours post-infection (Figure 5.7), whilst SEM analysis at 6 hours post-infection showed the formation of heterogeneous pneumococcal biofilm aggregates (Figure 5.8). Epithelial cell monolayers remained confluent for up to 6 hours post-infection with an MOI of 0.01:1, and up to 8 hours with an MOI of 0.001:1 (Figure 5.9).

However, for the remaining MOIs at these time-points and, for all MOIs during later time-points, the TEER of the infected monolayers decreased significantly in comparison to uninfected cultures (Figure 5.9). This response could be attributed to a number of factors including, the production of hydrogen peroxide, the release of pneumolysin upon pneumococcal cell lysis, and/or the shedding/dispersion of virulent planktonic cells from the developing nascent biofilm. To inhibit these putative causes of damage and, to extend the time of co-culture, the culture medium was replaced several times post-infection to remove any toxins and remove dispersed pneumococcal cells, whilst the medium was supplemented with catalase to counteract the production of hydrogen peroxide. Additionally, 16HBE cells were infected on day 5 after seeding. Collectively, these changes succeeded in extending the co-culture model to 12 hours for all the MOIs tested (0.1:1, 0.01:1 and 0.001:1), in both the presence and absence of catalase (Figure 5.10 and Figure 5.12). These results suggested that the replacement of the co-culture medium at regular intervals was crucial in preserving the integrity of the infected 16HBE cell monolayers by removing cytotoxic factors, such as pneumolysin, and by removing any accumulating planktonic cells.

Pneumolysin has been shown to be expressed in pneumococcal biofilms grown on both a fixed biotic epithelial surface and on an abiotic surface, with maximal expression found at 6-8 hours post-infection when grown on plastic (Shak et al., 2013b). The expression of pneumolysin is under the control of the luxS/AI-2 QS system (Joyce et al., 2004), which is important for pneumococcal biofilm assembly, competence and fratricide (Trappetti et al., 2011). A pneumolysin mutant resulted in pneumococcal biofilms with significantly less biomass on both an abiotic surface and on fixed respiratory epithelial

cells under both static and continuous-flow conditions (Shak et al., 2013b), suggesting that pneumolysin is important for the early formation of pneumococcal biofilms. Furthermore, two studies have shown lysis of pneumococcal biofilm cells when grown on either fixed lung cells (at 16 hours post-infection) or on an abiotic surface in a static model (Vidal et al., 2013, Wei and Håvarstein, 2012). However, in Vidal's flow system co-culture biofilm model, in which there was a complete turnover of the culture medium every 25 minutes, biofilms were still viable at 24 hours post-infection, suggesting that lysis may be triggered by a soluble factor (Vidal et al., 2013). Lysis is under the control of a competence-driven mechanism and it has been shown that competence and genetic transfer, which are intricately linked with bacterial growth and cell death, are significantly more efficient when pneumococci exist in a biofilm, and are even more efficient when a biofilm is grown on a biotic surface (Wei and Håvarstein, 2012, Marks et al., 2012b).

Therefore, it may be that in these two studies, and in the co-culture model developed in this project, that a subset of pneumococcal cells are lysed leading to released cellular contents that are taken up by competent pneumococcal cells for further biofilm assembly (Steinmoen et al., 2002, Wei and Håvarstein, 2012). The importance of lysis for pneumococcal biofilm growth was demonstrated when autolysin-negative pneumococci were grown on fixed epithelial cells and shown to be devoid of any extracellular matrix material; exhibiting low biomass, less structural complexity and heightened susceptibility to antibiotics (Marks et al., 2012a).

Taken together, lysis may be triggered more quickly when a pneumococcal biofilm is grown on live epithelial cells. This hypothesis may explain the decrease in TEER of 16HBE monolayers from 6 hours post-infection, when replacement of the co-culture medium was not performed to remove the build-up of cytotoxic factors released from lysed pneumococcal cells (Figure 5.9). Similarly, this hypothesis may explain why the TEER was preserved in experiments when the apical and baso-lateral medium was replaced multiple times post-infection, since pneumolysin was unable to accumulate in the co-culture model (Figure 5.10 and Figure 5.12). Replacement of the co-culture medium may also have prevented accumulation of any dispersed planktonic bacteria. It may be that a faster rate of cell lysis could be a defence mechanism in the presence of live epithelial cells and the associated production of antimicrobial peptides, such as cathelicidins and defensins. Specifically, pneumococcal-derived eDNA, which is released upon cell lysis, could be taken up and used for DNA repair to ensure the continued survival of the biofilm and possibly incorporated into the biofilm matrix as well.

As a 12-hour co-culture model had been established, the aims for the next chapter were to investigate the pneumococcal biofilm and to explore the epithelial response to nascent biofilm formation.

6 Chapter 6 – Characterising biofilm formation and host responses on epithelial cells

6.1 Introduction

In the previous chapter, human bronchial epithelial cells (16HBE cells) were inoculated with different MOIs of *S. pneumoniae* strain D39 on transwell membranes. The aim was to develop a co-culture model whereby pneumococcal biofilm development could be evaluated on live epithelial cells without the induction of cytotoxic effects by pneumococcus. Quantitative analysis of viable pneumococcal cells was achieved by measuring CFUs (Figure 5.7), while qualitative analysis of biofilm formation was evaluated using SEM (Figure 5.8), at various time-points post-infection. Epithelial cell monolayer integrity was determined by measuring the TEER across the monolayers. Two models were successfully developed: (i) an 8-hour static model in which there was no change of the co-culture medium post-infection (Figure 5.9) and, (ii) a 12-hour model with multiple changes of co-culture medium post-infection (Figure 5.12).

6.2 Aims

The individual aims for the experiments described in this chapter were as follows:

- Enumerate viable pneumococci colonising epithelial cells up to 12 hours post-infection.
- Analyse biofilm formation, architecture and surface area coverage up to 12 hours post-infection using SEM.
- Demonstrate epithelial cell integrity and viability at 12 hours post-infection.
- Investigate the epithelial cytokine response to pneumococcal biofilm formation by measuring the level of multiple cytokines present in the co-culture supernatants over time.

6.3 Measuring pneumococcal attachment to 16HBE cells

For the first set of experiments in this chapter, 16HBE cells were seeded on transwell inserts for 5 days, TEER measurements were taken and epithelial cell monolayers were infected with pneumococcal MOIs of 0.1:1, 0.01:1 and 0.001:1 in antibiotic-free sMEM per transwell. An uninfected monolayer was used as a control. Apical and baso-lateral medium from each culture was replaced at 0.5 hours post-infection and at 6, 8 and 10 hours post-infection. CFU analysis was performed at 0.5 hours and at 2, 6 and 12 hours post-infection, as previously described (Chapter 2, section 2.23).

The aims were as follows: 1) determine if the number of CFUs increased during the 12-hour co-culture period; 2) assess whether the number of adherent pneumococci correlated with MOI; 3) determine if there was a maximum number of pneumococcal cells that colonised 16HBE cell monolayers during co-culture and at what time-point this was reached. For each assay, CFUs were measured for all of the MOIs at a particular time-point (i.e. 0.5, 2, 6 or 12 hours post-infection). CFUs were measured a total of four times for each time-point.

At 0.5 hours post-infection, the number of pneumococcal cells reached $1x10^2$ for the MOI of 0.1:1, $1x10^1$ for the MOI of 0.01:1 and less than $1x10^1$ for the MOI of 0.001:1 (Figure 6.1, A). At 2 hours post-infection, the number of pneumococcal cells remained at $1x10^2$ for the MOI of 0.1:1, but increased to $1x10^2$ and $1x10^1$ for the MOIs of 0.01:1 and 0.001:1, respectively (Figure 6.1, B). At 6 hours post-infection, viable cells had increased to $1x10^5$ (0.1:1), $1x10^4$ (0.01:1) and $1x10^2$ (0.001:1) for the three MOIs (Figure 6.1, C). However, there was no increase in the number of pneumococcal cells from 6 hours to 12 hours post-infection for any of the three MOIs (Figure 6.1, D). In addition, there was not a significant difference between adjacent MOIs at any of the time-points measured, but there was a significant difference between the highest MOI (0.1:1) and the lowest MOI (0.001:1) at each time-point (Figure 6.1, A-D).

These results showed that cultured 16HBE cells supported the colonisation of up to $1x10^5$ pneumococcal cells with an MOI of 0.1:1 for up to 12 hours of co-culture, with pneumococci reaching a plateau at that number.

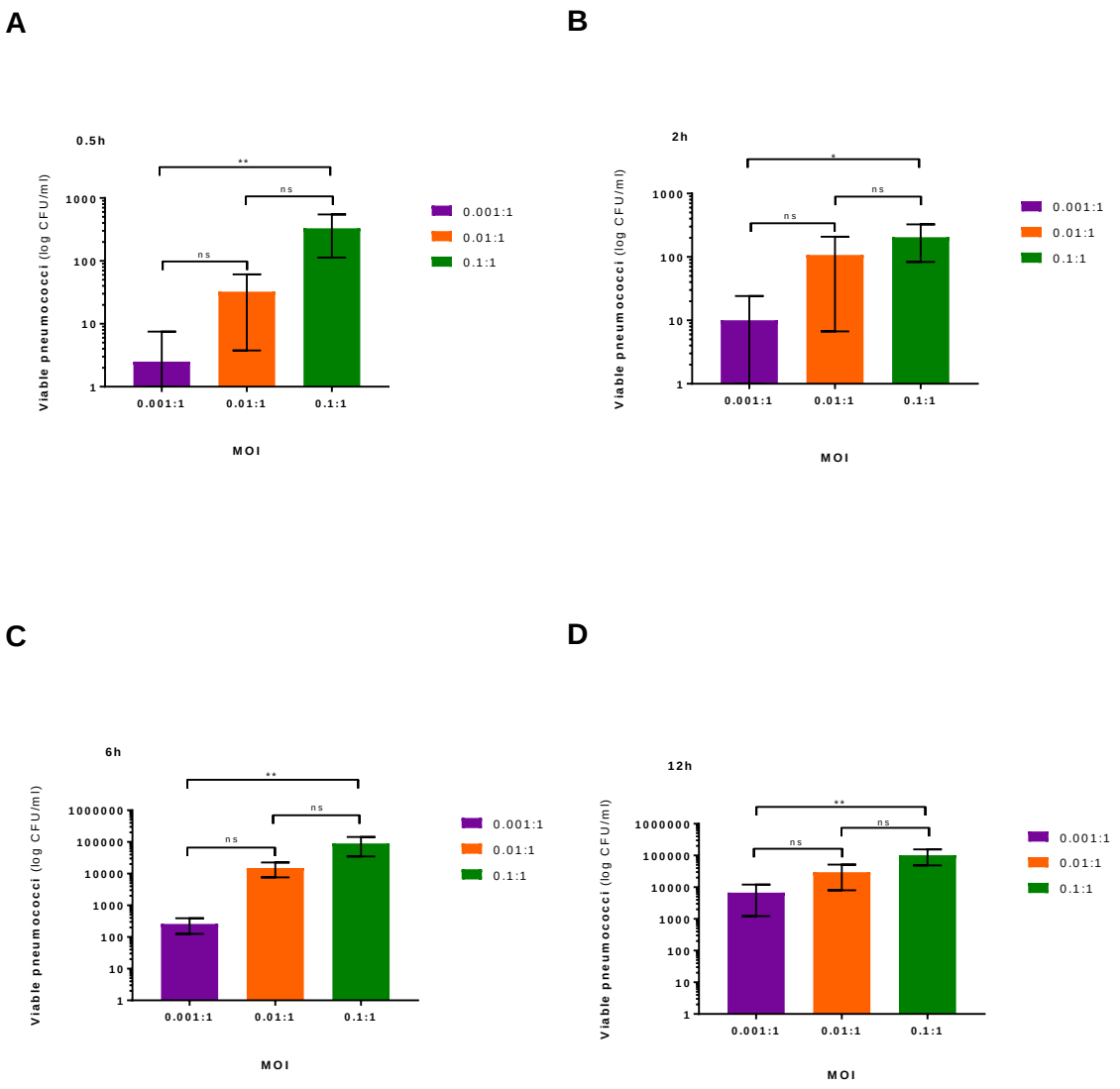

Figure 6.1: Time-course of pneumococcal adherence to 16HBE monolayers over 12 hours

16HBE cells were infected with different MOIs of the pneumococcal strain D39. At 0.5, 2, 6 and 12 hours post-infection transwell membranes were processed for CFU analysis (A). There was no statistically significant difference in the number of CFUs for adjacent MOIs at any of the time-points (A-D). Data points represent the mean and the error bars represent the standard errors of the mean, from four independent pooled experiments for each time-point. Significance is indicated as follows: *, $P < 0.05$; **, $P < 0.01$; ns, not significant.

6.4 Imaging pneumococcal biofilms on 16HBE cells using SEM

Having found an increase in the number of viable adherent pneumococci on 16HBE cell monolayers up to 12 hours post-infection (section 6.3), SEM was used to evaluate pneumococcal biofilm development. Cultured 16HBE cells were infected with MOIs of 0.1:1, 0.01:1 and 0.001:1 per transwell and the monolayers were processed for SEM analysis at 2, 6 and 12 hours post-infection, as previously described (Chapter 2, section 2.24). For each assay, the epithelial cells infected with all of the different MOIs were processed for SEM analysis at a particular time-point (i.e. 2, 6 or 12 hours post-infection). The epithelial cells were processed twice at each time-point for all of the MOIs.

At each time-point, surface-attached and aggregated pneumococci were found adherent to epithelial cells, surrounded by an extracellular matrix showing fibrous material, indicative of a pneumococcal biofilm (Figure 6.2, Figure 6.3 and Figure 6.4). Pneumococcal aggregates were heterogeneously distributed over the surface of the 16HBE cell monolayers and were only noticeable with a magnification of x1000 or higher. It was not possible to determine from all the images that were obtained (data not shown) whether there was a discernible difference in the size of D39 pneumococcal biofilm aggregates between MOIs at any time-point, or if there was an increase over time for each MOI.

A MOI 0.1:1

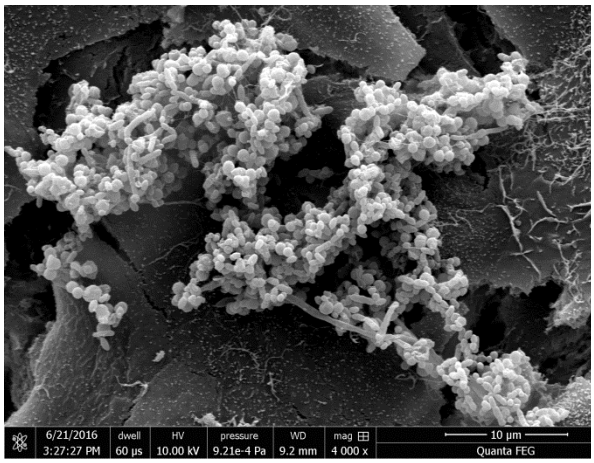

B MOI 0.1:1

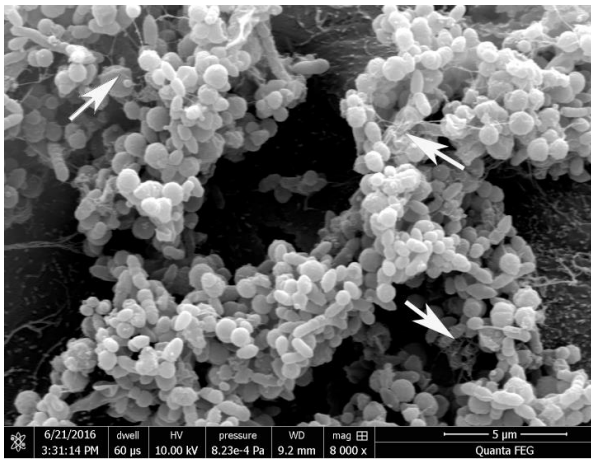

C MOI 0.01:1

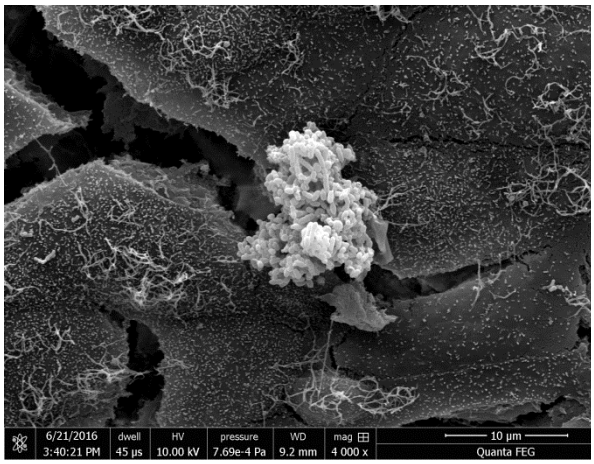

D MOI 0.01:1

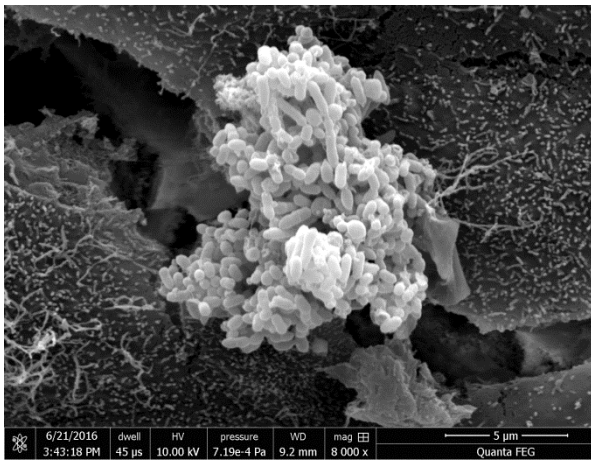

E MOI 0.001:1

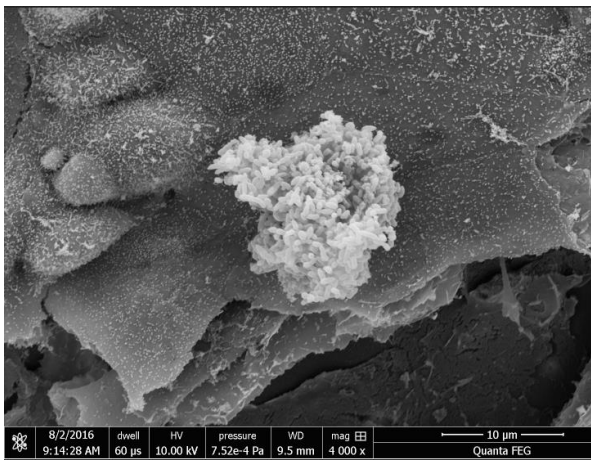

F MOI 0.001:1

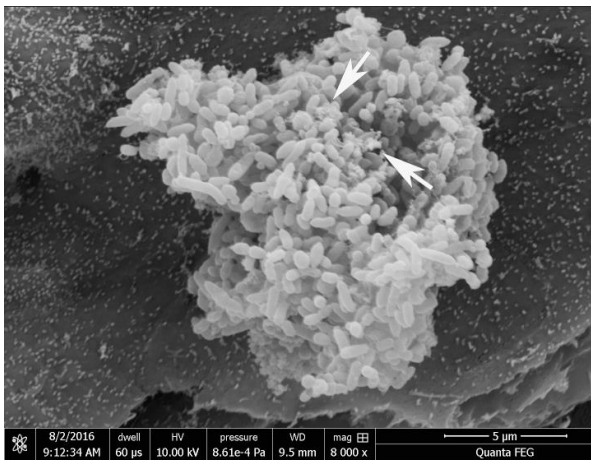

G Uninfected cells

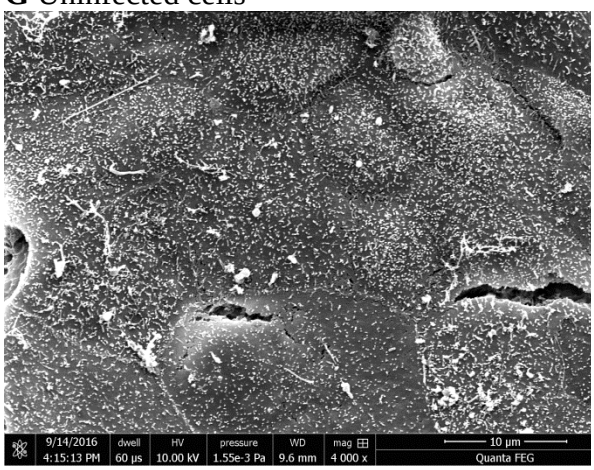

H Uninfected cells

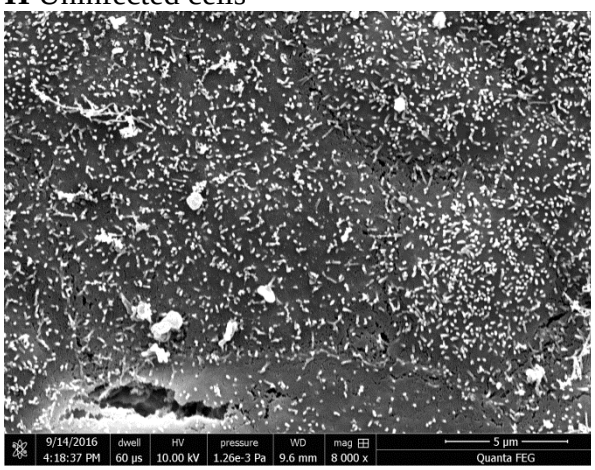

Figure 6.2: SEM analysis of D39 pneumococcal biofilms on 16HBE cell monolayers at 2 hours post-infection.

Cultured 16HBE cells were infected with different MOIs of the pneumococcal strain D39 and processed for SEM analysis after 2 hours. Representative images for the MOIs of 0.1:1 (A, B), 0.01:1 (C, D) and 0.001:1 (E, F) are shown, as well as an uninfected control (G, H). Pneumococcal biofilm formation was seen for all of the MOIs (A-F), with fibrous material and extracellular matrix detected (white arrows, B and F). Pneumococcal cells were not observed on uninfected monolayers (G, H).

A MOI 0.1:1

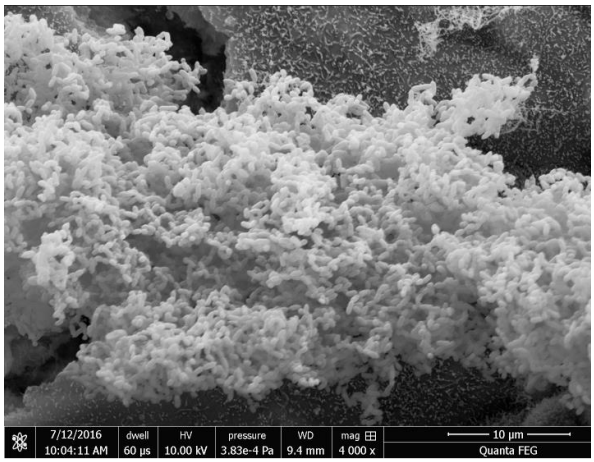

B MOI 0.1:1

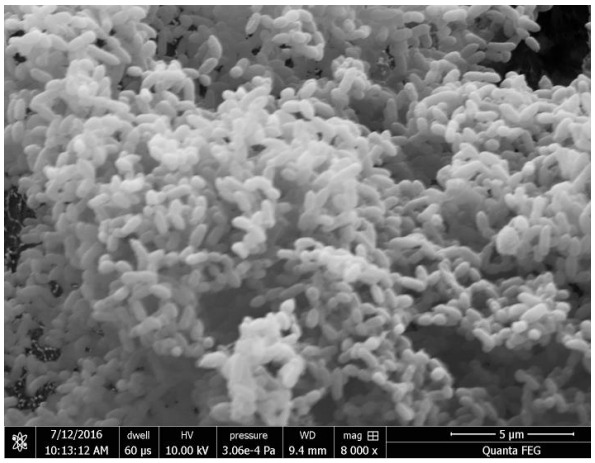

C MOI 0.01:1

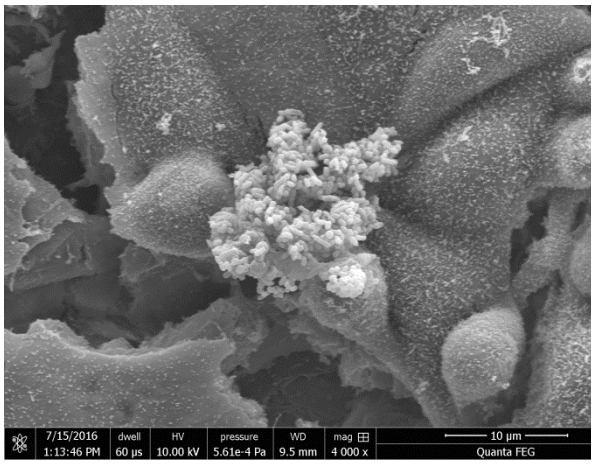

D MOI 0.01:1

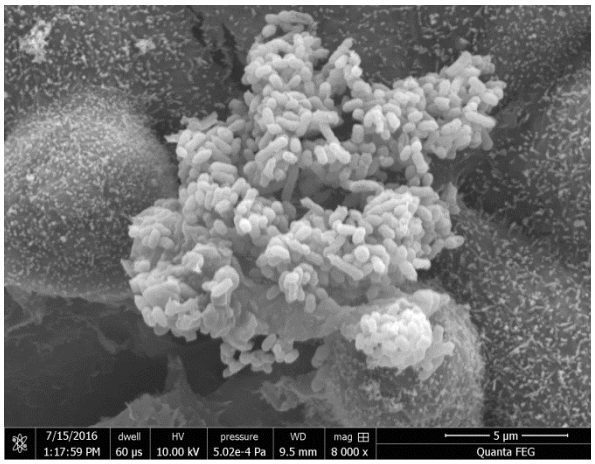

E MOI 0.001:1

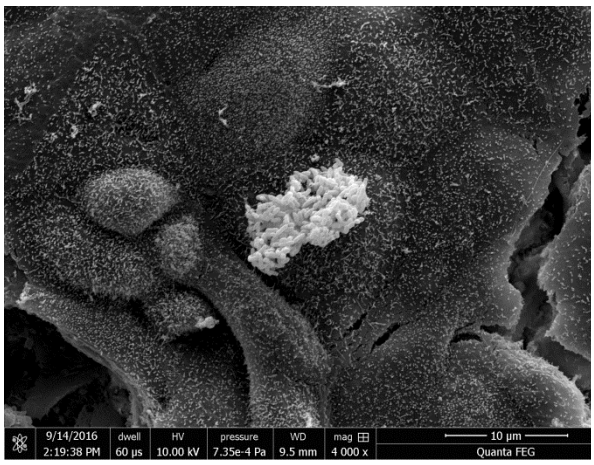

F MOI 0.001:1

G Uninfected cells

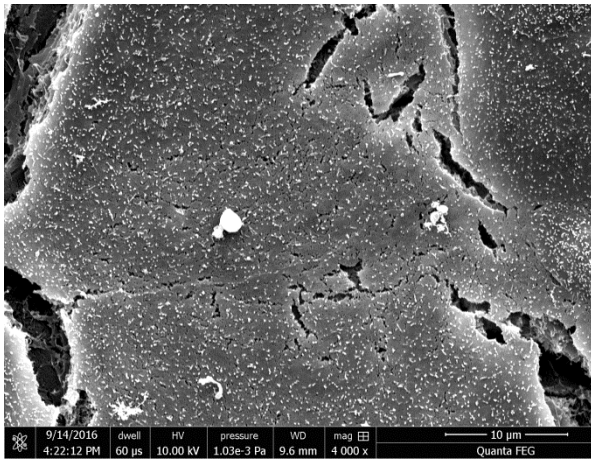

H Uninfected cells

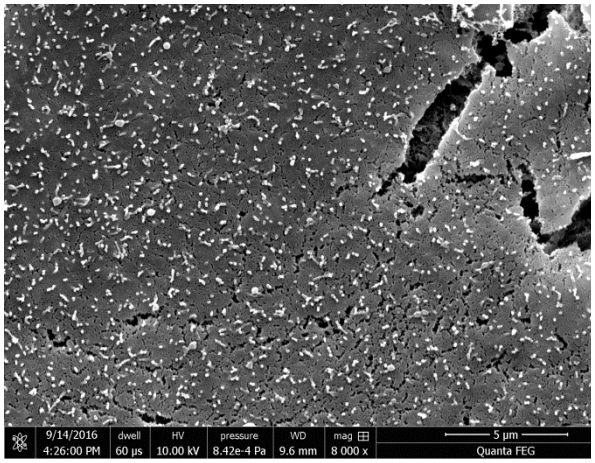

Figure 6.3: SEM analysis of D39 pneumococcal biofilms on 16HBE cell monolayers at 6 hours post-infection.

Cultured 16HBE cells were infected with different MOIs of the pneumococcal strain D39 and processed for SEM analysis after 6 hours. Representative images for the MOIs of 0.1:1 (A, B), 0.01:1 (C, D) and 0.001:1 (E, F) are shown, as well as an uninfected control (G, H). Pneumococcal biofilm formation was seen for all of the MOIs (A-F). Pneumococcal cells were not observed on uninfected monolayers (G, H).

A MOI 0.1:1

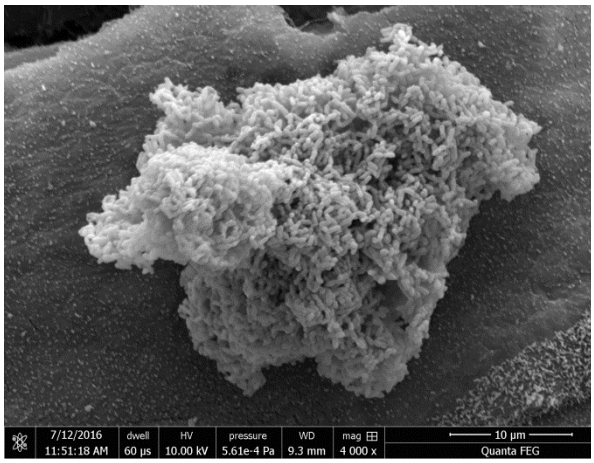

B MOI 0.1:1

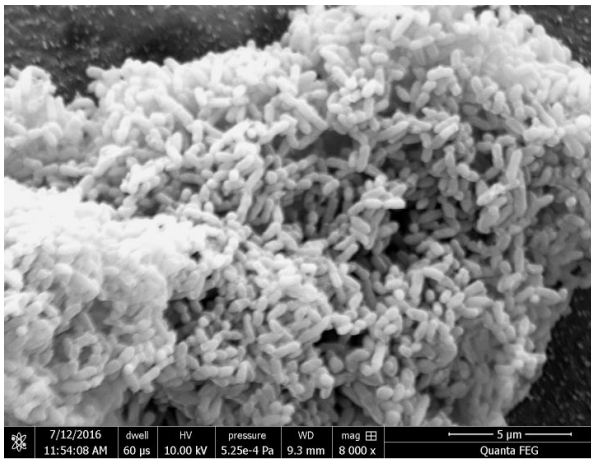

C MOI 0.01:1

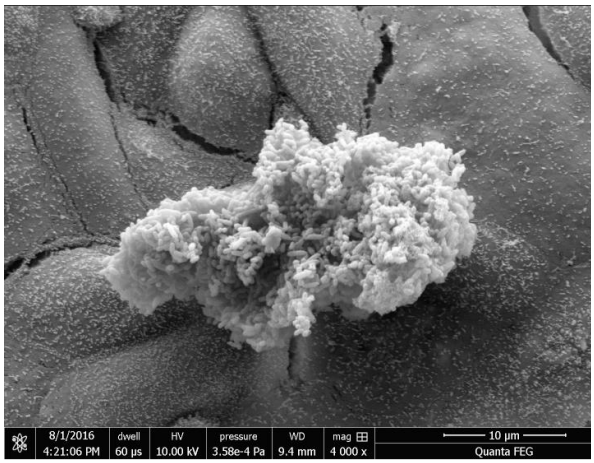

D MOI 0.01:1

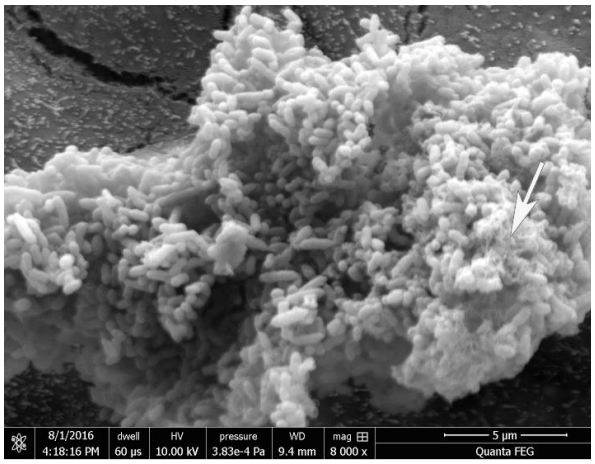

E MOI 0.001:1

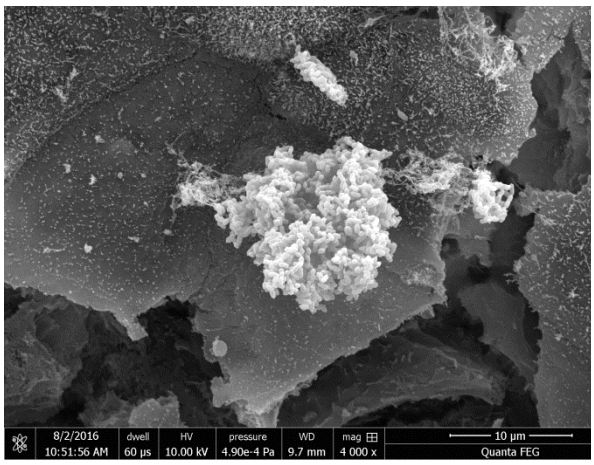

F MOI 0.001:1

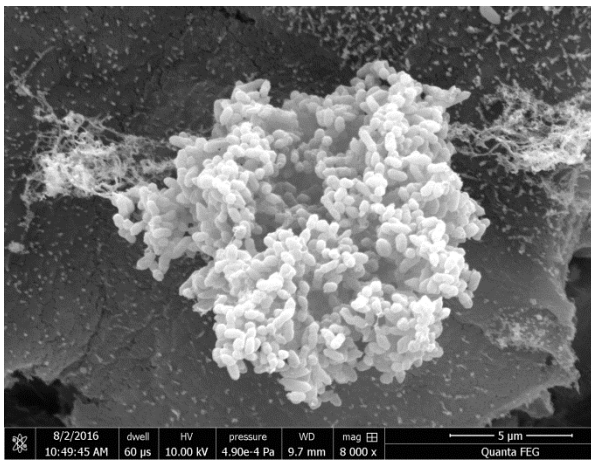

G Uninfected cells

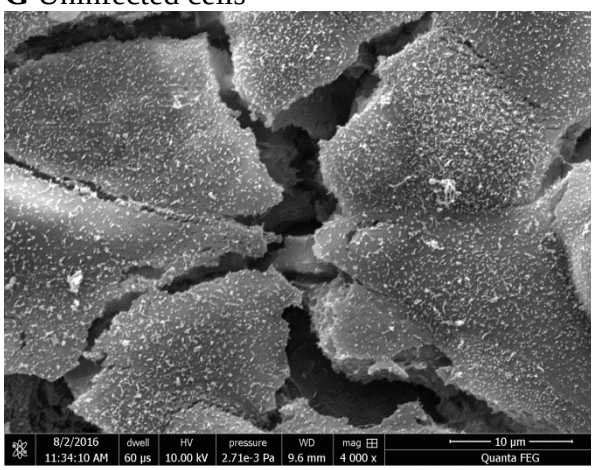

H Uninfected cells

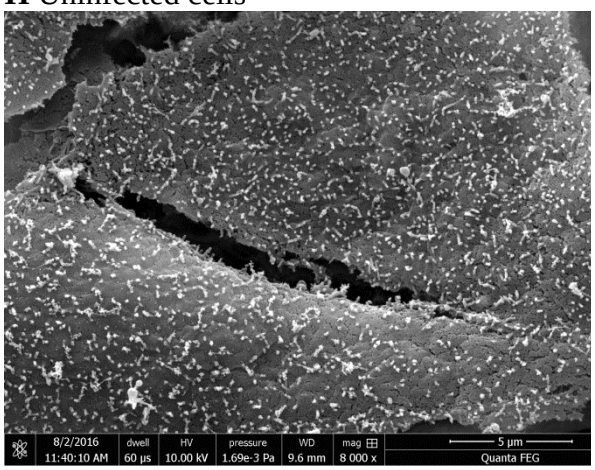

Figure 6.4: SEM analysis of D39 pneumococcal biofilms on 16HBE epithelial cells at 12 hours post-infection.

Cultured 16HBE cells were infected with different MOIs of the pneumococcal strain D39 and processed for SEM analysis after 12 hours. Representative images for the MOIs of 0.1:1 (A, B), 0.01:1 (C, D) and 0.001:1 (E, F) are shown, as well as an uninfected control (G, H). Pneumococcal biofilm formation was seen for all of the MOIs (A-F), with fibrous material also present (white arrows, D). Pneumococcal cells were not observed on uninfected monolayers (G, H).

6.5 Determination of epithelial cell cytotoxicity during pneumococcal co-culture

TEER indicated that epithelial cell monolayers remained intact up to 12 hours during co-culture (Chapter 5, Figure 5.12). To directly measure cell viability in the co-culture model, an LDH cytotoxicity assay was performed. LDH is a stable, cytosolic enzyme that is released upon cell lysis. The assay is a colorimetric method for determining cell-mediated cytotoxicity by measuring released LDH, which is quantified via a coupled enzymatic reaction. Firstly, LDH is responsible for the catalytic conversion of lactate to pyruvate, through NAD^+ reduction to NADH. Secondly, the enzyme diaphorase oxidises NADH to reduce a tetrazolium salt (iodonitrotetrazolium) into a red-coloured formazan product. The resulting formazan can be quantitatively measured using an absorbance plate reader, as previously described (Chapter 2, section 2.25), with the level detected directly proportional to the amount of extracellular LDH present.

16HBE cell monolayers were infected with MOIs of 0.1:1, 0.01:1 and 0.001:1, and two uninfected cultures were used. Apical and baso-lateral medium from all the monolayers was replaced at 0.5 hours post-infection and at 6, 8 and 10 hours post-infection. At 12 hours post-infection, the LDH assay was performed following the manufacturer's instructions. Briefly, the apical medium of the two uninfected cultures and the three infected monolayers was replaced with 300 µl of antibiotic-free sMEM, with 30 µl of Lysis Buffer added to one of the uninfected cultures. 100 µl of antibiotic-free sMEM was added to six wells of a 96-well plate, with three of the wells supplemented with 10 µl of Lysis Buffer. The co-culture plate and the 96-well plate were incubated for 45 minutes at 37°C/5% CO_2. After incubation, the apical medium of the two uninfected monolayers and the three infected monolayers was added to triplicate wells of the 96-well plate. The 96-well plate was centrifuged at 250 x *g* for 3 minutes before 50 µl of each sample was placed into a fresh 96-well plate supplemented with 50 µl of Reaction Mixture (Appendix 9.2). The plate was incubated for 30 minutes at room temperature in the dark. 50 µl of Stop Solution was added to each well and the plate was centrifuged at 250 x *g* for 3 minutes. The absorbance of each sample was then measured. The experiment was repeated two times ($n = 3$).

Cytotoxicity of the infected epithelial cell monolayers was compared to uninfected epithelial cells incubated with lysis buffer solution (representing 100% cytotoxicity) and to epithelial cells without lysis buffer (representing 0% cytotoxicity). For each MOI, the mean percentage of LDH release from three separate experiments was measured below 10%, with no statistically significant difference between the MOIs (Figure 6.5). These results indicated that the viability of the epithelial cell monolayers was maintained for up

to 12 hours in the presence of different MOIs, and in the presence of developing nascent pneumococcal biofilms on the cell surface.

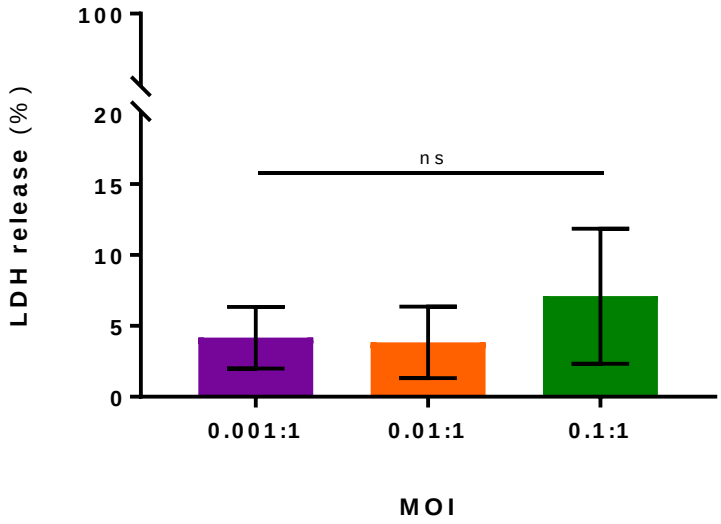

Figure 6.5: The effect of different MOIs of D39 pneumococci on LDH release from 16HBE cells at 12 hours post-infection.

Cultured 16HBE cells were infected with different MOIs of the pneumococcal strain D39. At 12 hours post-infection, viability was measured using an LDH cytotoxicity assay. Cytotoxicity was normalised against uninfected monolayers. Less than 10% cytotoxicity was found for all MOIs. Data points represent the mean and the error bars represent the standard errors of the mean, from three separate pooled experiments: ns, not significant.

TEER was also measured for all of the epithelial cell monolayers after each LDH assay had been performed. For each assay (n = 3), TEER of the uninfected 16HBE cells incubated with lysis buffer solution was at the baseline value of ~2000 Ohms.cm^2 (i.e. a transwell membrane without epithelial cells) (Figure 6.6). In contrast, there was no statistically significant difference between the TEER of the infected and uninfected monolayers (Figure 6.6).

Photomicrographic images were also taken of lysed and non-lysed uninfected epithelial cells, as well as infected epithelial cells for each assay (n = 3). One image was taken of each transwell per assay. Confluent monolayers of 16HBE cells were found for both an infected co-culture (MOI of 0.1:1) and uninfected 16HBE cells (0% cytotoxicity) after 12 hours, with no gaps seen on the transwell membranes (Figure 6.7, A-B). A confluent monolayer was not visible from uninfected, lysed epithelial cells (100% cytotoxicity) (Figure 6.7, C). Taken together, the results shown in Figure 6.5, Figure 6.6 and Figure 6.7 demonstrate that the integrity and viability of the 16HBE cells was preserved for up to 12 hours during co-culture with different pneumococcal loads (MOIs) in the presence of developing pneumococcal biofilms.

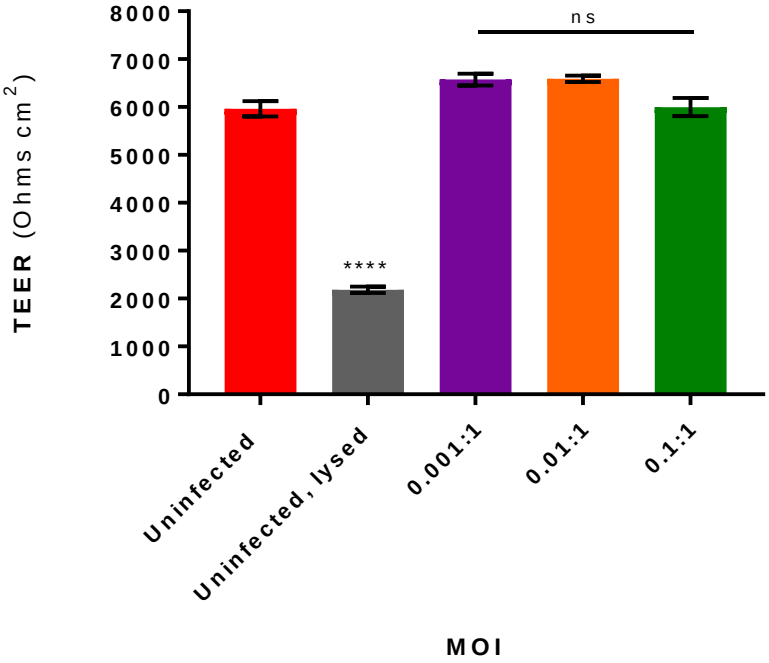

Figure 6.6: TEER of uninfected and infected 16HBE cell monolayers after pneumococcal challenge for 12 hours.

Cultured 16HBE cells were infected with different MOIs of the pneumococcal strain D39. TEER of uninfected epithelial cells incubated with lysis buffer solution was significantly different from uninfected epithelial cells incubated without lysis buffer, with the TEER at baseline level. There was no statistically significant difference between infected and uninfected (non-lysed) epithelial cells. Data points represent the mean and the error bars represent the standard errors of the mean, from three separate experiments. Significance is indicated as follows: ****, $P < 0.0001$; ns, not significant.

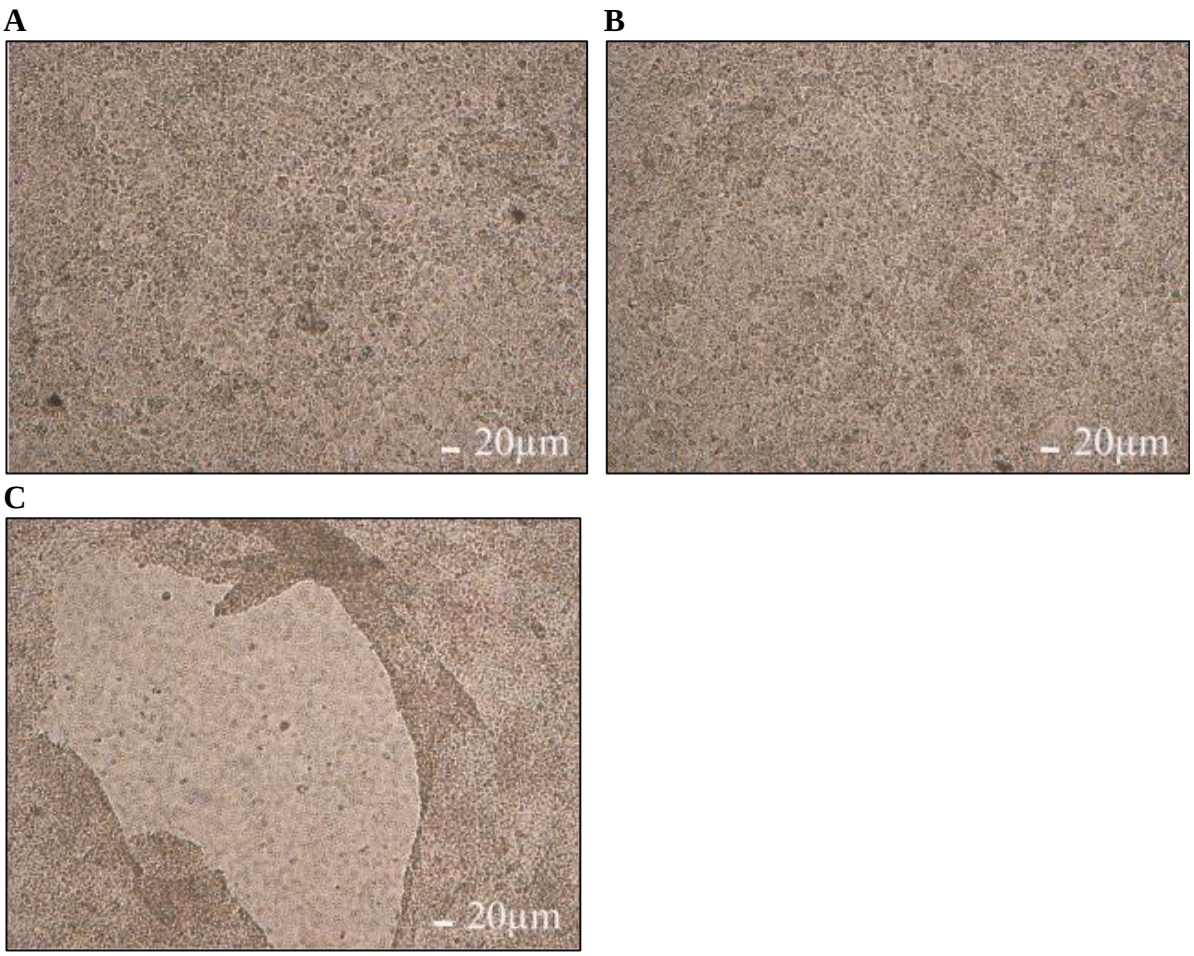

Figure 6.7: Micrographic images of 16HBE cell monolayers after pneumococcal challenge for 12 hours.

16HBE cells were grown for 5 days on transwell membranes and then infected with different MOIs of *S. pneumoniae* strain D39 for 12 hours. Representative images from three separate experiments are shown. A confluent monolayer was visible for epithelial cells infected with an MOI of 0.1:1 (A) and for uninfected epithelial cells (B). Large gaps were found with uninfected cultures treated with lysis buffer, since the cells had lysed and/or dislodged from the transwell membrane (C).

6.6 16HBE cell cytokine response to co-culture with *S. pneumoniae* strain D39

Having determined by CFU (Figure 6.1) and SEM analyses (Figure 6.2, Figure 6.3 and Figure 6.4) that *S. pneumoniae* were adherent and forming nascent biofilms on 16HBE cell monolayers at 12 hours of co-culture, without compromising epithelial cell integrity or viability (Figure 6.5, Figure 6.6 and Figure 6.7), the cytokine response of epithelial cells was measured.

Two independent studies by Blanchette-Cain et al. and Marks et al. showed that biofilm pneumococci induce a reduced cytokine response from epithelial cell lines (Detroit-562 human pharyngeal cells and NCI-H292 bronchial carcinoma cells) compared to planktonic pneumococci, with lower levels of pro-inflammatory cytokines (e.g. IL-6, IL-8 and TNF-α) detected (Blanchette-Cain et al., 2013, Marks et al., 2013). However, in both cases, live epithelial cells were only incubated with pneumococci for 4 hours before the culture supernatants were harvested. As it is likely that pneumococcal biofilms are present in the nasopharynx for longer than 4 hours, an extended *in vitro* co-culture model in which epithelial cell responses are assessed over a longer period would be more desirable and biologically relevant; yielding insights into how pneumococci may persist *in vivo*.

Consequently, the aim was to determine the cytokine response of 16HBE cell monolayers over 12 hours by measuring the concentration of a panel of cytokines at different time-points post-infection. The gradual increase in viable pneumococci on the 16HBE cells over time (Figure 6.1) and the low cytotoxicity (Figure 6.5) indicated that an MOI of 0.001:1 would be best to measure the extracellular concentration of cytokines in response to a growing pneumococcal biofilm. The apical medium was harvested prior to infection (0 hours) and at 4, 6, 8, 10 and 12 hours post-infection from infected (i.e. MOI of 0.001:1 only) and uninfected 16HBE cell monolayers. The apical medium was harvested as cytokine concentrations have been found to be considerably higher in the apical medium than in the baso-lateral medium (Ren et al., 2012b). The experiment was then repeated three more times ($n = 4$).

The following 11 cytokines were examined by using a customised human cytokine Luminex assay: interleukins (IL) 1α, 1β, 6, 8, 10, macrophage inflammatory protein (MIP) 1α and 1β, monocyte chemoattractant protein-1 (MCP-1), granulocyte-macrophage colony-stimulating factor (GM-CSF), tumour necrosis factor alpha (TNF-α), and interferon gamma (IFN-γ). The concentration of these cytokines have been investigated from planktonic and biofilm models of infection with epithelial cells, for pneumococci and other bacterial species (Starner et al., 2006, Hawdon et al., 2010, Raffel et al., 2013, Blanchette-Cain et al., 2013, Marks et al., 2013, Bowler et al., 2014). It was hypothesised that the

concentration of pro-inflammatory cytokines in the co-culture model would decrease with time, which would be in agreement with the attenuated immunoreactivity of a pneumococcal biofilm that is reported in the literature.

Cytokines were measured using a Luminex assay, as previously described (Chapter 2, section 2.26). Of the eleven cytokines that were measured, two (IL-1β and GM-CSF) were below the detectable range of the standard curve, whilst the concentrations of three cytokines (TNF-α, IFN-γ and IL-10) could not be interpreted due to inaccurate and incomplete standard curves. Results were obtained for the following cytokines: IL-1α, IL-6, IL-8, MIP-1α, MIP-1β and MCP-1 (Figure 6.8). No significant differences in concentration were found between infected and uninfected samples at any of the time-points measured.

A dampened cytokine response following exposure of epithelial cells to biofilm pneumococci in comparison to planktonic pneumococci has been shown in other studies with different pneumococcal strains using submerged culture with other epithelial cell lines (Blanchette-Cain et al., 2013, Marks et al., 2013). Additionally, it has been demonstrated that the epithelial cell inflammatory response is not correlated with the extent of pneumococcal adherence, but rather, with encapsulation, with unencapsulated pneumococcal strains shown to downregulate the expression of various pro-inflammatory cytokines (e.g. IL-1β, IL-6 and IL-8) (Bootsma et al., 2007). Therefore, the absence of a distinct cytokine response from the 16HBE cells may be due to the formation of a pneumococcal biofilm and downregulation of the capsule, a morphological change which has been found in previous studies illustrating pneumococcal adherence to epithelial cells and biofilm development (Hammerschmidt et al., 2005, Hall-Stoodley et al., 2008). Moreover, cytokine production by epithelial cells is enhanced by the presence of macrophage-derived factors (Krakauer, 2002, Morris et al., 2006, Xu et al., 2008, Marriott et al., 2012). Co-cultures of 16HBE cell monolayers and a macrophage cell line may induce an epithelial cell cytokine response in the presence of pneumococcal biofilms, which could be more reflective of conditions *in vivo*. Thus, the cytokine concentrations from infected and uninfected epithelial cells may represent baseline, constitutive expression. The Luminex assay was also only performed once, with 16HBE cell monolayers infected with an MOI of 0.001:1. Consequently, it would be desirable to repeat the assay with an MOI of 0.1:1, with more biological replicates.

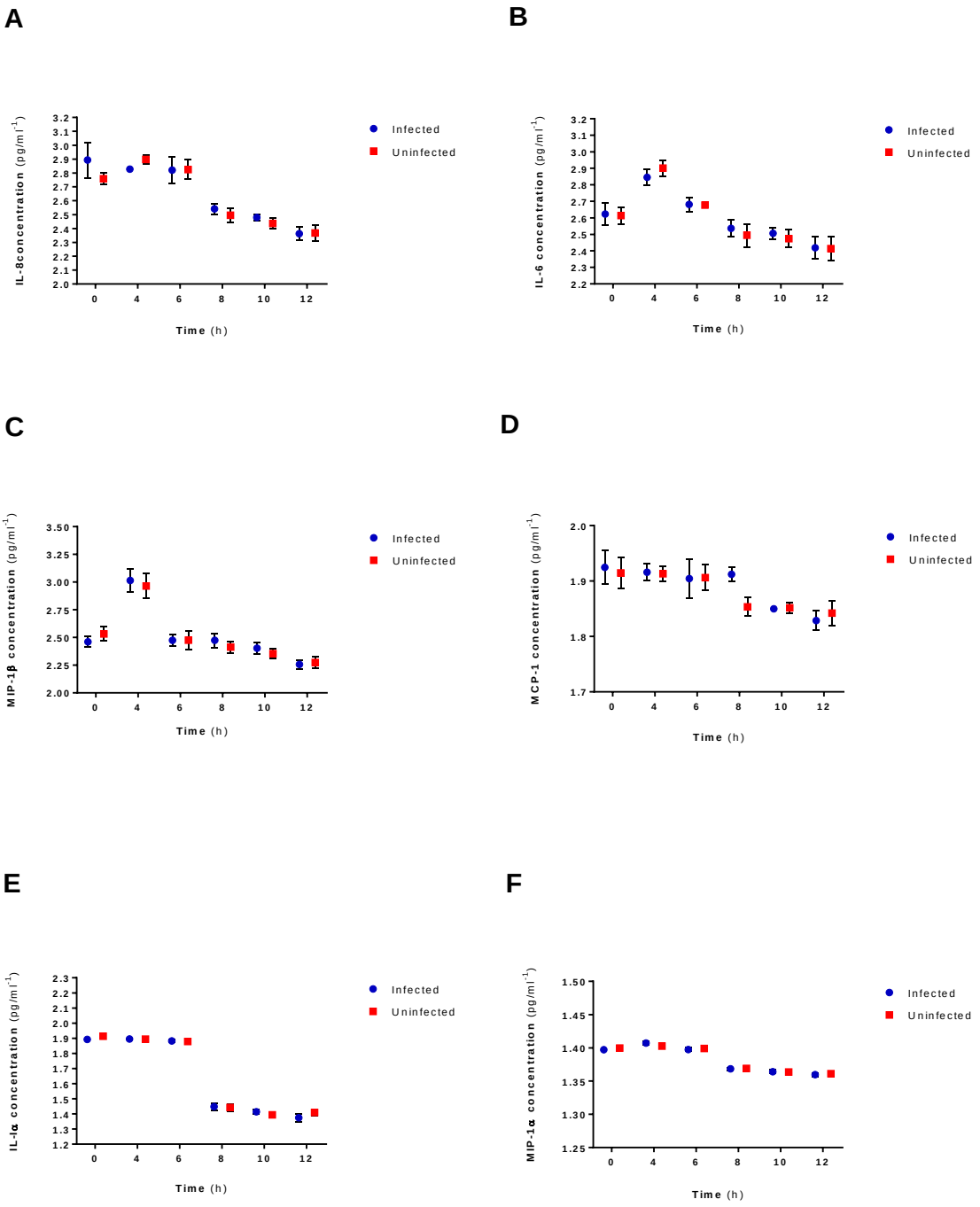

Figure 6.8: Cytokine concentrations in the apical supernatant of 16HBE cell monolayers co-cultured with *S. pneumoniae* strain D39.

16HBE cells were infected with the *S. pneumoniae* strain D39 with an MOI of 0.001:1. A statistically significant difference was not observed between infected and uninfected samples at the time-points measured for cytokines IL-8 (A), IL-6 (B), MIP-1β (C), MCP-1 (D), IL-1α (E) or MIP-1α (F).

6.7 Discussion

In Chapter 5, TEER measurements of infected 16HBE cell monolayers demonstrated that the integrity of epithelial cells could be maintained for up to 12 hours in the presence of different MOIs of a D39 pneumococcal strain. In this chapter, the initial aims were as follows: 1) to determine whether there was evidence for biofilm development over 12 hours of co-culture; 2) to show that the epithelial cells were viable at 12 hours post-infection; 3) to investigate the epithelial cytokine response to nascent pneumococcal biofilms.

CFU analysis (n = 4) at 12 hours post-infection demonstrated that the 16HBE cells supported pneumococcal colonisation of $1x10^5$ pneumococcal cells with an MOI of 0.1:1, with no significant increase in the number of pneumococci from 6 hours post-infection for any MOI (Figure 6.1). SEM analysis showed nascent biofilms formed with all of the MOIs at 12 hours post-infection, with evidence of extracellular fibrous material, heterogeneous structure and pleomorphic pneumococci (Figure 6.2, Figure 6.3 and Figure 6.4). LDH release (n = 3) from infected and uninfected 16HBE cell monolayers at 12 hours post-infection indicated there was a low percentage of cytotoxicity and cell death for all MOIs (Figure 6.5).

Having demonstrated 16HBE cell integrity and viability after 12 hours post-infection in the presence of adherent and aggregated biofilms of pneumococcus, the aim was to explore the epithelial cell cytokine response to co-culture with *S. pneumoniae*. Cytokine responses were comparable between infected and uninfected 16HBE cell monolayers, with no significant differences found. Since the assay was performed only once with an MOI of 0.001:1, the pathophysiological importance of the data is unclear. Repeated assays with a higher MOI and/or an alternative technique such as ELISA are proposed.

7 Chapter 7 - Discussion

S. pneumoniae is a bacterial pathogen associated with significant worldwide morbidity and mortality. As a prerequisite for pneumococcal infection, the pneumococcus must successfully colonise the mucosal epithelium of the nasopharynx in the upper respiratory tract (Bogaert et al., 2004, Simell et al., 2012). In immunocompromised individuals or during favourable conditions, such as a viral infection, pneumococci may spread to surrounding tissues or invade the bloodstream resulting in IPD. There has been growing evidence that pneumococci colonising the nasopharynx may be present in biofilms (Sanderson et al., 2006, Hoa et al., 2009, Nistico et al., 2011). Biofilm growth may be consistent with the persistence of pneumococci in the nasopharynx, where it can act as a reservoir for the dissemination of pneumococci in a colonised person to other sites, or facilitate transmission between individuals. Indeed, children with OM have been found to have denser and more extensive bacterial biofilms in their adenoids (Zuliani et al., 2009, Hoa et al., 2010, Saylam et al., 2010, Saafan et al., 2013, Tawfik et al., 2016).

Despite the emerging importance of the biofilm phenotype, research into the interactions between pneumococcal biofilms and the human host is limited. Instead, the majority of studies have used mouse models or grown pneumococcal biofilms on abiotic surfaces, such as glass or plastic. Mouse models have been an invaluable tool in allowing researchers to visualise a pneumococcal biofilm on a biotic surface (Marks et al., 2012a, Blanchette-Cain et al., 2013, Shak et al., 2013a, Blanchette et al., 2016), to assess virulence of a biofilm (invasiveness and antibiotic tolerance) (Sanchez et al., 2011b, Marks et al., 2013), and to determine the contribution of various bacterial factors to pneumococcal colonisation and accretion (Muñoz-Elías et al., 2008, Marks et al., 2012a, Blanchette-Cain et al., 2013, Hotomi et al., 2016). However, the clinical relevance of bacterial studies in mice, especially in cases studying host responses to pneumococcal colonisation (Joyce et al., 2009, Blanchette-Cain et al., 2013), is debatable, since pneumococci are not natural colonisers of mice and animal models do not recapitulate long-term human colonisation.

As for biofilm formation on abiotic surfaces, Marks et al. demonstrated that interaction with epithelial (fixed) cells is crucial for the development of a pneumococcal biofilm (biomass, structure and antibiotic tolerance) that more closely resembles a pneumococcal biofilm *in vivo* in mice (Marks et al., 2012a). These findings have been supported by another research group that used human-derived lung and pharyngeal epithelial cell lines as a substratum for the formation of a pneumococcal biofilm (Vidal et al., 2013).

The primary aims in this project were to determine: 1) if pneumococci could be visualised in adenoid tissue *ex vivo*; 2) if there was evidence of co-localisation with innate immune cells, and 3) if there was evidence of *S. pneumoniae* biofilm formation. An additional aim was to develop a co-culture model in which pneumococcal colonisation (adherence and nascent biofilm development) could be studied on live, cultured epithelial cell monolayers without compromising the integrity and viability of the epithelial cells.

Adenoids spiked with *S. pneumoniae* were used to successfully develop procedures to stain pneumococci in fixed tissue using immunohistochemistry and immunofluorescence. Distinct clusters of pneumococcal cells were detected near the epithelium and deeper within the tissue. Macrophages and neutrophils were also identified, with evidence of these cells co-localised with pneumococci. In patient adenoid tissue (n = 4), pneumococci were detected in half of the adenoids that were examined with only individual pneumococcal cells detected. This is consistent with a study by Nistico et al. whereby pneumococcus was found in half of the adenoids examined using fluorescence *in situ* hybridisation (FISH) (Nistico et al., 2011). Further patient adenoids will need to be examined in order to continue these investigations.

A co-culture model was developed using a bronchial epithelial cell line and *S. pneumoniae* D39. CFU and SEM analyses demonstrated that pneumococcal cells were viable, surface-attached and aggregated, which is indicative of the biofilm phenotype. Epithelial cell monolayer integrity and viability was shown using TEER measurements, LDH release and microscopic imaging of the cells. This model can be used to interrogate the characteristics of a *S. pneumoniae* biofilm and interactions with the host.

7.1 The host innate response to bacterial biofilms

Although it is widely reported in the literature that biofilms are resistant to the host cellular and immune response, limited research exists detailing how innate cells such as respiratory epithelial cells, neutrophils and macrophages interact with, and respond to, bacterial biofilms. Characterisation of host responses has predominantly been explored using *in vitro* co-culture models of neutrophils or macrophages with *P. aeruginosa* or staphylococcal biofilms.

For example, it has been shown when neutrophils encounter a *P. aeruginosa* biofilm the oxidative burst is diminished, and neutrophils are ineffective in eliminating the bacteria despite penetrating the biofilm (Jesaitis et al., 2003, Bjarnsholt et al., 2005, Walker et al., 2005). Similar findings have been found with *S. epidermidis* biofilms (Kristian et al., 2008).

Both *in vitro* and *in vivo* studies have found that macrophages associated with *S. aureus* biofilms induced less cytokine production (Thurlow et al., 2011, Hanke et al., 2013). It is believed that *S. aureus* biofilms are capable of skewing macrophages towards an alternatively activated, anti-inflammatory phenotype, which favours bacterial persistence (Thurlow et al., 2011, Hanke et al., 2012, Hanke et al., 2013).

Several studies have also reported reduced phagocytic function and production of pro-inflammatory cytokines in response to *S. epidermidis* biofilms (Schommer et al., 2011, Cerca et al., 2011, Spiliopoulou et al., 2012), in addition to attenuated phagocytic killing by macrophages (Spiliopoulou et al., 2012), neutrophils (Kristian et al., 2008) and antibody-mediated opsonophagocytosis (Cerca et al., 2006). Therefore, compared to planktonic bacteria, biofilm bacteria show greater survival in response to the effects of host innate cells. *S. epidermidis* biofilms have also been found to reduce complement (C3b) and antibody (IgG) deposition on the cell surface (Kristian et al., 2008).

Interestingly, neutrophils can penetrate newly formed *S. aureus* biofilms (Günther et al., 2009) and macrophages can phagocytose *S. aureus* from mechanically disrupted biofilms (Thurlow et al., 2011). Taken together, these results suggest that phagocytes are ineffective in phagocytosing a complex and mature biofilm, perhaps due to reduced surface deposition of opsonins (complement and antibody) (Kristian et al., 2008, Domenech et al., 2013). The reduced sensitivity of mature biofilms to neutrophil attack may be due to changes in the architecture and composition of the EPS of a growing biofilm, especially in studies where the number of bacteria in a biofilm and the thickness of a biofilm has remained the same over time (Günther et al., 2009). For instance, studies with *P. aeruginosa* have shown that the biofilm EPS can influence the capacity of neutrophils to phagocytose bacteria through EPS-derived compounds, such as rhamnolipids and alginate (Leid et al., 2005, Jensen et al., 2007, Alhede et al., 2009). The anti-phagocytic effects of the EPS may not be unique to *P. aeruginosa* biofilms since it has been shown that macrophages challenged with supernatants from *S. aureus* biofilms were unable to phagocytose planktonic bacteria, suggesting that biofilm bacteria can not only skew the activity of macrophages but impair their phagocytic potential completely (Scherr et al., 2015).

Despite the aforementioned studies, characterisation of the human cellular responses to pneumococcal biofilms is lacking. The presence of a biofilm in the nasopharynx has been proposed to correlate with increased persistence in the upper respiratory tract, and biofilm formation on adenoid tissue is implicated in the pathogenesis of COM, a very common disease that is not resolved by host innate cellular responses and is difficult to treat with antibiotics. Since pneumococcal biofilm association with adenoidal epithelial

cells has been demonstrated (Hoa et al., 2009, Nistico et al., 2011), an *ex vivo* adenoid tissue model was developed to investigate pneumococcal co-localisation with macrophages and neutrophils.

7.2 Development of an *ex vivo* adenoid model for examining the interaction between *S. pneumoniae* and host immune cells

In this project, spiked (S14) adenoid tissue samples were initially used to stain pneumococcus with an immunohistochemistry protocol. Optimisation experiments with different antibody dilutions (polyclonal rabbit anti-*S. pneumoniae*) and antigen retrieval techniques were performed, and macrophages and neutrophils were also successfully labelled in adenoid tissue.

Since immunohistochemistry proved to be a useful and cost-effective way of visualising pneumococci and host immune cells in adenoid tissue, co-localisation was first investigated in spiked adenoids. In each adenoid that was examined (n = 4), aggregates of pneumococci were observed beneath the parenchyma, and immune cells were also found in each adenoid sample. Aggregates of pneumococci were co-localised with phagocytic cells in two adenoids. However, evidence of co-localisation was inconclusive due to limitations of the methodology, whilst spiking of adenoid tissue is not representative of patient adenoids *in vivo*.

To obtain more representative results, fluorophore-conjugated secondary antibodies were used for immunofluorescent labelling of *S. pneumoniae* and macrophages in patient adenoids that were not spiked (n = 4). An Omni primary antibody was optimised with pure cultures of pneumococcus. *S. pneumoniae* was detected at the edges of the tissue in two patient adenoid samples, but pneumococcal aggregates were not observed anywhere in the tissue. Instead, only a single pneumococcal cell was identified, although it appeared to be co-localised with macrophages. Moreover, pneumococcus was amorphous in appearance compared to the morphology previously observed with S14 using pure cultures and spiked adenoids. This discrepancy may due to the fact that S14 was grown in optimal laboratory conditions in rich media at 37°C/5% CO_2 prior to spiking adenoid tissue. In contrast, pre-existent pneumococci in patient adenoids may have encountered stress in the host including, a paucity of nutrients, a lower temperature, other bacterial species, and the presence of host cells themselves.

Several groups have used SEM to demonstrate the formation of unidentified bacterial biofilms on adenoids (Al-Mazrou and Al-Khattaf, 2008, Kania et al., 2008, Hoa et al., 2010, Saylam et al., 2010, Saafan et al., 2013, Tawfik et al., 2016). Bacterial biofilms were

detected on the epithelial surface and within small crypts of the tissue. The same result was observed when Kania et al. used SEM and histological staining (Kania et al., 2008). Additionally, despite an extensive search, Winther et al. and Ivarsson et al. did not find bacterial biofilms in subepithelial parenchyma tissue using histological staining (Ivarsson and Lundberg, 2001, Winther et al., 2009). Phagocytes were found in the epithelium and penetrating the epithelial surface along with evidence of phagocytosis of planktonic bacteria. The authors of these studies hypothesised that surface-associated and invasive planktonic bacteria would likely be ingested by phagocytic cells, whilst surface-associated biofilms would withstand the activity of these innate immune cells.

Taken together, although the number of patient adenoids that were examined in this project were small (n = 4), these initial results exploring pneumococcal-host interactions in adenoid tissue are consistent with the aforementioned studies examining bacterial biofilms on adenoid samples and the non-invasive characteristics of pneumococcal biofilms reported in the literature. For instance, *in vitro* models have shown pneumococcal biofilms are considerably less invasive than their planktonic counterparts when grown on an epithelial substratum (Blanchette-Cain et al., 2013, Marks et al., 2013), with similar results found in mice (Sanchez et al., 2011b, Marks et al., 2013), including a study using confocal microscopy that showed pneumococci were located on the surface of the epithelial monolayer and not within lymphoid tissue in the nasopharynx (Joyce et al., 2009).

However, in the four patient adenoids that were examined, pneumococcal aggregates were not found on the epithelial surface either. It is possible that damage and/or loss of the epithelial surface during surgical removal of the tissue, and difficulty in orientating the adenoid prior to embedding the tissue in paraffin-wax, may have resulted in loss of aggregated *S. pneumoniae*. Moreover, inclusion criteria for patients undergoing adenoidectomy included children with either a middle ear infection or children without an infection but suffering from obstructive sleep apnea (OSA). It has been shown in the literature that in addition to children with middle ear disease harbouring an adenoid biofilm more frequently than children with OSA - as well as a higher grade and a denser biofilm - the surface area of the biofilm is considerably more extensive in patients with middle ear infections (Zuliani et al., 2009, Hoa et al., 2010, Saylam et al., 2010, Saafan et al., 2013, Tawfik et al., 2016). This discrepancy is not exclusive to children with otitis media as similar findings have been recorded in studies that compared adenoid biofilms from children with either OSA or chronic rhinosinusitis (CRS) (Zuliani et al., 2006, Coticchia et al., 2007). Thus, it is possible that the patient adenoids in this project were all taken from children without a clinical infection. These differences may account for why pneumococcal biofilms were not associated with phagocytic cells seen intracellularly or on the epithelial

surface. More adenoid samples are required to further investigate possible co-localisation between pneumococci and host innate immune cells to address the points raised above.

Human epithelial samples from adenoid tissue as well as from the sinus mucosa and in the middle ear have shown pneumococcal biofilms associated with epithelial cells (Hall-Stoodley et al., 2006, Sanderson et al., 2006, Hoa et al., 2009, Nistico et al., 2011). It would be a reasonable assumption that pneumococcal biofilms in the upper respiratory tract in the human host are present for more than 6 hours, but current *in vitro* co-culture models have involved a short contact time of only 4 hours on viable epithelial cells without a flow system model (Pracht et al., 2005, Bootsma et al., 2007, Sanchez et al., 2011b, Brittan et al., 2012, Blanchette-Cain et al., 2013, Blanchette et al., 2016). Therefore, the secondary aim in this project was to co-culture a nascent biofilm on live epithelial cells for a prolonged duration. This model would be more physiologically relevant to pneumococcal colonisation in the nasopharynx *in vivo*.

7.3 Current pneumococcal biofilm co-culture models

The number of models studying the interactions between human respiratory tract pathogens in general and living co- cultures of epithelial cells is limited. However, it is becoming increasingly evident that *in vitro* models which more closely mimic the *in vivo* environment are more physiologically relevant and insightful than studying bacterial biofilms on abiotic surfaces.

For instance, the development of a co-culture model of *P. aeruginosa* and a human bronchial epithelial cell line has been described in the literature, in which biofilm formation occurred 6-8 hours after co-culture (Anderson et al., 2008, Moreau-Marquis et al., 2010). The model has since been used in several *P. aeruginosa* studies, with a range of assays (Yu et al., 2012, Anderson et al., 2013, Redelman et al., 2014, Alshalchi and Anderson, 2014, Moreau-Marquis et al., 2015). *Actinobacillus pleuropneumoniae* and *Stenotrophomonas maltophilia* biofilms grown on a porcine epithelial cell line and on bronchial epithelial cell monolayers, respectively, have also been described (Pompilio et al., 2010, Tremblay et al., 2013). The authors of these studies emphasised how innovative these more biologically relevant models are for prospective studies investigating bacterial biofilm-host interactions, which could encompass: 1) investigating the response of the host to biofilm growth; 2) evaluating gene expression of bacterial biofilms on a biotic surface using RT-PCR and microarray analysis, or 3) performing biofilm prevention and/or disruption assays.

Current co-culture models with *S. pneumoniae* biofilms have involved challenging live epithelial cells with pneumococci for up to 4 hours without a flow system model. A major drawback of these models is that only a short contact time is used in which to study adherence, biofilm formation and/or host cellular responses. Alternative co-culture models have involved either fixing epithelial cells prior to inoculation with pneumococci (Marks et al., 2012a, Shak et al., 2013a, Vidal et al., 2013), or transplanting a biofilm grown on prefixed epithelia onto live epithelial cell cultures (Marks et al., 2013). Although it has been shown that fixed epithelia does not affect the extent of pneumococcal adherence or the biomass of a biofilm (Marks et al., 2012a), the host response cannot be investigated with non-viable cells. Furthermore, biofilm formation is arbitrarily created without the presence (stress) of host innate cells. To circumvent these pitfalls, one research group developed a continuous-flow bioreactor model (Shak et al., 2013b, Vidal et al., 2013). This model enabled researchers to grow pneumococcal biofilms on epithelial cell lines for up to 24 hours. However, a significant limitation of this bioreactor model is that it requires specialised and costly laboratory equipment, which is not accessible in all laboratories.

7.4 Development of a respiratory epithelial cell and *S. pneumoniae* co-culture model

In this project, a human bronchial epithelial cell line (16HBE cells) was used to develop a co-culture model with *S. pneumoniae* strain D39. Confluent 16HBE cells were challenged with different pneumococcal loads (MOIs) to determine an optimum MOI that would maintain epithelial cell monolayer integrity. The integrity and viability of infected epithelial cell monolayers was determined by TEER and LDH release, and CFU and SEM analyses were performed to evaluate biofilm development.

Biofilm formation was found for each MOI, evidenced by structurally complex *S. pneumoniae* aggregates. Similar to Marks et al. and Vidal et al., biofilm formation was found 6 hours after co-culture, but fixed epithelial cells were used in their studies (Marks et al., 2012a, Vidal et al., 2013). Consistent with pneumococci shedding their capsule during colonisation in the nasopharynx and, exhibiting lower capsule expression in the biofilm phenotype compared to planktonic cultures *in vitro* (Hammerschmidt et al., 2005, Hall-Stoodley et al., 2008), minimal capsule was observed with the nascent D39 biofilms. As reported in studies by Marks et al. and Vidal et al., extracellular matrix material was found on the D39 biofilms, evidenced by the presence of small globular-like debris on the surface of pneumococci, as well as fibrous material located between individual pneumococcal cells (Marks et al., 2012a, Vidal et al., 2013). It could be hypothesised that these features of a

pneumococcal biofilm may be more pronounced in response to stress since Marks et al. showed prominent matrix material even in pneumococcal biofilms grown on fixed epithelia, in comparison to biofilms grown on an abiotic substratum (Marks et al., 2012a).

To develop a more physiologically relevant co-culture model, changes were made to extend the duration of the co-culture including, seeding 16HBE cells for longer on transwell membranes and infecting confluent epithelial monolayers with *S. pneumoniae* in antibiotic-free sMEM supplemented with catalase. Additionally, since Moreau-Marquis et al. replaced co-culture medium with fresh medium (following incubation of human airway epithelial cells for 1 hour) to prevent cytotoxicity and facilitate *P. aeruginosa* biofilm formation, the co-culture medium was replaced multiple times from D39 pneumococci and 16HBE cell co-cultures (Moreau-Marquis et al., 2010). It was postulated that fresh co-culture medium would remove accumulating toxins, such as pneumolysin, as well as virulent planktonic pneumococci from the co-culture model.

These changes enabled 16HBE cell monolayers to be challenged for up to 12 hours without the loss of epithelial cell integrity. Studying the biofilm phenotype on a biotic surface enables important interactions between a biofilm and the host to be investigated. In the current models investigations are performed with: 1) developing biofilms on non-viable cells; 2) pre-formed biofilms from fixed epithelia; 3) developing biofilms on viable cells for only 4 hours. Therefore, the established 12-hour co-culture model developed in this project greatly improves upon current epithelial cell and pneumococcal biofilm co-cultures, by extending the co-culture duration for up to 3 times as long. As a result, investigations into pneumococcal biofilms or the host are considerably more representative of colonising pneumococcal biofilms in the upper respiratory tract *in vivo*.

The co-culture model described herein may also be used to evaluate the efficacy of antibiotic treatment of a pneumococcal biofilm on live epithelial cells. Marks et al. have already found that pneumococcal biofilms grown on fixed epithelial cells are less susceptible to gentamicin, penicillin and erythromycin than pneumococcal biofilms grown on either plastic or glass (Marks et al., 2012a). The ability of antibiotics to disrupt an established biofilm on epithelial cells has been evaluated for *P. aeruginosa*, with the promising results offering potential beneficial treatment for cystic fibrosis patients (Yu et al., 2012, Anderson et al., 2013, Moreau-Marquis et al., 2015). The recalcitrance of pneumococcal biofilms on 16HBE cell monolayers can be evaluated with clinically relevant antibiotics, such as amoxicillin.

More viable pneumococcal cells were adherent to the monolayers during co-culture. Blanchette-Cain et al. and Marks et al. found no intracellular pneumococci and reduced invasiveness, respectively, after two different epithelial cell lines were challenged with

pneumococcal biofilms, yet these studies involved either transplanting an already formed biofilm from pre-fixed epithelia or using a 4-hour contact time (Blanchette-Cain et al., 2013, Marks et al., 2013). It is not possible to determine whether mechanical disruption (cell scraping) of the transwell membranes in this project would be sufficient to lyse confluent epithelial cells and release internal pneumococci. Thus, the results from CFU analysis may only account for pneumococci associated with the epithelial cell surface, but it may be that pneumococci from a developing biofilm on live epithelial cells are non-invasive, which would corroborate with these studies in the literature.

To address the hypothesis in the field of biofilm research that bacterial biofilms do not stimulate a strong host cell response as an explanation for prolonged persistence in the human host, the production of multiple cytokines from infected and uninfected 16HBE cell monolayers was measured using a multi-analyte Luminex assay (n = 1). No differences were seen between the infected and uninfected samples. The absence of an immune response from infected monolayers in response to the development of nascent pneumococcal biofilms is similar to other reports of a dampened epithelial cell cytokine response following pneumococcal biofilm challenge for 4 hours (Blanchette-Cain et al., 2013, Marks et al., 2013). However, the Luminex assay must be repeated, with other MOIs, or an alternative technique (e.g. ELISA) could be utilised before any clear conclusions can be drawn.

7.5 Conclusion

In the first part of this project, the aim was to assess pneumococcal co-localisation with phagocytes in adenoid tissue. A novel approach was taken, whereby immunohistochemistry was used to determine the *in situ* localisation of pneumococcus in association with host cells. Immunohistochemistry was successful in reaching the following objectives (i) staining pure cultures of pneumococcus; (ii) identifying pneumococcus and macrophages and neutrophils in spiked adenoid tissue; (iii) showing the presence of *S. pneumoniae* biofilms. However, despite the effectiveness of immunohistochemistry, visualisation of pneumococcal co-localisation with host innate immune cells was inconclusive and unsuitable with immunohistochemistry and sequential section staining.

Thus, immunofluorescence was implemented. Immunofluorescent techniques effectively stained pure cultures of pneumococcus as well as pneumococcus and macrophages in patient (non-spiked) adenoids. Although aggregates of pneumococcus were not found, the sample size that was used was small (n = 4). Future studies would benefit from the continued use of immunofluorescence due to the more rapid detection of pneumococcus and the sharper images that are obtained with this technique.

In the second part of this project, the aim was to develop a prolonged co-culture of pneumococci on live epithelial cells and show evidence of nascent biofilm formation. The model was successfully established, with biofilms forming over 12 hours of culture without compromising epithelial cell integrity as determined by TEER, LDH production and photomicrographic images. This prolonged co-culture model improves upon existing pneumococcal models by establishing an extended co-culture on live epithelial cell monolayers without using a flow system model and, therefore, serves as a more representative model of pneumococcal biofilm colonisation *in vivo*.

Nascent biofilm formation was assessed through SEM, with the structural complexity, architecture and atypical cellular morphology consistent with pneumococcal biofilms examined from human biopsies *ex vivo*. Despite the effectiveness of SEM in showing pneumococcal biofilm topology, future studies could employ epifluorescence as a means of measuring surface area coverage on the confluent epithelial cells for all of the pneumococcal loads (multiplicities of infection) over several time-points of co-culture. Similarly, Luminex or an alternative technique, such as ELISA, could be used to explore the epithelial cell response to initial pneumococcal attachment and biofilm formation, and by concurrently using a higher pneumococcal load.

.

7.6 Prospective studies

In order to develop this work further, additional studies should be performed. These include:

1. **Examine co-localisation in additional patient adenoids from children undergoing adenoidectomy for the treatment of chronic or recurrent otitis media (OM) or obstructive sleep apnea (OSA).**

Dual immunofluorescence can be performed on more patient adenoids in order to increase the statistical power to determine whether aggregates of pneumococci are found in paediatric adenoid tissue and if pneumococci co-localise with macrophages.

2. **Measure antimicrobial peptide expression in 16HBE cells in response to *S. pneumoniae* D39.**

Antimicrobial peptides such as beta-defensins and cathelicidins are expressed by epithelial cells in response to bacterial challenge and form part of the innate immune system. Antimicrobial peptides may directly target a pathogen by forming a cytotoxic pore as well as orchestrating an immune response by influencing chemotaxis and cytokine release of inflammatory cells. The expression of antimicrobial peptides from 16HBE cells can be measured by harvesting the cell culture medium before and after pneumococcal challenge, and performing mRNA analysis via quantitative RT-PCR or Western blots.

3. **Assess antibiotic treatment of an established biofilm.**

The efficacy of antibiotic treatments against established D39 pneumococcal biofilms can be examined. Nascent pneumococcal biofilms will be exposed to either fresh medium alone or challenged with medium in combination with clinically relevant antibiotics including, amoxicillin, amoxicillin with clavulonic acid (co-amoxiclav) or azithromycin. Viable counts and analysis of biofilm formation will be determined by CFU and SEM analyses. The toxicity of the antibiotics towards the 16HBE cells will also be measured using the LDH cytotoxicity assay.

4. **Determine whether *S. pneumoniae* invades epithelial cells.**

The number of viable intracellular pneumococcal cells can be determined to assess whether pneumococci invade the 16HBE cells. An antibiotic exclusion assay would not be appropriate as this particular assay is dependent on all extracellular bacteria being killed by the chosen antibiotic. Instead, fluorescence microscopy can be used to distinguish between

extracellular pneumococci (bound by a lectin or pneumococcal-specific antibody) and then intracellular pneumococci (bound by membrane-permeable and membrane-impermeable fluorescent dyes) after permeabilising the 16HBE cells (Johnson and Criss, 2013).

5. **Investigate gene expression of *S. pneumoniae* and 16HBE cell monolayers in co-culture.**

S. pneumoniae gene expression can be analysed to potentially reveal genes that are up- or down-regulated during biofilm growth on the 16HBE cells. Similarly, investigations into 16HBE gene expression can also be performed. Together, these experiments may provide a deeper understanding of the interaction between a pneumococcal biofilm and live epithelial cells over time.

6. **Evaluate biofilm formation with mutant pneumococcal strains.**

Mutant strains can be used to investigate the specific role of pneumococcal virulence factors and adhesins. CFUs, SEM analysis and antibiotic treatment can then be used to assess the effect that a mutation has on biofilm formation and recalcitrance to antibiotics.

7. **Develop air-liquid interface co-culture models with other pneumococcal strains and with primary epithelial cells.**

Although the use of a biotic surface to examine pneumococcal biofilm-host interactions is more physiologically relevant than using an abiotic surface, such as glass or plastic, epithelial cell lines do not perfectly reproduce the *in* vivo nasopharynx environment. 16HBE cells do not contain cilia or an overlying mucosal surface unlike respiratory epithelial cells in the human host. Therefore, a co-culture model can be developed on primary epithelial cells, which will most likely be taken from nasal swabs of human volunteers; this technique will be less invasive than obtaining a biopsy during a bronchoscopy. Upon reaching confluency, the epithelial cells will then be cultured at an air-liquid interface (ALI) in which the apical medium is removed from the monolayers and only the baso-lateral medium is still used. These conditions lead to a differentiated epithelium with ciliated and mucus-producing cells. Finally, to develop the model even further, a more clinically relevant pneumococcal serotype can be used to seed the cultured primary epithelial cells. Specifically, a serotype that is not included in the pneumococcal vaccines.

8. Develop a mixed co-culture model with epithelial cells and macrophages.

The interaction of a pneumococcal biofilm in a mixed co-culture model of epithelial cells and macrophages can be investigated. Macrophages play an important role in the innate immune response to infection, and epithelial-macrophage interactions may modify the host response, such as cytokine production, to pneumococcal challenge.

8 References

Abidi, S. H., Sherwani, S. K., Siddiqui, T. R., Bashir, A. and Kazmi, S. U. (2013) 'Drug resistance profile and biofilm forming potential of Pseudomonas aeruginosa isolated from contact lenses in Karachi-Pakistan', *BMC Ophthalmol,* 13, pp. 57.

Agarwal, V., Hammerschmidt, S., Malm, S., Bergmann, S., Riesbeck, K. and Blom, A. M. (2012) 'Enolase of Streptococcus pneumoniae binds human complement inhibitor C4b-binding protein and contributes to complement evasion', *J Immunol,* 189(7), pp. 3575-84.

Al-Mazrou, K. A. and Al-Khattaf, A. S. (2008) 'Adherent biofilms in adenotonsillar diseases in children', *Arch Otolaryngol Head Neck Surg,* 134(1), pp. 20-3.

Al-Mutairi, D. and Kilty, S. J. (2011) 'Bacterial biofilms and the pathophysiology of chronic rhinosinusitis', *Curr Opin Allergy Clin Immunol,* 11(1), pp. 18-23.

Albrich, W. C., Madhi, S. A., Adrian, P. V., van Niekerk, N., Mareletsi, T., Cutland, C., Wong, M., Khoosal, M., Karstaedt, A., Zhao, P., Deatly, A., Sidhu, M., Jansen, K. U. and Klugman, K. P. (2012) 'Use of a rapid test of pneumococcal colonization density to diagnose pneumococcal pneumonia', *Clin Infect Dis,* 54(5), pp. 601-9.

Alhede, M., Bjarnsholt, T., Jensen, P., Phipps, R. K., Moser, C., Christophersen, L., Christensen, L. D., van Gennip, M., Parsek, M., Høiby, N., Rasmussen, T. B. and Givskov, M. (2009) 'Pseudomonas aeruginosa recognizes and responds aggressively to the presence of polymorphonuclear leukocytes', *Microbiology,* 155(Pt 11), pp. 3500-8.

Allan, R. N., Morgan, S., Brito-Mutunayagam, S., Skipp, P., Feelisch, M., Hayes, S. M., Hellier, W., Clarke, S. C., Stoodley, P., Burgess, A., Ismail-Koch, H., Salib, R. J., Webb, J. S., Faust, S. N. and Hall-Stoodley, L. (2016) 'Low Concentrations of Nitric Oxide Modulate Streptococcus pneumoniae Biofilm Metabolism and Antibiotic Tolerance', *Antimicrob Agents Chemother,* 60(4), pp. 2456-66.

Allan, R. N., Skipp, P., Jefferies, J., Clarke, S. C., Faust, S. N., Hall-Stoodley, L. and Webb, J. (2014) 'Pronounced metabolic changes in adaptation to biofilm growth by Streptococcus pneumoniae', *PLoS One,* 9(9), pp. e107015.

Allegrucci, M., Hu, F. Z., Shen, K., Hayes, J., Ehrlich, G. D., Post, J. C. and Sauer, K. (2006) 'Phenotypic characterization of Streptococcus pneumoniae biofilm development', *J Bacteriol,* 188(7), pp. 2325-35.

Allegrucci, M. and Sauer, K. (2007) 'Characterization of colony morphology variants isolated from Streptococcus pneumoniae biofilms', *J Bacteriol,* 189(5), pp. 2030-8.

Alshalchi, S. A. and Anderson, G. G. (2014) 'Involvement of stress-related genes polB and PA14_46880 in biofilm formation of Pseudomonas aeruginosa', *Infect Immun,* 82(11), pp. 4746-57.

Anderl, J. N., Franklin, M. J. and Stewart, P. S. (2000) 'Role of antibiotic penetration limitation in Klebsiella pneumoniae biofilm resistance to ampicillin and ciprofloxacin', *Antimicrob Agents Chemother,* 44(7), pp. 1818-24.

Anderl, J. N., Zahller, J., Roe, F. and Stewart, P. S. (2003) 'Role of nutrient limitation and stationary-phase existence in Klebsiella pneumoniae biofilm resistance to ampicillin and ciprofloxacin', *Antimicrob Agents Chemother,* 47(4), pp. 1251-6.

Anderson, G. G., Kenney, T. F., Macleod, D. L., Henig, N. R. and O'Toole, G. A. (2013) 'Eradication of Pseudomonas aeruginosa biofilms on cultured airway cells by a fosfomycin/tobramycin antibiotic combination', *Pathog Dis,* 67(1), pp. 39-45.

Anderson, G. G., Moreau-Marquis, S., Stanton, B. A. and O'Toole, G. A. (2008) 'In vitro analysis of tobramycin-treated Pseudomonas aeruginosa biofilms on cystic fibrosis-derived airway epithelial cells', *Infect Immun,* 76(4), pp. 1423-33.

Andersson, J., Boasso, A., Nilsson, J., Zhang, R., Shire, N. J., Lindback, S., Shearer, G. M. and Chougnet, C. A. (2005) 'The prevalence of regulatory T cells in lymphoid

tissue is correlated with viral load in HIV-infected patients', *J Immunol,* 174(6), pp. 3143-7.

Anwar, H., van Biesen, T., Dasgupta, M., Lam, K. and Costerton, J. W. (1989) 'Interaction of biofilm bacteria with antibiotics in a novel in vitro chemostat system', *Antimicrob Agents Chemother,* 33(10), pp. 1824-6.

Arnold, R. R., Brewer, M. and Gauthier, J. J. (1980) 'Bactericidal activity of human lactoferrin: sensitivity of a variety of microorganisms', *Infect Immun,* 28(3), pp. 893-8.

Aul, J. J., Anderson, K. W., Wadowsky, R. M., Doyle, W. J., Kingsley, L. A., Post, J. C. and Ehrlich, G. D. (1998) 'Comparative evaluation of culture and PCR for the detection and determination of persistence of bacterial strains and DNAs in the Chinchilla laniger model of otitis media', *Ann Otol Rhinol Laryngol,* 107(6), pp. 508-13.

Auler, M. E., Morreira, D., Rodrigues, F. F., Abr Ao, M. S., Margarido, P. F., Matsumoto, F. E., Silva, E. G., Silva, B. C., Schneider, R. P. and Paula, C. R. (2010) 'Biofilm formation on intrauterine devices in patients with recurrent vulvovaginal candidiasis', *Med Mycol,* 48(1), pp. 211-6.

Austrian, R. (1986) 'Some aspects of the pneumococcal carrier state', *J Antimicrob Chemother,* 18 Suppl A, pp. 35-45.

Bakaletz, L. O. (2007) 'Bacterial biofilms in otitis media: evidence and relevance', *Pediatr Infect Dis J,* 26(10 Suppl), pp. S17-9.

Bakaletz, L. O. (2010) 'Immunopathogenesis of polymicrobial otitis media', *J Leukoc Biol,* 87(2), pp. 213-22.

Balsells, E., Guillot, L., Nair, H. and Kyaw, M. H. (2017) 'Serotype distribution of Streptococcus pneumoniae causing invasive disease in children in the post-PCV era: A systematic review and meta-analysis', *PLoS One,* 12(5), pp. e0177113.

Barraud, N., Hassett, D. J., Hwang, S. H., Rice, S. A., Kjelleberg, S. and Webb, J. S. (2006) 'Involvement of nitric oxide in biofilm dispersal of Pseudomonas aeruginosa', *J Bacteriol,* 188(21), pp. 7344-53.

Barraud, N., Kelso, M. J., Rice, S. A. and Kjelleberg, S. (2015) 'Nitric oxide: a key mediator of biofilm dispersal with applications in infectious diseases', *Curr Pharm Des,* 21(1), pp. 31-42.

Barraud, N., Schleheck, D., Klebensberger, J., Webb, J. S., Hassett, D. J., Rice, S. A. and Kjelleberg, S. (2009) 'Nitric oxide signaling in Pseudomonas aeruginosa biofilms mediates phosphodiesterase activity, decreased cyclic di-GMP levels, and enhanced dispersal', *J Bacteriol,* 191(23), pp. 7333-42.

Bender, M. H. and Weiser, J. N. (2006) 'The atypical amino-terminal LPNTG-containing domain of the pneumococcal human IgA1-specific protease is required for proper enzyme localization and function', *Mol Microbiol,* 61(2), pp. 526-43.

Bennett, K. E., Haggard, M. P., Silva, P. A. and Stewart, I. A. (2001) 'Behaviour and developmental effects of otitis media with effusion into the teens', *Arch Dis Child,* 85(2), pp. 91-5.

Bergmann, S., Rohde, M., Chhatwal, G. S. and Hammerschmidt, S. (2001) 'alpha-Enolase of Streptococcus pneumoniae is a plasmin(ogen)-binding protein displayed on the bacterial cell surface', *Mol Microbiol,* 40(6), pp. 1273-87.

Bergmann, S., Schoenen, H. and Hammerschmidt, S. (2013) 'The interaction between bacterial enolase and plasminogen promotes adherence of Streptococcus pneumoniae to epithelial and endothelial cells', *Int J Med Microbiol,* 303(8), pp. 452-62.

Bertin, L., Pons, G., d'Athis, P., Duhamel, J. F., Maudelonde, C., Lasfargues, G., Guillot, M., Marsac, A., Debregeas, B. and Olive, G. (1996) 'A randomized, double-blind, multicentre controlled trial of ibuprofen versus acetaminophen and placebo for symptoms of acute otitis media in children', *Fundam Clin Pharmacol,* 10(4), pp. 387-92.

Bewick, T., Sheppard, C., Greenwood, S., Slack, M., Trotter, C., George, R. and Lim, W. S. (2012) 'Serotype prevalence in adults hospitalised with pneumococcal non-invasive community-acquired pneumonia', *Thorax,* 67(6), pp. 540-5.

Bjarnsholt, T., Jensen, P., Burmølle, M., Hentzer, M., Haagensen, J. A., Hougen, H. P., Calum, H., Madsen, K. G., Moser, C., Molin, S., Høiby, N. and Givskov, M. (2005) 'Pseudomonas aeruginosa tolerance to tobramycin, hydrogen peroxide and polymorphonuclear leukocytes is quorum-sensing dependent', *Microbiology,* 151(Pt 2), pp. 373-83.

Blanchette, K. A. and Orihuela, C. J. (2012) 'Future perspective on host-pathogen interactions during bacterial biofilm formation within the nasopharynx', *Future Microbiol,* 7(2), pp. 227-39.

Blanchette, K. A., Shenoy, A. T., Milner, J., Gilley, R. P., McClure, E., Hinojosa, C. A., Kumar, N., Daugherty, S. C., Tallon, L. J., Ott, S., King, S. J., Ferreira, D. M., Gordon, S. B., Tettelin, H. and Orihuela, C. J. (2016) 'Neuraminidase A-Exposed Galactose Promotes Streptococcus pneumoniae Biofilm Formation during Colonization', *Infect Immun,* 84(10), pp. 2922-32.

Blanchette-Cain, K., Hinojosa, C. A., Akula Suresh Babu, R., Lizcano, A., Gonzalez-Juarbe, N., Munoz-Almagro, C., Sanchez, C. J., Bergman, M. A. and Orihuela, C. J. (2013) 'Streptococcus pneumoniae biofilm formation is strain dependent, multifactorial, and associated with reduced invasiveness and immunoreactivity during colonization', *MBio,* 4(5), pp. e00745-13.

Bluestone, C. D. (1996) 'Pathogenesis of otitis media: role of eustachian tube', *Pediatr Infect Dis J,* 15(4), pp. 281-91.

Bogaert, D., De Groot, R. and Hermans, P. W. (2004) 'Streptococcus pneumoniae colonisation: the key to pneumococcal disease', *Lancet Infect Dis,* 4(3), pp. 144-54.

Boonacker, C. W., Rovers, M. M., Browning, G. G., Hoes, A. W., Schilder, A. G. and Burton, M. J. (2014) 'Adenoidectomy with or without grommets for children with otitis media: an individual patient data meta-analysis', *Health Technol Assess,* 18(5), pp. 1-118.

Bootsma, H. J., Egmont-Petersen, M. and Hermans, P. W. (2007) 'Analysis of the in vitro transcriptional response of human pharyngeal epithelial cells to adherent Streptococcus pneumoniae: evidence for a distinct response to encapsulated strains', *Infect Immun,* 75(11), pp. 5489-99.

Borriello, G., Werner, E., Roe, F., Kim, A. M., Ehrlich, G. D. and Stewart, P. S. (2004) 'Oxygen limitation contributes to antibiotic tolerance of Pseudomonas aeruginosa in biofilms', *Antimicrob Agents Chemother,* 48(7), pp. 2659-64.

Bothwell, M. R., Smith, A. L. and Phillips, T. (2003) 'Recalcitrant otorrhea due to Pseudomonas biofilm', *Otolaryngol Head Neck Surg,* 129(5), pp. 599-601.

Bowler, L. L., Ball, T. B. and Saward, L. L. (2014) 'A novel in vitro co-culture system allows the concurrent analysis of mature biofilm and planktonic bacteria with human lung epithelia', *J Microbiol Methods,* 101, pp. 49-55.

Brinkmann, V., Reichard, U., Goosmann, C., Fauler, B., Uhlemann, Y., Weiss, D. S., Weinrauch, Y. and Zychlinsky, A. (2004) 'Neutrophil extracellular traps kill bacteria', *Science,* 303(5663), pp. 1532-5.

Brittan, J. L., Buckeridge, T. J., Finn, A., Kadioglu, A. and Jenkinson, H. F. (2012) 'Pneumococcal neuraminidase A: an essential upper airway colonization factor for Streptococcus pneumoniae', *Mol Oral Microbiol,* 27(4), pp. 270-83.

Browall, S., Norman, M., Tångrot, J., Galanis, I., Sjöström, K., Dagerhamn, J., Hellberg, C., Pathak, A., Spadafina, T., Sandgren, A., Bättig, P., Franzén, O., Andersson, B., Örtqvist, Å., Normark, S. and Henriques-Normark, B. (2014) 'Intraclonal variations among Streptococcus pneumoniae isolates influence the likelihood of invasive disease in children', *J Infect Dis,* 209(3), pp. 377-88.

Brown, J. S., Hussell, T., Gilliland, S. M., Holden, D. W., Paton, J. C., Ehrenstein, M. R., Walport, M. J. and Botto, M. (2002) 'The classical pathway is the dominant

complement pathway required for innate immunity to Streptococcus pneumoniae infection in mice', *Proc Natl Acad Sci U S A,* 99(26), pp. 16969-74.

Brueggemann, A. B., Griffiths, D. T., Meats, E., Peto, T., Crook, D. W. and Spratt, B. G. (2003) 'Clonal relationships between invasive and carriage Streptococcus pneumoniae and serotype- and clone-specific differences in invasive disease potential', *J Infect Dis,* 187(9), pp. 1424-32.

Brueggemann, A. B., Peto, T. E., Crook, D. W., Butler, J. C., Kristinsson, K. G. and Spratt, B. G. (2004) 'Temporal and geographic stability of the serogroup-specific invasive disease potential of Streptococcus pneumoniae in children', *J Infect Dis,* 190(7), pp. 1203-11.

Brugger, S. D., Frey, P., Aebi, S., Hinds, J. and Mühlemann, K. (2010) 'Multiple colonization with S. pneumoniae before and after introduction of the seven-valent conjugated pneumococcal polysaccharide vaccine', *PLoS One,* 5(7), pp. e11638.

Brugger, S. D., Hathaway, L. J. and Mühlemann, K. (2009) 'Detection of Streptococcus pneumoniae strain cocolonization in the nasopharynx', *J Clin Microbiol,* 47(6), pp. 1750-6.

Butler, J. C., Dowell, S. F. and Breiman, R. F. (1998) 'Epidemiology of emerging pneumococcal drug resistance: implications for treatment and prevention', *Vaccine,* 16(18), pp. 1693-7.

Bättig, P. and Mühlemann, K. (2008) 'Influence of the spxB gene on competence in Streptococcus pneumoniae', *J Bacteriol,* 190(4), pp. 1184-9.

Casey, J. R. and Pichichero, M. E. (2004) 'Changes in frequency and pathogens causing acute otitis media in 1995-2003', *Pediatr Infect Dis J,* 23(9), pp. 824-8.

Cerca, F., Andrade, F., França, Â., Andrade, E. B., Ribeiro, A., Almeida, A. A., Cerca, N., Pier, G., Azeredo, J. and Vilanova, M. (2011) 'Staphylococcus epidermidis biofilms with higher proportions of dormant bacteria induce a lower activation of murine macrophages', *J Med Microbiol,* 60(Pt 12), pp. 1717-24.

Cerca, N., Jefferson, K. K., Oliveira, R., Pier, G. B. and Azeredo, J. (2006) 'Comparative antibody-mediated phagocytosis of Staphylococcus epidermidis cells grown in a biofilm or in the planktonic state', *Infect Immun,* 74(8), pp. 4849-55.

Ceri, H., Olson, M. E., Stremick, C., Read, R. R., Morck, D. and Buret, A. (1999) 'The Calgary Biofilm Device: new technology for rapid determination of antibiotic susceptibilities of bacterial biofilms', *J Clin Microbiol,* 37(6), pp. 1771-6.

Cevizci, R., Düzlü, M., Dündar, Y., Noyanalpan, N., Sultan, N., Tutar, H. and Bayazıt, Y. A. (2015) 'Preliminary results of a novel quorum sensing inhibitor against pneumococcal infection and biofilm formation with special interest to otitis media and cochlear implantation', *Eur Arch Otorhinolaryngol,* 272(6), pp. 1389-93.

Chaignon, P., Sadovskaya, I., Ragunah, C., Ramasubbu, N., Kaplan, J. B. and Jabbouri, S. (2007) 'Susceptibility of staphylococcal biofilms to enzymatic treatments depends on their chemical composition', *Appl Microbiol Biotechnol,* 75(1), pp. 125-32.

Chen, D. K., McGeer, A., de Azavedo, J. C. and Low, D. E. (1999) 'Decreased susceptibility of Streptococcus pneumoniae to fluoroquinolones in Canada. Canadian Bacterial Surveillance Network', *N Engl J Med,* 341(4), pp. 233-9.

Chen, J. D. and Morrison, D. A. (1987) 'Modulation of competence for genetic transformation in Streptococcus pneumoniae', *J Gen Microbiol,* 133(7), pp. 1959-67.

Chertow, D. S. and Memoli, M. J. (2013) 'Bacterial coinfection in influenza: a grand rounds review', *JAMA,* 309(3), pp. 275-82.

Cho, E. Y., Lee, H., Choi, E. H., Kim, Y. J., Eun, B. W., Cho, Y. K., Kim, Y. K., Jo, D. S., Lee, H. S., Lee, J., Kim, M. N., Kim, D. S. and Lee, H. J. (2014) 'Serotype distribution and antibiotic resistance of Streptococcus pneumoniae isolated from invasive infections after optional use of the 7-valent conjugate vaccine in Korea, 2006-2010', *Diagn Microbiol Infect Dis,* 78(4), pp. 481-6.

Christensen, L. D., van Gennip, M., Jakobsen, T. H., Alhede, M., Hougen, H. P., Høiby, N., Bjarnsholt, T. and Givskov, M. (2012) 'Synergistic antibacterial efficacy of early combination treatment with tobramycin and quorum-sensing inhibitors against Pseudomonas aeruginosa in an intraperitoneal foreign-body infection mouse model', *J Antimicrob Chemother,* 67(5), pp. 1198-206.

Ciofu, O., Beveridge, T. J., Kadurugamuwa, J., Walther-Rasmussen, J. and Høiby, N. (2000) 'Chromosomal beta-lactamase is packaged into membrane vesicles and secreted from Pseudomonas aeruginosa', *J Antimicrob Chemother,* 45(1), pp. 9-13.

Claverys, J. P. and Håvarstein, L. S. (2007) 'Cannibalism and fratricide: mechanisms and raisons d'être', *Nat Rev Microbiol,* 5(3), pp. 219-29.

Claverys, J. P., Martin, B. and Håvarstein, L. S. (2007) 'Competence-induced fratricide in streptococci', *Mol Microbiol,* 64(6), pp. 1423-33.

Coates, H., Thornton, R., Langlands, J., Filion, P., Keil, A. D., Vijayasekaran, S. and Richmond, P. (2008) 'The role of chronic infection in children with otitis media with effusion: evidence for intracellular persistence of bacteria', *Otolaryngol Head Neck Surg,* 138(6), pp. 778-81.

Coffey, T. J., Dowson, C. G., Daniels, M., Zhou, J., Martin, C., Spratt, B. G. and Musser, J. M. (1991) 'Horizontal transfer of multiple penicillin-binding protein genes, and capsular biosynthetic genes, in natural populations of Streptococcus pneumoniae', *Mol Microbiol,* 5(9), pp. 2255-60.

Coffey, T. J., Enright, M. C., Daniels, M., Morona, J. K., Morona, R., Hryniewicz, W., Paton, J. C. and Spratt, B. G. (1998) 'Recombinational exchanges at the capsular polysaccharide biosynthetic locus lead to frequent serotype changes among natural isolates of Streptococcus pneumoniae', *Mol Microbiol,* 27(1), pp. 73-83.

Cohen, J. M., Chimalapati, S., de Vogel, C., van Belkum, A., Baxendale, H. E. and Brown, J. S. (2012) 'Contributions of capsule, lipoproteins and duration of colonisation towards the protective immunity of prior Streptococcus pneumoniae nasopharyngeal colonisation', *Vaccine,* 30(30), pp. 4453-9.

Cohen, J. M., Khandavilli, S., Camberlein, E., Hyams, C., Baxendale, H. E. and Brown, J. S. (2011) 'Protective contributions against invasive Streptococcus pneumoniae pneumonia of antibody and Th17-cell responses to nasopharyngeal colonisation', *PLoS One,* 6(10), pp. e25558.

Cohen, R., Bingen, E., Varon, E., de La Rocque, F., Brahimi, N., Levy, C., Boucherat, M., Langue, J. and Geslin, P. (1997) 'Change in nasopharyngeal carriage of Streptococcus pneumoniae resulting from antibiotic therapy for acute otitis media in children', *Pediatr Infect Dis J,* 16(6), pp. 555-60.

Cohen, R., Levy, C., Bonnet, E., Grondin, S., Desvignes, V., Lecuyer, A., Fritzell, B. and Varon, E. (2010) 'Dynamic of pneumococcal nasopharyngeal carriage in children with acute otitis media following PCV7 introduction in France', *Vaccine,* 28(37), pp. 6114-21.

Cohen, R., Navel, M., Grunberg, J., Boucherat, M., Geslin, P., Derriennic, M., Pichon, F. and Goehrs, J. M. (1999) 'One dose ceftriaxone vs. ten days of amoxicillin/clavulanate therapy for acute otitis media: clinical efficacy and change in nasopharyngeal flora', *Pediatr Infect Dis J,* 18(5), pp. 403-9.

Conklin, L., Loo, J. D., Kirk, J., Fleming-Dutra, K. E., Deloria Knoll, M., Park, D. E., Goldblatt, D., O'Brien, K. L. and Whitney, C. G. (2014) 'Systematic review of the effect of pneumococcal conjugate vaccine dosing schedules on vaccine-type invasive pneumococcal disease among young children', *Pediatr Infect Dis J,* 33 Suppl 2, pp. S109-18.

Costerton, J. W., Lewandowski, Z., Caldwell, D. E., Korber, D. R. and Lappin-Scott, H. M. (1995) 'Microbial biofilms', *Annu Rev Microbiol,* 49, pp. 711-45.

Costerton, J. W., Lewandowski, Z., DeBeer, D., Caldwell, D., Korber, D. and James, G. (1994) 'Biofilms, the customized microniche', *J Bacteriol,* 176(8), pp. 2137-42.

Costerton, J. W., Stewart, P. S. and Greenberg, E. P. (1999) 'Bacterial biofilms: a common cause of persistent infections', *Science,* 284(5418), pp. 1318-22.

Coticchia, J., Zuliani, G., Coleman, C., Carron, M., Gurrola, J., Haupert, M. and Berk, R. (2007) 'Biofilm surface area in the pediatric nasopharynx: Chronic rhinosinusitis vs obstructive sleep apnea', *Arch Otolaryngol Head Neck Surg,* 133(2), pp. 110-4.

Coyte, P. C., Croxford, R., McIsaac, W., Feldman, W. and Friedberg, J. (2001) 'The role of adjuvant adenoidectomy and tonsillectomy in the outcome of the insertion of tympanostomy tubes', *N Engl J Med,* 344(16), pp. 1188-95.

Croucher, N. J., Harris, S. R., Fraser, C., Quail, M. A., Burton, J., van der Linden, M., McGee, L., von Gottberg, A., Song, J. H., Ko, K. S., Pichon, B., Baker, S., Parry, C. M., Lambertsen, L. M., Shahinas, D., Pillai, D. R., Mitchell, T. J., Dougan, G., Tomasz, A., Klugman, K. P., Parkhill, J., Hanage, W. P. and Bentley, S. D. (2011) 'Rapid pneumococcal evolution in response to clinical interventions', *Science,* 331(6016), pp. 430-4.

Cundell, D. R., Gerard, N. P., Gerard, C., Idanpaan-Heikkila, I. and Tuomanen, E. I. (1995a) 'Streptococcus pneumoniae anchor to activated human cells by the receptor for platelet-activating factor', *Nature,* 377(6548), pp. 435-8.

Cundell, D. R., Weiser, J. N., Shen, J., Young, A. and Tuomanen, E. I. (1995b) 'Relationship between colonial morphology and adherence of Streptococcus pneumoniae', *Infect Immun,* 63(3), pp. 757-61.

Curtis, M. M. and Way, S. S. (2009) 'Interleukin-17 in host defence against bacterial, mycobacterial and fungal pathogens', *Immunology,* 126(2), pp. 177-85.

Dabernat, H., Geslin, P., Megraud, F., Bégué, P., Boulesteix, J., Dubreuil, C., de La Roque, F., Trinh, A. and Scheimberg, A. (1998) 'Effects of cefixime or co-amoxiclav treatment on nasopharyngeal carriage of Streptococcus pneumoniae and Haemophilus influenzae in children with acute otitis media', *J Antimicrob Chemother,* 41(2), pp. 253-8.

Dagan, R., Leibovitz, E., Greenberg, D., Yagupsky, P., Fliss, D. M. and Leiberman, A. (1998) 'Dynamics of pneumococcal nasopharyngeal colonization during the first days of antibiotic treatment in pediatric patients', *Pediatr Infect Dis J,* 17(10), pp. 880-5.

Dalia, A. B., Standish, A. J. and Weiser, J. N. (2010) 'Three surface exoglycosidases from Streptococcus pneumoniae, NanA, BgaA, and StrH, promote resistance to opsonophagocytic killing by human neutrophils', *Infect Immun,* 78(5), pp. 2108-16.

Dalia, A. B. and Weiser, J. N. (2011) 'Minimization of bacterial size allows for complement evasion and is overcome by the agglutinating effect of antibody', *Cell Host Microbe,* 10(5), pp. 486-96.

Daly, K. A., Hunter, L. L. and Giebink, G. S. (1999) 'Chronic otitis media with effusion', *Pediatr Rev,* 20(3), pp. 85-93; quiz 94.

Daniel, M., Imtiaz-Umer, S., Fergie, N., Birchall, J. P. and Bayston, R. (2012) 'Bacterial involvement in otitis media with effusion', *Int J Pediatr Otorhinolaryngol,* 76(10), pp. 1416-22.

Daniels, C. C., Rogers, P. D. and Shelton, C. M. (2016) 'A Review of Pneumococcal Vaccines: Current Polysaccharide Vaccine Recommendations and Future Protein Antigens', *J Pediatr Pharmacol Ther,* 21(1), pp. 27-35.

Dave, S., Brooks-Walter, A., Pangburn, M. K. and McDaniel, L. S. (2001) 'PspC, a pneumococcal surface protein, binds human factor H', *Infect Immun,* 69(5), pp. 3435-7.

Davidson, R., Cavalcanti, R., Brunton, J. L., Bast, D. J., de Azavedo, J. C., Kibsey, P., Fleming, C. and Low, D. E. (2002) 'Resistance to levofloxacin and failure of treatment of pneumococcal pneumonia', *N Engl J Med,* 346(10), pp. 747-50.

Davies, D. G., Parsek, M. R., Pearson, J. P., Iglewski, B. H., Costerton, J. W. and Greenberg, E. P. (1998) 'The involvement of cell-to-cell signals in the development of a bacterial biofilm', *Science,* 280(5361), pp. 295-8.

Davis, K. M., Nakamura, S. and Weiser, J. N. (2011) 'Nod2 sensing of lysozyme-digested peptidoglycan promotes macrophage recruitment and clearance of S. pneumoniae colonization in mice', *J Clin Invest,* 121(9), pp. 3666-76.

de Beer, D., Stoodley, P., Roe, F. and Lewandowski, Z. (1994) 'Effects of biofilm structures on oxygen distribution and mass transport', *Biotechnol Bioeng,* 43(11), pp. 1131-8.

del Prado, G., Ruiz, V., Naves, P., Rodríguez-Cerrato, V., Soriano, F. and del Carmen Ponte, M. (2010) 'Biofilm formation by Streptococcus pneumoniae strains and effects of human serum albumin, ibuprofen, N-acetyl-l-cysteine, amoxicillin, erythromycin, and levofloxacin', *Diagn Microbiol Infect Dis,* 67(4), pp. 311-8.

Diamond, C., Sisson, P. R., Kearns, A. M. and Ingham, H. R. (1989) 'Bacteriology of chronic otitis media with effusion', *J Laryngol Otol,* 103(4), pp. 369-71.

Diavatopoulos, D. A., Short, K. R., Price, J. T., Wilksch, J. J., Brown, L. E., Briles, D. E., Strugnell, R. A. and Wijburg, O. L. (2010) 'Influenza A virus facilitates Streptococcus pneumoniae transmission and disease', *FASEB J,* 24(6), pp. 1789-98.

Dibdin, G. H., Assinder, S. J., Nichols, W. W. and Lambert, P. A. (1996) 'Mathematical model of beta-lactam penetration into a biofilm of Pseudomonas aeruginosa while undergoing simultaneous inactivation by released beta-lactamases', *J Antimicrob Chemother,* 38(5), pp. 757-69.

Dieudonné-Vatran, A., Krentz, S., Blom, A. M., Meri, S., Henriques-Normark, B., Riesbeck, K. and Albiger, B. (2009) 'Clinical isolates of Streptococcus pneumoniae bind the complement inhibitor C4b-binding protein in a PspC allele-dependent fashion', *J Immunol,* 182(12), pp. 7865-77.

Ding, F., Tang, P., Hsu, M. H., Cui, P., Hu, S., Yu, J. and Chiu, C. H. (2009) 'Genome evolution driven by host adaptations results in a more virulent and antimicrobial-resistant Streptococcus pneumoniae serotype 14', *BMC Genomics,* 10, pp. 158.

Dohar, J. E., Hebda, P. A., Veeh, R., Awad, M., Costerton, J. W., Hayes, J. and Ehrlich, G. D. (2005) 'Mucosal biofilm formation on middle-ear mucosa in a nonhuman primate model of chronic suppurative otitis media', *Laryngoscope,* 115(8), pp. 1469-72.

Domenech, M., García, E. and Moscoso, M. (2009) 'Versatility of the capsular genes during biofilm formation by Streptococcus pneumoniae', *Environ Microbiol,* 11(10), pp. 2542-55.

Domenech, M., García, E. and Moscoso, M. (2012) 'Biofilm formation in Streptococcus pneumoniae', *Microb Biotechnol,* 5(4), pp. 455-65.

Domenech, M., Ramos-Sevillano, E., García, E., Moscoso, M. and Yuste, J. (2013) 'Biofilm formation avoids complement immunity and phagocytosis of Streptococcus pneumoniae', *Infect Immun,* 81(7), pp. 2606-15.

Donkor, E. S., Bishop, C. J., Gould, K., Hinds, J., Antonio, M., Wren, B. and Hanage, W. P. (2011) 'High levels of recombination among Streptococcus pneumoniae isolates from the Gambia', *MBio,* 2(3), pp. e00040-11.

Donlan, R. M. (2001) 'Biofilms and device-associated infections', *Emerg Infect Dis,* 7(2), pp. 277-81.

Donlan, R. M. and Costerton, J. W. (2002) 'Biofilms: survival mechanisms of clinically relevant microorganisms', *Clin Microbiol Rev,* 15(2), pp. 167-93.

Dowson, C. G., Hutchison, A., Brannigan, J. A., George, R. C., Hansman, D., Liñares, J., Tomasz, A., Smith, J. M. and Spratt, B. G. (1989) 'Horizontal transfer of penicillin-binding protein genes in penicillin-resistant clinical isolates of Streptococcus pneumoniae', *Proc Natl Acad Sci U S A,* 86(22), pp. 8842-6.

Dunne, W. M. (1990) 'Effects of subinhibitory concentrations of vancomycin or cefamandole on biofilm production by coagulase-negative staphylococci', *Antimicrob Agents Chemother,* 34(3), pp. 390-3.

Echenique, J. R., Chapuy-Regaud, S. and Trombe, M. C. (2000) 'Competence regulation by oxygen in Streptococcus pneumoniae: involvement of ciaRH and comCDE', *Mol Microbiol,* 36(3), pp. 688-96.

Ehrlich, G. D., Veeh, R., Wang, X., Costerton, J. W., Hayes, J. D., Hu, F. Z., Daigle, B. J., Ehrlich, M. D. and Post, J. C. (2002) 'Mucosal biofilm formation on middle-ear mucosa in the chinchilla model of otitis media', *JAMA,* 287(13), pp. 1710-5.

Eldholm, V., Johnsborg, O., Haugen, K., Ohnstad, H. S. and Håvarstein, L. S. (2009) 'Fratricide in Streptococcus pneumoniae: contributions and role of the cell wall hydrolases CbpD, LytA and LytC', *Microbiology,* 155(Pt 7), pp. 2223-34.

Emaneini, M., Gharibpour, F., Khoramrooz, S. S., Mirsalehian, A., Jabalameli, F., Darban-Sarokhalil, D., Mirzaii, M., Sharifi, A. and Taherikalani, M. (2013) 'Genetic similarity between adenoid tissue and middle ear fluid isolates of Streptococcus pneumoniae, Haemophilus influenzae and Moraxella catarrhalis from Iranian children with otitis media with effusion', *Int J Pediatr Otorhinolaryngol,* 77(11), pp. 1841-5.

Epple, H. J., Loddenkemper, C., Kunkel, D., Tröger, H., Maul, J., Moos, V., Berg, E., Ullrich, R., Schulzke, J. D., Stein, H., Duchmann, R., Zeitz, M. and Schneider, T. (2006) 'Mucosal but not peripheral FOXP3+ regulatory T cells are highly increased in untreated HIV infection and normalize after suppressive HAART', *Blood,* 108(9), pp. 3072-8.

Falini, B., Abdulaziz, Z., Gerdes, J., Canino, S., Ciani, C., Cordell, J. L., Knight, P. M., Stein, H., Grignani, F. and Martelli, M. F. (1986) 'Description of a sequential staining procedure for double immunoenzymatic staining of pairs of antigens using monoclonal antibodies', *J Immunol Methods,* 93(2), pp. 265-73.

Fasching, C. E., Grossman, T., Corthésy, B., Plaut, A. G., Weiser, J. N. and Janoff, E. N. (2007) 'Impact of the molecular form of immunoglobulin A on functional activity in defense against Streptococcus pneumoniae', *Infect Immun,* 75(4), pp. 1801-10.

Fedson, D. S. (1999) 'The clinical effectiveness of pneumococcal vaccination: a brief review', *Vaccine,* 17 Suppl 1, pp. S85-90.

Feldman, C., Anderson, R., Cockeran, R., Mitchell, T., Cole, P. and Wilson, R. (2002) 'The effects of pneumolysin and hydrogen peroxide, alone and in combination, on human ciliated epithelium in vitro', *Respir Med,* 96(8), pp. 580-5.

Feldman, C., Anderson, R., Kanthakumar, K., Vargas, A., Cole, P. J. and Wilson, R. (1994) 'Oxidant-mediated ciliary dysfunction in human respiratory epithelium', *Free Radic Biol Med,* 17(1), pp. 1-10.

Feldman, C., Mitchell, T. J., Andrew, P. W., Boulnois, G. J., Read, R. C., Todd, H. C., Cole, P. J. and Wilson, R. (1990) 'The effect of Streptococcus pneumoniae pneumolysin on human respiratory epithelium in vitro', *Microb Pathog,* 9(4), pp. 275-84.

Ferreira, D. M., Neill, D. R., Bangert, M., Gritzfeld, J. F., Green, N., Wright, A. K., Pennington, S. H., Bricio-Moreno, L., Bricio Moreno, L., Moreno, A. T., Miyaji, E. N., Wright, A. D., Collins, A. M., Goldblatt, D., Kadioglu, A. and Gordon, S. B. (2013) 'Controlled human infection and rechallenge with Streptococcus pneumoniae reveals the protective efficacy of carriage in healthy adults', *Am J Respir Crit Care Med,* 187(8), pp. 855-64.

Flasche, S., Van Hoek, A. J., Sheasby, E., Waight, P., Andrews, N., Sheppard, C., George, R. and Miller, E. (2011) 'Effect of pneumococcal conjugate vaccination on serotype-specific carriage and invasive disease in England: a cross-sectional study', *PLoS Med,* 8(4), pp. e1001017.

Fleming-Dutra, K. E., Conklin, L., Loo, J. D., Knoll, M. D., Park, D. E., Kirk, J., Goldblatt, D., Whitney, C. G. and O'Brien, K. L. (2014) 'Systematic review of the effect of pneumococcal conjugate vaccine dosing schedules on vaccine-type nasopharyngeal carriage', *Pediatr Infect Dis J,* 33 Suppl 2, pp. S152-60.

Flemming, H. C. and Wingender, J. (2010) 'The biofilm matrix', *Nat Rev Microbiol,* 8(9), pp. 623-33.

Francolini, I. and Donelli, G. (2010) 'Prevention and control of biofilm-based medical-device-related infections', *FEMS Immunol Med Microbiol,* 59(3), pp. 227-38.

Fung, H. B. and Monteagudo-Chu, M. O. (2010) 'Community-acquired pneumonia in the elderly', *Am J Geriatr Pharmacother,* 8(1), pp. 47-62.

Fux, C. A., Costerton, J. W., Stewart, P. S. and Stoodley, P. (2005) 'Survival strategies of infectious biofilms', *Trends Microbiol,* 13(1), pp. 34-40.

García-Rodríguez, J. A. and Fresnadillo Martínez, M. J. (2002) 'Dynamics of nasopharyngeal colonization by potential respiratory pathogens', *J Antimicrob Chemother,* 50 Suppl S2, pp. 59-73.

Gates, G. A. (1999) 'Otitis media--the pharyngeal connection', *JAMA,* 282(10), pp. 987-9.

Gates, G. A., Avery, C. A. and Prihoda, T. J. (1988) 'Effect of adenoidectomy upon children with chronic otitis media with effusion', *Laryngoscope,* 98(1), pp. 58-63.

Gates, G. A., Avery, C. A., Prihoda, T. J. and Cooper, J. C. (1987) 'Effectiveness of adenoidectomy and tympanostomy tubes in the treatment of chronic otitis media with effusion', *N Engl J Med,* 317(23), pp. 1444-51.

Gates, G. A., Klein, J. O., Lim, D. J., Mogi, G., Ogra, P. L., Pararella, M. M., Paradise, J. L. and Tos, M. (2002) 'Recent advances in otitis media. 1. Definitions, terminology, and classification of otitis media', *Ann Otol Rhinol Laryngol Suppl,* 188, pp. 8-18.

Geno, K. A., Gilbert, G. L., Song, J. Y., Skovsted, I. C., Klugman, K. P., Jones, C., Konradsen, H. B. and Nahm, M. H. (2015) 'Pneumococcal Capsules and Their Types: Past, Present, and Future', *Clin Microbiol Rev,* 28(3), pp. 871-99.

Ghaffar, F., Friedland, I. R. and McCracken, G. H. (1999) 'Dynamics of nasopharyngeal colonization by Streptococcus pneumoniae', *Pediatr Infect Dis J,* 18(7), pp. 638-46.

Giebink, G. S. (1989) 'The microbiology of otitis media', *Pediatr Infect Dis J,* 8(1 Suppl), pp. S18-20.

Giebink, G. S., Juhn, S. K., Weber, M. L. and Le, C. T. (1982) 'The bacteriology and cytology of chronic otitis media with effusion', *Pediatr Infect Dis,* 1(2), pp. 98-103.

Goldblatt, D., Hussain, M., Andrews, N., Ashton, L., Virta, C., Melegaro, A., Pebody, R., George, R., Soininen, A., Edmunds, J., Gay, N., Kayhty, H. and Miller, E. (2005) 'Antibody responses to nasopharyngeal carriage of Streptococcus pneumoniae in adults: a longitudinal household study', *J Infect Dis,* 192(3), pp. 387-93.

Gosink, K. K., Mann, E. R., Guglielmo, C., Tuomanen, E. I. and Masure, H. R. (2000) 'Role of novel choline binding proteins in virulence of Streptococcus pneumoniae', *Infect Immun,* 68(10), pp. 5690-5.

Grebe, K. M., Takeda, K., Hickman, H. D., Bailey, A. L., Bailey, A. M., Embry, A. C., Bennink, J. R. and Yewdell, J. W. (2010) 'Cutting edge: Sympathetic nervous system increases proinflammatory cytokines and exacerbates influenza A virus pathogenesis', *J Immunol,* 184(2), pp. 540-4.

Green, M. and Wald, E. R. (1996) 'Emerging resistance to antibiotics: impact on respiratory infections in the outpatient setting', *Ann Allergy Asthma Immunol,* 77(3), pp. 167-73; quiz 173-5.

Guiral, S., Mitchell, T. J., Martin, B. and Claverys, J. P. (2005) 'Competence-programmed predation of noncompetent cells in the human pathogen Streptococcus pneumoniae: genetic requirements', *Proc Natl Acad Sci U S A,* 102(24), pp. 8710-5.

Günther, F., Wabnitz, G. H., Stroh, P., Prior, B., Obst, U., Samstag, Y., Wagner, C. and Hänsch, G. M. (2009) 'Host defence against Staphylococcus aureus biofilms infection: phagocytosis of biofilms by polymorphonuclear neutrophils (PMN)', *Mol Immunol,* 46(8-9), pp. 1805-13.

Güvenç, M. G., Midilli, K., Inci, E., Kuşkucu, M., Tahamiler, R., Ozergil, E., Ergin, S., Ada, M. and Altaş, K. (2010) 'Lack of Chlamydophila pneumoniae and predominance of Alloiococcus otitidis in middle ear fluids of children with otitis media with effusion', *Auris Nasus Larynx,* 37(3), pp. 269-73.

Hall-Stoodley, L., Costerton, J. W. and Stoodley, P. (2004) 'Bacterial biofilms: from the natural environment to infectious diseases', *Nat Rev Microbiol,* 2(2), pp. 95-108.

Hall-Stoodley, L., Hu, F. Z., Gieseke, A., Nistico, L., Nguyen, D., Hayes, J., Forbes, M., Greenberg, D. P., Dice, B., Burrows, A., Wackym, P. A., Stoodley, P., Post, J. C., Ehrlich, G. D. and Kerschner, J. E. (2006) 'Direct detection of bacterial biofilms on the middle-ear mucosa of children with chronic otitis media', *JAMA,* 296(2), pp. 202-11.

Hall-Stoodley, L., Nistico, L., Sambanthamoorthy, K., Dice, B., Nguyen, D., Mershon, W. J., Johnson, C., Hu, F. Z., Stoodley, P., Ehrlich, G. D. and Post, J. C. (2008) 'Characterization of biofilm matrix, degradation by DNase treatment and evidence of capsule downregulation in Streptococcus pneumoniae clinical isolates', *BMC Microbiol,* 8, pp. 173.

Hall-Stoodley, L. and Stoodley, P. (2005) 'Biofilm formation and dispersal and the transmission of human pathogens', *Trends Microbiol,* 13(1), pp. 7-10.

Hall-Stoodley, L. and Stoodley, P. (2009) 'Evolving concepts in biofilm infections', *Cell Microbiol,* 11(7), pp. 1034-43.

Hammerschmidt, S., Bethe, G., Remane, P. H. and Chhatwal, G. S. (1999) 'Identification of pneumococcal surface protein A as a lactoferrin-binding protein of Streptococcus pneumoniae', *Infect Immun,* 67(4), pp. 1683-7.

Hammerschmidt, S., Wolff, S., Hocke, A., Rosseau, S., Müller, E. and Rohde, M. (2005) 'Illustration of pneumococcal polysaccharide capsule during adherence and invasion of epithelial cells', *Infect Immun,* 73(8), pp. 4653-67.

Hammitt, L. L., Bruden, D. L., Butler, J. C., Baggett, H. C., Hurlburt, D. A., Reasonover, A. and Hennessy, T. W. (2006) 'Indirect effect of conjugate vaccine on adult carriage of Streptococcus pneumoniae: an explanation of trends in invasive pneumococcal disease', *J Infect Dis,* 193(11), pp. 1487-94.

Hanke, M. L., Angle, A. and Kielian, T. (2012) 'MyD88-dependent signaling influences fibrosis and alternative macrophage activation during Staphylococcus aureus biofilm infection', *PLoS One,* 7(8), pp. e42476.

Hanke, M. L., Heim, C. E., Angle, A., Sanderson, S. D. and Kielian, T. (2013) 'Targeting macrophage activation for the prevention and treatment of Staphylococcus aureus biofilm infections', *J Immunol,* 190(5), pp. 2159-68.

Hannig, C., Follo, M., Hellwig, E. and Al-Ahmad, A. (2010) 'Visualization of adherent micro-organisms using different techniques', *J Med Microbiol,* 59(Pt 1), pp. 1-7.

Harboe, Z. B., Dalby, T., Weinberger, D. M., Benfield, T., Mølbak, K., Slotved, H. C., Suppli, C. H., Konradsen, H. B. and Valentiner-Branth, P. (2014) 'Impact of 13-valent pneumococcal conjugate vaccination in invasive pneumococcal disease incidence and mortality', *Clin Infect Dis,* 59(8), pp. 1066-73.

Harmes, K. M., Blackwood, R. A., Burrows, H. L., Cooke, J. M., Harrison, R. V. and Passamani, P. P. (2013) 'Otitis media: diagnosis and treatment', *Am Fam Physician,* 88(7), pp. 435-40.

Hausdorff, W. P., Feikin, D. R. and Klugman, K. P. (2005) 'Epidemiological differences among pneumococcal serotypes', *Lancet Infect Dis,* 5(2), pp. 83-93.

Hawdon, N. A., Aval, P. S., Barnes, R. J., Gravelle, S. K., Rosengren, J., Khan, S., Ciofu, O., Johansen, H. K., Høiby, N. and Ulanova, M. (2010) 'Cellular responses of A549 alveolar epithelial cells to serially collected Pseudomonas aeruginosa from cystic fibrosis patients at different stages of pulmonary infection', *FEMS Immunol Med Microbiol,* 59(2), pp. 207-20.

Hendolin, P. H., Kärkkäinen, U., Himi, T., Markkanen, A. and Ylikoski, J. (1999) 'High incidence of Alloiococcus otitis in otitis media with effusion', *Pediatr Infect Dis J,* 18(10), pp. 860-5.

Hengzhuang, W., Wu, H., Ciofu, O., Song, Z. and Høiby, N. (2012) 'In vivo pharmacokinetics/pharmacodynamics of colistin and imipenem in Pseudomonas aeruginosa biofilm infection', *Antimicrob Agents Chemother,* 56(5), pp. 2683-90.

Hentzer, M., Wu, H., Andersen, J. B., Riedel, K., Rasmussen, T. B., Bagge, N., Kumar, N., Schembri, M. A., Song, Z., Kristoffersen, P., Manefield, M., Costerton, J. W., Molin, S., Eberl, L., Steinberg, P., Kjelleberg, S., Høiby, N. and Givskov, M. (2003) 'Attenuation of Pseudomonas aeruginosa virulence by quorum sensing inhibitors', *EMBO J,* 22(15), pp. 3803-15.

Herva, E., Luotonen, J., Timonen, M., Sibakov, M., Karma, P. and Mäkelä, P. H. (1980) 'The effect of polyvalent pneumococcal polysaccharide vaccine on nasopharyngeal and nasal carriage of Streptococcus pneumoniae', *Scand J Infect Dis,* 12(2), pp. 97-100.

Hicks, L. A., Harrison, L. H., Flannery, B., Hadler, J. L., Schaffner, W., Craig, A. S., Jackson, D., Thomas, A., Beall, B., Lynfield, R., Reingold, A., Farley, M. M. and Whitney, C. G. (2007) 'Incidence of pneumococcal disease due to non-pneumococcal conjugate vaccine (PCV7) serotypes in the United States during the era of widespread PCV7 vaccination, 1998-2004', *J Infect Dis,* 196(9), pp. 1346-54.

Hiller, N. L., Eutsey, R. A., Powell, E., Earl, J. P., Janto, B., Martin, D. P., Dawid, S., Ahmed, A., Longwell, M. J., Dahlgren, M. E., Ezzo, S., Tettelin, H., Daugherty, S. C., Mitchell, T. J., Hillman, T. A., Buchinsky, F. J., Tomasz, A., de Lencastre, H., Sá-Leão, R., Post, J. C., Hu, F. Z. and Ehrlich, G. D. (2011) 'Differences in genotype and virulence among four multidrug-resistant Streptococcus pneumoniae isolates belonging to the PMEN1 clone', *PLoS One,* 6(12), pp. e28850.

Hiller, N. L., Janto, B., Hogg, J. S., Boissy, R., Yu, S., Powell, E., Keefe, R., Ehrlich, N. E., Shen, K., Hayes, J., Barbadora, K., Klimke, W., Dernovoy, D., Tatusova, T., Parkhill, J., Bentley, S. D., Post, J. C., Ehrlich, G. D. and Hu, F. Z. (2007) 'Comparative genomic analyses of seventeen Streptococcus pneumoniae strains: insights into the pneumococcal supragenome', *J Bacteriol,* 189(22), pp. 8186-95.

Hoa, M., Syamal, M., Schaeffer, M. A., Sachdeva, L., Berk, R. and Coticchia, J. (2010) 'Biofilms and chronic otitis media: an initial exploration into the role of biofilms in the pathogenesis of chronic otitis media', *Am J Otolaryngol,* 31(4), pp. 241-5.

Hoa, M., Tomovic, S., Nistico, L., Hall-Stoodley, L., Stoodley, P., Sachdeva, L., Berk, R. and Coticchia, J. M. (2009) 'Identification of adenoid biofilms with middle ear pathogens in otitis-prone children utilizing SEM and FISH', *Int J Pediatr Otorhinolaryngol,* 73(9), pp. 1242-8.

Hoffman, L. R., D'Argenio, D. A., MacCoss, M. J., Zhang, Z., Jones, R. A. and Miller, S. I. (2005) 'Aminoglycoside antibiotics induce bacterial biofilm formation', *Nature,* 436(7054), pp. 1171-5.

Hoge, C. W., Reichler, M. R., Dominguez, E. A., Bremer, J. C., Mastro, T. D., Hendricks, K. A., Musher, D. M., Elliott, J. A., Facklam, R. R. and Breiman, R. F. (1994) 'An epidemic of pneumococcal disease in an overcrowded, inadequately ventilated jail', *N Engl J Med,* 331(10), pp. 643-8.

Holmes, A. R., McNab, R., Millsap, K. W., Rohde, M., Hammerschmidt, S., Mawdsley, J. L. and Jenkinson, H. F. (2001) 'The pavA gene of Streptococcus pneumoniae encodes a fibronectin-binding protein that is essential for virulence', *Mol Microbiol,* 41(6), pp. 1395-408.

Hostetter, M. K. (1986) 'Serotypic variations among virulent pneumococci in deposition and degradation of covalently bound C3b: implications for phagocytosis and antibody production', *J Infect Dis,* 153(4), pp. 682-93.

Hotomi, M., Yamanaka, N., Billal, D. S., Sakai, A., Yamauchi, K., Suzumoto, M., Takei, S., Yasui, N., Moriyama, S. and Kuki, K. (2004) 'Genotyping of Streptococcus pneumoniae and Haemophilus influenzae isolated from paired middle ear fluid and nasopharynx by pulsed-field gel electrophoresis', *ORL J Otorhinolaryngol Relat Spec,* 66(5), pp. 233-40.

Hotomi, M., Yuasa, J., Briles, D. E. and Yamanaka, N. (2016) 'Pneumolysin plays a key role at the initial step of establishing pneumococcal nasal colonization', *Folia Microbiol (Praha),* 61(5), pp. 375-83.

Howlin, R. P., Cathie, K., Hall-Stoodley, L., Cornelius, V., Duignan, C., Allan, R. N., Fernandez, B. O., Barraud, N., Bruce, K. D., Jefferies, J., Kelso, M., Kjelleberg, S., Rice, S. A., Rogers, G. B., Pink, S., Smith, C., Sukhtankar, P. S., Salib, R., Legg, J., Carroll, M., Daniels, T., Feelisch, M., Stoodley, P., Clarke, S. C., Connett, G., Faust, S. N. and Webb, J. S. (2017) 'Low-Dose Nitric Oxide as Targeted Anti-biofilm Adjunctive Therapy to Treat Chronic Pseudomonas aeruginosa Infection in Cystic Fibrosis', *Mol Ther*, 25(9), pp. 2104-2116.

Hsu, S. M., Raine, L. and Fanger, H. (1981) 'Use of avidin-biotin-peroxidase complex (ABC) in immunoperoxidase techniques: a comparison between ABC and unlabeled antibody (PAP) procedures', *J Histochem Cytochem*, 29(4), pp. 577-80.

Hussain, M., Melegaro, A., Pebody, R. G., George, R., Edmunds, W. J., Talukdar, R., Martin, S. A., Efstratiou, A. and Miller, E. (2005) 'A longitudinal household study of Streptococcus pneumoniae nasopharyngeal carriage in a UK setting', *Epidemiol Infect*, 133(5), pp. 891-8.

Hyams, C., Camberlein, E., Cohen, J. M., Bax, K. and Brown, J. S. (2010) 'The Streptococcus pneumoniae capsule inhibits complement activity and neutrophil phagocytosis by multiple mechanisms', *Infect Immun*, 78(2), pp. 704-15.

Hyams, C., Trzcinski, K., Camberlein, E., Weinberger, D. M., Chimalapati, S., Noursadeghi, M., Lipsitch, M. and Brown, J. S. (2013) 'Streptococcus pneumoniae capsular serotype invasiveness correlates with the degree of factor H binding and opsonization with C3b/iC3b', *Infect Immun*, 81(1), pp. 354-63.

Håvarstein, L. S., Coomaraswamy, G. and Morrison, D. A. (1995) 'An unmodified heptadecapeptide pheromone induces competence for genetic transformation in Streptococcus pneumoniae', *Proc Natl Acad Sci U S A*, 92(24), pp. 11140-4.

Håvarstein, L. S., Martin, B., Johnsborg, O., Granadel, C. and Claverys, J. P. (2006) 'New insights into the pneumococcal fratricide: relationship to clumping and identification of a novel immunity factor', *Mol Microbiol*, 59(4), pp. 1297-307.

Högberg, L., Geli, P., Ringberg, H., Melander, E., Lipsitch, M. and Ekdahl, K. (2007) 'Age- and serogroup-related differences in observed durations of nasopharyngeal carriage of penicillin-resistant pneumococci', *J Clin Microbiol*, 45(3), pp. 948-52.

Høiby, N., Bjarnsholt, T., Givskov, M., Molin, S. and Ciofu, O. (2010a) 'Antibiotic resistance of bacterial biofilms', *Int J Antimicrob Agents*, 35(4), pp. 322-32.

Høiby, N., Ciofu, O. and Bjarnsholt, T. (2010b) 'Pseudomonas aeruginosa biofilms in cystic fibrosis', *Future Microbiol*, 5(11), pp. 1663-74.

Høiby, N., Ciofu, O., Johansen, H. K., Song, Z. J., Moser, C., Jensen, P., Molin, S., Givskov, M., Tolker-Nielsen, T. and Bjarnsholt, T. (2011) 'The clinical impact of bacterial biofilms', *Int J Oral Sci*, 3(2), pp. 55-65.

Høiby, N., Döring, G. and Schiøtz, P. O. (1986) 'The role of immune complexes in the pathogenesis of bacterial infections', *Annu Rev Microbiol*, 40, pp. 29-53.

Ivarsson, M. and Lundberg, C. (2001) 'Phagocytosis in the nasopharyngeal secretion by cells from the adenoid', *Acta Otolaryngol*, 121(4), pp. 517-22.

Jain, R. and Douglas, R. (2014) 'When and how should we treat biofilms in chronic sinusitis?', *Curr Opin Otolaryngol Head Neck Surg*, 22(1), pp. 16-21.

Janeway, C. A. and Medzhitov, R. (2002) 'Innate immune recognition', *Annu Rev Immunol*, 20, pp. 197-216.

Jansen, A. G., Sanders, E. A., VAN DER Ende, A., VAN Loon, A. M., Hoes, A. W. and Hak, E. (2008) 'Invasive pneumococcal and meningococcal disease: association with influenza virus and respiratory syncytial virus activity?', *Epidemiol Infect*, 136(11), pp. 1448-54.

Jarva, H., Janulczyk, R., Hellwage, J., Zipfel, P. F., Björck, L. and Meri, S. (2002) 'Streptococcus pneumoniae evades complement attack and opsonophagocytosis by expressing the pspC locus-encoded Hic protein that binds to short consensus repeats 8-11 of factor H', *J Immunol*, 168(4), pp. 1886-94.

Jensch, I., Gámez, G., Rothe, M., Ebert, S., Fulde, M., Somplatzki, D., Bergmann, S., Petruschka, L., Rohde, M., Nau, R. and Hammerschmidt, S. (2010) 'PavB is a surface-exposed adhesin of Streptococcus pneumoniae contributing to nasopharyngeal colonization and airways infections', *Mol Microbiol,* 77(1), pp. 22-43.

Jensen, P., Bjarnsholt, T., Phipps, R., Rasmussen, T. B., Calum, H., Christoffersen, L., Moser, C., Williams, P., Pressler, T., Givskov, M. and Høiby, N. (2007) 'Rapid necrotic killing of polymorphonuclear leukocytes is caused by quorum-sensing-controlled production of rhamnolipid by Pseudomonas aeruginosa', *Microbiology,* 153(Pt 5), pp. 1329-38.

Jesaitis, A. J., Franklin, M. J., Berglund, D., Sasaki, M., Lord, C. I., Bleazard, J. B., Duffy, J. E., Beyenal, H. and Lewandowski, Z. (2003) 'Compromised host defense on Pseudomonas aeruginosa biofilms: characterization of neutrophil and biofilm interactions', *J Immunol,* 171(8), pp. 4329-39.

Johnson, M. B. and Criss, A. K. (2013) 'Fluorescence microscopy methods for determining the viability of bacteria in association with mammalian cells', *J Vis Exp,* (79).

Joyce, E. A., Kawale, A., Censini, S., Kim, C. C., Covacci, A. and Falkow, S. (2004) 'LuxS is required for persistent pneumococcal carriage and expression of virulence and biosynthesis genes', *Infect Immun,* 72(5), pp. 2964-75.

Joyce, E. A., Popper, S. J. and Falkow, S. (2009) 'Streptococcus pneumoniae nasopharyngeal colonization induces type I interferons and interferon-induced gene expression', *BMC Genomics,* 10, pp. 404.

Jurcisek, J. A. and Bakaletz, L. O. (2007) 'Biofilms formed by nontypeable Haemophilus influenzae in vivo contain both double-stranded DNA and type IV pilin protein', *J Bacteriol,* 189(10), pp. 3868-75.

Jönsson, G., Truedsson, L., Sturfelt, G., Oxelius, V. A., Braconier, J. H. and Sjöholm, A. G. (2005) 'Hereditary C2 deficiency in Sweden: frequent occurrence of invasive infection, atherosclerosis, and rheumatic disease', *Medicine (Baltimore),* 84(1), pp. 23-34.

Kadhim, A. L., Spilsbury, K., Semmens, J. B., Coates, H. L. and Lannigan, F. J. (2007) 'Adenoidectomy for middle ear effusion: a study of 50,000 children over 24 years', *Laryngoscope,* 117(3), pp. 427-33.

Kadioglu, A., Taylor, S., Iannelli, F., Pozzi, G., Mitchell, T. J. and Andrew, P. W. (2002) 'Upper and lower respiratory tract infection by Streptococcus pneumoniae is affected by pneumolysin deficiency and differences in capsule type', *Infect Immun,* 70(6), pp. 2886-90.

Kania, R. E., Lamers, G. E., Vonk, M. J., Dorpmans, E., Struik, J., Tran Ba Huy, P., Hiemstra, P., Bloemberg, G. V. and Grote, J. J. (2008) 'Characterization of mucosal biofilms on human adenoid tissues', *Laryngoscope,* 118(1), pp. 128-34.

Karlidağ, T., Demirdağ, K., Kaygusuz, I., Ozden, M., Yalçin, S. and Oztürk, L. (2002) 'Resistant bacteria in the adenoid tissues of children with otitis media with effusion', *Int J Pediatr Otorhinolaryngol,* 64(1), pp. 35-40.

Kaur, R., Casey, J. R. and Pichichero, M. E. (2011) 'Serum antibody response to five Streptococcus pneumoniae proteins during acute otitis media in otitis-prone and non-otitis-prone children', *Pediatr Infect Dis J,* 30(8), pp. 645-50.

Kelly, T., Dillard, J. P. and Yother, J. (1994) 'Effect of genetic switching of capsular type on virulence of Streptococcus pneumoniae', *Infect Immun,* 62(5), pp. 1813-9.

Kilian, M., Mestecky, J. and Schrohenloher, R. E. (1979) 'Pathogenic species of the genus Haemophilus and Streptococcus pneumoniae produce immunoglobulin A1 protease', *Infect Immun,* 26(1), pp. 143-9.

Kim, J. O., Romero-Steiner, S., Sørensen, U. B., Blom, J., Carvalho, M., Barnard, S., Carlone, G. and Weiser, J. N. (1999) 'Relationship between cell surface carbohydrates and intrastrain variation on opsonophagocytosis of Streptococcus pneumoniae', *Infect Immun,* 67(5), pp. 2327-33.

Kim, J. O. and Weiser, J. N. (1998) 'Association of intrastrain phase variation in quantity of capsular polysaccharide and teichoic acid with the virulence of Streptococcus pneumoniae', *J Infect Dis*, 177(2), pp. 368-77.

King, S. J., Hippe, K. R. and Weiser, J. N. (2006) 'Deglycosylation of human glycoconjugates by the sequential activities of exoglycosidases expressed by Streptococcus pneumoniae', *Mol Microbiol*, 59(3), pp. 961-74.

Kohanski, M. A., Dwyer, D. J. and Collins, J. J. (2010) 'How antibiotics kill bacteria: from targets to networks', *Nat Rev Microbiol*, 8(6), pp. 423-35.

Konstan, M. W. and Ratjen, F. (2012) 'Effect of dornase alfa on inflammation and lung function: potential role in the early treatment of cystic fibrosis', *J Cyst Fibros*, 11(2), pp. 78-83.

Kovács, M., Halfmann, A., Fedtke, I., Heintz, M., Peschel, A., Vollmer, W., Hakenbeck, R. and Brückner, R. (2006) 'A functional dlt operon, encoding proteins required for incorporation of d-alanine in teichoic acids in gram-positive bacteria, confers resistance to cationic antimicrobial peptides in Streptococcus pneumoniae', *J Bacteriol*, 188(16), pp. 5797-805.

Kowalko, J. E. and Sebert, M. E. (2008) 'The Streptococcus pneumoniae competence regulatory system influences respiratory tract colonization', *Infect Immun*, 76(7), pp. 3131-40.

Krakauer, T. (2002) 'Stimulant-dependent modulation of cytokines and chemokines by airway epithelial cells: cross talk between pulmonary epithelial and peripheral blood mononuclear cells', *Clin Diagn Lab Immunol*, 9(1), pp. 126-31.

Kristian, S. A., Birkenstock, T. A., Sauder, U., Mack, D., Götz, F. and Landmann, R. (2008) 'Biofilm formation induces C3a release and protects Staphylococcus epidermidis from IgG and complement deposition and from neutrophil-dependent killing', *J Infect Dis*, 197(7), pp. 1028-35.

Kronenberg, A., Zucs, P., Droz, S. and Mühlemann, K. (2006) 'Distribution and invasiveness of Streptococcus pneumoniae serotypes in Switzerland, a country with low antibiotic selection pressure, from 2001 to 2004', *J Clin Microbiol*, 44(6), pp. 2032-8.

Kumar, K. L., Ashok, V., Ganaie, F. and Ramesh, A. C. (2014) 'Nasopharyngeal carriage, antibiogram & serotype distribution of Streptococcus pneumoniae among healthy under five children', *Indian J Med Res*, 140(2), pp. 216-20.

Käyhty, H., Auranen, K., Nohynek, H., Dagan, R. and Mäkelä, H. (2006) 'Nasopharyngeal colonization: a target for pneumococcal vaccination', *Expert Rev Vaccines*, 5(5), pp. 651-67.

Launes, C., de-Sevilla, M. F., Selva, L., Garcia-Garcia, J. J., Pallares, R. and Muñoz-Almagro, C. (2012) 'Viral coinfection in children less than five years old with invasive pneumococcal disease', *Pediatr Infect Dis J*, 31(6), pp. 650-3.

Lebeaux, D., Ghigo, J. M. and Beloin, C. (2014) 'Biofilm-related infections: bridging the gap between clinical management and fundamental aspects of recalcitrance toward antibiotics', *Microbiol Mol Biol Rev*, 78(3), pp. 510-43.

Lee, G. M., Kleinman, K., Pelton, S. I., Hanage, W., Huang, S. S., Lakoma, M., Dutta-Linn, M., Croucher, N. J., Stevenson, A. and Finkelstein, J. A. (2014) 'Impact of 13-Valent Pneumococcal Conjugate Vaccination on Streptococcus pneumoniae Carriage in Young Children in Massachusetts', *J Pediatric Infect Dis Soc*, 3(1), pp. 23-32.

Leid, J. G., Shirtliff, M. E., Costerton, J. W. and Stoodley, P. (2002) 'Human leukocytes adhere to, penetrate, and respond to Staphylococcus aureus biofilms', *Infect Immun*, 70(11), pp. 6339-45.

Leid, J. G., Willson, C. J., Shirtliff, M. E., Hassett, D. J., Parsek, M. R. and Jeffers, A. K. (2005) 'The exopolysaccharide alginate protects Pseudomonas aeruginosa biofilm bacteria from IFN-gamma-mediated macrophage killing', *J Immunol*, 175(11), pp. 7512-8.

Leung, M. H., Oriyo, N. M., Gillespie, S. H. and Charalambous, B. M. (2011) 'The adaptive potential during nasopharyngeal colonisation of Streptococcus pneumoniae', *Infect Genet Evol,* 11(8), pp. 1989-95.

Levy, C., Varon, E., Picard, C., Béchet, S., Martinot, A., Bonacorsi, S. and Cohen, R. (2014) 'Trends of pneumococcal meningitis in children after introduction of the 13-valent pneumococcal conjugate vaccine in France', *Pediatr Infect Dis J,* 33(12), pp. 1216-21.

Lewis, K. (2000) 'Programmed death in bacteria', *Microbiol Mol Biol Rev,* 64(3), pp. 503-14.

Lewis, K. (2001) 'Riddle of biofilm resistance', *Antimicrob Agents Chemother,* 45(4), pp. 999-1007.

Lewis, K. (2008) 'Multidrug tolerance of biofilms and persister cells', *Curr Top Microbiol Immunol,* 322, pp. 107-31.

Lewis, K. (2010) 'Persister cells', *Annu Rev Microbiol,* 64, pp. 357-72.

Li, Q., Li, Y. X., Douthitt, K., Stahl, G. L., Thurman, J. M. and Tong, H. H. (2012) 'Role of the alternative and classical complement activation pathway in complement mediated killing against Streptococcus pneumoniae colony opacity variants during acute pneumococcal otitis media in mice', *Microbes Infect,* 14(14), pp. 1308-18.

Li, Q., Li, Y. X., Stahl, G. L., Thurman, J. M., He, Y. and Tong, H. H. (2011) 'Essential role of factor B of the alternative complement pathway in complement activation and opsonophagocytosis during acute pneumococcal otitis media in mice', *Infect Immun,* 79(7), pp. 2578-85.

Li, Y., Weinberger, D. M., Thompson, C. M., Trzciński, K. and Lipsitch, M. (2013) 'Surface charge of Streptococcus pneumoniae predicts serotype distribution', *Infect Immun,* 81(12), pp. 4519-24.

Lim, W. S., Macfarlane, J. T., Boswell, T. C., Harrison, T. G., Rose, D., Leinonen, M. and Saikku, P. (2001) 'Study of community acquired pneumonia aetiology (SCAPA) in adults admitted to hospital: implications for management guidelines', *Thorax,* 56(4), pp. 296-301.

Lizcano, A., Chin, T., Sauer, K., Tuomanen, E. I. and Orihuela, C. J. (2010) 'Early biofilm formation on microtiter plates is not correlated with the invasive disease potential of Streptococcus pneumoniae', *Microb Pathog,* 48(3-4), pp. 124-30.

Loose, M., Hudel, M., Zimmer, K. P., Garcia, E., Hammerschmidt, S., Lucas, R., Chakraborty, T. and Pillich, H. (2015) 'Pneumococcal hydrogen peroxide-induced stress signaling regulates inflammatory genes', *J Infect Dis,* 211(2), pp. 306-16.

Lu, Y. J., Gross, J., Bogaert, D., Finn, A., Bagrade, L., Zhang, Q., Kolls, J. K., Srivastava, A., Lundgren, A., Forte, S., Thompson, C. M., Harney, K. F., Anderson, P. W., Lipsitch, M. and Malley, R. (2008) 'Interleukin-17A mediates acquired immunity to pneumococcal colonization', *PLoS Pathog,* 4(9), pp. e1000159.

López, R. (2006) 'Pneumococcus: the sugar-coated bacteria', *Int Microbiol,* 9(3), pp. 179-90.

Magee, A. D. and Yother, J. (2001) 'Requirement for capsule in colonization by Streptococcus pneumoniae', *Infect Immun,* 69(6), pp. 3755-61.

Mah, T. F. and O'Toole, G. A. (2001) 'Mechanisms of biofilm resistance to antimicrobial agents', *Trends Microbiol,* 9(1), pp. 34-9.

Malley, R. (2010) 'Antibody and cell-mediated immunity to Streptococcus pneumoniae: implications for vaccine development', *J Mol Med (Berl),* 88(2), pp. 135-42.

Malley, R., Henneke, P., Morse, S. C., Cieslewicz, M. J., Lipsitch, M., Thompson, C. M., Kurt-Jones, E., Paton, J. C., Wessels, M. R. and Golenbock, D. T. (2003) 'Recognition of pneumolysin by Toll-like receptor 4 confers resistance to pneumococcal infection', *Proc Natl Acad Sci U S A,* 100(4), pp. 1966-71.

Malley, R., Trzcinski, K., Srivastava, A., Thompson, C. M., Anderson, P. W. and Lipsitch, M. (2005) 'CD4+ T cells mediate antibody-independent acquired immunity to pneumococcal colonization', *Proc Natl Acad Sci U S A,* 102(13), pp. 4848-53.

Manzenreiter, R., Kienberger, F., Marcos, V., Schilcher, K., Krautgartner, W. D., Obermayer, A., Huml, M., Stoiber, W., Hector, A., Griese, M., Hannig, M., Studnicka, M., Vitkov, L. and Hartl, D. (2012) 'Ultrastructural characterization of cystic fibrosis sputum using atomic force and scanning electron microscopy', *J Cyst Fibros,* 11(2), pp. 84-92.

Marks, L. R., Davidson, B. A., Knight, P. R. and Hakansson, A. P. (2013) 'Interkingdom signaling induces Streptococcus pneumoniae biofilm dispersion and transition from asymptomatic colonization to disease', *MBio,* 4(4).

Marks, L. R., Parameswaran, G. I. and Hakansson, A. P. (2012a) 'Pneumococcal interactions with epithelial cells are crucial for optimal biofilm formation and colonization in vitro and in vivo', *Infect Immun,* 80(8), pp. 2744-60.

Marks, L. R., Reddinger, R. M. and Hakansson, A. P. (2012b) 'High levels of genetic recombination during nasopharyngeal carriage and biofilm formation in Streptococcus pneumoniae', *MBio,* 3(5).

Marriott, H. M., Gascoyne, K. A., Gowda, R., Geary, I., Nicklin, M. J., Iannelli, F., Pozzi, G., Mitchell, T. J., Whyte, M. K., Sabroe, I. and Dockrell, D. H. (2012) 'Interleukin-1β regulates CXCL8 release and influences disease outcome in response to Streptococcus pneumoniae, defining intercellular cooperation between pulmonary epithelial cells and macrophages', *Infect Immun,* 80(3), pp. 1140-9.

McClay, J. E. (2000) 'Resistant bacteria in the adenoids: a preliminary report', *Arch Otolaryngol Head Neck Surg,* 126(5), pp. 625-9.

McCool, T. L., Cate, T. R., Moy, G. and Weiser, J. N. (2002) 'The immune response to pneumococcal proteins during experimental human carriage', *J Exp Med,* 195(3), pp. 359-65.

McCool, T. L. and Weiser, J. N. (2004) 'Limited role of antibody in clearance of Streptococcus pneumoniae in a murine model of colonization', *Infect Immun,* 72(10), pp. 5807-13.

McCoy, W. F., Bryers, J. D., Robbins, J. and Costerton, J. W. (1981) 'Observations of fouling biofilm formation', *Can J Microbiol,* 27(9), pp. 910-7.

McCullers, J. A. (2006) 'Insights into the interaction between influenza virus and pneumococcus', *Clin Microbiol Rev,* 19(3), pp. 571-82.

McCullers, J. A. (2014) 'The co-pathogenesis of influenza viruses with bacteria in the lung', *Nat Rev Microbiol,* 12(4), pp. 252-62.

McCullers, J. A. and Bartmess, K. C. (2003) 'Role of neuraminidase in lethal synergism between influenza virus and Streptococcus pneumoniae', *J Infect Dis,* 187(6), pp. 1000-9.

McGrath, F. D., Brouwer, M. C., Arlaud, G. J., Daha, M. R., Hack, C. E. and Roos, A. (2006) 'Evidence that complement protein C1q interacts with C-reactive protein through its globular head region', *J Immunol,* 176(5), pp. 2950-7.

McLinn, S. and Williams, D. (1996) 'Incidence of antibiotic-resistant Streptococcus pneumoniae and beta-lactamase-positive Haemophilus influenzae in clinical isolates from patients with otitis media', *Pediatr Infect Dis J,* 15(9 Suppl), pp. S3-9.

Medzhitov, R., Preston-Hurlburt, P. and Janeway, C. A. (1997) 'A human homologue of the Drosophila Toll protein signals activation of adaptive immunity', *Nature,* 388(6640), pp. 394-7.

Melegaro, A. and Edmunds, W. J. (2004) 'The 23-valent pneumococcal polysaccharide vaccine. Part II. A cost-effectiveness analysis for invasive disease in the elderly in England and Wales', *Eur J Epidemiol,* 19(4), pp. 365-75.

Melin, M., Trzciński, K., Meri, S., Käyhty, H. and Väkeväinen, M. (2010) 'The capsular serotype of Streptococcus pneumoniae is more important than the genetic background for resistance to complement', *Infect Immun,* 78(12), pp. 5262-70.

Millar, E. V., O'Brien, K. L., Watt, J. P., Bronsdon, M. A., Dallas, J., Whitney, C. G., Reid, R. and Santosham, M. (2006) 'Effect of community-wide conjugate pneumococcal

vaccine use in infancy on nasopharyngeal carriage through 3 years of age: a cross-sectional study in a high-risk population', *Clin Infect Dis,* 43(1), pp. 8-15.

Millar, E. V., Pimenta, F. C., Roundtree, A., Jackson, D., Carvalho, M. a. G., Perilla, M. J., Reid, R., Santosham, M., Whitney, C. G., Beall, B. W. and O'Brien, K. L. (2010) 'Pre- and post-conjugate vaccine epidemiology of pneumococcal serotype 6C invasive disease and carriage within Navajo and White Mountain Apache communities', *Clin Infect Dis,* 51(11), pp. 1258-65.

Millar, M. R., Brown, N. M., Tobin, G. W., Murphy, P. J., Windsor, A. C. and Speller, D. C. (1994) 'Outbreak of infection with penicillin-resistant Streptococcus pneumoniae in a hospital for the elderly', *J Hosp Infect,* 27(2), pp. 99-104.

Miller, E., Andrews, N. J., Waight, P. A., Slack, M. P. and George, R. C. (2011) 'Herd immunity and serotype replacement 4 years after seven-valent pneumococcal conjugate vaccination in England and Wales: an observational cohort study', *Lancet Infect Dis,* 11(10), pp. 760-8.

Mitchell, T. J., Andrew, P. W., Saunders, F. K., Smith, A. N. and Boulnois, G. J. (1991) 'Complement activation and antibody binding by pneumolysin via a region of the toxin homologous to a human acute-phase protein', *Mol Microbiol,* 5(8), pp. 1883-8.

Mitchell, T. J. and Dalziel, C. E. (2014) 'The biology of pneumolysin', *Subcell Biochem,* 80, pp. 145-60.

Mold, C., Rodic-Polic, B. and Du Clos, T. W. (2002) 'Protection from Streptococcus pneumoniae infection by C-reactive protein and natural antibody requires complement but not Fc gamma receptors', *J Immunol,* 168(12), pp. 6375-81.

Monasta, L., Ronfani, L., Marchetti, F., Montico, M., Vecchi Brumatti, L., Bavcar, A., Grasso, D., Barbiero, C. and Tamburlini, G. (2012) 'Burden of disease caused by otitis media: systematic review and global estimates', *PLoS One,* 7(4), pp. e36226.

Montanaro, L., Poggi, A., Visai, L., Ravaioli, S., Campoccia, D., Speziale, P. and Arciola, C. R. (2011) 'Extracellular DNA in biofilms', *Int J Artif Organs,* 34(9), pp. 824-31.

Moreau-Marquis, S., Coutermarsh, B. and Stanton, B. A. (2015) 'Combination of hypothiocyanite and lactoferrin (ALX-109) enhances the ability of tobramycin and aztreonam to eliminate Pseudomonas aeruginosa biofilms growing on cystic fibrosis airway epithelial cells', *J Antimicrob Chemother,* 70(1), pp. 160-6.

Moreau-Marquis, S., Redelman, C. V., Stanton, B. A. and Anderson, G. G. (2010) 'Co-culture models of Pseudomonas aeruginosa biofilms grown on live human airway cells', *J Vis Exp,* (44).

Morris, G. E., Parker, L. C., Ward, J. R., Jones, E. C., Whyte, M. K., Brightling, C. E., Bradding, P., Dower, S. K. and Sabroe, I. (2006) 'Cooperative molecular and cellular networks regulate Toll-like receptor-dependent inflammatory responses', *FASEB J,* 20(12), pp. 2153-5.

Mortier-Barrière, I., de Saizieu, A., Claverys, J. P. and Martin, B. (1998) 'Competence-specific induction of recA is required for full recombination proficiency during transformation in Streptococcus pneumoniae', *Mol Microbiol,* 27(1), pp. 159-70.

Moscoso, M. and Claverys, J. P. (2004) 'Release of DNA into the medium by competent Streptococcus pneumoniae: kinetics, mechanism and stability of the liberated DNA', *Mol Microbiol,* 54(3), pp. 783-94.

Moscoso, M., García, E. and López, R. (2006) 'Biofilm formation by Streptococcus pneumoniae: role of choline, extracellular DNA, and capsular polysaccharide in microbial accretion', *J Bacteriol,* 188(22), pp. 7785-95.

Moscoso, M., García, E. and López, R. (2009) 'Pneumococcal biofilms', *Int Microbiol,* 12(2), pp. 77-85.

Mukerji, R., Mirza, S., Roche, A. M., Widener, R. W., Croney, C. M., Rhee, D. K., Weiser, J. N., Szalai, A. J. and Briles, D. E. (2012) 'Pneumococcal surface protein A inhibits complement deposition on the pneumococcal surface by competing with the binding of C-reactive protein to cell-surface phosphocholine', *J Immunol,* 189(11), pp. 5327-35.

Mulcahy, H., Charron-Mazenod, L. and Lewenza, S. (2008) 'Extracellular DNA chelates cations and induces antibiotic resistance in Pseudomonas aeruginosa biofilms', *PLoS Pathog,* 4(11), pp. e1000213.

Mulcahy, L. R., Burns, J. L., Lory, S. and Lewis, K. (2010) 'Emergence of Pseudomonas aeruginosa strains producing high levels of persister cells in patients with cystic fibrosis', *J Bacteriol,* 192(23), pp. 6191-9.

Murakami, M., Nishi, Y., Seto, K., Kamashita, Y. and Nagaoka, E. (2015) 'Dry mouth and denture plaque microflora in complete denture and palatal obturator prosthesis wearers', *Gerodontology,* 32(3), pp. 188-94.

Musher, D. M. (1992) 'Infections caused by Streptococcus pneumoniae: clinical spectrum, pathogenesis, immunity, and treatment', *Clin Infect Dis,* 14(4), pp. 801-7.

Muñoz-Almagro, C., Jordan, I., Gene, A., Latorre, C., Garcia-Garcia, J. J. and Pallares, R. (2008) 'Emergence of invasive pneumococcal disease caused by nonvaccine serotypes in the era of 7-valent conjugate vaccine', *Clin Infect Dis,* 46(2), pp. 174-82.

Muñoz-Elías, E. J., Marcano, J. and Camilli, A. (2008) 'Isolation of Streptococcus pneumoniae biofilm mutants and their characterization during nasopharyngeal colonization', *Infect Immun,* 76(11), pp. 5049-61.

Nakamura, S., Davis, K. M. and Weiser, J. N. (2011) 'Synergistic stimulation of type I interferons during influenza virus coinfection promotes Streptococcus pneumoniae colonization in mice', *J Clin Invest,* 121(9), pp. 3657-65.

Nash, J. A., Ballard, T. N., Weaver, T. E. and Akinbi, H. T. (2006) 'The peptidoglycan-degrading property of lysozyme is not required for bactericidal activity in vivo', *J Immunol,* 177(1), pp. 519-26.

Nasrin, D., Collignon, P. J., Roberts, L., Wilson, E. J., Pilotto, L. S. and Douglas, R. M. (2002) 'Effect of beta lactam antibiotic use in children on pneumococcal resistance to penicillin: prospective cohort study', *BMJ,* 324(7328), pp. 28-30.

Nelson, A. L., Roche, A. M., Gould, J. M., Chim, K., Ratner, A. J. and Weiser, J. N. (2007) 'Capsule enhances pneumococcal colonization by limiting mucus-mediated clearance', *Infect Immun,* 75(1), pp. 83-90.

Nguyen, D., Joshi-Datar, A., Lepine, F., Bauerle, E., Olakanmi, O., Beer, K., McKay, G., Siehnel, R., Schafhauser, J., Wang, Y., Britigan, B. E. and Singh, P. K. (2011) 'Active starvation responses mediate antibiotic tolerance in biofilms and nutrient-limited bacteria', *Science,* 334(6058), pp. 982-6.

Nieto, C. and Espinosa, M. (2003) 'Construction of the mobilizable plasmid pMV158GFP, a derivative of pMV158 that carries the gene encoding the green fluorescent protein', *Plasmid,* 49(3), pp. 281-5.

Nistico, L., Kreft, R., Gieseke, A., Coticchia, J. M., Burrows, A., Khampang, P., Liu, Y., Kerschner, J. E., Post, J. C., Lonergan, S., Sampath, R., Hu, F. Z., Ehrlich, G. D., Stoodley, P. and Hall-Stoodley, L. (2011) 'Adenoid reservoir for pathogenic biofilm bacteria', *J Clin Microbiol,* 49(4), pp. 1411-20.

Nokso-Koivisto, J., Marom, T. and Chonmaitree, T. (2015) 'Importance of viruses in acute otitis media', *Curr Opin Pediatr,* 27(1), pp. 110-5.

O'Brien, K. L., Millar, E. V., Zell, E. R., Bronsdon, M., Weatherholtz, R., Reid, R., Becenti, J., Kvamme, S., Whitney, C. G. and Santosham, M. (2007) 'Effect of pneumococcal conjugate vaccine on nasopharyngeal colonization among immunized and unimmunized children in a community-randomized trial', *J Infect Dis,* 196(8), pp. 1211-20.

O'Brien, K. L., Wolfson, L. J., Watt, J. P., Henkle, E., Deloria-Knoll, M., McCall, N., Lee, E., Mulholland, K., Levine, O. S., Cherian, T. and Team, H. a. P. G. B. o. D. S. (2009) 'Burden of disease caused by Streptococcus pneumoniae in children younger than 5 years: global estimates', *Lancet,* 374(9693), pp. 893-902.

O'Toole, G., Kaplan, H. B. and Kolter, R. (2000) 'Biofilm formation as microbial development', *Annu Rev Microbiol,* 54, pp. 49-79.

Ochoa-Gondar, O., Figuerola-Massana, E., Vila-Corcoles, A., Aguirre, C. A., de Diego, C., Satue, E., Gomez, F., Raga, X. and Group, E. S. (2015) 'Epidemiology of Streptococcus pneumoniae causing acute otitis media among children in Southern Catalonia throughout 2007-2013: Incidence, serotype distribution and vaccine's effectiveness', *Int J Pediatr Otorhinolaryngol,* 79(12), pp. 2104-8.

Oggioni, M. R., Trappetti, C., Kadioglu, A., Cassone, M., Iannelli, F., Ricci, S., Andrew, P. W. and Pozzi, G. (2006) 'Switch from planktonic to sessile life: a major event in pneumococcal pathogenesis', *Mol Microbiol,* 61(5), pp. 1196-210.

Okshevsky, M., Regina, V. R. and Meyer, R. L. (2015) 'Extracellular DNA as a target for biofilm control', *Curr Opin Biotechnol,* 33, pp. 73-80.

Orihuela, C. J., Gao, G., Francis, K. P., Yu, J. and Tuomanen, E. I. (2004) 'Tissue-specific contributions of pneumococcal virulence factors to pathogenesis', *J Infect Dis,* 190(9), pp. 1661-9.

Pagella, F., Colombo, A., Gatti, O., Giourgos, G. and Matti, E. (2010) 'Rhinosinusitis and otitis media: the link with adenoids', *Int J Immunopathol Pharmacol,* 23(1 Suppl), pp. 38-40.

Pai, R., Moore, M. R., Pilishvili, T., Gertz, R. E., Whitney, C. G., Beall, B. and Team, A. B. C. S. (2005) 'Postvaccine genetic structure of Streptococcus pneumoniae serotype 19A from children in the United States', *J Infect Dis,* 192(11), pp. 1988-95.

Paradise, J. L., Bluestone, C. D., Rogers, K. D., Taylor, F. H., Colborn, D. K., Bachman, R. Z., Bernard, B. S. and Schwarzbach, R. H. (1990) 'Efficacy of adenoidectomy for recurrent otitis media in children previously treated with tympanostomy-tube placement. Results of parallel randomized and nonrandomized trials', *JAMA,* 263(15), pp. 2066-73.

Parker, D., Martin, F. J., Soong, G., Harfenist, B. S., Aguilar, J. L., Ratner, A. J., Fitzgerald, K. A., Schindler, C. and Prince, A. (2011) 'Streptococcus pneumoniae DNA initiates type I interferon signaling in the respiratory tract', *MBio,* 2(3), pp. e00016-11.

Parker, D., Soong, G., Planet, P., Brower, J., Ratner, A. J. and Prince, A. (2009) 'The NanA neuraminidase of Streptococcus pneumoniae is involved in biofilm formation', *Infect Immun,* 77(9), pp. 3722-30.

Parsek, M. R. and Singh, P. K. (2003) 'Bacterial biofilms: an emerging link to disease pathogenesis', *Annu Rev Microbiol,* 57, pp. 677-701.

Paton, J. C. and Ferrante, A. (1983) 'Inhibition of human polymorphonuclear leukocyte respiratory burst, bactericidal activity, and migration by pneumolysin', *Infect Immun,* 41(3), pp. 1212-6.

Paton, J. C., Rowan-Kelly, B. and Ferrante, A. (1984) 'Activation of human complement by the pneumococcal toxin pneumolysin', *Infect Immun,* 43(3), pp. 1085-7.

Pearson, M. M., Laurence, C. A., Guinn, S. E. and Hansen, E. J. (2006) 'Biofilm formation by Moraxella catarrhalis in vitro: roles of the UspA1 adhesin and the Hag hemagglutinin', *Infect Immun,* 74(3), pp. 1588-96.

Peltola, V., Heikkinen, T., Ruuskanen, O., Jartti, T., Hovi, T., Kilpi, T. and Vainionpää, R. (2011) 'Temporal association between rhinovirus circulation in the community and invasive pneumococcal disease in children', *Pediatr Infect Dis J,* 30(6), pp. 456-61.

Percival, S. L., Hill, K. E., Williams, D. W., Hooper, S. J., Thomas, D. W. and Costerton, J. W. (2012) 'A review of the scientific evidence for biofilms in wounds', *Wound Repair Regen,* 20(5), pp. 647-57.

Perez, A. C., Pang, B., King, L. B., Tan, L., Murrah, K. A., Reimche, J. L., Wren, J. T., Richardson, S. H., Ghandi, U. and Swords, W. E. (2014) 'Residence of Streptococcus pneumoniae and Moraxella catarrhalis within polymicrobial biofilm promotes antibiotic resistance and bacterial persistence in vivo', *Pathog Dis,* 70(3), pp. 280-8.

Pericone, C. D., Overweg, K., Hermans, P. W. and Weiser, J. N. (2000) 'Inhibitory and bactericidal effects of hydrogen peroxide production by Streptococcus pneumoniae on other inhabitants of the upper respiratory tract', *Infect Immun,* 68(7), pp. 3990-7.

Pettigrew, M. M., Gent, J. F., Pyles, R. B., Miller, A. L., Nokso-Koivisto, J. and Chonmaitree, T. (2011) 'Viral-bacterial interactions and risk of acute otitis media complicating upper respiratory tract infection', *J Clin Microbiol,* 49(11), pp. 3750-5.

Pettigrew, M. M., Marks, L. R., Kong, Y., Gent, J. F., Roche-Hakansson, H. and Hakansson, A. P. (2014) 'Dynamic changes in the Streptococcus pneumoniae transcriptome during transition from biofilm formation to invasive disease upon influenza A virus infection', *Infect Immun,* 82(11), pp. 4607-19.

Pichichero, M. E. (2000) 'Recurrent and persistent otitis media', *Pediatr Infect Dis J,* 19(9), pp. 911-6.

Pilishvili, T., Lexau, C., Farley, M. M., Hadler, J., Harrison, L. H., Bennett, N. M., Reingold, A., Thomas, A., Schaffner, W., Craig, A. S., Smith, P. J., Beall, B. W., Whitney, C. G., Moore, M. R. and Network, A. B. C. S. E. I. P. (2010a) 'Sustained reductions in invasive pneumococcal disease in the era of conjugate vaccine', *J Infect Dis,* 201(1), pp. 32-41.

Pilishvili, T., Zell, E. R., Farley, M. M., Schaffner, W., Lynfield, R., Nyquist, A. C., Vazquez, M., Bennett, N. M., Reingold, A., Thomas, A., Jackson, D., Schuchat, A. and Whitney, C. G. (2010b) 'Risk factors for invasive pneumococcal disease in children in the era of conjugate vaccine use', *Pediatrics,* 126(1), pp. e9-17.

Pittet, L. A., Hall-Stoodley, L., Rutkowski, M. R. and Harmsen, A. G. (2010) 'Influenza virus infection decreases tracheal mucociliary velocity and clearance of Streptococcus pneumoniae', *Am J Respir Cell Mol Biol,* 42(4), pp. 450-60.

Plasschaert, A. I., Rovers, M. M., Schilder, A. G., Verheij, T. J. and Hak, E. (2006) 'Trends in doctor consultations, antibiotic prescription, and specialist referrals for otitis media in children: 1995-2003', *Pediatrics,* 117(6), pp. 1879-86.

Pompilio, A., Crocetta, V., Confalone, P., Nicoletti, M., Petrucca, A., Guarnieri, S., Fiscarelli, E., Savini, V., Piccolomini, R. and Di Bonaventura, G. (2010) 'Adhesion to and biofilm formation on IB3-1 bronchial cells by Stenotrophomonas maltophilia isolates from cystic fibrosis patients', *BMC Microbiol,* 10, pp. 102.

Porat, N., Arguedas, A., Spratt, B. G., Trefler, R., Brilla, E., Loaiza, C., Godoy, D., Bilek, N. and Dagan, R. (2004) 'Emergence of penicillin-nonsusceptible Streptococcus pneumoniae clones expressing serotypes not present in the antipneumococcal conjugate vaccine', *J Infect Dis,* 190(12), pp. 2154-61.

Post, J. C., Aul, J. J., White, G. J., Wadowsky, R. M., Zavoral, T., Tabari, R., Kerber, B., Doyle, W. J. and Ehrlich, G. D. (1996a) 'PCR-based detection of bacterial DNA after antimicrobial treatment is indicative of persistent, viable bacteria in the chinchilla model of otitis media', *Am J Otolaryngol,* 17(2), pp. 106-11.

Post, J. C., Hiller, N. L., Nistico, L., Stoodley, P. and Ehrlich, G. D. (2007) 'The role of biofilms in otolaryngologic infections: update 2007', *Curr Opin Otolaryngol Head Neck Surg,* 15(5), pp. 347-51.

Post, J. C., Preston, R. A., Aul, J. J., Larkins-Pettigrew, M., Rydquist-White, J., Anderson, K. W., Wadowsky, R. M., Reagan, D. R., Walker, E. S., Kingsley, L. A., Magit, A. E. and Ehrlich, G. D. (1995) 'Molecular analysis of bacterial pathogens in otitis media with effusion', *JAMA,* 273(20), pp. 1598-604.

Post, J. C., White, G. J., Aul, J. J., Zavoral, T., Wadowsky, R. M., Zhang, Y., Preston, R. A. and Ehrlich, G. D. (1996b) 'Development and Validation of a Multiplex PCR-Based Assay for the Upper Respiratory Tract Bacterial Pathogens Haemophilus influenzae, Streptococcus pneumoniae, and Moraxella catarrhalis', *Mol Diagn,* 1(1), pp. 29-39.

Potera, C. (1999) 'Forging a link between biofilms and disease', *Science,* 283(5409), pp. 1837, 1839.

Pracht, D., Elm, C., Gerber, J., Bergmann, S., Rohde, M., Seiler, M., Kim, K. S., Jenkinson, H. F., Nau, R. and Hammerschmidt, S. (2005) 'PavA of Streptococcus pneumoniae modulates adherence, invasion, and meningeal inflammation', *Infect Immun,* 73(5), pp. 2680-9.

Principi, N., Marchisio, P., Schito, G. C. and Mannelli, S. (1999) 'Risk factors for carriage of respiratory pathogens in the nasopharynx of healthy children. Ascanius Project Collaborative Group', *Pediatr Infect Dis J,* 18(6), pp. 517-23.

Qin, L., Kida, Y., Imamura, Y., Kuwano, K. and Watanabe, H. (2013) 'Impaired capsular polysaccharide is relevant to enhanced biofilm formation and lower virulence in Streptococcus pneumoniae', *J Infect Chemother,* 19(2), pp. 261-71.

Qin, Z., Ou, Y., Yang, L., Zhu, Y., Tolker-Nielsen, T., Molin, S. and Qu, D. (2007) 'Role of autolysin-mediated DNA release in biofilm formation of Staphylococcus epidermidis', *Microbiology,* 153(Pt 7), pp. 2083-92.

Quin, L. R., Carmicle, S., Dave, S., Pangburn, M. K., Evenhuis, J. P. and McDaniel, L. S. (2005) 'In vivo binding of complement regulator factor H by Streptococcus pneumoniae', *J Infect Dis,* 192(11), pp. 1996-2003.

Raffel, F. K., Szelestey, B. R., Beatty, W. L. and Mason, K. M. (2013) 'The Haemophilus influenzae Sap transporter mediates bacterium-epithelial cell homeostasis', *Infect Immun,* 81(1), pp. 43-54.

Ramos-Sevillano, E., Urzainqui, A., Campuzano, S., Moscoso, M., González-Camacho, F., Domenech, M., Rodríguez de Córdoba, S., Sánchez-Madrid, F., Brown, J. S., García, E. and Yuste, J. (2015) 'Pleiotropic effects of cell wall amidase LytA on Streptococcus pneumoniae sensitivity to the host immune response', *Infect Immun,* 83(2), pp. 591-603.

Rani, S. A., Pitts, B., Beyenal, H., Veluchamy, R. A., Lewandowski, Z., Davison, W. M., Buckingham-Meyer, K. and Stewart, P. S. (2007) 'Spatial patterns of DNA replication, protein synthesis, and oxygen concentration within bacterial biofilms reveal diverse physiological states', *J Bacteriol,* 189(11), pp. 4223-33.

Ravin, A. W. (1959) 'Reciprocal capsular transformations of pneumococci', *J Bacteriol,* 77(3), pp. 296-309.

Rayner, M. G., Zhang, Y., Gorry, M. C., Chen, Y., Post, J. C. and Ehrlich, G. D. (1998) 'Evidence of bacterial metabolic activity in culture-negative otitis media with effusion', *JAMA,* 279(4), pp. 296-9.

Redelman, C. V., Chakravarty, S. and Anderson, G. G. (2014) 'Antibiotic treatment of Pseudomonas aeruginosa biofilms stimulates expression of the magnesium transporter gene mgtE', *Microbiology,* 160(Pt 1), pp. 165-78.

Reid, S. D., Hong, W., Dew, K. E., Winn, D. R., Pang, B., Watt, J., Glover, D. T., Hollingshead, S. K. and Swords, W. E. (2009) 'Streptococcus pneumoniae forms surface-attached communities in the middle ear of experimentally infected chinchillas', *J Infect Dis,* 199(6), pp. 786-94.

Ren, B., Li, J., Genschmer, K., Hollingshead, S. K. and Briles, D. E. (2012a) 'The absence of PspA or presence of antibody to PspA facilitates the complement-dependent phagocytosis of pneumococci in vitro', *Clin Vaccine Immunol,* 19(10), pp. 1574-82.

Ren, D., Nelson, K. L., Uchakin, P. N., Smith, A. L., Gu, X. X. and Daines, D. A. (2012b) 'Characterization of extended co-culture of non-typeable Haemophilus influenzae with primary human respiratory tissues', *Exp Biol Med (Maywood),* 237(5), pp. 540-7.

Rice, K. C., Mann, E. E., Endres, J. L., Weiss, E. C., Cassat, J. E., Smeltzer, M. S. and Bayles, K. W. (2007) 'The cidA murein hydrolase regulator contributes to DNA release and biofilm development in Staphylococcus aureus', *Proc Natl Acad Sci U S A,* 104(19), pp. 8113-8.

Richards, L., Ferreira, D. M., Miyaji, E. N., Andrew, P. W. and Kadioglu, A. (2010) 'The immunising effect of pneumococcal nasopharyngeal colonisation; protection

against future colonisation and fatal invasive disease', *Immunobiology,* 215(4), pp. 251-63.

Richter, S. S., Heilmann, K. P., Dohrn, C. L., Riahi, F., Diekema, D. J. and Doern, G. V. (2013) 'Pneumococcal serotypes before and after introduction of conjugate vaccines, United States, 1999-2011(1.)', *Emerg Infect Dis,* 19(7), pp. 1074-83.

Ritchie, N. D., Mitchell, T. J. and Evans, T. J. (2012) 'What is different about serotype 1 pneumococci?', *Future Microbiol,* 7(1), pp. 33-46.

Rivera-Olivero, I. A., del Nogal, B., Sisco, M. C., Bogaert, D., Hermans, P. W. and de Waard, J. H. (2011) 'Carriage and invasive isolates of Streptococcus pneumoniae in Caracas, Venezuela: the relative invasiveness of serotypes and vaccine coverage', *Eur J Clin Microbiol Infect Dis,* 30(12), pp. 1489-95.

Robbins, J. B., Austrian, R., Lee, C. J., Rastogi, S. C., Schiffman, G., Henrichsen, J., Mäkelä, P. H., Broome, C. V., Facklam, R. R. and Tiesjema, R. H. (1983) 'Considerations for formulating the second-generation pneumococcal capsular polysaccharide vaccine with emphasis on the cross-reactive types within groups', *J Infect Dis,* 148(6), pp. 1136-59.

Roche, A. M., Richard, A. L., Rahkola, J. T., Janoff, E. N. and Weiser, J. N. (2015) 'Antibody blocks acquisition of bacterial colonization through agglutination', *Mucosal Immunol,* 8(1), pp. 176-85.

Rodgers, G. L., Arguedas, A., Cohen, R. and Dagan, R. (2009) 'Global serotype distribution among Streptococcus pneumoniae isolates causing otitis media in children: potential implications for pneumococcal conjugate vaccines', *Vaccine,* 27(29), pp. 3802-10.

Rosenow, C., Ryan, P., Weiser, J. N., Johnson, S., Fontan, P., Ortqvist, A. and Masure, H. R. (1997) 'Contribution of novel choline-binding proteins to adherence, colonization and immunogenicity of Streptococcus pneumoniae', *Mol Microbiol,* 25(5), pp. 819-29.

Rubin, L. G. (2000) 'Pneumococcal vaccine', *Pediatr Clin North Am,* 47(2), pp. 269-85, v.

Rubins, J. B. and Janoff, E. N. (1998) 'Pneumolysin: a multifunctional pneumococcal virulence factor', *J Lab Clin Med,* 131(1), pp. 21-7.

Rupprecht, T. A., Angele, B., Klein, M., Heesemann, J., Pfister, H. W., Botto, M. and Koedel, U. (2007) 'Complement C1q and C3 are critical for the innate immune response to Streptococcus pneumoniae in the central nervous system', *J Immunol,* 178(3), pp. 1861-9.

Römling, U. and Balsalobre, C. (2012) 'Biofilm infections, their resilience to therapy and innovative treatment strategies', *J Intern Med,* 272(6), pp. 541-61.

Saafan, M. E., Ibrahim, W. S. and Tomoum, M. O. (2013) 'Role of adenoid biofilm in chronic otitis media with effusion in children', *Eur Arch Otorhinolaryngol,* 270(9), pp. 2417-25.

Sanchez, C. J., Hurtgen, B. J., Lizcano, A., Shivshankar, P., Cole, G. T. and Orihuela, C. J. (2011a) 'Biofilm and planktonic pneumococci demonstrate disparate immunoreactivity to human convalescent sera', *BMC Microbiol,* 11, pp. 245.

Sanchez, C. J., Kumar, N., Lizcano, A., Shivshankar, P., Dunning Hotopp, J. C., Jorgensen, J. H., Tettelin, H. and Orihuela, C. J. (2011b) 'Streptococcus pneumoniae in biofilms are unable to cause invasive disease due to altered virulence determinant production', *PLoS One,* 6(12), pp. e28738.

Sanchez, C. J., Shivshankar, P., Stol, K., Trakhtenbroit, S., Sullam, P. M., Sauer, K., Hermans, P. W. and Orihuela, C. J. (2010) 'The pneumococcal serine-rich repeat protein is an intra-species bacterial adhesin that promotes bacterial aggregation in vivo and in biofilms', *PLoS Pathog,* 6(8), pp. e1001044.

Sanderson, A. R., Leid, J. G. and Hunsaker, D. (2006) 'Bacterial biofilms on the sinus mucosa of human subjects with chronic rhinosinusitis', *Laryngoscope,* 116(7), pp. 1121-6.

Sandgren, A., Sjostrom, K., Olsson-Liljequist, B., Christensson, B., Samuelsson, A., Kronvall, G. and Henriques Normark, B. (2004) 'Effect of clonal and serotype-specific properties on the invasive capacity of Streptococcus pneumoniae', *J Infect Dis,* 189(5), pp. 785-96.

Santos, A. P., Watanabe, E. and Andrade, D. (2011) 'Biofilm on artificial pacemaker: fiction or reality?', *Arq Bras Cardiol,* 97(5), pp. e113-20.

Saylam, G., Tatar, E. C., Tatar, I., Ozdek, A. and Korkmaz, H. (2010) 'Association of adenoid surface biofilm formation and chronic otitis media with effusion', *Arch Otolaryngol Head Neck Surg,* 136(6), pp. 550-5.

Schauder, S., Shokat, K., Surette, M. G. and Bassler, B. L. (2001) 'The LuxS family of bacterial autoinducers: biosynthesis of a novel quorum-sensing signal molecule', *Mol Microbiol,* 41(2), pp. 463-76.

Scherr, T. D., Hanke, M. L., Huang, O., James, D. B., Horswill, A. R., Bayles, K. W., Fey, P. D., Torres, V. J. and Kielian, T. (2015) 'Staphylococcus aureus Biofilms Induce Macrophage Dysfunction Through Leukocidin AB and Alpha-Toxin', *MBio,* 6(4).

Scherr, T. D., Heim, C. E., Morrison, J. M. and Kielian, T. (2014) 'Hiding in Plain Sight: Interplay between Staphylococcal Biofilms and Host Immunity', *Front Immunol,* 5, pp. 37.

Schommer, N. N., Christner, M., Hentschke, M., Ruckdeschel, K., Aepfelbacher, M. and Rohde, H. (2011) 'Staphylococcus epidermidis uses distinct mechanisms of biofilm formation to interfere with phagocytosis and activation of mouse macrophage-like cells 774A.1', *Infect Immun,* 79(6), pp. 2267-76.

Scott, J. R., Millar, E. V., Lipsitch, M., Moulton, L. H., Weatherholtz, R., Perilla, M. J., Jackson, D. M., Beall, B., Craig, M. J., Reid, R., Santosham, M. and O'Brien, K. L. (2012) 'Impact of more than a decade of pneumococcal conjugate vaccine use on carriage and invasive potential in Native American communities', *J Infect Dis,* 205(2), pp. 280-8.

Shah, D., Zhang, Z., Khodursky, A., Kaldalu, N., Kurg, K. and Lewis, K. (2006) 'Persisters: a distinct physiological state of E. coli', *BMC Microbiol,* 6, pp. 53.

Shainheit, M. G., Mulé, M. and Camilli, A. (2014) 'The core promoter of the capsule operon of Streptococcus pneumoniae is necessary for colonization and invasive disease', *Infect Immun,* 82(2), pp. 694-705.

Shak, J. R., Ludewick, H. P., Howery, K. E., Sakai, F., Yi, H., Harvey, R. M., Paton, J. C., Klugman, K. P. and Vidal, J. E. (2013a) 'Novel role for the Streptococcus pneumoniae toxin pneumolysin in the assembly of biofilms', *MBio,* 4(5), pp. e00655-13.

Shak, J. R., Vidal, J. E. and Klugman, K. P. (2013b) 'Influence of bacterial interactions on pneumococcal colonization of the nasopharynx', *Trends Microbiol,* 21(3), pp. 129-35.

Sharma, S. K., Casey, J. R. and Pichichero, M. E. (2012) 'Reduced serum IgG responses to pneumococcal antigens in otitis-prone children may be due to poor memory B-cell generation', *J Infect Dis,* 205(8), pp. 1225-9.

Shenoy, A. T. and Orihuela, C. J. (2016) 'Anatomical site-specific contributions of pneumococcal virulence determinants', *Pneumonia (Nathan),* 8.

Shimada, J., Moon, S. K., Lee, H. Y., Takeshita, T., Pan, H., Woo, J. I., Gellibolian, R., Yamanaka, N. and Lim, D. J. (2008) 'Lysozyme M deficiency leads to an increased susceptibility to Streptococcus pneumoniae-induced otitis media', *BMC Infect Dis,* 8, pp. 134.

Short, K. R., Reading, P. C., Brown, L. E., Pedersen, J., Gilbertson, B., Job, E. R., Edenborough, K. M., Habets, M. N., Zomer, A., Hermans, P. W., Diavatopoulos, D. A. and Wijburg, O. L. (2013) 'Influenza-induced inflammation drives pneumococcal otitis media', *Infect Immun,* 81(3), pp. 645-52.

Shouval, D. S., Greenberg, D., Givon-Lavi, N., Porat, N. and Dagan, R. (2006) 'Site-specific disease potential of individual Streptococcus pneumoniae serotypes in

pediatric invasive disease, acute otitis media and acute conjunctivitis', *Pediatr Infect Dis J*, 25(7), pp. 602-7.

Shrestha, S., Foxman, B., Weinberger, D. M., Steiner, C., Viboud, C. and Rohani, P. (2013) 'Identifying the interaction between influenza and pneumococcal pneumonia using incidence data', *Sci Transl Med*, 5(191), pp. 191ra84.

Siegel, S. J., Roche, A. M. and Weiser, J. N. (2014) 'Influenza promotes pneumococcal growth during coinfection by providing host sialylated substrates as a nutrient source', *Cell Host Microbe*, 16(1), pp. 55-67.

Simell, B., Auranen, K., Käyhty, H., Goldblatt, D., Dagan, R., O'Brien, K. L. and Group, P. C. (2012) 'The fundamental link between pneumococcal carriage and disease', *Expert Rev Vaccines*, 11(7), pp. 841-55.

Singh, R., Ray, P., Das, A. and Sharma, M. (2009) 'Role of persisters and small-colony variants in antibiotic resistance of planktonic and biofilm-associated Staphylococcus aureus: an in vitro study', *J Med Microbiol*, 58(Pt 8), pp. 1067-73.

Sjöström, K., Spindler, C., Ortqvist, A., Kalin, M., Sandgren, A., Kühlmann-Berenzon, S. and Henriques-Normark, B. (2006) 'Clonal and capsular types decide whether pneumococci will act as a primary or opportunistic pathogen', *Clin Infect Dis*, 42(4), pp. 451-9.

Sleeman, K. L., Griffiths, D., Shackley, F., Diggle, L., Gupta, S., Maiden, M. C., Moxon, E. R., Crook, D. W. and Peto, T. E. (2006) 'Capsular serotype-specific attack rates and duration of carriage of Streptococcus pneumoniae in a population of children', *J Infect Dis*, 194(5), pp. 682-8.

Smith, C. M., Fadaee-Shohada, M. J., Sawhney, R., Baker, N., Williams, G., Hirst, R. A., Andrew, P. W. and O'Callaghan, C. (2013) 'Ciliated cultures from patients with primary ciliary dyskinesia do not produce nitric oxide or inducible nitric oxide synthase during early infection', *Chest*, 144(5), pp. 1671-1676.

Song, Z., Borgwardt, L., Høiby, N., Wu, H., Sørensen, T. S. and Borgwardt, A. (2013) 'Prosthesis infections after orthopedic joint replacement: the possible role of bacterial biofilms', *Orthop Rev (Pavia)*, 5(2), pp. 65-71.

Spiliopoulou, A. I., Kolonitsiou, F., Krevvata, M. I., Leontsinidis, M., Wilkinson, T. S., Mack, D. and Anastassiou, E. D. (2012) 'Bacterial adhesion, intracellular survival and cytokine induction upon stimulation of mononuclear cells with planktonic or biofilm phase Staphylococcus epidermidis', *FEMS Microbiol Lett*, 330(1), pp. 56-65.

Spoering, A. L. and Lewis, K. (2001) 'Biofilms and planktonic cells of Pseudomonas aeruginosa have similar resistance to killing by antimicrobials', *J Bacteriol*, 183(23), pp. 6746-51.

Starner, T. D., Zhang, N., Kim, G., Apicella, M. A. and McCray, P. B. (2006) 'Haemophilus influenzae forms biofilms on airway epithelia: implications in cystic fibrosis', *Am J Respir Crit Care Med*, 174(2), pp. 213-20.

Steinmoen, H., Knutsen, E. and Håvarstein, L. S. (2002) 'Induction of natural competence in Streptococcus pneumoniae triggers lysis and DNA release from a subfraction of the cell population', *Proc Natl Acad Sci U S A*, 99(11), pp. 7681-6.

Stewart, P. S. and Costerton, J. W. (2001) 'Antibiotic resistance of bacteria in biofilms', *Lancet*, 358(9276), pp. 135-8.

Stewart, P. S. and Franklin, M. J. (2008) 'Physiological heterogeneity in biofilms', *Nat Rev Microbiol*, 6(3), pp. 199-210.

Stone, G., Wood, P., Dixon, L., Keyhan, M. and Matin, A. (2002) 'Tetracycline rapidly reaches all the constituent cells of uropathogenic Escherichia coli biofilms', *Antimicrob Agents Chemother*, 46(8), pp. 2458-61.

Stoodley, P., Debeer, D. and Lewandowski, Z. (1994) 'Liquid flow in biofilm systems', *Appl Environ Microbiol*, 60(8), pp. 2711-6.

Stroeher, U. H., Paton, A. W., Ogunniyi, A. D. and Paton, J. C. (2003) 'Mutation of luxS of Streptococcus pneumoniae affects virulence in a mouse model', *Infect Immun*, 71(6), pp. 3206-12.

Sun, K. and Metzger, D. W. (2008) 'Inhibition of pulmonary antibacterial defense by interferon-gamma during recovery from influenza infection', *Nat Med*, 14(5), pp. 558-64.

Sá-Leão, R., Nunes, S., Brito-Avô, A., Frazão, N., Simões, A. S., Crisóstomo, M. I., Paulo, A. C., Saldanha, J., Santos-Sanches, I. and de Lencastre, H. (2009) 'Changes in pneumococcal serotypes and antibiotypes carried by vaccinated and unvaccinated day-care centre attendees in Portugal, a country with widespread use of the seven-valent pneumococcal conjugate vaccine', *Clin Microbiol Infect*, 15(11), pp. 1002-7.

Sá-Leão, R., Pinto, F., Aguiar, S., Nunes, S., Carriço, J. A., Frazão, N., Gonçalves-Sousa, N., Melo-Cristino, J., de Lencastre, H. and Ramirez, M. (2011) 'Analysis of invasiveness of pneumococcal serotypes and clones circulating in Portugal before widespread use of conjugate vaccines reveals heterogeneous behavior of clones expressing the same serotype', *J Clin Microbiol*, 49(4), pp. 1369-75.

Tapiainen, T., Kujala, T., Kaijalainen, T., Ikäheimo, I., Saukkoriipi, A., Renko, M., Salo, J., Leinonen, M. and Uhari, M. (2010) 'Biofilm formation by Streptococcus pneumoniae isolates from paediatric patients', *APMIS*, 118(4), pp. 255-60.

Tawfik, S. A., Ibrahim, A. A., Talaat, I. M., El-Alkamy, S. S. and Youssef, A. (2016) 'Role of bacterial biofilm in development of middle ear effusion', *Eur Arch Otorhinolaryngol*, 273(11), pp. 4003-4009.

Taylor, S., Marchisio, P., Vergison, A., Harriague, J., Hausdorff, W. P. and Haggard, M. (2012) 'Impact of pneumococcal conjugate vaccination on otitis media: a systematic review', *Clin Infect Dis*, 54(12), pp. 1765-73.

Temime, L., Boëlle, P. Y., Valleron, A. J. and Guillemot, D. (2005) 'Penicillin-resistant pneumococcal meningitis: high antibiotic exposure impedes new vaccine protection', *Epidemiol Infect*, 133(3), pp. 493-501.

Thornton, R. B., Rigby, P. J., Wiertsema, S. P., Filion, P., Langlands, J., Coates, H. L., Vijayasekaran, S., Keil, A. D. and Richmond, P. C. (2011) 'Multi-species bacterial biofilm and intracellular infection in otitis media', *BMC Pediatr*, 11, pp. 94.

Thornton, R. B., Wiertsema, S. P., Kirkham, L. A., Rigby, P. J., Vijayasekaran, S., Coates, H. L. and Richmond, P. C. (2013) 'Neutrophil extracellular traps and bacterial biofilms in middle ear effusion of children with recurrent acute otitis media--a potential treatment target', *PLoS One*, 8(2), pp. e53837.

Thurlow, L. R., Hanke, M. L., Fritz, T., Angle, A., Aldrich, A., Williams, S. H., Engebretsen, I. L., Bayles, K. W., Horswill, A. R. and Kielian, T. (2011) 'Staphylococcus aureus biofilms prevent macrophage phagocytosis and attenuate inflammation in vivo', *J Immunol*, 186(11), pp. 6585-96.

Tocheva, A. S., Jefferies, J. M., Christodoulides, M., Faust, S. N. and Clarke, S. C. (2010) 'Increase in serotype 6C pneumococcal carriage, United Kingdom', *Emerg Infect Dis*, 16(1), pp. 154-5.

Tocheva, A. S., Jefferies, J. M., Rubery, H., Bennett, J., Afimeke, G., Garland, J., Christodoulides, M., Faust, S. N. and Clarke, S. C. (2011) 'Declining serotype coverage of new pneumococcal conjugate vaccines relating to the carriage of Streptococcus pneumoniae in young children', *Vaccine*, 29(26), pp. 4400-4.

Toll, E. C. and Nunez, D. A. (2012) 'Diagnosis and treatment of acute otitis media: review', *J Laryngol Otol*, 126(10), pp. 976-83.

Tomasz, A. (1995) 'The pneumococcus at the gates', *N Engl J Med*, 333(8), pp. 514-5.

Tomasz, A., Jamieson, J. D. and Ottolenghi, E. (1964) 'The fine structure of diplococcus pneumoniae', *J Cell Biol*, 22, pp. 453-67.

Tong, H. H., Fisher, L. M., Kosunick, G. M. and DeMaria, T. F. (2000) 'Effect of adenovirus type 1 and influenza A virus on Streptococcus pneumoniae

nasopharyngeal colonization and otitis media in the chinchilla', *Ann Otol Rhinol Laryngol,* 109(11), pp. 1021-7.

Tonnaer, E. L., Graamans, K., Sanders, E. A. and Curfs, J. H. (2006) 'Advances in understanding the pathogenesis of pneumococcal otitis media', *Pediatr Infect Dis J,* 25(6), pp. 546-52.

Tonnaer, E. L., Rijkers, G. T., Meis, J. F., Klaassen, C. H., Bogaert, D., Hermans, P. W. and Curfs, J. H. (2005) 'Genetic relatedness between pneumococcal populations originating from the nasopharynx, adenoid, and tympanic cavity of children with otitis media', *J Clin Microbiol,* 43(7), pp. 3140-4.

Torres, A., Blasi, F., Dartois, N. and Akova, M. (2015) 'Which individuals are at increased risk of pneumococcal disease and why? Impact of COPD, asthma, smoking, diabetes, and/or chronic heart disease on community-acquired pneumonia and invasive pneumococcal disease', *Thorax,* 70(10), pp. 984-9.

Tran, P. L., Lowry, N., Campbell, T., Reid, T. W., Webster, D. R., Tobin, E., Aslani, A., Mosley, T., Dertien, J., Colmer-Hamood, J. A. and Hamood, A. N. (2012) 'An organoselenium compound inhibits Staphylococcus aureus biofilms on hemodialysis catheters in vivo', *Antimicrob Agents Chemother,* 56(2), pp. 972-8.

Trappetti, C., Potter, A. J., Paton, A. W., Oggioni, M. R. and Paton, J. C. (2011) 'LuxS mediates iron-dependent biofilm formation, competence, and fratricide in Streptococcus pneumoniae', *Infect Immun,* 79(11), pp. 4550-8.

Tremblay, Y. D., Lévesque, C., Segers, R. P. and Jacques, M. (2013) 'Method to grow Actinobacillus pleuropneumoniae biofilm on a biotic surface', *BMC Vet Res,* 9, pp. 213.

Trombe, M. C. (1993) 'Characterization of a calcium porter of Streptococcus pneumoniae involved in calcium regulation of growth and competence', *J Gen Microbiol,* 139(3), pp. 433-9.

Trzciński, K., Thompson, C. M. and Lipsitch, M. (2004) 'Single-step capsular transformation and acquisition of penicillin resistance in Streptococcus pneumoniae', *J Bacteriol,* 186(11), pp. 3447-52.

Trzciński, K., Thompson, C. M., Srivastava, A., Basset, A., Malley, R. and Lipsitch, M. (2008) 'Protection against nasopharyngeal colonization by Streptococcus pneumoniae is mediated by antigen-specific CD4+ T cells', *Infect Immun,* 76(6), pp. 2678-84.

Tseng, B. S., Zhang, W., Harrison, J. J., Quach, T. P., Song, J. L., Penterman, J., Singh, P. K., Chopp, D. L., Packman, A. I. and Parsek, M. R. (2013) 'The extracellular matrix protects Pseudomonas aeruginosa biofilms by limiting the penetration of tobramycin', *Environ Microbiol,* 15(10), pp. 2865-78.

Tu, A. H., Fulgham, R. L., McCrory, M. A., Briles, D. E. and Szalai, A. J. (1999) 'Pneumococcal surface protein A inhibits complement activation by Streptococcus pneumoniae', *Infect Immun,* 67(9), pp. 4720-4.

Turner, P., Hinds, J., Turner, C., Jankhot, A., Gould, K., Bentley, S. D., Nosten, F. and Goldblatt, D. (2011) 'Improved detection of nasopharyngeal cocolonization by multiple pneumococcal serotypes by use of latex agglutination or molecular serotyping by microarray', *J Clin Microbiol,* 49(5), pp. 1784-9.

van den Aardweg, M. T., Schilder, A. G., Herkert, E., Boonacker, C. W. and Rovers, M. M. (2010) 'Adenoidectomy for otitis media in children', *Cochrane Database Syst Rev,* (1), pp. CD007810.

van Hoek, A. J., Andrews, N., Waight, P. A., Stowe, J., Gates, P., George, R. and Miller, E. (2012) 'The effect of underlying clinical conditions on the risk of developing invasive pneumococcal disease in England', *J Infect,* 65(1), pp. 17-24.

van Rossum, A. M., Lysenko, E. S. and Weiser, J. N. (2005) 'Host and bacterial factors contributing to the clearance of colonization by Streptococcus pneumoniae in a murine model', *Infect Immun,* 73(11), pp. 7718-26.

Vandevelde, N. M., Tulkens, P. M. and Van Bambeke, F. (2014) 'Antibiotic activity against naive and induced Streptococcus pneumoniae biofilms in an in vitro pharmacodynamic model', *Antimicrob Agents Chemother,* 58(3), pp. 1348-58.

Varon, E., Levy, C., De La Rocque, F., Boucherat, M., Deforche, D., Podglajen, I., Navel, M. and Cohen, R. (2000) 'Impact of antimicrobial therapy on nasopharyngeal carriage of Streptococcus pneumoniae, Haemophilus influenzae, and Branhamella catarrhalis in children with respiratory tract infections', *Clin Infect Dis,* 31(2), pp. 477-81.

Vidal, J. E., Howery, K. E., Ludewick, H. P., Nava, P. and Klugman, K. P. (2013) 'Quorum-sensing systems LuxS/autoinducer 2 and Com regulate Streptococcus pneumoniae biofilms in a bioreactor with living cultures of human respiratory cells', *Infect Immun,* 81(4), pp. 1341-53.

Vidal, J. E., Ludewick, H. P., Kunkel, R. M., Zähner, D. and Klugman, K. P. (2011) 'The LuxS-dependent quorum-sensing system regulates early biofilm formation by Streptococcus pneumoniae strain D39', *Infect Immun,* 79(10), pp. 4050-60.

von Bodman, S. B., Willey, J. M. and Diggle, S. P. (2008) 'Cell-cell communication in bacteria: united we stand', *J Bacteriol,* 190(13), pp. 4377-91.

Voynow, J. A. and Rubin, B. K. (2009) 'Mucins, mucus, and sputum', *Chest,* 135(2), pp. 505-12.

Vu, H. T., Yoshida, L. M., Suzuki, M., Nguyen, H. A., Nguyen, C. D., Nguyen, A. T., Oishi, K., Yamamoto, T., Watanabe, K. and Vu, T. D. (2011) 'Association between nasopharyngeal load of Streptococcus pneumoniae, viral coinfection, and radiologically confirmed pneumonia in Vietnamese children', *Pediatr Infect Dis J,* 30(1), pp. 11-8.

Waite, R. D., Struthers, J. K. and Dowson, C. G. (2001) 'Spontaneous sequence duplication within an open reading frame of the pneumococcal type 3 capsule locus causes high-frequency phase variation', *Mol Microbiol,* 42(5), pp. 1223-32.

Walker, C. L., Rudan, I., Liu, L., Nair, H., Theodoratou, E., Bhutta, Z. A., O'Brien, K. L., Campbell, H. and Black, R. E. (2013) 'Global burden of childhood pneumonia and diarrhoea', *Lancet,* 381(9875), pp. 1405-16.

Walker, T. S., Tomlin, K. L., Worthen, G. S., Poch, K. R., Lieber, J. G., Saavedra, M. T., Fessler, M. B., Malcolm, K. C., Vasil, M. L. and Nick, J. A. (2005) 'Enhanced Pseudomonas aeruginosa biofilm development mediated by human neutrophils', *Infect Immun,* 73(6), pp. 3693-701.

Walport, M. J. (2001) 'Complement. First of two parts', *N Engl J Med,* 344(14), pp. 1058-66.

Walters, M. C., Roe, F., Bugnicourt, A., Franklin, M. J. and Stewart, P. S. (2003) 'Contributions of antibiotic penetration, oxygen limitation, and low metabolic activity to tolerance of Pseudomonas aeruginosa biofilms to ciprofloxacin and tobramycin', *Antimicrob Agents Chemother,* 47(1), pp. 317-23.

Wartha, F., Beiter, K., Albiger, B., Fernebro, J., Zychlinsky, A., Normark, S. and Henriques-Normark, B. (2007) 'Capsule and D-alanylated lipoteichoic acids protect Streptococcus pneumoniae against neutrophil extracellular traps', *Cell Microbiol,* 9(5), pp. 1162-71.

Watson, D. A. and Musher, D. M. (1999) 'A brief history of the pneumococcus in biomedical research', *Semin Respir Infect,* 14(3), pp. 198-208.

Webster, J., Theodoratou, E., Nair, H., Seong, A. C., Zgaga, L., Huda, T., Johnson, H. L., Madhi, S., Rubens, C., Zhang, J. S., El Arifeen, S., Krause, R., Jacobs, T. A., Brooks, A. W., Campbell, H. and Rudan, I. (2011) 'An evaluation of emerging vaccines for childhood pneumococcal pneumonia', *BMC Public Health,* 11 Suppl 3, pp. S26.

Wei, H. and Håvarstein, L. S. (2012) 'Fratricide is essential for efficient gene transfer between pneumococci in biofilms', *Appl Environ Microbiol,* 78(16), pp. 5897-905.

Weimer, K. E., Armbruster, C. E., Juneau, R. A., Hong, W., Pang, B. and Swords, W. E. (2010) 'Coinfection with Haemophilus influenzae promotes pneumococcal biofilm formation during experimental otitis media and impedes the progression of pneumococcal disease', *J Infect Dis*, 202(7), pp. 1068-75.

Weimer, K. E., Juneau, R. A., Murrah, K. A., Pang, B., Armbruster, C. E., Richardson, S. H. and Swords, W. E. (2011) 'Divergent mechanisms for passive pneumococcal resistance to β-lactam antibiotics in the presence of Haemophilus influenzae', *J Infect Dis*, 203(4), pp. 549-55.

Weinberger, D. M., Dagan, R., Givon-Lavi, N., Regev-Yochay, G., Malley, R. and Lipsitch, M. (2008) 'Epidemiologic evidence for serotype-specific acquired immunity to pneumococcal carriage', *J Infect Dis*, 197(11), pp. 1511-8.

Weinberger, D. M., Malley, R. and Lipsitch, M. (2011) 'Serotype replacement in disease after pneumococcal vaccination', *Lancet*, 378(9807), pp. 1962-73.

Weinberger, D. M., Trzciński, K., Lu, Y. J., Bogaert, D., Brandes, A., Galagan, J., Anderson, P. W., Malley, R. and Lipsitch, M. (2009) 'Pneumococcal capsular polysaccharide structure predicts serotype prevalence', *PLoS Pathog*, 5(6), pp. e1000476.

Weiser, J. N. (2010) 'The pneumococcus: why a commensal misbehaves', *J Mol Med (Berl)*, 88(2), pp. 97-102.

Weiser, J. N., Austrian, R., Sreenivasan, P. K. and Masure, H. R. (1994) 'Phase variation in pneumococcal opacity: relationship between colonial morphology and nasopharyngeal colonization', *Infect Immun*, 62(6), pp. 2582-9.

Weiser, J. N., Bae, D., Epino, H., Gordon, S. B., Kapoor, M., Zenewicz, L. A. and Shchepetov, M. (2001) 'Changes in availability of oxygen accentuate differences in capsular polysaccharide expression by phenotypic variants and clinical isolates of Streptococcus pneumoniae', *Infect Immun*, 69(9), pp. 5430-9.

Weiser, J. N., Bae, D., Fasching, C., Scamurra, R. W., Ratner, A. J. and Janoff, E. N. (2003) 'Antibody-enhanced pneumococcal adherence requires IgA1 protease', *Proc Natl Acad Sci U S A*, 100(7), pp. 4215-20.

Weiser, J. N., Markiewicz, Z., Tuomanen, E. I. and Wani, J. H. (1996) 'Relationship between phase variation in colony morphology, intrastrain variation in cell wall physiology, and nasopharyngeal colonization by Streptococcus pneumoniae', *Infect Immun*, 64(6), pp. 2240-5.

Whitchurch, C. B., Tolker-Nielsen, T., Ragas, P. C. and Mattick, J. S. (2002) 'Extracellular DNA required for bacterial biofilm formation', *Science*, 295(5559), pp. 1487.

Whitney, C. G., Farley, M. M., Hadler, J., Harrison, L. H., Bennett, N. M., Lynfield, R., Reingold, A., Cieslak, P. R., Pilishvili, T., Jackson, D., Facklam, R. R., Jorgensen, J. H., Schuchat, A. and Network, A. B. C. S. o. t. E. I. P. (2003) 'Decline in invasive pneumococcal disease after the introduction of protein-polysaccharide conjugate vaccine', *N Engl J Med*, 348(18), pp. 1737-46.

Whitney, C. G., Pilishvili, T., Farley, M. M., Schaffner, W., Craig, A. S., Lynfield, R., Nyquist, A. C., Gershman, K. A., Vazquez, M., Bennett, N. M., Reingold, A., Thomas, A., Glode, M. P., Zell, E. R., Jorgensen, J. H., Beall, B. and Schuchat, A. (2006) 'Effectiveness of seven-valent pneumococcal conjugate vaccine against invasive pneumococcal disease: a matched case-control study', *Lancet*, 368(9546), pp. 1495-502.

Williams, I., Venables, W. A., Lloyd, D., Paul, F. and Critchley, I. (1997) 'The effects of adherence to silicone surfaces on antibiotic susceptibility in Staphylococcus aureus', *Microbiology*, 143 (Pt 7), pp. 2407-13.

Wilson, R., Cohen, J. M., Jose, R. J., de Vogel, C., Baxendale, H. and Brown, J. S. (2015) 'Protection against Streptococcus pneumoniae lung infection after nasopharyngeal colonization requires both humoral and cellular immune responses', *Mucosal Immunol*, 8(3), pp. 627-39.

Wilson, R., Cohen, J. M., Reglinski, M., Jose, R. J., Chan, W. Y., Marshall, H., de Vogel, C., Gordon, S., Goldblatt, D., Petersen, F. C., Baxendale, H. and Brown, J. S. (2017) 'Naturally Acquired Human Immunity to Pneumococcus Is Dependent on Antibody to Protein Antigens', *PLoS Pathog,* 13(1), pp. e1006137.

Winkelstein, J. A. (1981) 'The role of complement in the host's defense against Streptococcus pneumoniae', *Rev Infect Dis,* 3(2), pp. 289-98.

Winkelstein, J. A. and Tomasz, A. (1977) 'Activation of the alternative pathway by pneumococcal cell walls', *J Immunol,* 118(2), pp. 451-4.

Winskel, H. (2006) 'The effects of an early history of otitis media on children's language and literacy skill development', *Br J Educ Psychol,* 76(Pt 4), pp. 727-44.

Winther, B., Gross, B. C., Hendley, J. O. and Early, S. V. (2009) 'Location of bacterial biofilm in the mucus overlying the adenoid by light microscopy', *Arch Otolaryngol Head Neck Surg,* 135(12), pp. 1239-45.

Wolcott, R. D. and Ehrlich, G. D. (2008) 'Biofilms and chronic infections', *JAMA,* 299(22), pp. 2682-4.

Wolter, N., Tempia, S., Cohen, C., Madhi, S. A., Venter, M., Moyes, J., Walaza, S., Malope-Kgokong, B., Groome, M., du Plessis, M., Magomani, V., Pretorius, M., Hellferscee, O., Dawood, H., Kahn, K., Variava, E., Klugman, K. P. and von Gottberg, A. (2014) 'High nasopharyngeal pneumococcal density, increased by viral coinfection, is associated with invasive pneumococcal pneumonia', *J Infect Dis,* 210(10), pp. 1649-57.

Wright, A. K., Bangert, M., Gritzfeld, J. F., Ferreira, D. M., Jambo, K. C., Wright, A. D., Collins, A. M. and Gordon, S. B. (2013) 'Experimental human pneumococcal carriage augments IL-17A-dependent T-cell defence of the lung', *PLoS Pathog,* 9(3), pp. e1003274.

Wyllie, A. L., Chu, M. L., Schellens, M. H., van Engelsdorp Gastelaars, J., Jansen, M. D., van der Ende, A., Bogaert, D., Sanders, E. A. and Trzciński, K. (2014) 'Streptococcus pneumoniae in saliva of Dutch primary school children', *PLoS One,* 9(7), pp. e102045.

Wyres, K. L., Lambertsen, L. M., Croucher, N. J., McGee, L., von Gottberg, A., Liñares, J., Jacobs, M. R., Kristinsson, K. G., Beall, B. W., Klugman, K. P., Parkhill, J., Hakenbeck, R., Bentley, S. D. and Brueggemann, A. B. (2013) 'Pneumococcal capsular switching: a historical perspective', *J Infect Dis,* 207(3), pp. 439-49.

Xu, F., Droemann, D., Rupp, J., Shen, H., Wu, X., Goldmann, T., Hippenstiel, S., Zabel, P. and Dalhoff, K. (2008) 'Modulation of the inflammatory response to Streptococcus pneumoniae in a model of acute lung tissue infection', *Am J Respir Cell Mol Biol,* 39(5), pp. 522-9.

Xu, G., Kiefel, M. J., Wilson, J. C., Andrew, P. W., Oggioni, M. R. and Taylor, G. L. (2011) 'Three Streptococcus pneumoniae sialidases: three different products', *J Am Chem Soc,* 133(6), pp. 1718-21.

Xu, Q., Casey, J. R. and Pichichero, M. E. (2015) 'Higher levels of mucosal antibody to pneumococcal vaccine candidate proteins are associated with reduced acute otitis media caused by Streptococcus pneumoniae in young children', *Mucosal Immunol,* 8(5), pp. 1110-7.

Yadav, M. K., Kwon, S. K., Cho, C. G., Park, S. W., Chae, S. W. and Song, J. J. (2012) 'Gene expression profile of early in vitro biofilms of Streptococcus pneumoniae', *Microbiol Immunol,* 56(9), pp. 621-9.

Yu, Q., Griffin, E. F., Moreau-Marquis, S., Schwartzman, J. D., Stanton, B. A. and O'Toole, G. A. (2012) 'In vitro evaluation of tobramycin and aztreonam versus Pseudomonas aeruginosa biofilms on cystic fibrosis-derived human airway epithelial cells', *J Antimicrob Chemother,* 67(11), pp. 2673-81.

Yuste, J., Botto, M., Paton, J. C., Holden, D. W. and Brown, J. S. (2005) 'Additive inhibition of complement deposition by pneumolysin and PspA facilitates Streptococcus pneumoniae septicemia', *J Immunol,* 175(3), pp. 1813-9.

Yuste, J., Khandavilli, S., Ansari, N., Muttardi, K., Ismail, L., Hyams, C., Weiser, J., Mitchell, T. and Brown, J. S. (2010) 'The effects of PspC on complement-mediated immunity to Streptococcus pneumoniae vary with strain background and capsular serotype', *Infect Immun,* 78(1), pp. 283-92.

Yuste, J., Sen, A., Truedsson, L., Jönsson, G., Tay, L. S., Hyams, C., Baxendale, H. E., Goldblatt, F., Botto, M. and Brown, J. S. (2008) 'Impaired opsonization with C3b and phagocytosis of Streptococcus pneumoniae in sera from subjects with defects in the classical complement pathway', *Infect Immun,* 76(8), pp. 3761-70.

Zhang, Q., Bernatoniene, J., Bagrade, L., Pollard, A. J., Mitchell, T. J., Paton, J. C. and Finn, A. (2006) 'Serum and mucosal antibody responses to pneumococcal protein antigens in children: relationships with carriage status', *Eur J Immunol,* 36(1), pp. 46-57.

Zhang, Q., Leong, S. C., McNamara, P. S., Mubarak, A., Malley, R. and Finn, A. (2011) 'Characterisation of regulatory T cells in nasal associated lymphoid tissue in children: relationships with pneumococcal colonization', *PLoS Pathog,* 7(8), pp. e1002175.

Zhang, Z., Clarke, T. B. and Weiser, J. N. (2009) 'Cellular effectors mediating Th17-dependent clearance of pneumococcal colonization in mice', *J Clin Invest,* 119(7), pp. 1899-909.

Zheng, Z. and Stewart, P. S. (2002) 'Penetration of rifampin through Staphylococcus epidermidis biofilms', *Antimicrob Agents Chemother,* 46(3), pp. 900-3.

Zhou, H., Haber, M., Ray, S., Farley, M. M., Panozzo, C. A. and Klugman, K. P. (2012) 'Invasive pneumococcal pneumonia and respiratory virus co-infections', *Emerg Infect Dis,* 18(2), pp. 294-7.

Zhu, L., Kuang, Z., Wilson, B. A. and Lau, G. W. (2013) 'Competence-independent activity of pneumococcal EndA [corrected] mediates degradation of extracellular dna and nets and is important for virulence', *PLoS One,* 8(7), pp. e70363.

Zuliani, G., Carlisle, M., Duberstein, A., Haupert, M., Syamal, M., Berk, R., Du, W. and Coticchia, J. (2009) 'Biofilm density in the pediatric nasopharynx: recurrent acute otitis media versus obstructive sleep apnea', *Ann Otol Rhinol Laryngol,* 118(7), pp. 519-24.

Zuliani, G., Carron, M., Gurrola, J., Coleman, C., Haupert, M., Berk, R. and Coticchia, J. (2006) 'Identification of adenoid biofilms in chronic rhinosinusitis', *Int J Pediatr Otorhinolaryngol,* 70(9), pp. 1613-7.

9 Appendix

9.1 Immunohistochemistry reagents

9.1.1 Washing buffer

TBS was mixed in 1 litre of reverse osmosis water (ROW) and adjusted to pH 7.6 by adding 35 ml of 1M hydrochloric acid (HCL). ROW was added for a total volume of 10 litres and mixed well.

9.1.2 Culture medium blocking solution

Dulbecco's Modified Eagles Medium (DMEM) was dissolved in ROW and added to sodium hydrogen carbonate ($NaHCO_3$). 5 g of bovine serum albumin (BSA) was dissolved in 400 ml DMEM and 100 ml of fetal calf serum (FCS).

9.1.3 Diaminobenzidine (DAB) kit

32 µl of chromogen was added to 1 ml of buffer and 50 µl of 15% azide, and then applied to tissue sections. This working solution was sufficient for 5 slides. Volumes were scaled-up for more slides when required.

9.1.4 Mayer's haematoxylin counterstain

1 g of Mayer's haematoxylin was dissolved with 50 g of ammonium alum (Fisher Scientific, U.K.) and 0.2 g of sodium iodate in 1 litre of distilled water overnight. 50 g of chloral hydrate (BDH Chemicals, U.K.) and 1 g of citric acid was added, mixed and boiled for 5 minutes.

9.1.5 Methyl green counterstain

2.72 g of sodium acetate, trihydrate (BDH Chemicals, U.K.) was added to 200 ml of distilled water, mixed, and adjusted to pH 4.2 using concentrated glacial acetic acid (BDH Chemicals, U.K.). 1 g of Methyl green was then added to the sodium acetate buffer and mixed to dissolve.

9.2 Lactate dehydrogenase cytotoxicity kit reagents

9.2.1 LDH Positive Control

1 µl of LDH Positive Control was diluted in 10 ml of TBS containing 1% BSA. 50 µl of the diluted LDH Positive Control was used in triplicate wells.

9.2.2 Reaction Mixture

11.4 ml of ultrapure water was added to one vial of Substrate Mix and mixed gently. 0.6 ml of Assay Buffer was then added to the 11.4 ml Substrate Mix and mixed well.

9.3 Human Magnetic Custom Luminex Kit reagents

9.3.1 Wash solution

15 ml of Wash Solution Concentrate was added to 285 ml of deionised water and mixed well.

9.3.2 Standard curve

150 µl of Assay Diluent was pipetted into six 1.5 ml microcentrifuge tubes and supplemented with 150 µl of antibiotic-free sMEM. 150 µl of the reconstituted standards was pipetted into the first tube. 150 µl was then taken from this tube and placed into the next one for 1:3 serial dilutions. Blanks were made with 150 µl of Assay Diluent and 150 µl of antibiotic-free sMEM.

9.3.3 Washing steps

200 µl of Wash Solution was pipetted into each well of the 96-flat bottom plate. The plate was placed onto a magnetic 96-well separator (Fisher Scientific, U.K.) and left for 1 minute. The magnetic separator was then turned upside down to decant the fluid from each well and excess fluid was blotted on dry paper towels.

9.3.4 Antibody beads

The Antibody Bead Concentrate was vortexed for 30 seconds. For a single well of a 96-well plate, 2.5 µl of the vortexed beads was supplemented with 25 µl of Wash Solution. Volumes were scaled-up to the number of wells required. 25 µl of the total solution was pipetted into each well.

9.3.5 Biotinylated detector antibody

For a single well of a 96-well plate, 10 µl of Biotinylated Antibody was supplemented with 100 µl of Biotin Diluent. Volumes were scaled-up to the number of wells required. 100 µl of the total solution was pipetted into each well.

9.3.6 Streptavidin-RPE solution

For a single well of a 96-well plate, 10 µl of Streptavidin-RPE was supplemented with 100 µl of RPE-Diluent. Volumes were scaled-up to the number of wells required. 100 µl of the total solution was pipetted into each well.

9.4 ENT Project Information Sheets and Consent Forms

9.4.1 Information sheet for parents of children undergoing ENT procedures

We are conducting some research into new ways of treating infection in chronic and recurrent ear, nose and throat (ENT) conditions. Your child is being invited to take part in a research study because they have either been diagnosed with an ENT condition or are being cared for by the ENT service. Before you decide it is important for you to understand why the research is being done and what it will involve. Please take time to read the following information carefully and discuss it with friends, relatives and your GP if you wish. Ask us if there is anything that is not clear or if you would like more information. Take time to decide whether or not you wish your child to take part.

Children with chronic ENT problems often require surgery to effectively treat their illness. Infection can play a part in causing or making these conditions worse. The research we are doing looks at new ways of growing bacteria from samples taken routinely during surgery and finding possible ways of enhancing antibiotic treatment of infection. By investigating these things we hope to improve our understanding of how infection may cause chronic ENT disease. Finding out about the bacteria involved in chronic ENT diseases is important so we can better understand the processes involved in ENT infection and inflammation and hopefully devise new treatments.

It is up to you to decide whether or not your child takes part. If you decide they can take part you will be asked to sign a consent form and your GP will be notified of their participation by letter. Even after you decide to participate you are still free to withdraw your child from the study at any time and without giving a reason. This will not affect the standard of care they receive.

What will happen if my child takes part?
If you agree for your child to take part we will retain tissue normally removed during their surgery as research samples. Acquisition of these samples will not alter the surgery in any way. It is only the processing of the sample once they get to the laboratory that will change. Part of the specimen will be sent for routine processing (as clinically indicated) and the rest will be used for research purposes. Some of the sample will be frozen and stored for analysis at a later date. All samples will be given study numbers, which cannot be directly traced back to your child. A doctor involved in the study will also check your child's notes to record details of symptoms, history and treatment, which will help in the analysis of the samples. A research study number will also be given to any documentation so that it cannot be traced back to your child. Section B on the consent form asks you to give us permission to store the sample for use in future studies. The official name for such permission is linked anonymised, whereby results of future studies can be linked with your child's medical details but the researchers will not have access to his or her identity.

What are the side effects of taking part?
None.

What are the possible disadvantages and risks of taking part?
None. The extra laboratory tests will not affect your child in any way.

What are the possible benefits of taking part?
The information we get from this study may help us to better treat children with chronic and recurrent ENT diseases. It will not directly benefit your child now but may help them

or children with similar problems in the future.

Will my taking part in this study be kept confidential?
Yes. Any information about your child that leaves the hospital will have their details removed so that they cannot be identified.

What will happen to the results of the research?
The results may be published in a scientific or medical journal. They may also be presented at a scientific conference. Confidentiality will not be broken by publication, as the information presented will not be related to named children.

What if something goes wrong?
Any complaint about the way you have been dealt with during the study or any possible harm you might suffer will be addressed. Please raise your concerns in the first instance with the Principal Investigator (that is the lead researcher), Dr Saul Faust – his contact details are at the end of this form. If you wish to make a more formal complaint, please contact the Patient Advice and Liaison Service (available from 9am-4.30pm Monday to Friday, out of hours there is an answer phone), PALS, C level, Centre Block, Mailpoint 81, Southampton General Hospital. Email PALS@suht.swest.nhs.uk Tel 02380 798498

What insurance provisions are in place?
In the event that something does go wrong and you are harmed during the research and this is due to someone's negligence then you may have grounds for a legal action for compensation against the sponsor, Southampton University Hospitals NHS Trust but you may have to pay your legal costs. The former National Health Service complaints mechanism will still be available to you. As the Principal Investigator is an employee of the University of Southampton, additional professional indemnity and clinical investigation insurance is in place.

Contact for further information:
If you have any questions relating to this research you will have the opportunity to discuss them with a children's doctor either on the ward or when you come to clinic. Otherwise you can contact:

-Mr William Hellier, Consultant otolaryngologist, Southampton University Hospitals NHS Trust, Tremona Road, Southampton, SO16 6YD, Tel: 02380825526.

-Dr Saul Faust, Senior Lecturer in Paediatric Immunology and Infectious Diseases, University of Southampton, C level, West Wing, Mailpoint 218, Southampton Universities Hospital Trust, Tremona Road, Southampton, SO16 6YD, Tel: 02380796883

General information about participating in research in the NHS is available on the National Patient Safety Agency website http://www.nres.npsa.nhs.uk/public/index.htm.

9.4.2 Information sheet for children aged 5-9 undergoing ENT procedures

Please ask your mum or your dad to help you read this form

Your mum or dad has said that you will be able to help other children while you are in hospital by taking part in our project.

What are we doing?
We are looking at better ways of helping other children with problems like yours. To do this, we would like to study the poorly parts the doctors take out of you during your operation to make you feel better.

Do I have to take part?
No, but you must decide this with your mum or dad. You or your parents can ask for you to stop taking part at any time. We are happy to answer any questions that you may have.

Will anything be different about my trip to hospital if I take part?
No. You will not have to have anything extra done if you take part.

9.4.3 ENT Consent Forms

Parent consent form (staged) – ENT Surgery

PART A **Consent for the main study**

PLEASE **INITIAL** THE BOXES FOR EACH SECTION YOU WISH YOUR CHILD TO TAKE PART IN (please put a cross through any you do not wish to consent to):

1 I confirm that I have read the information sheet for the above study version 1.2 dated 25/08/09. I have had the opportunity to ask questions, I understand why the research is being done and any possible risks to my child have been explained to me.

2 I understand that my child's participation is voluntary and that we can withdraw at any time without our legal rights or medical care being affected.

3 I give permission for sections of my child's notes to be looked at by individuals from the local NHS Trust, the study sponsor (Southampton University Hospital NHS Trust) and from regulatory authorities where it is relevant to my taking part in this research. I give permission for these individuals to have access to my records.

4 I agree to take part in the above study and for researchers to retain infectious material removed during my child's ear/tonsil surgery (delete as appropriate).

5 I agree that my child's samples be stored and tested to investigate the causes of ear, nose and throat problems.

6 I agree that the researchers may keep a sample of my child's blood taken at the time of cannulation.

7 I give permission for my general practitioner to be notified of my involvement in this study.

SAMPLES GIFTED FOR STORAGE AND USE IN FUTURE STUDIES

PART B **Linked Anonymised Samples**

8 I agree to my child's anonymised data relevant to this trial being collected and stored on electronic databases in accordance with the Data Protection Act 1998

9 I indicate my consent for the samples to be stored (potentially for many years) for the following types of studies (provided they have gained ethical approval):

a I give permission for the samples to be used for treatments/investigations of ear, nose and throat diseases in children and adults.

b I give permission for the samples to be stored for use in other unrelated research studies, the precise nature of which will depend upon future scientific advances.

c In the case of linked anonymised samples, I give permission for a member of the research team to look at my child's medical records.

d I understand that the samples may be used for commercial development, without financial or other benefit to myself in keeping with the gift nature of the sample.

_____ _____ _____

Name of Parent Date Signature

_____ _____ _____

Name of Person taking consent (if different from researcher) Date Signature

_____ _____

Signature of Researcher Date

For children >12 years:

I agree to take part in this study

_____ _____

Name Date

When completed 1 for patient, 1 for researcher, 1(original) to be kept with hospital notes.

9.5 First author papers from PhD

9.5.1 Review paper published in The Journal of Infection

Journal of Infection (2014) 69, S47—S52

BIAM British Infection Association

www.elsevierhealth.com/journals/jinf

New approaches to the treatment of biofilm-related infections

Matthew Wilkins [a,b], Luanne Hall-Stoodley [b,c], Raymond N. Allan [a,b], Saul N. Faust [a,b,*]

[a] *Academic Unit of Clinical and Experimental Sciences, Faculty of Medicine and Institute of Life Sciences, University of Southampton, Southampton, UK*
[b] *NIHR Wellcome Trust Clinical Research Facility, C Level, West Wing, Mailpoint 218, University Hospital Southampton NHS Foundation Trust, Tremona Road, Southampton, SO16 6YD, UK*
[c] *Microbial Infection and Immunity, Centre for Microbial Interface Biology, The Ohio State University, 793 Biomedical Research Tower, 460 W. 12th Avenue, Columbus, OH, 43210-2210, USA*

Accepted 18 July 2014
Available online 17 September 2014

KEYWORDS
Clinical biofilm infection;
Bacterial infection;
Pathophysiology;
Diagnosis;
Treatment

Summary Bacteria causing chronic infections predominately grow as surface-attached, sessile communities known as biofilms. Biofilm-related infections including cystic fibrosis lung infection, chronic and recurrent otitis media, chronic wounds and implant- and catheter-associated infections, are a significant cause of morbidity and mortality and financial cost. Chronic biofilm-based infections are recalcitrant to conventional antibiotic therapy and are often unperturbed by host immune responses such as phagocytosis, despite a sustained presence of host inflammation.

The diagnosis of clinically important biofilm infections is often difficult as Koch's postulates are rarely met. If treatment is required, surgical removal of the infected implant, or debridement of wound or bone, is the most efficient means of eradicating a clinically significant biofilm. New approaches to treatment are under investigation.

Discovery and definition

The concept that bacteria exist as single, free-floating ("planktonic") organisms in nature was radically overturned in the 1970s upon the observation that bacteria were capable of attaching to and growing on a surface, and that these adherent bacteria predominate numerically in natural, clinical and industrial aquatic ecosystems.[1] It is now widely

* Corresponding author. NIHR Wellcome Trust Clinical Research Facility, C Level, West Wing, Mailpoint 218, University Hospital Southampton NHS Foundation Trust, Tremona Road, Southampton, SO16 6YD, UK.
E-mail address: s.faust@soton.ac.uk (S.N. Faust).

http://dx.doi.org/10.1016/j.jinf.2014.07.014
0163-4453/

accepted that biofilms represent a mode of bacterial growth, allowing survival in hostile environments and colonisation of new niches through dispersal.[2] Biofilms are associated with a self-produced hydrated matrix of extracellular polymeric substances (EPS),[3,4] comprised of polysaccharides, proteins, lipids and extracellular DNA (eDNA).[5] This matrix confers structure and protection to the complex biofilm community against changing environmental conditions.

Biofilms — the clinical importance and burden on public health

Bacteria in biofilms can specifically mediate infections which differ from those caused by planktonic bacteria.[6] Aside from surface association, aggregation, and the production of a matrix, there are two main differences between biofilm-associated microorganisms and their planktonic counterparts. Biofilms are inherently more tolerant to antibiotics and other forms of antimicrobial treatment, and to host immune responses, despite a sustained presence of inflammatory cells and effector functions.[7–9] Clinically, this can result in chronic or recurrent infections such as chronic and recurrent otitis media (COM),[10] chronic wounds,[11] cystic fibrosis lung infection[12] and chronic rhinosinusitis[13] (Table 1).

Biofilm contamination occurs in a range of indwelling medical devices leading to hospital-acquired infections (Table 1). The US Centres for Disease Control and Prevention (CDC) estimates that biofilms are responsible for more than 65% of such nosocomial infections.[14] Currently, the most effective means of treating these infections, and often the only feasible solution, is to physically remove the infected medical device.

Why do bacteria form biofilms?

There are a number of evolutionary advantages for bacterial cells to aggregate and attach to a surface.

Table 1 Biofilm-associated clinical infections.[48]

Chronic Otitis media
Recurrent tonsillitis
Chronic wounds
Cystic fibrosis lung infection
Urinary tract infections
Chronic rhinosinusitis
Dental caries
Periodontitis
Device-related infections
Urinary catheters
Mechanical heart valves
Prosthetic joints
Contact lenses
Intrauterine devices
Pacemakers
Endotracheal tubes
Voice prostheses
Tympanostomy tubes

Defence

In the process of infection or colonisation, bacteria come up against a variety of host defence mechanisms, including pH changes, phagocytic attack, and the presence of antimicrobial agents (natural and administered). Biofilm bacteria can withstand these mechanisms far better than planktonic bacteria, displaying enhanced resistance to cell lysis by complement, opsonisation and phagocytosis.[4] Phagocytes that attempt to engulf and ingest bacteria in a biofilm may harm surrounding healthy tissue, through the secretion of toxins, in a process known as "frustrated phagocytosis".[4] In *Pseudomonas aeruginosa* biofilms, phagocytic killing has also been reported to be reduced despite polymorphonuclear leukocytes (PMN) penetrating through the EPS and apparent phagocytosis occurring.[15]

Interactive communities and quorum sensing

Bacteria in biofilms are often described as living in a community comparable to those of multicellular organisms. Individual bacterial cells in biofilms are capable of sensing environmental conditions and, through cell-to-cell communication, undergoing changes in their gene expression to increase survival. However, such phenotypic change after adaption of gene expression is only transient and, depending on the conditions, biofilm bacteria may convert back to planktonic growth. Nevertheless, the communal existence and closely packed environment within a biofilm is ideal for intercellular interactions between cells of either the same or different species, benefitting other members of the community and the biofilm as a whole.

To communicate with one another, bacteria synthesise and respond to signalling molecules in a process known as quorum sensing (QS). In low density, as in planktonic populations, bacteria secrete low molecular weight, highly diffusible, signal molecules (autoinducers, such as oligopeptides in Gram positive bacteria and *N*-acyl-L-homoserine lactones in Gram negative bacteria) at levels that are too low to induce changes in gene expression. Once the close proximity bacterial population reaches a critical mass, the increased concentration of autoinducer molecules in the EPS allows individual bacterial to sense the presence of other bacteria. Physiological processes under QS control include surface attachment, EPS production, competence, bioluminescence and secretion of virulence factors.[16]

Biofilm formation

The biofilm life cycle is regarded as a dynamic, continually evolving process characterised by several distinct phases, each regulated by a number of specific genes (Fig. 1).

Attachment

When free-floating, planktonic bacteria initially attach to a surface they are not irreversibly bound and are susceptible to antibiotic treatment, gentle rinsing, or changes in conditions.

Bacterial surface attachment is complex. The rate and extent of microbial attachment is not simply dependent on the properties of the bacteria, but of the surface itself and

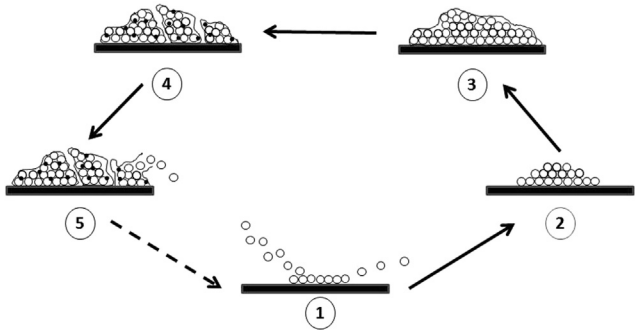

Figure 1 Biofilm life cycle: (1) Planktonic bacteria adhere to the surface, but the attachment is reversible at this stage. (2) Following adhesion, irreversible attachment occurs. Microcolonies begin to form as the bacteria start to undergo cell division, enabling more adhesion sites for the recruitment of other cells. (3) Extracellular polymeric substances (EPS) are secreted, which results in a self-produced matrix that provides the basis of the biofilm's structure and signals the beginning of biofilm maturation. (4) The biofilm is now fully mature, with the tower-like structures interspersed with water channels for the circulation of oxygen and nutrients and the removal of waste products. Cell-to-cell communication, through quorum sensing (QS), regulates a number of physiological processes such as the secretion of virulence factors via changes in bacterial gene expression, to promote survival. (5) The life cycle of a biofilm ends with the detachment of small segments from the biofilm. These planktonic bacteria may relocate and colonise other surfaces.

the immediate environment. Generally, bacterial attachment is more likely on surfaces that are hydrophobic, rougher, or coated by a conditioning film comprised of polymers from the surrounding environment, with an increase in cation and nutrient concentration also playing a role.[17] Once in contact with a surface, bacterial cells overcome common repulsive forces due to net negative electrostatic charges, mediated by cell surface appendages, fimbriae and flagella. Following attachment, cells aggregate into structures known as microcolonies and begin to undergo cell division, which enables the recruitment of other cells by providing more adhesion sites.

Gene regulation

A profound change in phenotypic expression occurs on the switch from the planktonic to the biofilm growth mode. Microarray studies demonstrate that numerous species variably express as much as ten percent of their genomes in established biofilms compared to planktonic growth conditions.[18–21] In some cases, biofilms from different strains of the same bacterial species may be as different from one another as they are from planktonic bacteria.[22]

The extracellular matrix

After microcolony formation, an extracellular matrix is produced. Consisting of polysaccharides, proteins and eDNA, the matrix confers physical protection and defines a biofilm by providing the basis for the structure.[23] Bacteria also produce increasing amounts of EPS as biofilms become more mature.[24] The matrix is crucial in allowing biofilm bacteria to withstand adverse conditions such as high osmotic stress, low nutrient and oxygen availability, antibiotics and host immune responses.

Three dimensional structure

A biofilm is not a homogenous monolayer, but a three dimensional structure with significant spatial and temporal heterogeneity.[25] In addition, the architecture and composition varies according to the bacterial species and the surrounding environment, for instance *P. aeruginosa* often forms mushroom-shaped microcolonies whereas *Streptococcus pneumoniae* forms tower-like structures. These structures are interspersed with water channels that enable fluid to penetrate, facilitating efficient exchange of nutrients and oxygen as well as the removal of potentially toxic metabolites.[26] This structured consortium of bacteria may also include host proteins such as immunoglobulins, fibrin and platelets.

Biofilm bacteria do not preferentially consume nutrients for growth but rather to make the exopolysaccharide material of the scaffold matrix. However, when nutrients are scarce, the scaffold can be digested by secreted enzymes and used for consumption.[27]

Detachment and dispersal

The life cycle of bacterial biofilms ends with the liberation of planktonic bacteria or the detachment of small segments from the mature biofilm that can propagate to other sites. Detachment and dispersal may occur through one of three different mechanisms, which vary according to the bacterial species: clumping dispersal, swarming/seeding dispersal and surface dispersal.[28]

Clumping dispersal occurs when a collection of cells are shed from a biofilm as clumps or emboli. For example, in *Staphylococcus aureus* biofilms, clumps are continually shed[29] and remain surrounded by the EPS, more closely resembling the attached biofilm than planktonic cells, and exhibiting similar antibiotic resistance. The ability of these non-directed emboli to reattach to a surface may account for the tendency of *S. aureus* to induce metastasis.[30]

Swarming dispersal occurs when many individual bacteria cells from microcolonies are released into either the bulk fluid or the substratum through the degradative activity of endogenous enzymes.[31,32] Unlike clumping dispersal, bacteria that detach via swarming dispersal are motile, self-propelled and directional, and no longer protected against the host environment.[2] Swarming dispersal may be important clinically in cystic fibrosis or bronchiectasis, where infective exacerbations are due to dispersal of bacteria from chronic pseudomonal or multispecies biofilms.[33]

Additional biofilm characteristics

Oxygen and nutrient gradients

Diffusion is the main mechanism for nutrient and oxygen entry into biofilms. However, it is limited because of the

tightly packed bacteria, and impacts upon the overall size of the three dimensional structure. Characteristically, oxygen and nutrient gradients exist within biofilms, with oxygen and nutrient depletion observed with increasing biofilm depth. Cells residing in the depths of a biofilm may be anaerobic, resulting in a slow-growing or even a non-growing (dormant) state giving rise to metabolic quiescence. Cells near the surface of a biofilm are aerobic and more rapidly growing in association with robust metabolic activity, since oxygen and nutrients can readily diffuse to these cells.[26] There are also local variations in pH and metabolites, which contribute to the existence of multiple microenvironments within a biofilm.

Species diversity

Clinical biofilms are increasingly recognised as being made up of more than one bacterial species. Although not a characteristic of all clinical biofilms, multispecies consortia potentially benefit from interspecies exchange of metabolic substrates and products that allows two or more distinctly different organisms to co-operate with one another in close proximity (known as syntrophism).[34,35]

Biofilms and antibiotic tolerance

Bacteria in biofilms are highly recalcitrant to conventional antimicrobial treatment.[36,37] Biofilms have been reported to tolerate antimicrobial agents at concentrations 10—1000 times that which are required to eradicate genetically equivalent planktonic bacteria.[7] Such resistance is multifactorial, and may be intrinsic (inherent) and/or acquired due to an exchange of genetic information.

Firstly, the self-produced matrix biofilm protects bacteria by retarding the diffusion and penetration of antimicrobials. The matrix of *P. aeruginosa* biofilms decreases the tobramycin concentration reaching the bacteria by binding to the antibiotic,[38] whilst β-lactamases at a concerted concentration degrade routinely used beta-lactam based antibiotics.[39] Similarly, multidrug resistance (MDR) pumps may contribute to biofilm resistance against low antibiotic concentrations, by transporting antimicrobial molecules out of the cell.[40]

Secondly, metabolically inactive cells within biofilms are rendered non-susceptible to antimicrobial attack,[41,42] since growth or metabolic activity is a prerequisite for most antibiotic action. In addition, "persister" cells are deeply buried cells insensitive to killing by antibiotics, which can persevere until antibiotic treatment ceases.[43]

Importantly, the persister phenotype is not due to nutrient constraints; nor are persisters mutants since their progeny, which are indistinguishable from the original strain, display similar susceptibility to antibiotics as those in the parent biofilm. Instead, persisters appear to be a pre-programmed response to the biofilm mode of growth, a survival mechanism to forego replication in favour of ensuring that some cells will survive such an environmental stress, to subsequently repopulate the biofilm.[44]

Detecting and diagnosing biofilm infections

Diagnosis of biofilm-associated infection (BAI) is a challenge since biofilm bacteria may not be cultured from infected tissues. For example, in otitis media with effusion (OME), a pathogen was identified in 25—30% of cases using culture compared to more than 90% in acute otitis media (AOM).[45] However, pathogens can be detected using polymerase chain reaction (PCR) and with 16S ribosomal probes.

Because conventional culture techniques may fail to detect bacteria in biofilms molecular methods may be helpful in detecting and identifying bacteria when there is a high clinical suspicion of infection. Diagnostic approaches include PCR, fluorescence *in situ* hybridisation (FISH) in tandem with confocal laser scanner microscopy (CLSM), and more recent novel technologies such as PLEX-ID.[46] In OME, pathogens were identified in 80—100% of cases investigated using PCR and/or FISH.[10,45]

Criteria for characterising biofilm-associated infections

Specific criteria have been developed to aid in the formal diagnosis of biofilms causing clinically significant infection (Table 2). An important distinction is that although a BAI may appear to respond to antibiotic treatment,[10] presumed to be due to the release and killing of susceptible

Table 2 Diagnostic criteria for biofilm-associated infections.[56]

1) The association of pathogenic bacteria with a surface. Where an infection is found in a patient in association with various types of epithelium, for example, middle ear mucosa in chronic otitis media, or skin in chronic wounds; with endocardium, in endocarditis; or associated with medical devices such as catheters and prostheses.
2) Direct examination of infected tissue demonstrates aggregated cells in cell clusters surrounded by a matrix, which may be of bacterial and host origin (e.g. fibrin, collagen and fibronectin).
3) Infection is confined to a particular site in the host.
4) Recalcitrance to antibiotic treatment despite demonstrated susceptibility of planktonic bacteria.[a]
5) Culture-negative result in spite of clinically documented high suspicion of infection (as localised bacteria in a biofilm may be missed in a conventional blood sample or aspirate).
6) Ineffective host clearance shown by the location of bacterial cell clusters (macrocolonies) in discrete areas in the host tissue associated with host inflammatory cells.

[a] Antibiotic susceptibility of planktonic cultures can only be tested upon positive culture from a clinical specimen. Therefore, it is suggested that in the absence of culture, recalcitrance to antibiotic therapy may be inferred from the presence of live bacterial cells in the biofilm from *in situ* viability staining or reverse transcription polymerase chain reaction (RT-PCR).

planktonic bacterial cells,[4] the underlying infection will not be eradicated. Chronic or recurrent infection, along with recalcitrance to antibiotic treatment, are significant clinical indicators of BAI.[47,48]

Treating biofilm infections

Current strategies

Conventional approaches used to treat acute infections may not clear chronic biofilm infections and in many cases promotes resistance and further biofilm formation. Some advocate administration of conventional antibiotics at high doses for prolonged periods of time,[49] though no large randomised controlled trials have been carried out. Most current treatment regimens target acute exacerbations caused by planktonic release of bacteria from biofilms, without overall cure.

Currently, the most efficient means of eradicating a clinically significant biofilm remains the surgical removal of the infected implant, or debridement of wound or bone. Such treatment is not always feasible, nor without risk of complications. Clinically significant biofilms remain a challenge to treat.

Future directions

A number of novel approaches for the treatment of clinical biofilm infections are under investigation, such as targeting the QS systems or metabolic pathway manipulation.

QS inhibitors (QSI) may be an effective future therapeutic option. QS-deficient *P. aeruginosa* biofilms demonstrated enhanced susceptibility to the synergistic effects of a QSI and tobramycin *in vitro* and in a mouse model.[50,51] Mice treated with a QSI and tobramycin prophylactically or early post-infection demonstrated substantially reduced colony forming units and increased *P. aeruginosa* clearance, where prevention of QS-controlled eDNA release and rhamnolipid production inhibited subsequent antibiotic activity neutralisation and lysis of polymorphonuclear leukocytes, which otherwise promotes biofilm survival.[51]

Another example of a potential clinically-useful strategy is modulation of biofilm metabolic pathways. For instance, the intracellular second messenger cyclic di-GMP (c-di-GMP) governs a wide range of cellular functions, including biofilm formation, virulence, motility and dispersal.[52] Low-dose nitric oxide (NO) signalling has been shown to stimulate specific phosphodiesterases (PDEs), which trigger degradation of c-di-GMP and concomitant enhanced dispersal of *P. aeruginosa* biofilms.[53] *In vitro*, low-dose NO has been the prime candidate for dispersal,[54] but prodrugs that only release NO upon contact with a biofilm and reaction with biofilm-specific enzymes, could allow for targeted enhancement of antibacterial efficacy while limiting potential toxic effects to the target tissue.[55]

Conclusions

Bacterial biofilms are a significant cause of morbidity and mortality, and are a major economic burden on global health systems. Novel methods have emerged to diagnose and treat clinical biofilm infections alongside surgical removal and conventional antibiotic therapy. Because antibiotic treatment may be ineffective in eradicating chronic biofilm-related infections, new therapeutic approaches are needed.

Conflict of interest

The authors have no conflict of interest to report.

Acknowledgements

MW is funded by a PhD Studentship provided by the Sir Jules Thorne Trust. RA, LH-S and SNF were in part funded by the Southampton NIHR Wellcome Trust Clinical Research Facility and NIHR Respiratory Biomedical Research Unit.

References

1. Costerton JW, Geesey GG, Cheng KJ. How bacteria stick. *Sci Am* 1978;**238**(1):86—95.
2. Hall-Stoodley L, Stoodley P. Biofilm formation and dispersal and the transmission of human pathogens. *Trends Microbiol* 2005;**13**(1):7—10.
3. Donlan RM, Costerton JW. Biofilms: survival mechanisms of clinically relevant microorganisms. *Clin Microbiol Rev* 2002; **15**(2):167—93.
4. Costerton JW, Stewart PS, Greenberg EP. Bacterial biofilms: a common cause of persistent infections. *Science* 1999; **284**(5418):1318—22.
5. Flemming HC, Wingender J. The biofilm matrix. *Nat Rev Microbiol* 2010;**8**(9):623—33.
6. Costerton JW, Irvin RT, Cheng KJ. The bacterial glycocalyx in nature and disease. *Annu Rev Microbiol* 1981;**35**:299—324.
7. Gilbert P, Das J, Foley I. Biofilm susceptibility to antimicrobials. *Adv Dent Res* 1997;**11**(1):160—7.
8. Fux CA, Costerton JW, Stewart PS, Stoodley P. Survival strategies of infectious biofilms. *Trends Microbiol* 2005;**13**(1): 34—40.
9. Foreman A, Holtappels G, Psaltis AJ, Jervis-Bardy J, Field J, Wormald PJ, et al. Adaptive immune responses in *Staphylococcus aureus* biofilm-associated chronic rhinosinusitis. *Allergy* 2011;**66**(11):1449—56.
10. Hall-Stoodley L, Hu FZ, Gieseke A, Nistico L, Nguyen D, Hayes J, et al. Direct detection of bacterial biofilms on the middle-ear mucosa of children with chronic otitis media. *J Am Med Assoc* 2006;**296**(2):202—11.
11. Kirketerp-Møller K, Jensen P, Fazli M, Madsen KG, Pedersen J, Moser C, et al. Distribution, organization, and ecology of bacteria in chronic wounds. *J Clin Microbiol* 2008;**46**(8):2717—22.
12. Starner TD, Zhang N, Kim G, Apicella MA, McCray PB. *Haemophilus influenzae* forms biofilms on airway epithelia: implications in cystic fibrosis. *Am J Respir Crit Care Med* 2006; **174**(2):213—20.
13. Psaltis AJ, Ha KR, Beule AG, Tan LW, Wormald PJ. Confocal scanning laser microscopy evidence of biofilms in patients with chronic rhinosinusitis. *Laryngoscope* 2007;**117**(7):1302—6.
14. Potera C. Forging a link between biofilms and disease. *Science* 1999;**283**(5409). 1837, 1839.
15. Jesaitis AJ, Franklin MJ, Berglund D, Sasaki M, Lord CI, Bleazard JB, et al. Compromised host defense on *Pseudomonas aeruginosa* biofilms: characterization of neutrophil and biofilm interactions. *J Immunol* 2003;**171**(8):4329—39.

16. Fuqua WC, Winans SC, Greenberg EP. Quorum sensing in bacteria: the LuxR-LuxI family of cell density-responsive transcriptional regulators. *J Bacteriol* 1994;**176**(2):269—75.
17. Donlan RM. Biofilms: microbial life on surfaces. *Emerg Infect Dis* 2002;**8**(9):881—90.
18. Whiteley M, Bangera MG, Bumgarner RE, Parsek MR, Teitzel GM, Lory S, et al. Gene expression in *Pseudomonas aeruginosa* biofilms. *Nature* 2001;**413**(6858):860—4.
19. Schoolnik GK, Voskuil MI, Schnappinger D, Yildiz FH, Meibom K, Dolganov NA, et al. Whole genome DNA microarray expression analysis of biofilm development by *Vibrio cholerae* O1 E1 Tor. *Methods Enzymol* 2001;**336**:3—18.
20. Schembri MA, Kjaergaard K, Klemm P. Global gene expression in *Escherichia coli* biofilms. *Mol Microbiol* 2003;**48**(1):253—67.
21. Beenken KE, Dunman PM, McAleese F, Macapagal D, Murphy E, Projan SJ, et al. Global gene expression in *Staphylococcus aureus* biofilms. *J Bacteriol* 2004;**186**(14):4665—84.
22. Beloin C, Ghigo JM. Finding gene-expression patterns in bacterial biofilms. *Trends Microbiol* 2005;**13**(1):16—9.
23. Sutherland I. Biofilm exopolysaccharides: a strong and sticky framework. *Microbiology* 2001;**147**(Pt 1):3—9.
24. Leriche V, Sibille P, Carpentier B. Use of an enzyme-linked lectin sorbent assay to monitor the shift in polysaccharide composition in bacterial biofilms. *Appl Environ Microbiol* 2000;**66**(5):1851—6.
25. Costerton W, Veeh R, Shirtliff M, Pasmore M, Post C, Ehrlich G. The application of biofilm science to the study and control of chronic bacterial infections. *J Clin Invest* 2003;**112**(10):1466—77.
26. Costerton JW, Lewandowski Z, Caldwell DE, Korber DR, Lappin-Scott HM. Microbial biofilms. *Annu Rev Microbiol* 1995;**49**:711—45.
27. Allison DG, Ruiz B, SanJose C, Jaspe A, Gilbert P. Extracellular products as mediators of the formation and detachment of *Pseudomonas fluorescens* biofilms. *FEMS Microbiol Lett* 1998;**167**(2):179—84.
28. Hall-Stoodley L, Costerton JW, Stoodley P. Bacterial biofilms: from the natural environment to infectious diseases. *Nat Rev Microbiol* 2004;**2**(2):95—108.
29. Stoodley P, Wilson S, Hall-Stoodley L, Boyle JD, Lappin-Scott HM, Costerton JW. Growth and detachment of cell clusters from mature mixed-species biofilms. *Appl Environ Microbiol* 2001;**67**(12):5608—13.
30. Lowy FD. *Staphylococcus aureus* infections. *N Engl J Med* 1998;**339**(8):520—32.
31. Boyd A, Chakrabarty AM. Role of alginate lyase in cell detachment of *Pseudomonas aeruginosa*. *Appl Environ Microbiol* 1994;**60**(7):2355—9.
32. Lee SF, Li YH, Bowden GH. Detachment of *Streptococcus mutans* biofilm cells by an endogenous enzymatic activity. *Infect Immun* 1996;**64**(3):1035—8.
33. Staudinger BJ, Muller JF, Halldórsson S, Boles B, Angermeyer A, Nguyen D, et al. Conditions associated with the cystic fibrosis defect promote chronic *Pseudomonas aeruginosa* infection. *Am J Respir Crit Care Med* 2014;**189**(7):812—24.
34. Møller S, Sternberg C, Andersen JB, Christensen BB, Ramos JL, Givskov M, et al. In situ gene expression in mixed-culture biofilms: evidence of metabolic interactions between community members. *Appl Environ Microbiol* 1998;**64**(2):721—32.
35. Bryant MP, Wolin EA, Wolin MJ, Wolfe RS. *Methanobacillus omelianskii*, a symbiotic association of two species of bacteria. *Arch Mikrobiol* 1967;**59**(1):20—31.
36. Stewart PS, Costerton JW. Antibiotic resistance of bacteria in biofilms. *Lancet* 2001;**358**(9276):135—8.
37. Fux CA, Stoodley P, Hall-Stoodley L, Costerton JW. Bacterial biofilms: a diagnostic and therapeutic challenge. *Expert Rev Anti Infect Ther* 2003;**1**(4):667—83.
38. Hoyle BD, Wong CK, Costerton JW. Disparate efficacy of tobramycin on Ca(2+)-, Mg(2+)-, and HEPES-treated *Pseudomonas aeruginosa* biofilms. *Can J Microbiol* 1992;**38**(11):1214—8.
39. Giwercman B, Jensen ET, Høiby N, Kharazmi A, Costerton JW. Induction of beta-lactamase production in *Pseudomonas aeruginosa* biofilm. *Antimicrobial Agents Chemother* 1991;**35**(5):1008—10.
40. Maira-Litrán T, Allison DG, Gilbert P. An evaluation of the potential of the multiple antibiotic resistance operon (mar) and the multidrug efflux pump acrAB to moderate resistance towards ciprofloxacin in *Escherichia coli* biofilms. *J Antimicrob Chemother* 2000;**45**(6):789—95.
41. Borriello G, Werner E, Roe F, Kim AM, Ehrlich GD, Stewart PS. Oxygen limitation contributes to antibiotic tolerance of *Pseudomonas aeruginosa* in biofilms. *Antimicrob Agents Chemother* 2004;**48**(7):2659—64.
42. Anderl JN, Zahller J, Roe F, Stewart PS. Role of nutrient limitation and stationary-phase existence in *Klebsiella pneumoniae* biofilm resistance to ampicillin and ciprofloxacin. *Antimicrob Agents Chemother* 2003;**47**(4):1251—6.
43. Lewis K. Riddle of biofilm resistance. *Antimicrob Agents Chemother* 2001;**45**(4):999—1007.
44. Dawson CC, Intapa C, Jabra-Rizk MA. "Persisters": survival at the cellular level. *PLoS Pathog* 2011;**7**(7):e1002121.
45. Post JC, Preston RA, Aul JJ, Larkins-Pettigrew M, Rydquist-White J, Anderson KW, et al. Molecular analysis of bacterial pathogens in otitis media with effusion. *J Am Med Assoc* 1995;**273**(20):1598—604.
46. Ecker DJ, Sampath R, Massire C, Blyn LB, Hall TA, Eshoo MW, et al. Ibis T5000: a universal biosensor approach for microbiology. *Nat Rev Microbiol* 2008;**6**(7):553—8.
47. Hall-Stoodley L, Stoodley P. Evolving concepts in biofilm infections. *Cell Microbiol* 2009;**11**(7):1034—43.
48. Hall-Stoodley L, Stoodley P, Kathju S, Høiby N, Moser C, Costerton JW, et al. Towards diagnostic guidelines for biofilm-associated infections. *FEMS Immunol Med Microbiol* 2012;**65**(2):127—45.
49. Høiby N, Bjarnsholt T, Givskov M, Molin S, Ciofu O. Antibiotic resistance of bacterial biofilms. *Int J Antimicrob Agents* 2010;**35**(4):322—32.
50. Hentzer M, Wu H, Andersen JB, Riedel K, Rasmussen TB, Bagge N, et al. Attenuation of *Pseudomonas aeruginosa* virulence by quorum sensing inhibitors. *EMBO J* 2003;**22**(15):3803—15.
51. Christensen LD, van Gennip M, Jakobsen TH, Alhede M, Hougen HP, Høiby N, et al. Synergistic antibacterial efficacy of early combination treatment with tobramycin and quorum-sensing inhibitors against *Pseudomonas aeruginosa* in an intraperitoneal foreign-body infection mouse model. *J Antimicrob Chemother* 2012;**67**(5):1198—206.
52. Römling U, Galperin MY, Gomelsky M. Cyclic di-GMP: the first 25 years of a universal bacterial second messenger. *Microbiol Mol Biol Rev* 2013;**77**(1):1—52.
53. Barraud N, Schleheck D, Klebensberger J, Webb JS, Hassett DJ, Rice SA, et al. Nitric oxide signaling in *Pseudomonas aeruginosa* biofilms mediates phosphodiesterase activity, decreased cyclic di-GMP levels, and enhanced dispersal. *J Bacteriol* 2009;**191**(23):7333—42.
54. Barraud N, Hassett DJ, Hwang SH, Rice SA, Kjelleberg S, Webb JS. Involvement of nitric oxide in biofilm dispersal of *Pseudomonas aeruginosa*. *J Bacteriol* 2006;**188**(21):7344—53.
55. Barraud N, Kardak BG, Yepuri NR, Howlin RP, Webb JS, Faust SN, et al. Cephalosporin-3′-diazeniumdiolates: targeted NO-donor prodrugs for dispersing bacterial biofilms. *Angew Chem Int Ed Engl* 2012;**51**(36):9057—60.
56. Parsek MR, Singh PK. Bacterial biofilms: an emerging link to disease pathogenesis. *Annu Rev Microbiol* 2003;**57**:677—701.